Study on the neurobiological bases of autism spectrum disorders : behavioural and molecular characterisation of Shank3 mutant mice

Allain-Thibeault Ferhat

Thèse de doctorat

Université Sorbonne Paris Cité

Préparée à l'Université Paris Diderot

École doctorale Bio Sorbonne Paris Cité 562

Génétique Humaine et Fonctions Cognitives / UMR3571 Gènes, Synapses et Cognition

Study on the neurobiological bases of autism spectrum disorders: Behavioural and molecular characterisation of *Shank3* mutant mice

Allain-Thibeault FERHAT

Thèse de doctorat de Neurobiologie

Présentée et soutenue publiquement à Paris le 18 septembre 2018

Président	Dr. Pierre Gressens
Rapporteur	Dr. Win Crusio
Rapporteur	Dr. Markus Wöhr
Examinateur	Dr. Camilla Bellone
Directeur de thèse	Dr. Elodie EY
Directeur d'unité	Prof. Thomas Bourgeron

CITATIONS

“One day, I’ll go live in 'Theory'! Because in Theory… EVERYTHING is fine!”

“If you ever get close to a human and human behaviour, be ready to get confused. There's definitely no logic to human behaviour, but yet so, yet so irresistible.”
Human behaviour, Björk

REMERCIEMENTS

To the all members of my jury

Before all, I would like to thank all member of my jury for give me the honor of judging my research during this Ph.D. I sincerely thank Dr Wim Crusio and Dr Markus Wöhr to have accepted to be my thesis rapporteurs and for bringing their expertise. I also would like to thank Dr Pierre Gresens to chair my jury as well as Camilla Bellone to review my work.

Aux laboratoire GHFC et aux membres de l'Institut Pasteur

Je tiens à remercier sincèrement Elodie Ey de m'avoir proposé ce stage de M2 ainsi que cette thèse. Merci d'avoir encadré mon travail pendant ces 4 ans et de m'avoir permis, je pense, d'améliorer mes compétences et mes connaissances scientifiques. Merci encore pour tous tes conseils lors de la rédaction de ce manuscrit et pendant toutes mes présentations.

Merci beaucoup Thomas Bourgeron de m'avoir accueilli au sein de ton laboratoire pour mon stage de M2 et de m'avoir fait confiance tout au long de cette thèse afin de mener à bien ce projet. Merci aussi pour toutes ces discussions et ces échanges scientifiques que l'on a pu avoir pendant ces 4ans.

Anne-Marie Le Sourd, un grand merci pour toute ton aide, pour tout le travail que tu as fait et qui m'a grandement aidé et pour ta bonne humeur quotidienne, tes encouragements. Je te souhaite le meilleur pour ta retraite et sache que tu nous as manquée pour ma dernière année de thèse.

Un énorme merci à Anne Biton, qui m'a grandement aidé pour l'étude d'ARN. Heureusement que tu restais toujours de bonne humeur devant ces résultats et on va finir par la terminer !

A tous mes co-thésard, les anciens, Laura, Marion et Coralie, la plus ou moins ancien, Ophélie, et les encore moins anciens, Oscar, Aline et Min. Merci à vous pour votre bonne humeur, votre gentillesse (ça dépend qui bien évidemment), et toutes ces discussions intellectuelles (tout est relatif).

Je tiens également à remercier chaleureusement tous les membres, ancien et présent, du laboratoire GHFC. Merci à Nathalie Lemiere et Hany Goudran-Botros pour leurs aides multiples apportées pour les différentes expériences que j'ai pu faire ainsi que pour les multiples conversations lors des repas. Merci à Thomas Roland, Gaël Millot et Guillaume Dumas pour leurs aides en bio-informatique et statistique. Je me dois de dire un grand merci à Claire Leblond pour son aide et une thèse rose. Merci à Sophie Calderari et Alexandre Mathieu pour ces compétitions lorsqu'on partageait le bureau. Merci à toute l'équipe de psy, Anita Begiato, Anne Claude Tabet, Anna Maruani, Frédérique Amsellem et Richard Delorme, pour toutes ces riches conversations et leurs bonnes humeurs et leurs conseils.

Merci à toute l'équipe de l'animalerie Lwoff et Metchnikoff pour leurs précieuses aides pour s'occuper des animaux et en particulier à Miguel Gasalho et Martine Jacob. Merci également à Marion Bérard d'avoir tout fait pour que l'on puisse travailler dans l'animalerie malgré tous les problèmes et les nombreuses réclamations.

En dehors de Pasteur, merci à Michael Schmeisser, Tobias Boeckers et Dominik Reims de m'avoir accueilli au sein du laboratoire à Ulm ainsi que les nombreux échanges et remarques au sujet des Shank.

De manière plus personnelle, je tiens réellement à remercier toutes les personnes proches de moi, que l'on se connaisse depuis 23 ans ou 3ans, que vous soyez thésard ou non. Merci d'avoir toujours été là et d'être toujours là.

Je souhaite remercier chaleureusement mes parents, mon frère et de ma sœur. Merci de m'avoir toujours soutenu, motivé et cru en moi pendant ces quatre années mais également bien avant. Je ne saurai jamais comment vous remercier.

Pour finir, j'aimerais remercier, autant que faire se peut, la personne qui me supporte et soutien depuis les premières semaines de cette thèse. Sans toi et ton humour cela n'aurait pas été pareil ni faisable. Merci pour tout Chloé.

SUMMARY

Autism spectrum disorders (ASD) are neurodevelopmental psychiatric disorders characterised by alterations in social communication, including social interactions and social signals such as speech, as well as stereotyped behaviours and restricted interests (American Psychiatric Association 2013). Behind this apparently unified definition, an important phenotypic variability is present, from severe disabilities to subtle impairments of personality traits (Leblond et al. 2014). Furthermore, individuals with ASD display several comorbidities, like intellectual disability, hyperactivity or epilepsy. ASD affect approximately 1-2% of people in the population.

More than 1000 genes were associated with ASD, the majority of them encoding synaptic proteins (Huguet, Ey, and Bourgeron 2013; Thomas Bourgeron 2015). Among these genes, the *SHANK* family, encoding synaptic scaffolding proteins and composed by *SHANK1*, *SHANK2* and *SHANK3*, is significantly associated with ASD. All *SHANK* genes are expressed in the post-synaptic density of glutamatergic synapses, but each member displays different brain expression patterns. There is a phenotypic inter-individual variability between patients carrying a deleterious *SHANK* mutation (Leblond et al. 2014). *SHANK3* mutations account for 1-2% of patients with ASD and intellectual disability. Interestingly, different studies reported a worsening of the phenotype and a regression of some aspects of behaviour in adolescence and adulthood for *SHANK3* patients (Guilmatre et al. 2014; De Rubeis et al. 2018).

Following these clinical and genetic observations, we propose to characterise a specific *Shank3* mouse models, displaying mutation in exon 11, at the behavioural level (a longitudinal study between three and twelve months of age) and at the molecular level (transcriptome analysis using RNA sequencing). We performed behavioural tests on male and female littermates. Then, we performed RNA sequencing on 12-months old animals in four brain structures (cortex, striatum, hippocampus, cerebellum).

We observed a decrease of exploratory behaviours, an increase of socio-sexual interactions as well as an increase of stereotyped behaviours. We also noticed a worsening of stereotyped behaviour with increasing age. These behaviours can be explained by impairments in cell signalling of specific neurons in striatum, based on RNA sequencing data.

Altogether, this project provides a comprehensive characterisation of a mouse model of ASD. It sheds some light on the molecular mechanisms possibly involved in a subgroup of patients with ASD and mutated in *SHANK3*. This insight could reveal new therapeutic approaches for the patients targeting the imbalance in striatal neurons.

RESUME

Les troubles du spectre autistique (TSA) sont des troubles psychiatriques neurodéveloppementaux caractérisés par des altérations de la communication et de l'interaction sociale, ainsi que des comportements stéréotypés et des intérêts restreints (American Psychiatric Association, 2013). Derrière cette définition, une importante variabilité phénotypique est présente, allant de handicaps sévères à des altérations plus subtiles (Leblond et al., 2014). De plus, les personnes atteintes de TSA présentent plusieurs comorbidités, comme une déficience intellectuelle, de l'hyperactivité ou de l'épilepsie. Les TSA touchent 1 à 2% de la population.

Plus de 1000 gènes sont actuellement associés aux TSA, la majorité d'entre eux codant pour des protéines synaptiques (Bourgeron, 2015, Huguet, Ey et Bourgeron, 2013). Parmi ces gènes, la famille *SHANK*, codant pour les protéines d'échafaudage synaptique et composée de *SHANK1*, *SHANK2* et *SHANK3*, est très associée aux TSA. Ces protéines sont exprimées dans la densité post-synaptique des synapses glutamatergiques, mais chaque membre affiche des profils d'expression cérébrale différents. Il existe une variabilité interindividuelle phénotypique entre les patients porteurs d'une mutation dans un gène *SHANK* (Leblond et al., 2014). Les mutations *SHANK3* concernent 1-2% des patients atteints de TSA et de déficience intellectuelle. Différentes études ont révélé une aggravation du phénotype et une régression de certains aspects du comportement à l'adolescence et à l'âge adulte chez les patients portant une mutation dans *SHANK3* (De Rubeis et coll., 2018, Guilmatre, Huguet, Delorme et Bourgeron, 2014).

Suite à ces observations cliniques et génétiques, nous proposons de caractériser un modèle de souris *Shank3*, présentant une mutation dans l'exon 11, au niveau comportemental (étude longitudinale entre trois et douze mois) et au niveau moléculaire (analyse du transcriptome en utilisant le séquençage d'ARNm). Nous avons effectué des tests de comportement chez les mâles et les femelles de même portée. Nous avons ensuite effectué le séquençage de l'ARN sur des animaux de 12 mois dans quatre structures cérébrales (cortex, hippocampe, striatum, cervelet).

Nous avons observé une diminution des comportements exploratoires, une augmentation des interactions socio-sexuelles ainsi qu'une augmentation des comportements stéréotypés. Nous avons également remarqué une aggravation du comportement stéréotypé au cours de l'âge. Ces comportements peuvent s'expliquer par une altération de la signalisation cellulaire de neurones spécifiques au striatum, selon nos données issues du séquençage de l'ARN.

Pour conclure, ce projet fournit une caractérisation complète d'un modèle murin des TSA. Il apporte un éclairage sur les mécanismes moléculaires éventuellement impliqués dans un sous-groupe de patients atteints de TSA et mutés dans *SHANK3*. Nos résultats pourraient révéler une nouvelle approche thérapeutique pour les patients en ciblant le déséquilibre dans les neurones du striatum.

Content

Citations 2

Remerciements 3

Summary 5

Résumé 6

Abbreviations 10

Introduction 12

I. Clinical aspects of autism spectrum disorders 14

I.A. History 14

I.B. Main clinical criteria 14

I.C. Epidemiology 17

I.D. Comorbidities 18

I.D.1. Intellectual disability (ID) 18

I.D.2. Psychiatric disorders 19

I.D.3. Epilepsy 19

I.E. Diagnosis 19

I.F. Causes 20

I.F.1. Genetic factors 20

I.F.2. Environmental factors 23

I.F.3. Epigenetic factors 24

II. Neurobiology of autism 25

II.A. Neuro-developmental disorders 25

II.A.1. Brain development 25

II.A.1. Gene expression 26

II.B. Imbalanced Excitatory/inhibitory synapses 27

II.C. Pathways associated with ASD core symptoms 28

II.C.1. Social pathway 28

II.C.2. Stereotyped pathway 32

III. *SHANK* gene: structure and implication 35

III.A. Structure of genes and proteins 35

III.A.1. Structure of the Shank genes 35

III.A.2. Structure of the proteins 37

III.A.3. Implication in neurons 40

III.A.4. Expression 42

III.B. Implication of Shank family in neuro-pathology 44

III.B.1. Heterogeneity of symptoms 44

III.B.2. Autism spectrum disorder 45
III.B.3. Bipolar disorder 47
III.B.4. Schizophrenia 47
III.B.5. Alzheimer disease (AD) 47
IV. Mouse models for autism 49
IV.A. Benefits of mouse models for autism 49
IV.B. Mouse models carrying mutations in SHANK genes 50
IV.B.1. Shank1 50
IV.B.1. Shank2 51
IV.B.2. Shank3 55
V. Aims 62
Material & methods 64
I. Mouse cohorts 66
I.A. General 66
I.A. Weaning 66
I.A. Behavioural procedures 67
II. Behavioural tests 68
II.A. General health 68
II.B. Dark/light anxiety-like test 68
II.C. Elevated Plus-maze anxiety-like test 69
II.D. Locomotion and exploratory test in Open field 69
II.E. Stereotyped behaviour observation 70
II.F. Occupant/new-comer social test with vocalisation recording 70
II.G. Male behaviour in presence of an oestrus female 72
II.H. Three-chambered social test 73
II.I. Behavioural statistics 73
III. Biochemical & molecular biology test 74
III.A. Tissue collection 74
III.B. Total RNA extraction 74
III.C. RNA-Seq samples 74
III.D. Mapping and reference genome 75
III.E. Calling variants from the RNAseq data 75
III.F. Differential Expression Analysis 76
III.G. Gene set analysis 76
III.H. RNA isolation and dd-PCR 77
III.I. Protein-protein interaction network analysis 77
Results 78

I. Molecular and behavioural characterisation of *Shank3Δ11* mutant mice 80

I.A. Context 80

I.B. Article manuscript 80

II. Behavioural characterisation of *Shank2*/*Shank3* double mutant mice 104

II.A. Context 104

II.B. Results 104

Discussion* *110

I. Comparison between studies 112

II. Behaviour & transcriptomics 113

III. Specific gene expression impaired 118

IV. Perpectives and conclusion 119

References* *122

Annexes* *150

I. Article 1: "Social Communication in Mice – Are There Optimal Cage Conditions? 152

II. Article 2: "Recording Mouse Ultrasonic Vocalizations to Evaluate Social Communication" 175

III. Review: "Chapter 5: Behavioural Phenotypes and Neural Circuit Dysfunctions in Mouse Models of Autism Spectrum Disorder" 188

ABBREVIATIONS

Δ	Deletion
ABP1	Abelson tyrosine kinase interacting
AC	Adenylate cyclase
ACI	Autism Comorbidity Interview
AD	Alzheimer's disease
ADHD	Attention-deficit with hyperactivity disorder
ADI-R	Autism Diagnostic Interview, Revised
ADOS	Autism Diagnostic Observation Schedule
AMPA	α-amino-3-hydroxy-5-methyl-4-isoxazolepropionic acid
ANK	Ankyrins
AOB	Accessory olfactory bulb
ASD	Autism spectrum disorders
Aβ	Amyloid-beta
BLA	Basolateral amygdala
BPD	Bipolar disorder
CARS	Childhood Autism Rating Scale
CCS	Children Communication Scale
CDC	Centers for Disease Control and Prevention
CNV	Copy number variation
CSL	Corticostriatal loops
dmPFC	Dorsomedian PFC
DR	Dopamine receptor 1/2
DREADD	Designer receptor exclusively activated by designer drugs
DRN	Dorsal raphe nucleus
DSM	Diagnostic and Statistical Manual of Mental Disorders
fEPSP	Field excitatory postsynaptic potential
FISH	Fluorescent in Situ Hybridization
GKAP	Guanylate Kinase-Associated Protein
GluA	AMPA glutamate receptor
GluN	NMDA glutamate receptor
GPCR	G-Protein-Coupled-Receptor
Gpi/e	Globus palidus intern / extern
GRIP	Glutamate receptor-interaction protein
HDAC2	Histone deacetylase-2
ID	Intellectual disability
InsG	Insertion of Guanine
IP3	Inositol 1,4,5-triphosphate
IQ	Intelligence quotient
KO	Knock-out
LGD	Likely gene-disrupting
LTP	Long-Term potentiation
mEPSP	Miniature excitatory postsynaptic potential
mGluR	Metabotropic glutamate receptor

mPFC	Median PFC
MRI	Magnetic resonance imaging
MSN	Medium spiny neurons
NAcc	Nucleus accumbens
NC	New-comer
NLGN	Neuroligin
NMDA	N-methyl-D-aspartate
NOS1	Nitric oxide synthase 1
NRXN	Neurexin
OB	Olfactory bulb
PAG	Periaqueductal grey
PCW	Post conception week
PDD	Pervasive developmental disorder
PDZ	PSD-95/Disc-large/ZO-1
PFC	Prefrontal cortex
PLPc	Phospholipase C
PK A-B-C	Protein kinase A-B or C
PMS	Phelan-McDermid syndrome
PND	Post-natal day
PPI	Protein-protein interaction
Pro	Proline rich
PSD	Post-synaptic density
PVN	Paraventricular nucleus
RBS	Repetitive Behaviour Scale
SAM	Sterile alpha motif
SCZ	Schizophrenia
SEM	Standard error of the mean
SFARI	Simons Foundation Autism Research Initiative
SH3	Src homology 3
SHANK	SH3 and multiple Ankyrin repeat domains
SNP/SNV	Single nucleotide polymorphism/ variant
SNr/c	Substantia nigria reticulata / compacta
SRS	Social Responsiveness Scale
STN	Subthalamic nucleus
USV	Ultrasonic vocalisations
vmPFC	Ventromedian PFC
VPA	Valproic acid
VTA	Ventral tegmental area
WAIS	Wechsler Adult Intelligence Scale
WISC	Wechsler Intelligence Scale for Children

INTRODUCTION

I. Clinical aspects of autism spectrum disorders

I.A. *History*

In 1943, Leo Kanner published an article, entitled "*Autistic Disturbance of Affective Contact*". In this study, he described 11 children, eight boys and three girls, with "*inability to relate themselves in the ordinary way to people and to situation from beginning of life*". He linked several impairments observed in children under the same terminology: "*Autism"* (Kanner 1943). Kanner borrowed the term "*autism*" to schizophrenia terminology, used to qualify a schizophrenic patient with unusual social interactions (Stotz-Ingenlath 2000). Furthermore, Kanner described impairments in language and intellectual disabilities (ID) for several of these patients.

In parallel, Hans Asperger published a study on four children who presented similar characteristics as described by Kanner without ID and language deficits (Frith 1991; Asperger 1944). Furthermore, Asperger described these children as having a lack of empathy, a very specific centre of interest and being clumsy.

In 1956, Kanner and Einsenberg noticed that repetitive behaviour could be seen in several children with intellectual defidiency and "*autistic disturbance*" and proposed to use "*the presence of elaborately conceived rituals together with the characteristic aloneness*" as a proxy "*to differentiate the autistic patients*" (Eisenberg and Kanner 1956).

I.B. *Main clinical criteria*

In the following years, several studies validated the observation of Kanner and Asperger and, in 1980, a unified definition and semiology of infantile autism was proposed in the Diagnostic and Statistical Manual of Mental Disorders III (DSM-III) (American Psychiatric Association 1980). In the DSM-III, infantile autism is related to pervasive developmental disorder (PDD) and characterised by "*a lack of responsiveness to other people (autism), gross impairment in communicative skills, and bizarre responses to various aspects of the environment, all developing within the first 30 months of age*". This last element of the definition implies a neuro-developmental aspect of autism.

A. Persistent deficits in social communication and social interaction across multiple contexts, as manifested by the following, currently or by history (examples are illustrative, not exhaustive; see text):

1. Deficits in social-emotional reciprocity, ranging, for example, from abnormal social approach and failure of normal back-and-forth conversation; to reduced sharing of interests, emotions, or affect; to failure to initiate or respond to social interactions.

2. Deficits in nonverbal communicative behaviours used for social interaction, ranging, for example, from poorly integrated verbal and nonverbal communication; to abnormalities in eye contact and body language or deficits in understanding and use of gestures; to a total lack of facial expressions and nonverbal communication.

3. Deficits in developing, maintaining, and understanding relationships, ranging, for example, from difficulties adjusting behaviour to suit various social contexts; to difficulties in sharing imaginative play or in making friends; to absence of interest in peers.

B. Restricted, repetitive patterns of behaviour, interests, or activities, as manifested by at least two of the following, currently or by history (examples are illustrative, not exhaustive; see text):

1. Stereotyped or repetitive motor movements, use of objects, or speech (e.g., simple motor stereotypes, lining up toys or flipping objects, echolalia, idiosyncratic phrases).

2. Insistence on sameness, inflexible adherence to routines, or ritualized patterns of verbal or nonverbal behaviour (e.g., extreme distress at small changes, difficulties with transitions, rigid thinking patterns, greeting rituals, need to take same route or eat same food every day).

3. Highly restricted, fixated interests that are abnormal in intensity or focus (e.g., strong attachment to or preoccupation with unusual objects, excessively circumscribed or perseverative interests).

4. Hyper- or hypo-reactivity to sensory input or unusual interest in sensory aspects of the environment (e.g., apparent indifference to pain/temperature, adverse response to specific sounds or textures, excessive smelling or touching of objects, visual fascination with lights or movement).

C. Symptoms must be present in the early developmental period (but may not become fully manifest until social demands exceed limited capacities or may be masked by learned strategies in later life).

D. Symptoms cause clinically significant impairment in social, occupational, or other important areas of current functioning.

E. These disturbances are not better explained by intellectual disability (intellectual developmental disorder) or global developmental time. Intellectual disability and autism spectrum disorder frequently co-occur; to make comorbid diagnoses of autism spectrum disorder and intellectual disability, social communication should be below that expected for general developmental level.

Table 1: Diagnostic criteria for autism spectrum disorder in the 2013 Diagnostic and Statistical Manual of Mental Disorders Fifth Edition, DSM-5 (American Psychiatric Association 2013).

In 1994, an update of the DSM was published, DSM-IV, which introduced autistic disorder, as a heterogeneous group into the PDD and not as the infantile autism (American Psychiatric Association 2000). The DSM-IV characterised the autistic disorder with an abnormal or an absence of social interaction and communication as well as a restricted repertoire of activities and interests, the autistic triad. This DSM introduced the presence of variability between patients. Since the last version of DSM-5, published in 2013, Asperger's Syndrome is associated with the autistic disorders into PDD-Not Otherwise Specified and childhood disintegrative disorders. The annotation for autistic disorder is also changed by Autism Spectrum Disorders (ASD) and precise criteria are defined (Table 1) (American Psychiatric Association 2013).

However, the inclusion of Asperger's syndrome in PDD then ASD, in DSM-IV and DSM-5, are debated due to the phenotypic difference between autistic patients and several Asperger patients (Yu et al. 2011; Ghaziuddin 2010). ASD are characterised by a deficit in social communication, verbal and non-verbal, and presence of restricted interests and repetitive behaviour (Table 1). Social interaction and social communication criteria, from DSM-IV, are hardly distinguishable and are grouped in DSM-5 (Hazen, McDougle, and Volkmar 2013). The DSM-5 introduced the notion of spectrum in autism, suggesting an important variability in semiology of patients, already proposed in DSM-IV. To characterise as well as possible the phenotype of patients, a scale of severity levels in

ASD is also proposed, from level 1 (the patient requires small support) to level 3 (the patient requires very substantial support) (Table 2). In the following part, we will base all descriptions and discussion on the DSM-5 ASD characterisation.

Severity level	Social communication	Restricted, repetitive behaviours
Level 1 "Requiring support"	Without supports in place, deficits in social communication cause noticeable impairments. Difficulty initiating social interactions, and clear examples of atypical or unsuccessful responses to social overtures of others. May appear to have decreased interest in social interactions. For example, a person who is able to speak in full sentences and engages in communication, but whose to-and-fro conversation with others fails, and whose attempts to make friends are odd and typically unsuccessful.	Inflexibility of behaviour causes significant interference with functioning in one or more contexts. Difficulty switching between activities. Problems of organization and planning hamper independence.
Level 2 "Requiring substantial support"	Marked deficits in verbal and nonverbal social communication skills; social impairments apparent even with supports in place; limited initiation of social interactions; and reduced or abnormal responses to social overtures from others. For example, a person who speaks simple sentences, whose interaction is limited to narrow special interests, and who has markedly odd nonverbal communication.	Inflexibility of behaviours, difficulty coping with change or other restricted / repetitive behaviours appears frequently enough to be obvious to the casual observer and interfere with functioning in a variety of contexts. Distress and/ or difficulty changing focus or action.
Level 3 "Requiring very substantial support"	Severe deficits in verbal and nonverbal social communication skills cause severe impairments in functioning, very limited initiation of social interactions, and minimal response to social overtures from others. For example, a person with few words of intelligible speech who rarely initiates interaction and, when he or she does, makes unusual approaches to meet needs only and responds to only very direct social approaches.	Inflexibility of behaviour, extreme difficulty coping with change, or other restricted/ repetitive behaviours markedly interferes with functioning in all spheres. Great distress/ difficulty changing focus or action.

Table 2: Severity levels for autism spectrum disorder based on the DSM-5 diagnostic criteria (American Psychiatric Association 2013).

I.C. *Epidemiology*

The current prevalence of ASD is 1-2% of the population. In a recent publication from the Centers for Disease Control and Prevention (CDC), the prevalence of ASD in the United States of America (USA) was estimated at 16.8 per 1000 children, 1.7% of the population, aged eight years (Baio et al. 2018). The prevalence varied between states from 13.1 to 29.3 per 1000 children. This variability between states can be explained by the number of paediatricians, psychiatrist, and health centres in each state (Mandell and Palmer 2005). The sex ratio for ASD is unbalanced, with four boys affected for one girl (Baio et al. 2018). When focusing on intellectual and adaptive functioning in children with ASD aged 8 years, 31% displayed intellectual disabilities (ID; intelligence quotient [IQ] ≤70), 25% classified as borderline (71≤IQ≤85) and 44% displayed average and above-average IQ (IQ>85). In the USA, the prevalence of ASD steadily increases over years, according to the CDC report (2000: 6.7/1000; 2006: 9.0/1000; 2008: 11.3/1000; 2014: 14.7/1000) (Figure 1.A).

This increase of ASD prevalence in the USA could be directly related to the increase of ASD cases, due to environmental effects for example (see I.F.2), but this theory is neither validated nor excluded. It is more likely that the increase is due to the improvement of the medical practices (Lyall et al. 2017; Hansen, Schendel, and Parner 2015), with an enlargement of DSM diagnosis criteria especially between DSM-III and DSM-VI (see I.B.), the improvement of detection and inclusion in the spectrum, the set-up of standardised tests for the diagnosis, and the possibility to detect children with ASD in schools (Turnbull 2005). Furthermore, a study in Sweden revealed a stable prevalence between 1993 and 2002, but an increase of diagnosis (Figure 1.B) (Lundström et al. 2015).

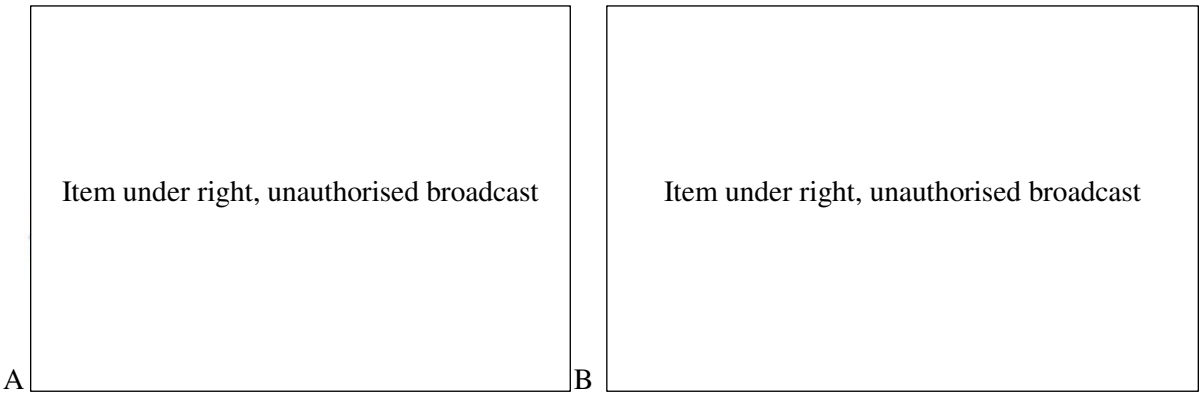

Figure 1: Evolution of prevalence of ASD over years.
*(A) Estimated prevalence of autism spectrum disorder in the United States of America from 2004 to 2018 based on Centers for Disease Control and Prevention (CDC) reports (Autism Speaks). (B) Estimated prevalence of autism spectrum disorder in Sweden based on Child and Adolescent Twin Study in Sweden (CATSS), national patient register (NPR), and NPR diagnoses in Swedish twins. *Prevalence calculated on 19993 people responding in twin study born 1993-2002* (Lundström et al. 2015).

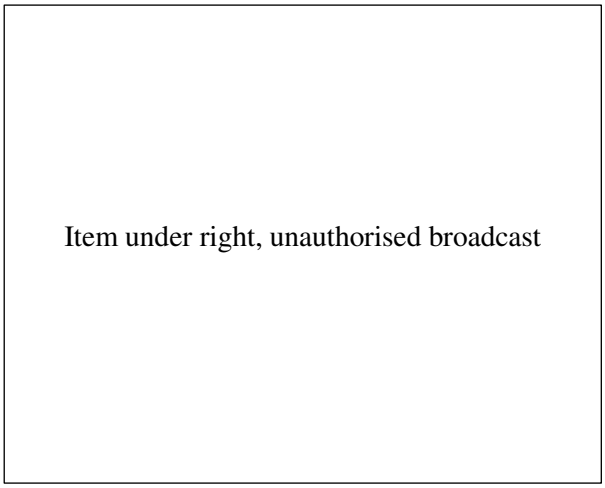

Figure 2: Core symptoms and most frequent comorbidities in ASD. *Red line defines the level of severity, low at the centre (dotted circle) and high at the periphery (full circle). Colours represent the combination of clinical features. From* (Huguet, Ey, and Bourgeron 2013).

I.D. *Comorbidities*

The two main criteria of ASD, deficits in social communication and repetitive and stereotyped behaviour, are often associated with other disorders, named comorbidities. The most frequent comorbidities are described hereafter (Figure 2).

I.D.1. *Intellectual disability (ID)*

ID is the most frequent comorbidity in patients with ASD. Seventy percent of patients display ID at different severity levels (Mefford, Batshaw, and Hoffman 2012; Newschaffer et al. 2007; Wilkins and Matson 2009). The DSM-5 qualified ID as a deficit in intellectual functioning (quantified by the intellectual quotient, IQ) and a deficit in adaptive functioning observed during childhood (American Psychiatric Association 2013).

To quantify IQ, different scales are used, such as the WISC (Wechsler Intelligence Scale for Children) and WAIS (Wechsler Adult Intelligence Scale). For patients without verbal impairments, standard tests are proposed as the Raven's Progressive Matrices.

In the DSM-IV and DSM-5, four qualitative levels define ID (Boat et al. 2015):

- Mild ID: $50 \leq IQ \leq 69$; the patient lives independently with a minimum level of support and can acquire basic skills such as reading and writing;
- Moderate: $36 \leq IQ \leq 49$; the patient lives independently with important support and requires specific supervision for learning.
- Severe: $20 \leq IQ \leq 35$; the patient requires daily assistance.

- Profound: IQ≤19; the patient requires 24-hour assistance.

Patients with ASD, but without ID (IQ>70) are said to display high-functioning autism.

I.D.2. *Psychiatric disorders*

Several studies showed that psychiatric disorders are more common in patients with ASD. The Autism Comorbidity Interview (ACI) is used to quantify these aspects (Leyfer et al. 2006). The most common psychiatric disorders are anxiety, attention-deficit with hyperactivity disorder (ADHD) and mood disorders.

Anxiety disorders are characterised by increased anxiety and fear, and can be expressed through specific phobia, social anxiety disorder, agoraphobia (American Psychiatric Association 2013). Anxiety disorders are present in 11-84% in children with ASD, according to the type of measure, reported by parents or observed by practitioners (White et al. 2009). Patients with ASD may also have ADHD (28-27%) and mood disorders, including bipolar disorders and depression (2-57%) (Mansour et al. 2017; Ghaziuddin and Greden 1998). In neurotypical population, anxiety is found in 3-30% according to the criteria, ADHD is found in 3.4%, and mood disorder in 3.8% (Martin 2003; Boat et al. 2015; Fayyad et al. 2007).

I.D.3. *Epilepsy*

Epilepsy is a neurological disorder characterised by an excessive and abnormal neuronal activity in the brain followed by seizure (Fisher et al. 2005). It occurs more often in patients with ASD than in the neurotypical population, with 5-38% of patients with ASD displaying seizure (Frye et al. 2016). This prevalence in ASD patients varies between studies and with the associated comorbidities (Spence and Schneider 2009). Indeed, 21.5% of patients with ASD and ID suffer from epilepsy while only 8% of patients with ASD, but without ID display epilepsy (Amiet et al. 2008).

I.E. *Diagnosis*

Despite the improvements of biological and medical techniques, no biological markers allow any precise diagnosis of ASD. The diagnostic is generated using clinical and psychological evaluations with standardised tools based on interviews with the patient and his/her relatives. The two most used tools are:

- The *Autism Diagnostic Interview, Revised* (ADI-R) (C Lord, Rutter, and Le Couteur 1994) which consists in an interview with the parents. This interview allows to list and evaluate the deficits and to notice the outbreak and evolution of the disorders;
- The Autism Diagnostic Observation Schedule (ADOS) (Catherine Lord et al. 2000) which consists in a structured interview with the patient based on short activities and games. This tool allows the evaluation of the different deficits and can be adapted depending on the age and the language level of the patient.

Other tools have been developed allowing a quantitative evaluation of the patient:

- The Childhood Autism Rating Scale (CARS) (Schopler et al. 1980) which allows an evaluation of the global deficit associated with ASD core symptoms;
- The Social Responsiveness Scale (SRS) (Constantino et al. 2000) which evaluates more specifically the social behaviours;
- The Children Communication Scale (CCS) (Bishop 1998) which tests the social communication;
- The Repetitive Behaviour Scale (RBS) (Bodfish et al. 2000) which quantifies the repetitive and the stereotyped behaviours.

The first clinical signs of ASD usually emerges in the first years of life of the patients and the first consistent diagnostic can be performed at three years of age (Ozonoff et al. 2010). In the majority of cases, the psychological evaluation is followed by a diagnostic of comorbidities.

I.F. *Causes*

The aetiology of ASD is very complex and different factors could influence the brain development and cause ASD. In this part, we will discuss the three main effects that influence brain development: genetics, epigenetics and environment.

I.F.1. *Genetic factors*

The most studied aetiology of autism is the genetic factors. Early ASD heritability studies, during the seventies and the eighties, were conducted on twins and showed a higher concordance of ASD and ID in monozygotic twins compared to dizygotic twins and siblings (August, Stewart, and Tsai 1981; Folstein and Rutter 1977). In the nineties, Bailey and colleagues proposed a first estimation of the concordance rates in ASD at 92% for monozygotic twins versus 10% for dizygotic twins (Bailey et al. 1995). A recent study on a larger cohort shows that the concordance rate for dizygotic twins is around 20% (Hallmayer et al. 2011). Furthermore, a study on siblings calculated an increase

of 20% of recurrence rate if the first born displayed ASD versus 1% if the first born did not display ASD (Ozonoff et al. 2010).

More recently, several studies on large cohorts estimated the heritability of ASD at 50-59% (Lundström et al. 2012; Sandin et al. 2014). Interestingly, Colvert and colleagues (2015) showed that the estimation of heritability largely depends on diagnostic tools, with 56% with ADI-R, 76% with ADOS and 95% with other tools (Colvert et al. 2015). This study highlights the importance of a united definition of ASD and the use of standardised diagnostic tools. Importantly, all studies highlighted an incomplete heritability, indicating the presence of other factors (Huguet, Ey, and Bourgeron 2013).

The first genetic causes of ASD were identified in different syndromes, counting for 10% of cases (Zafeiriou et al. 2013). These syndromes are due to monogenic mutations especially in Fragile X syndrome (gene Fragile X Mental Retardation, *FRM1*) and Rett syndrome (gene Methyl CpG binding protein 2, *MECP2*) (Pieretti et al. 1991; Amir et al. 1999). Later, thanks to better sequencing methods, whole genome/exome/RNA sequencing, studies on the genetic aetiology of ASD became more confident. Studies based on the whole genome or whole exome revealed deleterious mutations in patients with ASD non-associated with any syndrome. To date, more than 1000 genes associated with ASD are listed in the SFARI (Simons Foundation Autism Research Initiative) database. The majority of these genes are categorised according to the strength of their association with ASD:

- Category S: ≈140 genes associated with syndromic disorders; these genes are more or less associated with ASD according to the following category, e.g. *MECP2*;
- Category 1: ≈ 25 genes strongly associated with ASD with rigorous criteria, e.g. *SHANK3*;
- Category 2: ≈ 59 genes strongly associated with ASD with less rigorous criteria by several studies, e.g. *FOXP1*;
- Category 3: ≈ 175 genes with supporting suggestive evidence, e.g. *Neurexin* 1 (*NRXN1*);
- Category 4: ≈ 405 genes with supporting minimal evidence, e.g. *GRIN2A*;
- Category 5: ≈ 160 genes not rigorously tested in humans;
- Category 6: ≈ 20 genes tested in humans without robust evidence;
- No category: ≈ 165 genes not categorized.

Yuen and colleagues proposed another classification based on the degree of involvement in ASD: genes known to be associated with ASD (Class I), possible gene candidates (Class II), putative genes (Class III) and genes known to be associated with neurodevelopmental disorders (Class IV) (Yuen et al. 2015).

All these genes associated with ASD are involved in cellular functions, including synaptic function, chromatin remodelling and RNA translation (see I.F.3 & **Figure 3**) (Huguet, Ey, and Bourgeron 2013). However, different mutations can affect the same pathway in the neuronal functioning (Guilmatre et al. 2014).

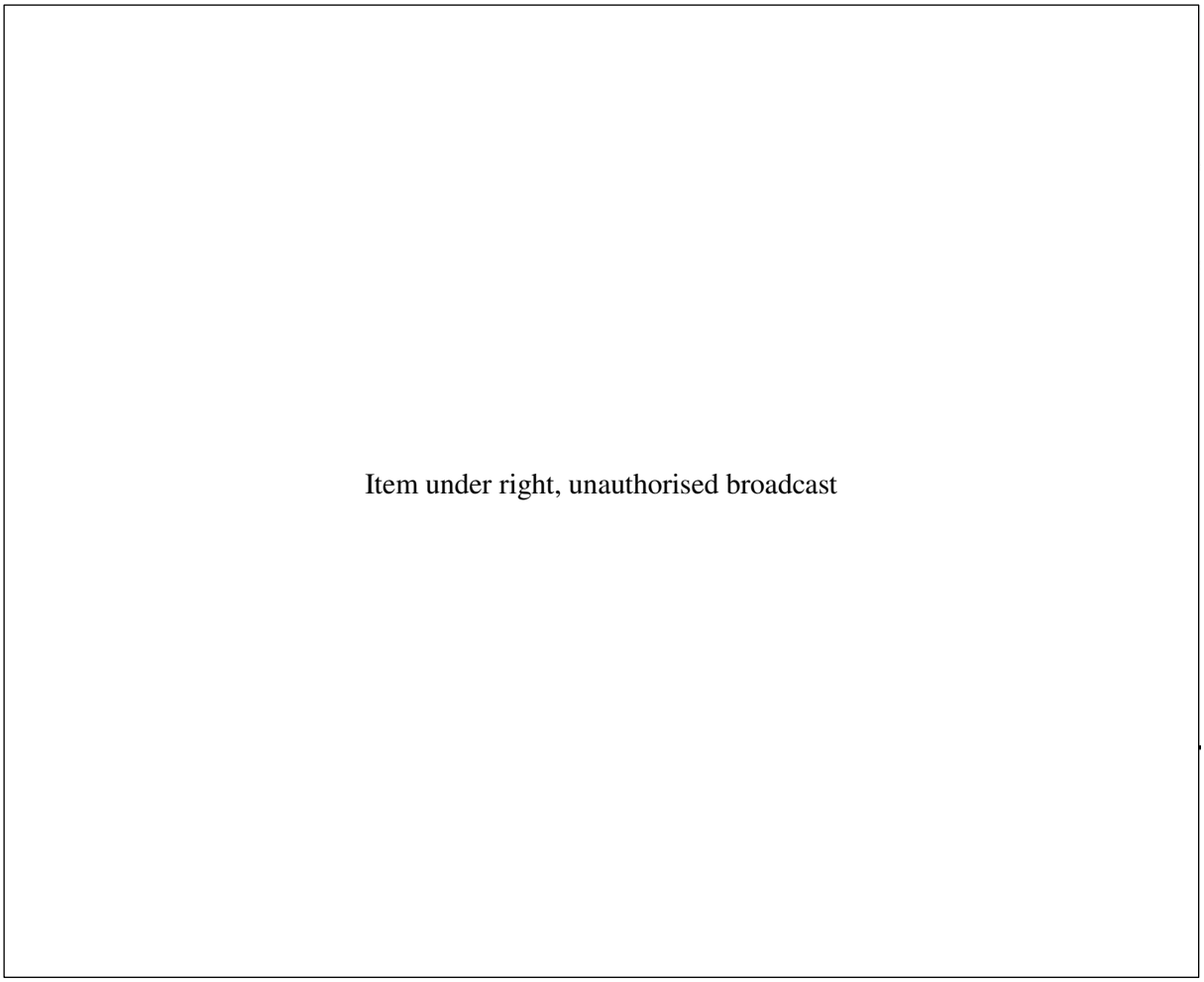

Figure 3: Biological pathways of pre- and post-synaptic proteins mutated in ASD or other disorders.
These proteins are involved in many functions, including the organization of the postsynaptic density, cytoskeleton dynamics, cellular signalling cascades, epigenetic regulation of transcription, and release of neurotransmitters. Proteins associated with ASD are in red, those associated with other psychiatric disorders are in purple, and those associated with intellectual disability are in blue. Panel a illustrates the pre- and post-synapse; panel b illustrates the synapse and gene transcription regulation in the nucleus (from Huguet et al., 2013).

The mutations involved in ASD are mostly dominant (Casey et al. 2012). Chromosomic abnomalities are observed in 3% of cases with duplication, deletion, inversion or translocation (Reddy 2005), and *de novo* copy number variants (CNVs) are more present in individuals with ASD than in non-affected siblings or controls (Huguet, Ey, and Bourgeron 2013), no matter the size of the CNV. The frequency of *de novo* CNV is 7% in ASD patients from simplex families (one affected individual) and 4% in ASD patients from multiplex families (at least two affected individuals) and less than 2% in non-affected siblings and controls (Huguet, Ey, and Bourgeron 2013). Recent analysis of the whole exome showed a higher number of single nucleotide variants (SNVs) in patients than in non-affected siblings and controls (Iossifov et al. 2014). The SNV can be of different types: missense mutation, stop-losses, or *likely gene-disrupting* (LGD), including nonsense mutation and frameshift mutation due to the insertion or deletion of nucleotide(s).

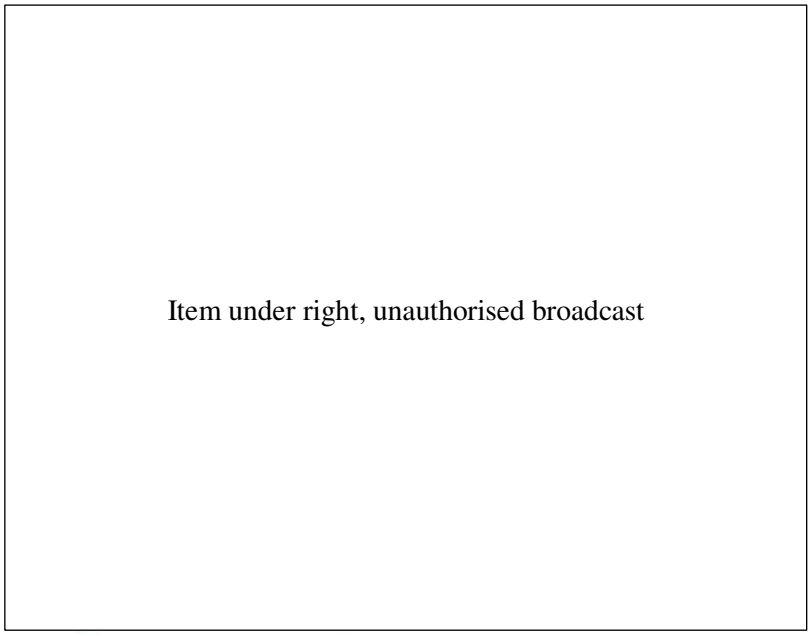

Figure 4: Possible transmission of ASD. *(Far left) De novo highly penetrant mutation non-present in parents; (left-of-middle) child inherits of rare variant; (right-of-middle) combination of rare variant and genetic background; (far right) child inherits of high risk genetic background. Adapted from* (Bourgeron 2015).

Monogenic forms of ASD (i.e., one gene is enough to trigger impairment) are estimated to represent 10-20% for monogenic dominant forms and 3-6% for monogenic recessive forms of ASD (Bourgeron 2015; E. T. Lim et al. 2013). Polygenic forms of ASD also exist and are determined by a combination of low risk alleles or by specific genetic backgrounds. Indeed, combinations between rare deleterious variants, monogenic causes and genetic variants could generate different phenotypes or reveal impairment not present in parents and lead to ASD (Figure 4) (Thomas Bourgeron 2015). The genetic background can also influence the sensitivity to gene expression dosage (Toro et al. 2010).

I.F.2. *Environmental factors*

Environmental factors increase the risk of autism. However, this aspect is less rigorously studied and more difficult to control. Only few environmental factors are fully validated to date (Karimi et al. 2017). Familial factors such as parental age increase the risk of ASD. Parents older than 34 years seem to increase the ASD risk by 29%, and this risk is increased each 10 years for the father (Sasanfar et al. 2010). However, a study on risk factors in children born between 1991 and 2001 associated an increased risk of ASD with the father's age only, as the germline is more likely to develop *de novo* mutations (Reichenberg et al. 2006; Lauritsen, Pedersen, and Mortensen 2005). The prenatal exposition to drugs is the most robust factor associated with ASD and can increase the risk by 46% (Gardener, Spiegelman, and Buka 2009). Several studies showed an impact of anti-epileptic drugs (Valproic acid, VPA) or antidepressant drugs on social behaviour, motor activities and post-

natal development of the child (Narita et al. 2010; Rai et al. 2013). Other prenatal factors impact the brain development and induce autism, like infections of the mother during pregnancy (Berger, Navar-Boggan, and Omer 2011; Ornoy, Weinstein-Fudim, and Ergaz 2015) or caesarean delivery (Gardener, Spiegelman, and Buka 2011).

I.F.3. *Epigenetic factors*

Epigenetics is defined by mechanisms provoking a heritable and reversible change of gene expression which do not modify the nucleotide sequence, like DNA methylation. Gene expression can be disturbed at different steps, for instance transcriptional and translational control, RNA transport, or protein activity. Few studies linked ASD with epigenetic modulations, although a strong evidence of an epigenetic impact in ASD was shown (Siu and Weksberg 2017). Indeed, a significant number of genes associated with syndromic or non-syndromic ASD are involved in the control of gene expression. Some genes strongly associated with ASD directly control gene expression, like *MECP2* (SFARI-category: 2) in Rett syndrome, while others modulate it indirectly, like *FMR1* (SFARI-category:1) in Fragile X syndrome (Siu and Weksberg 2017). For instance, a mutation in *MECP2*, a gene encoding a methyl-CpG binding protein, causes Rett syndrome (Amir et al. 1999). The CpG sites in DNA sequence, composed by a cytosine followed by a guanine, are involved in gene expression. Methylation of these sites causes stable silencing of a specific gene and allows a regulation of the transcription (Bird 2002). The *MECP2* protein methylates CpG sites, establishing epigenetic marks and gene silencing. Therefore, a mutation in this gene can lead to gene regulation impairments. The Fragile X syndrome is due to an abnormally high number of CGG repetitions in *FMR1*. This mutated region becomes an abnormal methylation site, resulting in an inhibition of the expression of the protein, FMRP (Crawford, Acuña, and Sherman 2001). Other mutations associated with non-syndromic ASD are related to epigenetics. The gene *CHD8* (SFARI-category: 1) encodes for a protein involved in chromatin remodelling (Merner et al. 2016). Mutations of this gene have a penetrance of 85%. More recently, a study on mice showed that the gene *SHANK3*, encoding a post-synaptic scaffolding protein and strongly associated with ASD (see III.B), interacts with a histone deacetylase-2 (HDAC2) and disturbs the chromatin expansion and gene transcription (Qin et al. 2018).

In the following part, we will mainly focus on the genetic causes of ASD. We will discuss about SH3 and multiple Ankyrin repeat domains (*SHANKs*) gene family, and especially *SHANK3*. These genes encode scaffolding proteins at excitatory synapses. This gene family is strongly associated with ASD and was identified by Fluorescent In Situ Hybridization (FISH) analysis and whole genome sequencing (Durand et al. 2007). Following a meta-analysis on *SHANK* family, almost 1% of ASD patients display mutation (*SHANK1*: 0.04%; *SHANK2: 0.17%; SHANK3: 0.70%*) and 2% of patients with ASD and ID display mutation in *SHANK3* (Leblond et al. 2014).

II. Neurobiology of autism

II.A. *Neuro-developmental disorders*

II.A.1. *Brain development*

Based on the DSM-5, we qualified above (see I.B) ASD as a PDD condition, with an emergence of clinical signs in the first three years of life (see I.E). The first direct link between neuronal impairments and ASD was established by comorbidities like epilepsy. Neurobiological analyses revealed brain abnormalities in ASD patients. Indeed, magnetic resonance imaging (MRI) studies showed that the cerebral volume and the head circumference were increased by 20% in ASD patients compared to neuro-typical controls, during early childhood (Sacco, Gabriele, and Persico 2015; Redcay and Courchesne 2005). The brain size is reduced at birth compared to neuro-typical controls, but radically growths the first years to reach, in the majority of cases, a normal size at puberty (Redcay and Courchesne 2005; Xiao et al. 2014; Courchesne, Campbell, and Solso 2011). MRI analyses pointed more specifically to abnormalities in the size of the brain structures. They highlighted the increase of the white matter in early life (Courchesne, Campbell, and Solso 2011; Carper and Courchesne 2005; Hazlett et al. 2005; Herbert et al. 2004). Abnormalities in gyrus formation on the cerebral cortex were observed, with an increase of the cortical folds or an increase of the gyrus size (Wallace et al. 2013; Ecker et al. 2016). A recent meta-analysis on a large cohort of patients with ASD refuted previous studies proposing a relationship between the size of the corpus callosum and ASD (Lefebvre et al. 2015). At the neuronal organisation level, a modification of cortical columns was reported with an increase of the number of columns, combined with fewer cells. This structural modification describes abnormal circuitry without significant difference in neuronal density in cerebrum cortex (M. F. Casanova et al. 2002; M. Casanova and Trippe 2009).

Other brain structures appeared to be concerned. The volume of the amygdala is increased in children with ASD, in comparison with neuro-typical controls (Nordahl et al. 2012; Schumann et al. 2004). The number of neurons is increased in the prefrontal cortex while it is decreased in the amygdala (Lai et al. 2015; Courchesne, Campbell, and Solso 2011). Interestingly, these two structures are strongly associated with social interactions (see II.C.1).

II.A.1. *Gene expression*

The observed impairments in brain development may be related to the spatiotemporal gene expression. Indeed, in non-pathologic conditions, the brain development depends on the accurate regulation of gene expression in the prenatal period and in infancy, as depicted in comprehensive spatiotemporal gene expression maps (Kang et al. 2011; Colantuoni et al. 2011). Berchtold and colleagues (2008) highlighted the modulation of gene expression during early age, but also in later age. They suggested the existence of a critical period for the formation of neural circuitry, and of a gender difference in gene expression in the brain (Berchtold et al. 2008). For ASD patients, the dysregulation of gene expression in young brain might lead to brain atypical development. For example, Chow and colleagues (2012) showed that several cellular pathways leading to cell multiplication and cell differentiation are dysregulated in the prefrontal cortex (PFC) of ASD toddlers (Chow et al. 2012). Several genes associated with ASD, such as Neuroligin 4 (*NLGN4)*, Neurexin1 (*NRXN1)* or *SHANK3*, display different expression profiles during development (**Figure 5**). Mutations in these genes impact the formation of early neural circuits (M. W. State and Šestan 2012).

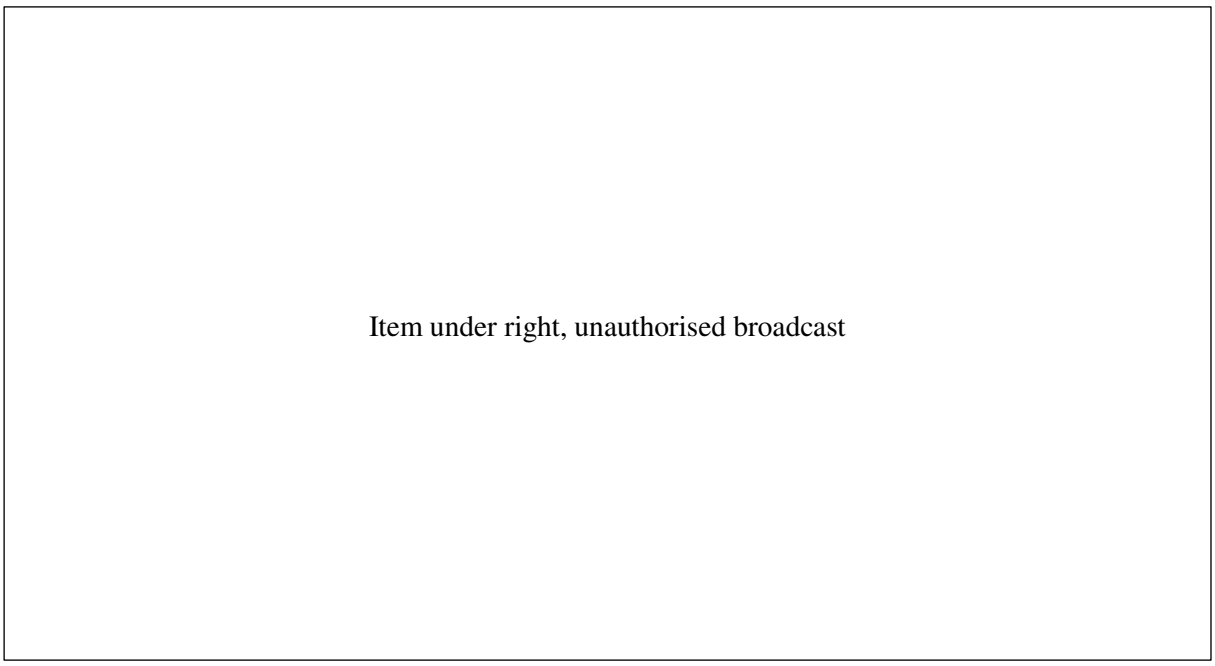

Figure 5: Developmental neurobiology of ASD risk genes*. (A) A subset of genes associated with ASD are expressed in neurons. (B) Expression profiles of several genes associated with ASD during development of the human neocortex (from State & Šestan, 2012).*

II.B. *Imbalanced Excitatory/inhibitory synapses*

Many genes associated with ASD are expressed in synaptic areas or have an impact on synaptic transmission. For example, mutations in *FMR1*, the gene associated with fragile X syndrome, impact the expression of NOS1 (nitric oxide synthase 1), that generates the neurotransmitter NO, in the cortex during the foetal period, but also the expression of N-methyl-D-aspartate (NMDA) glutamate receptor 1 (GluN1) and Dopamine receptor 1 (D1R) (H. Wang, Kim, and Zhuo 2010; Soden and Chen 2010; Kwan et al. 2012). These observations reveal impairments in synaptic transmission.

A precise balance between excitation and inhibition (E:I) inputs in neural circuits is necessary for neuro-typical brain development and functions (Isaacson and Scanziani 2011). Several mechanisms lead to the perturbation of the E: I balance, such as reduction of neurogenesis and synapse formation, and deficit of receptors at excitatory synapses, like glutamate receptors, or at inhibitory synapses, like γ-Amino, butyric acid (GABA) receptors. We discuss hereafter the relationship between E:I balance and ASD-associated genes.

A hypothesis relates the physiological and behavioural defects in patients with ASD and in rodent models with impairment in E:I balance (Rubenstein and Merzenich 2003; Gogolla et al. 2009; S. B. Nelson and Valakh 2015; T Bourgeron 2007). The E:I balance is impacted in ASD cases, with an increase of neural excitation (Rubenstein and Merzenich 2003). Using optogenetic techniques in mouse models, Yizhar and colleagues (2011) showed that an activation of excitatory synapses leads to impairments in social interactions (Yizhar et al. 2011). Furthermore, a decrease of GABAergic signalling is often observed in patients, but also in ASD mouse models which lead to a rise of intracellular calcium and impairment in synaptic transduction (Cellot and Cherubini 2014). Nevertheless, other studies showed opposite observations with an increase of GABA inhibition (Bertone et al. 2005; Gonçalves et al. 2017). Altogether, impairments in ASD seem to be related to excitatory and inhibitory synapses, and the imbalance between the two is an attractive hypothesis based on neurobiological observation. However, it is difficult to validate this hypothesis due to the variation of the E:I ratio according to the cell type and the brain structure (Xue, Atallah, and Scanziani 2014).

Some genes associated with ASD are linked to excitatory synaptic impairments, like the *Shank* family, or to inhibitory synaptic impairments, like *NLGN* and *GABRb* (Tabuchi et al. 2007; Földy, Malenka, and Südhof 2013; Rothwell et al. 2014; DeLorey et al. 2008). Therefore, the implication of ASD genes, in either excitatory or inhibitory synapses, shows that the synaptic impairment can be due to dysregulations on both sides. However, identical mouse models can reveal impairments in excitatory or inhibitory input according to the study, complicating the understanding of the impact of the E:I balance in ASD (see IV.B.2.b).

II.C. *Pathways associated with ASD core symptoms*

Depending on the brain structure, the E:I imbalance can be local, i.e. limited to a brain nucleus, or distant, i.e. in cortico-striatal loop (Belmonte et al. 2004). These two types of imbalance affect several brain pathways including those involved in ASD: the social-associated pathways, also called social brain, and the stereotyped-associated pathway. However, the exact implication of each structure in social impairment or stereotyped behaviour still needs further investigations. The following parts are adapted from (see Annexes III) (Ferhat et al. 2017).

II.C.1. *Social pathway*

The brain structures associated with social cognition, often termed "social brain", comprise areas involved in perception (somatosensory cortices), emotions (amygdala), motivation (ventral striatum and tegmental area), decision-making and executive control (prefrontal cortex, PFC). However, behind this apparent specification, other brain structures are involved in different aspects of social behaviours and all structures interact together. Despite the new techniques of brain imaging (electro-encephalogram, MRI) in humans, the experiments on mice are more effective and the brain structures involved in social behaviours are more documented in mice than in humans. Furthermore, several mouse brain structures are considered homologous to human brain structures (Wise 2008; Karten 2015).

II.C.1.a. Sensory input

Social interactions are regulated by social signals, forming social communication. In mice, these signals include ultrasonic vocalisations (USV), odours, pheromones, tactile stimuli, involving whisking and body contacts, and visual signals using body postures (Latham and Mason 2004; Brennan and Kendrick 2006; Portfors 2007).

Appropriate social reactions depend, in first place, on a good acquisition of stimuli. The sensory perception is, therefore, the first step in the social brain. Several stimuli can be integrated like vision via eye and occipital visual cortex, auditory signal via ear and primary and secondary auditory cortex (Arriaga, Zhou, and Jarvis 2012), or odour information through the olfactory and vomeronasal system (**Figure 6**.A) (Matsuo et al. 2015). All these sensory inputs can be integrated at different levels, in the primary sensory cortex or in specific pathways.

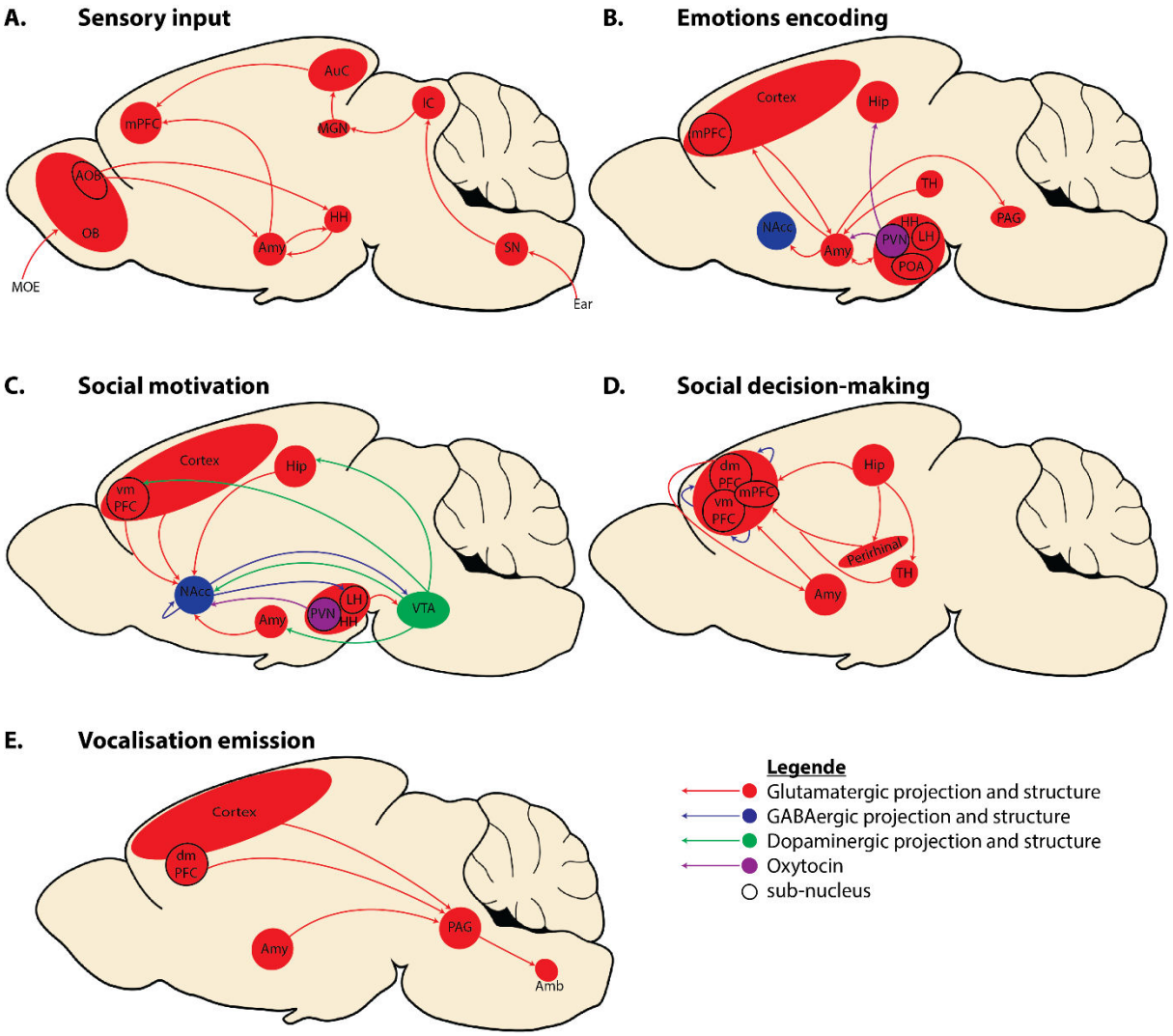

Figure 6: Schematic representation of interaction between structures for sensory input (A), Emotions encoding (B), Social motivation (C) and Vocalisation emission (D). *OB: olfactory bulb; AOB: Accessory olfactory bulb; PFC: prefrontal cortex; mPFC: median PFC; dmPFC: dorsomedian PFC; vmPFC: ventromedian PFC; Amy: amygdala; HH: hypothalamus; Auc: auditory cortex; MGM: medial geniculate nucleus; SON: superior olivary nucleus; IC: inferior colliculus; Hip: hippocampus; TH: thalamus; PAG: periaqueductal grey; NAcc: nucleus accumbens; PVN: paraventricular nucleus; LH: lateral hypothalamus; POA: preoptic area; VTA: ventral tegmental area; Perirhinal: perirhinal cortex; Amb: nucleus ambiguus*

In rodents, when the animal detects a scent, the olfactory bulb (OB) and the accessory olfactory bulb (AOB) send the information to several nuclei of the amygdala and several nuclei of the hypothalamus (Keverne 1999; Matsuo et al. 2015). After the detection of noise or vocalisation, the cochlear nucleus is activated. It sends information to the auditory cortex through the superior olivary nucleus, inferior colliculus and medial geniculate nucleus (Figure 6.A). Amygdala and different sensory cortices send information to the PFC for appropriate responses (see II.C.1.d).

II.C.1.b. Emotions encoding

Following the appropriate stimulation and the integration of stimulus, the amygdala and hypothalamus are activated (Figure 6.B). The amygdala is a complex structure located in the temporal lobe and contains several nuclei playing a crucial role in valence processing (positive or negative event), in emotion-based social interactions, such as arousal, freezing and aggression (Maren 2003). The medial amygdala is activated by positive or negative valence especially in social recognition (Bosch and Neumann 2012). It receives projections from different brain structures to integrate stimuli, as the AOB (Keverne 1999; Matsuo et al. 2015) and the pre-optic area (Popik and van Ree 1991). This last structure, a sub-nucleus of hypothalamus, is strongly associated with mating and social reward (McHenry et al. 2017). The basolateral amygdala (BLA) is involved in affection and in close social interaction and receives input from the cortex and the thalamus. Composed by glutamatergic neurons, the BLA projects to several brain structures involved in social interaction, entorhinal cortex (involved in the assessment of familiarity in stimuli), PFC (social hierarchy), hypothalamus, nucleus accumbens (NAcc), the mid-brain reticular formation and the periaqueductal gray (PAG) (Price 2006). The activity of the amygdala is modulated by reciprocal connections with the hypothalamus. The medial amygdala projects to the hypothalamus, sending information about the valence of the stimuli, while the hypothalamus projects back on the medial amygdala and the central amygdala to switch between aggressive and affiliative responses (Veening et al. 2005).

The hippocampus plays also an important role in social memory and emotion. This structure is associated with the encoding of declarative memory (Squire and Wixted 2011) and lesions in Cornu Ammonis (CA) one (CA1) or three (CA3) reveal impairment in learning and memory. However, little is known about the CA2, which has recently been associated with social memory processing (Hitti and Siegelbaum 2014).

The hypothalamus integrates stimuli from the external environment, but also from the internal state (Kruk, De Vos-frerichs, and Van Der Poel 1979; Matsuo et al. 2015). Especially, the paraventricular nucleus (PVN) is strongly associated with management of social stimuli. A sub-population of neurons in the PVN, the magnocellular neurons, releases oxytocin and vasopressin locally (Swanson and Sawchenko 1983), but also in other brain structures, like the amygdala, previously described, and the NAcc. Oxytocin, playing a central role in reproduction, was associated with social memory by modulating the firing of hippocampal inhibitory neuron (Ferguson et al. 2000; Owen et al. 2013).

II.C.1.c. Social motivation

Social motivation is directly linked to the reward circuit. A social interaction can be rewarding for an individual and can be pleasurable or aversive. The NAcc is an important structure for integration and release of this information.

The NAcc is part of the striatum with the putamen and the caudate, especially the ventral striatum, and is included in the mesocorticolimbic dopamine system, also called reward circuit. This system is associated with goal directed behaviours and motivation, as well as higher cognitive functions such as learning and memory. Dysfunctions of this circuitry can lead to different forms of addictions. The reward circuit reinforces social behaviours and social motivation (Chevallier et al. 2012) and is involved in the mediation of social motivation, mating, maternal behaviour and formation of pair bonds (Kohls et al. 2013; Robinson, Zitzman, and Williams 2011).

The reward circuit is composed by three main structures: the ventromedial PFC (vmPFC), the NAcc and the ventral tegmental area (VTA) (Figure 6.C). Nevertheless, these three structures are not isolated. The NAcc is composed by GABAergic neurons, the medium spiny neurons (MSN), which project on the VTA and the hypothalamus. It receives glutamatergic inputs from the vmPFC, the cortex, the BLA and the hippocampus. The VTA projects dopaminergic axons on MSNs, but also on vmPFC, BLA and hippocampus and receives glutamatergic inputs from the lateral hypothalamus (Russo and Nestler 2013). Therefore, a control loop is present with a GABAergic link from NAcc to VTA and a dopaminergic link from VTA to NAcc. The MSN, which release GABA in the VTA, express two types of dopamine receptors, D1R and D2R. At the cellular level, D1R activate adenylate cyclase (AC) while D2R inhibit AC. The MSN are so-called D1-MSN or D2-MSN and go through the ventral pallidum via direct projection (D1-MSN) or indirect (D2-MSN). Historically, the direct pathway promotes social behaviour (reward) and the indirect pathway inhibits social behaviour (Fernández, Mollinedo-Gajate, and Peñagarikano 2018). However, recent investigations revealed that MSNs can express D1R and D2R simultaneously, which complicates the classical “dichotomy” of NAcc (Kupchik et al. 2015). Furthermore, D1- and D2-MSNs receive oxytocin input from the PVN. Recent investigations in social behaviour support the implication of reward circuit with an activation of dopaminergic neurons in the VTA followed by MSN, mainly D1-MSNs (Gunaydin et al. 2014).

II.C.1.d. Social decision-making

The PFC is involved in different cognitive processes, such as reinforcement (see II.C.1.c), working memory, attention and decision-making, especially during social interaction. The PFC is mainly composed by glutamatergic neurons and GABAergic interneurons (Schubert, Martens, and Kolk 2015).

The PFC is usually separated in three parts: dorsomedian (dmPFC), ventromedian (vmPFC) and medial (mPFC) based on human PFC homology (Bicks 2015). However, the number of sub-nucleus of PCF is subject to debate. These areas interact together. The mPFC organizes, among others, the temporal sequences of actions, taking into account the rapid changes in the social environment and in the emotional state of the animal (Fuster 2008). The dmPFC, also called the anterior cingulate cortex, is one of the major structures implicated in the establishment and maintenance of social hierarchy and dominance among littermates. It projects axons on the BLA (F. Wang, Kessels, and Hu 2014). The vmPFC is involved in the organisation of cooperative relationships, valuing rewarding social interaction and regulating emotional reactions (Rilling and Sanfey 2011). The vmPFC is linked to the amygdala as a part of reward circuit. The hippocampus projects axons on PFC, especially on vmPFC, through direct pathway and indirect pathway, via thalamus or perirhinal cortex (Eichenbaum 2017). Connexions between these two structures support functions in episodic and long-term memory.

II.C.1.e. Vocalisations emission

Rodents, as several mammals, use vocalisations, among other signals, to communicate. Mice emit a variety of ultrasonic vocalisations (USVs) in different contexts (Ferhat et al. 2016). USVs, with a frequency range between 30kHz and 110kHz (Heckman et al. 2016), are considered innate with very little evidence of learning (Hammerschmidt et al. 2012; Portfors and Perkel 2014). The complete pathway, toward the emission of USVs, is not completely known. The amygdala and the dmPFC are two structures implicated in control of type of USVs emitted, but not in ability of emission, by a regulation of arousal and emotion (Figure 6.D). Amygdala and dmPFC project axons to the PAG in the midbrain. The PAG innervates the nucleus ambiguus in the brainstem. This structure innervates the respiratory premotor nuclei and the cranial nerve nuclei which directly innervates the larynx (Arriaga and Jarvis 2013). Furthermore, a direct cortical projection to the nucleus ambiguus has been highlighted, which can support the idea of voluntary control of emission (Arriaga and Jarvis 2013).

II.C.2. *Stereotyped pathway*

In humans, stereotyped behaviours take different forms (see I.B) and seem to be related to the corticostriatal circuits and basal ganglia. Stereotyped behaviours and restricted interests vary in kind, but also in degree (Langen, Durston, et al. 2011). Stereotyped behaviours occur in mice under different forms: excessive self-grooming, repetitive climbing, rearing or jumping in specific locations of the cage, and atypical digging in the bedding.

Several studies showed the involvement of the basal ganglia in the modulation of repetitive or stereotyped behaviours. The basal ganglia usually include the striatum (caudate nucleus and putamen),

the pallidum (globus pallidus), the ventral pallidum, the subthalamic nucleus and the substantia nigra (Ikemoto, Yang, and Tan 2015). All these structures are interconnected, and they are strongly connected to the cortex, to form corticostriatal loops (CSL) (Alexander, DeLong, and Strick 1986). Other structures, such as hippocampus or amygdala, allow a modulation of the CSL activation (Bachevalier 1996).

The CSL is involved in the control of movement and motor coordination via two pathways: the striatonigral "direct pathway" and the striatopallidal "indirect pathway". In the direct pathway, the cortex, with glutamatergic neurons, and the substantia nigria compacta (SNc), with dopaminergic neurons, activate dorsal striatal MSNs (Figure 7). MSNs project GABAergic axons on globus palidus intern (GPi) which activates thalamus via GABAergic connexions. The thalamus is connected to the motor cortex via glutamatergic synapses. In the indirect pathway, MSNs project through globus palidus extern (GPe). The GPe inhibits the subthalamic nucleus (STN) that projects glutamatergic synapses to the GPi and SNr. These two pathways have antagonist effects on movements. The direct pathway promotes movements by activation of the thalamo-cortical projection, and the indirect pathway inhibits movements by inactivation of the thalamo-cortical projection. A subtle E:I balance is required and a dysfunction could generate impairment in movement and stereotyped behaviour (Langen, Kas, et al. 2011; Langen, Durston, et al. 2011). Impairments in direct and indirect pathways could produce stereotyped behaviours in mice, but also in humans. For instance, several mouse models mutated in ASD risk genes display stereotyped behaviours (see IV.B). The type of stereotyped behaviours observed seems to be linked to the type of impairments in this circuit (Langen, Durston, et al. 2011).

The cortico-striatal circuitry can be manipulated by targeting agents, which bind to inhibitory GABA receptors or to excitatory glutamate receptors (e.g. Presti et al. 2004). Dopaminergic drugs can also modulate stereotypic behaviours by stimulating the direct pathway or inhibiting the indirect pathway. Furthermore, the dorsal striatum, associated with motor functions, and the ventral striatum, NAcc, associated with reward and cognitive functions, are two structures near each other, and studies shows the inter connection between these two structures, from ventral to dorsal (Haber, Fudge, and McFarland 2000; Sesack and Grace 2010). This interconnection allows the modulation of information in the different cortico-striatal circuits (Haber, Fudge, and McFarland 2000) and could influence the presence of motor stereotyped behaviours, but also the presence of cognitive repetitive behaviours (Table 1) (Groenewegen 2003). This observation reinforced the idea of implication of striatum in ASD at different levels (Fuccillo 2016).

Item under right, unauthorised broadcast

Figure 8: Circuit diagram for direct (left panel) & indirect pathways (right panel)*. Ach, acetylcholine; DA, dopamine; Glu, glutamate; Enk, enkaphalin; SP, substance P. Nuclei: SNc, substantia nigra pars compacta; SNr, substantia nigra pars reticulata; GPe, extern globus pallidus; GPi, intern globus pallidus; STN, subthalamic nucleus; VL, ventral lateral nucleus; VA, ventral anterior nucleus* (Leisman, Melillo, and R. 2013).

III. *SHANK* gene: structure and implication

In the following part, we will mainly focus on the genetic causes of ASD. We will discuss about SH3 and multiple Ankyrin repeat domains (*SHANKs*) gene family that includes three members: *SHANK1*, *SHANK2/PROSAP1* (hereafter *SHANK2*) and *SHANK3/PROSAP2* (hereafter *SHANK3*). This gene family is strongly associated with ASD and was identified by Fluorescent In Situ Hybridization (FISH) analysis and whole genome sequencing (Durand et al. 2007). Following a meta-analysis on patients with mutations in the *SHANK* gene family, almost 1% of ASD patients display a mutation (*SHANK1*: 0.04%; *SHANK2: 0.17%; SHANK3: 0.70%*) and 2% of patients with ASD and ID display a mutation in *SHANK3* (Leblond et al. 2014). These genes encode scaffolding proteins in the post-synaptic density (PSD) of glutamatergic synapses. Because of their scaffolding function at the synapse, SHANK proteins make the link between synaptic receptors, adhesion proteins, signalisation proteins and cytoskeleton. We will describe the different domains composing SHANK proteins as well as the main interactions with other proteins.

III.A. *Structure of genes and proteins*

III.A.1. *Structure of the Shank genes*

In the human genome, *SHANK1* is located on chromosome 19 in position 19q13.33 and the mRNA measures 6.6 kb. This gene contains 23 exons and displays two promoters leading to, at least, two isoforms (*Shank1*a-b; Figure 8). *SHANK2* is located on chromosome 11 in position 11q13.3 and the mRNA measures 7.2 kb. There are 25 exons and three promoters for, at least, three distinct isoforms (*Shank2*a-b-e; Figure 8). The last member of *SHANK* family, *SHANK3,* is located on chromosome 22 in position 22q13.3 and the mRNA measures 7.1 kb. This gene displays 22 exons with six promoters, which generate at least six main isoforms (*Shank3*a-f; Figure 7; reviewed in Jiang and Ehlers 2013; Sala et al. 2015).

The organisation of the *Shank* gene family in the mouse genome is very similar to the one in the human genome. *Shank1* and *Shank2* are located on chromosome 7, respectively in 7B3 and 7F5. *Shank1* displays 23 exons and two main promoters and *Shank2* displays 25 exons with three promoters. *Shank3* is located on chromosome 15, in position 15E3, and has 22 exons with, at least, six promoters.

Little is currently known on the expression of the different isoforms for *Shank1* and *Shank2*, *Shank3* being more studied. According to Wang and colleagues (2014), the presence of multiple intragenic promoters generate six isoforms, *Shank3*a-f (X. Wang et al. 2014). Furthermore, alternative

splicing is present between exons 10 and 12 (five alternative splicing), between exons 18 and 20 (three alternative splicing) and between exons 21 and 22 (four alternative splicing). All isoforms display different expression profiles, in the spatial scale, but also in the temporal domain (see III.A.4).

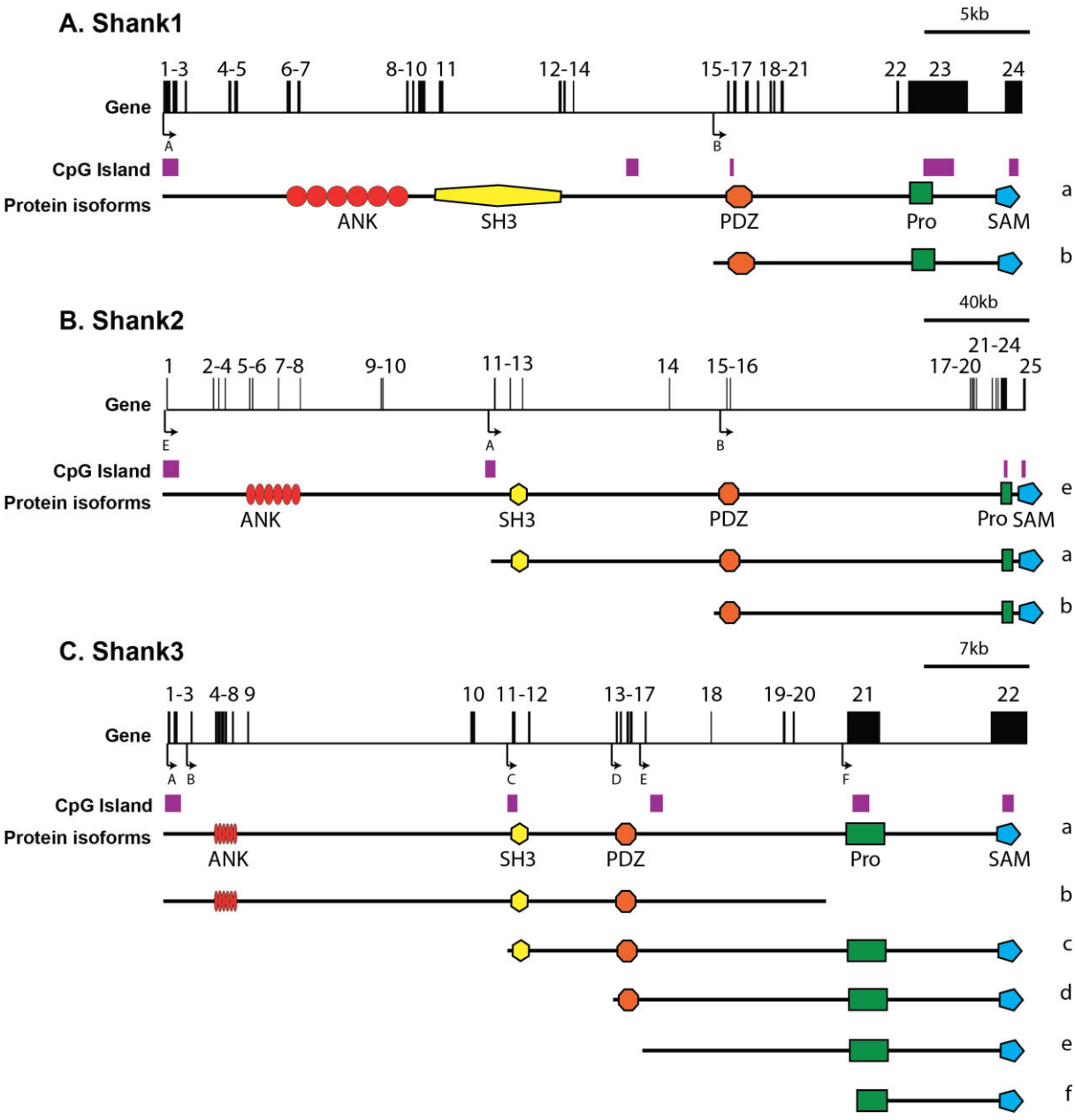

Figure 8: Schematic representations of Shank1 (A), Shank2 (B) and Shank3 (C) genes and proteins in the mouse. *Gene: Black squares are exons. Black arrows are intragenic promoters. Purples squares are position of CpG islands Protein: black lines are amino acids sequence; geometrical figures are domains. The protein domains are aligned with the corresponding exons. The diagram was drawn on the basis of the information contained at the National Centre for Biotechnology Information (NCBI) and Uniprot database.*

III.A.2. *Structure of the proteins*

The three *SHANK* genes encode for three main proteins, which present structural similarities. Each SHANK protein contains five conserved domains, from N-terminal to C-terminal: the Ankyrins (ANK) domain, the Src homology 3 (SH3) domains, the PSD-95/Disc-large/ZO-1 (PDZ) domain, the proline (Pro) rich domain and the sterile alpha motif (SAM) domain. These domains allow interactions with more than thirty synaptic proteins such as receptors, other scaffolding proteins, synaptic anchor proteins or cytoskeleton proteins (Kreienkamp 2008). Based on protein-protein interaction (PPI) database (Biogrid database; thebiogrid.org), the number of proteins directly interacting with SHANK can reach 170 for Shank3 in mice. Here, we will describe the main proteins interacting with different Shank domains.

III.A.2.a. Ankyrin (ANK) domain

The first domain found in N-terminal position of SHANK is composed by six Ankyrin motifs repetitions (Figure 8). It interacts with α-FODRIN, an actin-based cytoskeleton protein, allowing indirect interaction with actin cytoskeleton. The SHARPIN (SHANK Associated RH domain interactor) protein can also interact with the ANK domain. SHARPIN is mainly known as a regulator of the immune and skin inflammatory responses (Figure 9).

III.A.2.b. Src homology 3 (SH3) domain

The SH3 domain, second domain in N-terminal, is a short amino-acid sequence allowing indirect interaction with actin-based cytoskeleton via the DENSIN-180 (Figure 8). Many interactions, direct or indirect, with ion channels were observed. Indeed, GRIP1 (Glutamate receptor-interaction protein), a protein containing seven PDZ domains, allows an indirect connection between Shank proteins and sub-units of AMPA (α-amino-3-hydroxy-5-methyl-4-isoxazolepropionic acid) receptor, GluA1-GluA2 (Brückner et al. 1999; Dong et al. 1997; Sheng and Kim 2000). Furthermore, a voltage-dependent calcium channel, CaV1.3, directly interacts with the SH3 domain of Shank proteins (Figure 9) (Zhang et al. 2005).

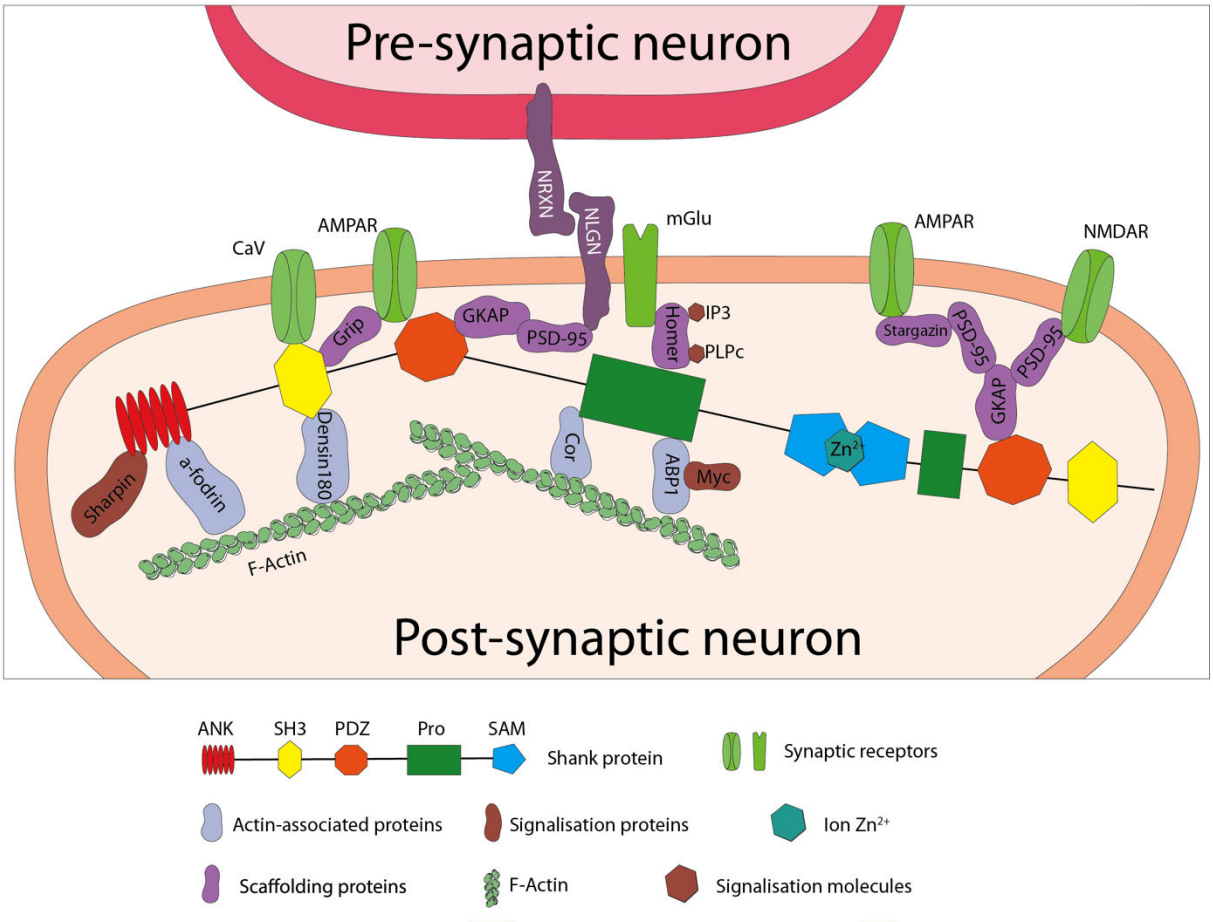

Figure 9: Schematic representation of the partial proteins interacting with Shank protein at the post-synaptic density of glutamatergic synapses. *CaV: Calcium-voltage gate; AMPAR: α-amino-3-hydroxy-5-methyl-4-isoxazolepropionic acid receptor; NMDAR: N-Methyl-D-aspartic acid or N-Methyl-D-aspartate receptor; mGlu: metabotropic glutamatergic receptor; NRXN: Neurexin; NLGN: Neuroligin; Grip: Glutamate receptor-interaction protein; GKAP: Guanylate Kinase-Associated Protein; PSD-95: Post-synaptic density protein 95; Cor: Cortactin; IP3:Inositol triphosphate; PLPc: Phospholipase C.*

III.A.2.c. PSD-95/Disc-large/ZO-1 (PDZ) domain

This domain mainly interacts with other scaffolding proteins like Guanylate Kinase-Associated Protein (GKAP)/SAPAP (Figure 9). GKAP is an abundant protein in PSD and allows indirect interaction between the PDZ domain of SHANK3 and the scaffolding protein PSD-95 (Boeckers et al. 1999). Interestingly, the bond between GKAP and SHANK is modulated by GKAP isoform. Indeed, GKAP is associated with SHANK by a c-terminal domain (GQSK sequence) and one isoform of GKAP, GKAP1b, does not display this sequence. An over-expression of this isoform seems to inhibit the synaptic localisation of SHANK.

SHANK, via the PDZ domain, also interacts with different glutamatergic receptors. Direct interaction between PDZ and AMPA receptors are present especially with GluA2 (Uemura, Mori, and Mishina 2004) and GluA1 by a C-terminal motif (Uemura, Mori, and Mishina 2004). Furthermore, direct interaction seems to be involved between SHANK PDZ domain and mGLUR1 (metabotropic

glutamate receptor 1), but this observation is still unclear in vivo (Tu et al. 1999). But, the majority of interactions with glutamatergic receptors are indirect via the PSD-95 and GKAP scaffold proteins and its multiple PDZ domains. PSD-95 interacts directly with sub-unit of NMDA receptor (N-methyl-D-aspartate receptor), GluN1-GluN2A-B or indirectly with sub-units of AMPAR by the STARGAZIN protein (L. Chen et al. 2000). Furthermore, PSD-95 directly interacts with the intracellular domain of Neuroligin (NLGN) protein. Extracellular domain of NLGN protein interacts with Neurexin (NRXN), located at the presynaptic membrane, to form a synaptic adhesion complex.

III.A.2.d. Proline - rich domain (Pro)

The Proline rich domain is the longest domain in SHANK proteins with more than 1000 residues (Figure 8 & Figure 9). The beginning and the end of this domain are very rich in proline and also serine. Three main proteins interact with this domain: HOMER, CORTACTIN and ABP-1.

HOMER is a scaffolding protein, interacting with several proteins by an EVH1 domain, which recognises a proline-rich motif, the PPXXF (Proline-Proline-X-X-Phenylalanine) motif. By this motif, HOMER proteins interact with SHANK proteins. Furthermore, HOMER proteins interact with proteins mGLUR1, mGLUR5, and second messenger PLPc (phospholipase C) and IP3 (inositol 1, 4, 5-triphosphate). These interactions, with several effectors of cellular signalisation, reveal the central role of HOMER proteins, and, by extension, SHANK proteins, in signal transduction. Indeed, HOMER impacts the intracellular calcium release, the synaptic transmission (Tu et al. 1999) and the structural and functional organisation of the dendritic spine (Sala et al. 2001).

The proline-rich domain also interacts with CORTACTIN proteins. CORTACTIN is a F-actin-binding protein and is involved as an actin regulatory protein (Naisbitt et al. 1999). In response to glutamate stimulation, CORTACTIN recruits and allows the polymerisation of actin-based cytoskeleton. The interaction SHANK/CORTACTIN seems to be crucial for the synaptic cytoskeleton dynamism and links the synaptic cleft and the dendritic spine.

The third main protein partner with proline-rich domain is the Abelson tyrosine kinase interacting (ABP1) protein. This kinase interacts with F-actin to allow the organisation of dynamic post-synaptic cytoskeleton (Qualmann 2004). It also interacts with the transcription factor complex MYC/MAX by a translocation in nucleus. In this last case, ABP1 is implicated in spine maturation and synapse morphology (Proepper et al. 2007).

III.A.2.e. Sterile alpha motif (SAM) domain

The last domain in C-terminal position of SHANK is the SAM domain (Figure 8). This domain seems to be necessary for the synaptic targeting of SHANK proteins and the recruitment as a scaffolding protein (Boeckers et al. 2005). Furthermore, several studies showed a homo-multimerisation of SHANK proteins through the SAM domain. In this case, the two SAM domains interact through a Zn^{2+} ion and this ion is crucial for the recruitment of SHANKs and their binding (Figure 9) (Y. Lee, Ryu, et al. 2017; Grabrucker 2014; E.-J. Lee et al. 2015).

III.A.3. *Implication in neurons*

As we saw above, SHANKs/Shanks proteins interact with several glutamatergic receptors at the PSD of glutamatergic synapses. Glutamate is the major excitatory neurotransmitter in the nervous system.

Two mains types of glutamatergic receptors are associated with Shank, fast acting ionotropic receptors, composed by AMPAR, NMDAR and Kainate receptors, and slow acting metabotropic receptors, composed by two main groups of mGluR. The ionotropic receptors are activated by glutamate neurotransmitter and let flowed in sodium ions (NA^{+}) through all receptors, and calcium ions (Ca^{2+}) through NMDAR, and let potassium ions (K^{+}) flow out (Kandel et al. 2013). The activation of these receptors can be modulated by cytosolic protein, like Cornichon Family AMPA Receptor Auxiliary Protein (CNIH) which modulates the type of sub-unit and activation of AMPAR (Herring et al. 2013). This ionic input triggers membrane depolarization in post-synaptic area and allow signal propagation (**Figure 10**) (Dingledine and McBain 1999). The rise of intracellular Ca^{2+} concentration also activates shared signalling pathway with metabotropic receptors (Beaulieu and Gainetdinov 2011).

Two main groups of metabotropic receptors are present, Group I composed by mGluR1 and mGluR5, and Group II composed by mGluR2 and mGluR3. They regulate the degree of neurotransmission by modulating the expression of proteins at the synapse. The group I is associated with a Gq protein that activates PLPc and allows calcium ions to come out from the endoplasmic reticulum. The combination of Ca^{2+} and PLPc activates the protein kinase C, phosphorylating and regulating downstream proteins. The mGluR group I also activates an intracellular mTOR signalling pathway. The Phosphoinositide 3-kinase (PI3K) activates the protein kinase B (PKB). In turn, PKB activates mTOR, a protein inhibiting or activating different transcription factor (Gladding et al. 2009). The receptor mGlur5 is a promising target for Fragile X syndrome target (Pop et al. 2014).

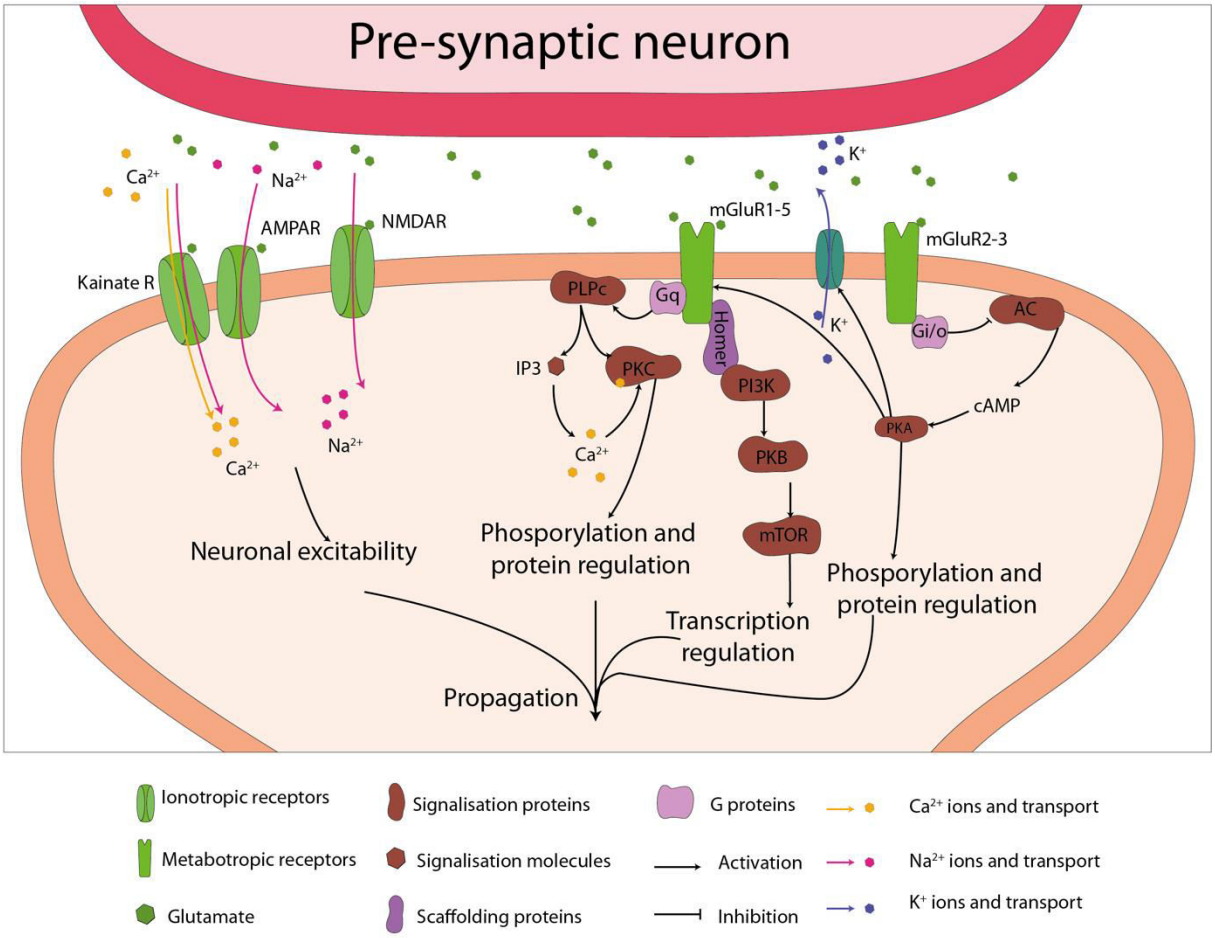

Figure 10: Schematic of interaction of glutamatergic receptors at the post synaptic density of glutamatergic synapses. *AMPAR: α-amino-3-hydroxy-5-methyl-4-isoxazolepropionic acid receptor; NMDAR: N-Methyl-D-aspartic acid or N-Methyl-D-aspartate receptor; mGlu: metabotropic glutamatergic receptor; PLPc: Phospholipase C; IP3:Inositol triphosphate; PKC: Protein kinase C; PI3K: Phosphoinositide3-kinase; PKB: Protein kinase B; AC: Adenylate cyclase; PKA: Protein kinase A; cAMP: cyclic adenosine monophosphate;Ca2+: calcium ions; NA2+: sodium ions; K+: potassium ions.*

The group II is associated with Gi/o protein. This G protein inhibits adenylate cyclase and reduces the cytosolic concentration of cyclic adenosine-monophosphate (cAMP), a signalling second messenger. The reduction of cAMP generates among other a reduction of activation of protein kinase A (PKA) (Yin and Niswender 2014). In normal condition, PKA allows phosphorylation and regulation of several proteins, including mGluR5 especially in D2-MSN (**Figure 10**) (Uematsu et al. 2015). PKA also allows activation of potassium channels (K^+ output) and inhibition of Ca^{2+} channels (Niswender and Conn 2010). The shank protein interacts and maintains these glutamatergic receptors at the synapse.

Interestingly, through the implication on cell signalisation, Shank have an important role in neurons expressing glutamatergic and other receptor, like dopamine in striatum, due to the shared signalling pathway to mediate information in post-synaptic compartment (Beaulieu and Gainetdinov 2011). Furthermore, due to the direct or indirect interaction with the glutamatergic receptors,

SHANKs play an important role in upholding the excitatory transmission through the synapse. They also have a central function in the formation of the synapse and the maintenance of the synapse reinforced by the direct and indirect interaction with Neuroligin and actin cytoskeleton (Sala et al. 2015; Naisbitt et al. 1999; Tu et al. 1999).

The first studies on SHANK showed the presence of these proteins, co-localizing with Cortactin, in cone growth in developing neurons (Du et al. 1998; Naisbitt et al. 1999; Durand et al. 2007). These observations validate the importance of SHANK protein in synaptic formation. A recent study shows the presence of *Shank3* in the nucleus, more specifically *Shank3*b (X. Wang et al. 2014), and the relation between *Shank3* mutation in mice and a histone deacetylase (HDAC2) that is strongly implicated in the transcriptomic regulation (Qin et al. 2018). These observations support the implication of SHANK in nucleus and in epigenetic modulation on neurons.

III.A.4. *Expression*

The three *SHANK* genes code for several mRNA splices and display complex transcription profiles. These profiles were mainly studied in mouse models; few studies were conducted in humans. Shank proteins are involved in neuronal functions, such as synaptogenesis, cytoskeleton, and glutamate receptor setting up (III.A.2); their expression varies according to the brain structures. Little information can be found about the expression of the different isoforms and their structure specificity for *Shank1* and *Shank2*. Most of the studies are based on the mouse brain for the expression of *Shank1* and *Shank2*.

Shank1 mRNA is strongly expressed in cortex, hippocampus (CA1 and CA3), amygdala, substantia nigra, and cerebellar Purkinje cells in the mouse brain (Figure 11.A-B) (Peça et al. 2011; Harony-Nicolas et al. 2015). In these regions, Shank1 is expressed close to the membrane in the PSD of neurons, but also in astrocytes (Collins et al. 2017). According to the NCBI database, two main isoforms of *Shank1* exist: *Shank1*a and *Shank1*b (Figure 8.A).

Three main isoforms of *Shank2* exist*: Shank2*e*, Shank2*a and *Shank2*b (Figure 8.B). *Shank2* is mainly expressed in cerebellar Purkinje cells, but can also be found in hippocampus, olfactory bulb and central gray and cortex in the mouse brain to a lesser extent (Figure 11.A-B) (Du et al. 1998; S. Lim et al. 1999; Peça et al. 2011; Harony-Nicolas et al. 2015). Shank2 is also present in the kidneys and the liver (Du et al. 1998; S. Lim et al. 1999; Uhlen et al. 2015). In subcellular level, Shank2 is found close to the membrane in the PSD.

Based on the literature, *Shank3* generates at least six main isoforms, *Shank3*a to f, related to the six intragenic promoters (Figure 8.C) (X. Wang et al. 2014). The expression of *Shank3* varies according to the brain regions and the age. When considering all isoforms together, *Shank3* is expressed in adult mouse brain in the olfactory bulb, the thalamus, the CA3 hippocampus, the

cerebellar granule cells, the cortex, and the striatum (Figure 11.A-B) (Boeckers et al. 1999; Peça et al. 2011). *Shank3* is also expressed in the heart, the spleen and at the neuro-muscular junction. In the brain, *Shank3* is highly enriched at cortico-striatal glutamatergic synapses. However, each isoform displays a specific expression pattern. *Shank3*a-b-e are strongly expressed in the striatum compared to other brain structures, while *Shank3*c-d are mainly expressed in cerebellar granule cells (X. Wang et al. 2014). Surprisingly, only Shank3b seems to be expressed in neuronal nucleus while the other isoforms are expressed close to the membrane in PSD. *Shank3* is expressed relatively at low levels at birth in the whole brain; then its expression increases after the post-natal day 10 (PND10) to get stable during adolescence and in adulthood in mice. In humans, based on the Allen brain atlas, the expression of SHANK3 starts to increase from 35-36 postconceptional weeks with a peak at four months after birth and remains stable while ageing (Figure 11.C).

Furthermore, *SHANK* genes contain several CpG islands that can regulate expression (Figure 8). The methylation profile of CpG in *SHANK1* and *SHANK2* seems to be similar between structure (Beri et al. 2007). Concerning *SHANK3*, CpG islands displayed a tissue-specific methylation profile, especially between cerebellum and the rest of the brain (Beri et al. 2007). These observations underlie a CpG-dependent regulation of the Shank expression. Furthermore, a post-transcriptional regulation of *SHANK3* is present, by micro-RNAs, playing a role on splicing and SHANK3 protein expression (Choi et al. 2015)

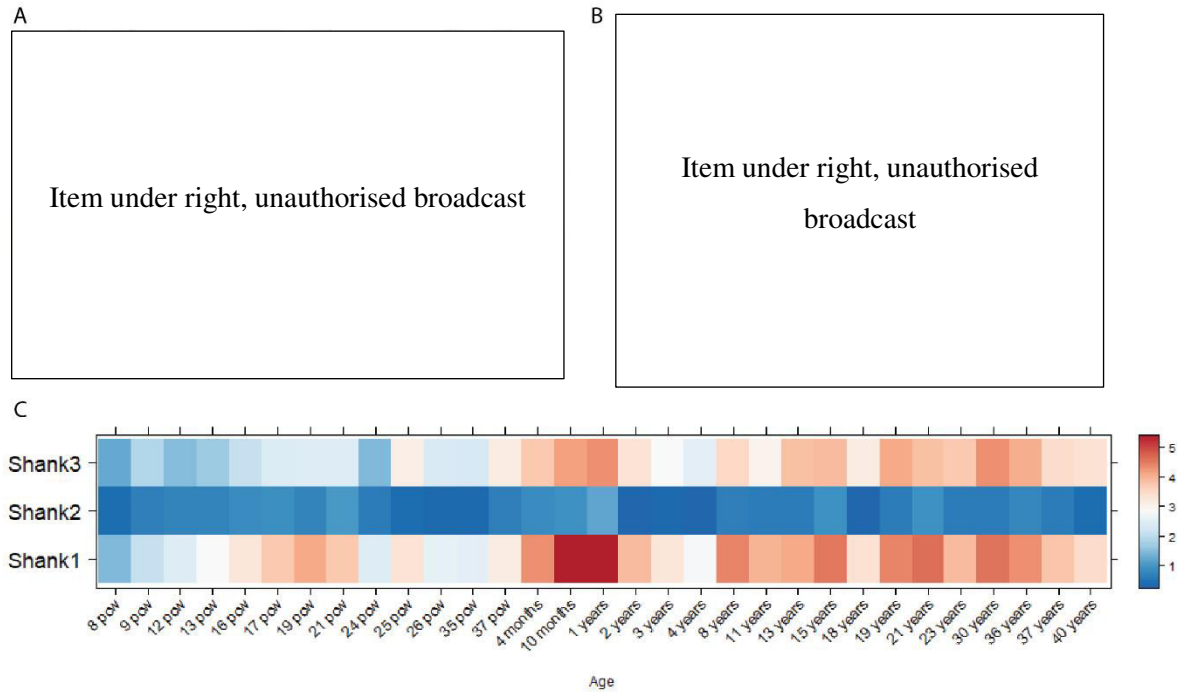

Figure 11: Expression of Shank proteins and RNAs in mice (A-B) and humans (C).
(A) mRNA in situ hybridization of coronal, medial parasagittal and lateral parasagittal mouse brain section from 5 week old mice of Shank family of genes (from Peça et al., 2011). (B) Relative Expression of Shank family of proteins in different structure of the brain from 5 week old mice (++++++ highest expression; - no detectable expression) (From Peça et al., 2011). (C) Representation of mean RNA expression of SHANK1, SHANK2 and SHANK3 in humans over age for the whole brain. PCW: post conception week; mos: months: yrs Years. Based on BrainSpan Allen brain atlas.

III.B. *Implication of Shank family in neuro-pathology*

III.B.1. *Heterogeneity of symptoms*

As stated in the previous part (see I.F), ASD phenotype may result from a complex interaction between genetic, environmental and epigenetic factors, but also a stochastic impact can be proposed (Huguet, Ey, and Bourgeron 2013). Few studies analysed the impact of the environment and epigenetics on the phenotype. However, we know that one mutation in the same gene can lead to different phenotypes in different genetics backgrounds (Guilmatre et al. 2014). All these aspects explain the important variability and heterogeneity in ASD, hence the use of the term *spectrum*.

As mentioned earlier, the *SHANK* family is widely involved in ASD. However, due to the numerous variants of the genes and existing mutations found in patients, *SHANK3* patients can display different psychiatric disorders and important heterogeneity (**Figure 12**.A) (Guilmatre et al. 2014). These observations imply an important heterogeneity between *SHANK3* patients, but also in the genetic background of these patients (Guilmatre et al. 2014). Interestingly, Guilmatre and colleagues (2014) described a possible evolution of the phenotype for different patients and noticed a worsening of this phenotype especially for individuals with Phelan-McDermid (Guilmatre et al. 2014).

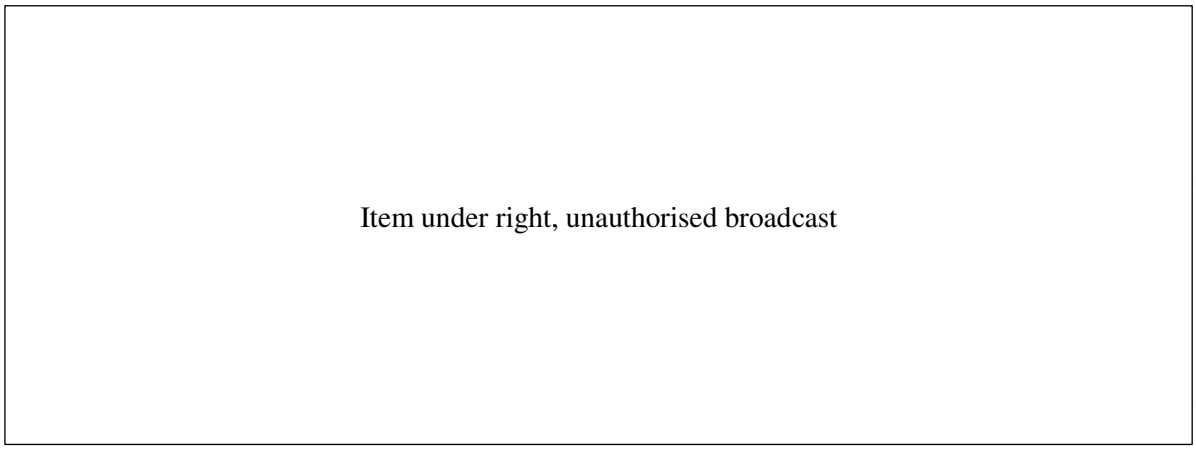

Figure 12: Clinical features and possible trajectories of patients carrying heterozygous deleterious mutations or copy number variations in the different SHANK genes.
(A) SHANK3 mutations/deletions/ translocations are associated with Phelan-McDermid syndrome (PMS), ASD, severe intellectual disability, and patients can develop schizophrenia, bipolar disorder, attention deficit with hyperactivity (ADHD), epilepsy and Alzheimer's disease. A regression is observed in childhood and from adolescence. (B) SHANK1 deletions and mutations are associated with high-functioning autism in males, and patients can develop schizophrenia (SCZ), bipolar disorder (BPD) and Alzheimer's disease (AD). (C) SHANK2 mutations/deletions/translocations are found in patients with ASD and mild to moderate intellectual disability (ID), and patients can develop schizophrenia, bipolar disorder and Alzheimer's disease. Plain lines indicate

phenotypic outcomes already associated with SHANK genes mutations and dotted lines show candidate disorders that should be screened for SHANK genes (from Guilmatre et al., 2014).

More recently, De Rubeis and associates (2018) documented a regression for 65% of *SHANK3* patients, characterized by a loss of language skills, motor skills, permanently or for a prolonged period of time in early childhood or in adolescence (De Rubeis et al. 2018). Interestingly, the case study of Serret and colleagues presented two patients with mutation in *Shank3* treated by lithium who displayed a reversal of language regression after two years of treatment (Serret et al. 2015).

SHANK1 and *SHANK2* are associated with several psychiatric disorders in patients (**Figure 12**.B-C). However, the genetic bases of this heterogeneity are still unknown and any information on heterogeneity will help to understand the genetic, environmental or epigenetic factors.

III.B.2. *Autism spectrum disorder*

Autism spectrum disorders are strongly associated with genetic variations (Geschwind 2009; Huguet, Ey, and Bourgeron 2013; Thomas Bourgeron 2016). Mutations in the *SHANK* gene family are significantly associated with syndromic or non-syndromic autism.

III.B.2.a. Association with non-syndromic autism

Mutations in the three members of the *SHANK* gene family can be deletions, duplications or SNV (Durand et al. 2007; Leblond et al. 2014, 2012; Pinto et al. 2010). All patients displayed heterozygous mutation on *SHANK* family, revealing a haploinsufficiency.

The main clinical signs associated with *SHANK1* mutations are ASD symptoms with a normal IQ (mean IQ=107). These mutations were *de novo* mutations, and they were found in 0.04% of patients with ASD, but never in control people (Leblond et al. 2014). Nevertheless, a recent study described a patient carrying a *SHANK1* mutation in exon 22 (T. Wang et al. 2016) displaying ASD with moderate IQ ($35 \leq IQ \leq 55$). This suggests that SHANK1 can also be involved in cognitive processes, and can be related with studies in mouse models (see IV.B.1).

De novo truncating mutations or *de novo* deletions in *SHANK2* affect 0.17 % of patients with ASD (Leblond et al. 2014). These patients appeared to present more severe symptoms than patients mutated in *SHANK1*. They displayed ASD or PDD- not otherwise specified with mild intellectual disability (ID; mean IQ=62 ± 17) and delayed development, like motor delay or late language development. Patients with *SHANK2* mutations often present comorbidities such as dysmorphic features, abnormal neurological examination, hypotonia, oral dyspraxia or cerebellar syndromes.

Mutations in *SHANK3* were found in 0.69 % of all patients with ASD and in up to 2.12 % of ASD patients with moderate to profound ID (mean IQ=31 ± 8) (Leblond et al. 2014). These mutations

can be deletions, duplications or truncating mutations. If the deletion is large, patients usually display PMS (see III.B.2.b). In the case of duplication, the patient can display Asperger syndrome (see III.B.2.c) and ADHD. In the case of non-syndromic ASD, in addition to ASD core symptoms, patients with a deletion might display developmental delay, severe language delay or epilepsy (Waga et al. 2011; Gauthier et al. 2010; Moessner et al. 2007; Leblond et al. 2014; Boccuto et al. 2013).

III.B.2.b. Phelan-McDermid syndrome

SHANK3 was the first and the most studied gene of the *SHANK* family due to its role in PMS, also known as 22q13 syndrome (Guilmatre et al. 2014; Phelan and McDermid 2012). The PMS is a severe genetic condition associated with ASD. PMS is characterized by a variety of clinical symptoms with heterogeneous degrees of severity, including hypotonia, global developmental delay, intellectual disability, absent or delayed speech and ASD core symptoms (Kolevzon et al. 2014; Leblond et al. 2014; Phelan and McDermid 2012). Several comorbidities can also appear, like seizures, kidney malformation and abnormalities, cardiac defects, gastro-intestinal disorders or dysmorphic features. These symptoms are associated with the genetic deletion of a large part of the long arm of chromosome 22, 22q13.3. The prevalence of this condition is uncertain, but PMS are present in 0.2-0.4% of patients with neurodevelopmental disorders (Tabet et al. 2017).

The modification of 22q13.3 region can be due to ring chromosome (14%), unbalanced translocations (7%), interstitial deletion (11%) or simple deletion (68%) (Bonaglia et al. 2011). In this case, the size of this deletion can vary between patients, ranging from less than 100 kb to 9 Mb. In the majority of cases, this deletion includes *SHANK3*. However, in rare cases, *SHANK3* is not deleted, suggesting the implication of other genes or an influence of other genes on *SHANK3* expression (Disciglio et al. 2014; Wilson et al. 2008). The deletion of some specific regions of 22q13 seems to be associated with different features like absence of speech, seizure or ophthalmic features (Tabet et al. 2017). Interestingly, Tabet and colleagues (2017) presented a family in which all children displayed a deletion in *SHANK3* (the first exons), mild to severe ID and an important speech delay. However, the mother displayed similar *SHANK3* deletion without cognitive dysfunction (Tabet et al. 2017). This observation suggests that compensatory mechanisms in neuronal pathway might help to reduce the severity of the phenotype observed. Further investigations in this direction could provide clues for novel treatments.

III.B.2.c. Asperger's syndrome

Asperger's syndrome is a form of ASD without ID and developmental delay. Surprisingly, Durand and colleagues showed a partial trisomy of the terminal part of the chromosome 22, including

SHANK3, in a boy with Asperger's syndrome (Durand et al. 2007). Another patient with Asperger's syndrome displayed a mutation in PDZ domain in *SHANK3* (Boccuto et al. 2013). Sato and colleagues (2012) showed three members of a family with Asperger's syndrome carrying a large deletion in *SHANK1* (Sato et al. 2012). To date, no mutation in *SHANK2* has been associated with Asperger's syndrome.

III.B.3. *Bipolar disorder*

Bipolar disorder is a psychiatric condition characterised by a fluctuation of the mood of the patient, with periods of depression and periods of elevated mood with manic-like behaviours. Among the studies analysing the association of *SHANK3* with bipolar disorders, all bipolar disorder patients displayed PMS, except in the study of Vucurovic and colleagues (Sovner, Stone, and Fox 1996; Ma Verhoeven et al. 2012; Verhoeven et al. 2013; Willemsen et al. 2011; Vucurovic et al. 2012; Denayer et al. 2012). The patient in the Vucurovic's study displayed a multiple deletion of at least six exons of *SHANK3,* as well as the genes *ACR, RAPL2B* and RPL23AP82. A recent case study proposed an effective therapy, using lithium treatment, to reduce mood disorders for PMS patients (Egger et al. 2017). A partial duplication of *SHANK2* was highlighted in a patient with bipolar disorder (Noor et al. 2014). Recently, four points mutations in *SHANK2* (c.3979G>A; c.2900A>G; c.4461C>T ;c.4926G>A) were found in patients with bipolar disorder and could be related to the disorder (Y. Yang, Wang, and Jiang 2018). To date, no link was made between *SHANK1* and bipolar disorder.

III.B.4. *Schizophrenia*

Schizophrenia is a psychiatric disorder characterised by delusions, hallucinations, difficulties in thinking and concentration as well as a lack of motivation (American Psychiatric Association 2013). In 2010, two *de novo SHANK3* mutations were found in patients with schizophrenic symptoms in two separate families. The first one was a R536W (after SH3 Domain) mutation and the second a R111X truncating mutation (Gauthier et al. 2010). The patients displayed ADHD, ID or seizure. Another study highlighted a significant association of five SNVs located in *SHANK1* promoter and reduced auditory working memory in schizophrenic patients (Lennertz et al. 2012). Recently, a mutation A1731S of *SHANK2* (in the proline-rich domain) was identified in four unrelated schizophrenic patients, but not in controls (Peykov et al. 2015).

III.B.5. *Alzheimer disease (AD)*

Several studies showed a possible link between AD and the expression of *SHANK*. The protein Amyloid-beta (Aβ), a marker of AD, is increased in the forebrain of AD patients (Hardy and Selkoe 2002). This increase of Aβ observed in AD patients was accompanied by an increase of *SHANK2* expression and a decrease of *SHANK3* expression in brain tissues from AD patients (Gong et al. 2009). In parallel, a significant negative correlation between the level of Aβ and the level of expression of *Shank1*, *Shank3*, Homer1B and mGluR1 was found in APPTg mouse model and in iPSC model from patients (Roselli et al. 2009; Pham et al. 2010). To conclude, these studies revealed an association between Aβ level and *SHANK* expression in AD, but further studies are needed to unravel the causes and consequences of the two aspects.

IV. Mouse models for autism

IV.A. *Benefits of mouse models for autism*

The *SHANK* gene family has been associated with ASD based on genetic studies in humans (see above); however, the mechanisms leading mutations in these genes to physiological and behavioural effects remain to be clarified. Many studies analysed animal models expressing such mutations as a proxy and studied the molecular, cellular and behavioural phenotypes to elucidate the mechanisms.

Mice were often used as a study model because of their phylogenetic (they carry orthologous genes) and physiological similarity to humans (Chinwalla et al. 2002; Brown, Hancock, and Gates 2006). Furthermore, mice are social animals and some of their behavioural traits can be paralleled with some traits of human behaviour. The generation and exploration of mouse models bring knowledge about the biology of autism (Crawley 2012). Studies on mouse models facilitate the understanding of the different neuronal circuits mediating ASD-related phenotypes and could provide innovative knowledge-based treatments in ASD.

At the behavioural level, the two core symptoms of ASD, deficits in social communication and stereotyped-like behaviours, can be evaluated in mice (Silverman et al. 2010). Different protocols, supposed to measure similar behavioural traits, are used to quantify the ASD-like level. The social behaviour, in juvenile and adult mice, is explored according to three main axes: social motivation for interaction with a same-sex unfamiliar mouse, social motivation during socio-sexual interaction, and interest in social novelty, i.e., the ability and motivation to discriminate between a familiar mouse and an unfamiliar one. The last one is often associated with social memory (see II.C.1). The social motivation, during socio-sexual interaction, is often studied using direct and free social interaction between the tested mouse and an unfamiliar mouse (Ferhat et al. 2015). The social motivation and the social memory can be studied using the three-chambered test and free interaction test. The three-chambered test, divided in three different phases, allows the discrimination between social interest and interest in novelty (M. Yang, Silverman, and Crawley 2011). The social communication and interaction in pups are tested during brief maternal separation with a recording of USVs emitted.

Stereotyped behaviours are usually characterised by repeated body movements such as excessive self-grooming, digging, marble burying, jumping or circling behaviour. Direct observation allows a quantification of the time spent in each category of stereotyped behaviour. Mainly motor repetitive behaviour can be observed in mice.

To understand the implication of cerebral pathways (see II.C), studies analysed electrophysiology, protein composition or neuronal development. However, the majority of brain

studies performed analysis on CA1 or CA3 in the hippocampus and few on the striatum or cortex. We will focus in the following part on the behaviour and neurophysiology of *Shank* mouse models.

IV.B. *Mouse models carrying mutations in SHANK genes*

IV.B.1. *Shank1*

The unique mouse model had been generated by Hung and colleagues (2008) (Hung et al. 2008). This mutant mouse displayed a deletion (Δ) of exons 14 and 15 in *Shank1* (Δ14-15; Figure 13.A; Table 3). These exons carry one of the two promoters and are present in the two known isoforms (Shank1a-b). Therefore, this model should be a complete knock-out (KO) (Hung et al. 2008), according to the current knowledge about *Shank1* isoform expression (Figure 8.A; (X. Wang et al. 2014)).

IV.B.1.a. Behavioural analysis

The *Shank1* mutant mouse was the first ASD model mutated in one gene of the *Shank* family generated (Hung et al. 2008). *Shank1*-/- mice displayed few impairments in ASD core symptoms, and *Shank1*+/- mice displayed even more limited impairments (Hung et al. 2008; Silverman et al. 2011; Wöhr et al. 2011; Sungur et al. 2014; Sungur, Schwarting, and Wöhr 2016; Sungur et al. 2017). Normal social interaction was observed in the three-chambered test and free social interaction (Sungur et al. 2017). Only *Shank1*-/- female mice displayed impairment in social recognition with a decrease of the time spent in contact with new unfamiliar mice in the third phase of the three-chambered test. Furthermore, a reduction of the communication can be observed in *Shank1*-/- mice with a decreased number of ultrasonic vocalisations emitted by pups during development and in adult males during their interaction with an oestrus female and a reduction of sniffing time of *Shank1*-/- adult males during scent marking test with female urine in comparison with wild-type mice (Wöhr et al. 2011; Sungur, Schwarting, and Wöhr 2016). *Shank1*-/- adult mice also displayed stereotyped behaviour with an increase of self-grooming behaviour (Sungur et al. 2014). Surprisingly, these *Shank1*-/- mice displayed a reduction of marbles burying behaviour as well as exploration behaviour in the open-field in comparison with *Shank1*+/+ mice (Silverman et al. 2011; Sungur et al. 2014). In humans, patients did not display intellectual disabilities, but can exhibit anxiety. *Shank1*-/- mice manifested impairment during a memory test, object recognition test (Sungur et al. 2017), and slight anxiety-like behaviour, in the dark/light test (Hung et al. 2008) contrary to human patients (Leblond et al. 2014).

IV.B.1.b. Neurobiology and electrophysiology

In this model, only one study analysed the neuronal pattern (Hung et al. 2008). *Shank1*-/- mice showed an abnormal PSD protein composition with a reduction of GKAP/SAPAP and Homer protein. In anatomic morphology, they showed smaller dendritic spines as well as thinner PSD in mutant mice. At the electrophysiological level, *Shank1*-/- mice displayed a decrease of synaptic strength with a decrease of field excitatory postsynaptic potential (fEPSP) and miniature excitatory postsynaptic potential (mEPSP) frequency.

IV.B.1. *Shank2*

Three independent mouse models were generated (Figure 13 & Table 3). The first one, displayed a deletion of exon 16 and 17 (*Shank2*Δ**16-17**; Figure 13.B; Table 3; (Won et al. 2012)), the second one a deletion in exon 17 (*Shank2*Δ**17**; Figure 13.C; Table 3; (Schmeisser et al. 2012)) and the third, recently generated, displayed a mutation in exon 24 (*Shank2*Δ**24**; Figure 13.D; Table 3; (Pappas et al. 2017)). The mouse model *Shank2*Δ16-17 and *Shank2*Δ17 are often annotated as *Shank2*Δ6-7 and *Shank2*Δ7 based on the exons from *Shank2a* isoforms (Figure 8).

In parallel of mouse models expressing the mutation in the whole body, four floxed conditional models were generated, specific to excitatory (c*Shank2*Δe) or inhibitory neurons (c*Shank2*Δi) (Kim et al. 2018), and two specific to the Purkinje cells of the cerebellum, using *Shank2*Δ16-17 mutation (c*Shank2*Δ16-17) (Peter et al. 2016) (Peter 2016) or *Shank2*Δ17 mutation (c*Shank2*Δ17) (Ha et al. 2016). According to the actual knowledge of *Shank2* expression, all models should be complete KO (Figure 8.B; (X. Wang et al. 2014)). Even if all *Shank2* models displayed complete suppression of expression, they displayed important diversity, mainly at the electrophysiological level (see IV.B.1.b) (Ferhat et al. 2017). This observation can reveal the poor knowledge about *Shank2* expression in mice. These differences can also reveal the important impact of "laboratory effect" and the different protocols used.

IV.B.1.a. Behavioural analysis

The *Shank2*-/- mouse models exhibited behavioural impairments, compared to *Shank2*+/+ mice. These impairments could be related to ASD core symptoms in patients. In *Shank2*Δ16-17, studies showed different results for social interactions. *Shank2*Δ16-17-/- mice showed a decrease of social motivation or interest in social novelty (E.-J. Lee et al. 2015; Won et al. 2012). However, Lim and colleagues (2016) showed no significant difference between genotypes (C.-S. Lim et al. 2017).

Concerning communication, according to Won and colleagues (2012), *Shank2*Δ16-17-/- mice showed a decrease of call rate in males during mating behaviour. *Shank2*Δ17-/- displayed a decrease

of the time spent in contact and a decrease of call rate during same-sex social interaction (Schmeisser et al. 2012; Ey et al. 2013). *Shank2*Δ24-/- mice displayed a decrease of time spent in contact compared to *Shank2*Δ24+/+ in the three-chambered test and dyadic social test (Pappas et al. 2017). Interestingly, Pappas and colleagues (2017) showed a decrease of bi-directional interaction during dyadic test. The social aspect seems to be perturbed in these models and can be related with *SHANK2* patients, who manifested mild social impairments (Leblond et al. 2014).

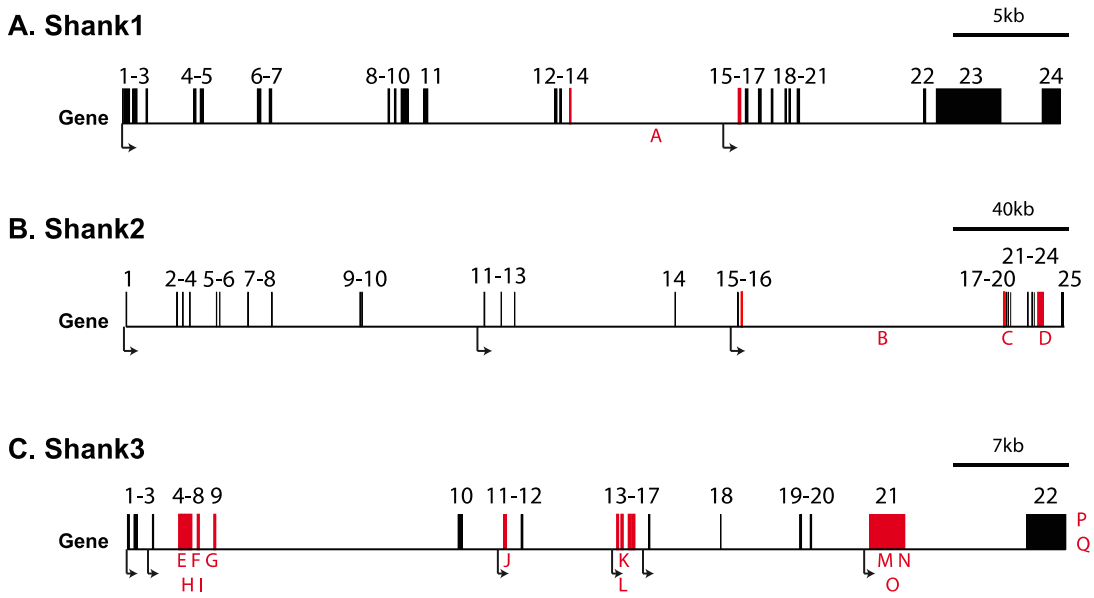

Figure 13: Schematic representation of mutation in Shank1 (A), Shank2 (B) and Shank3 (C) genes in the mouse genome.
Black squares are exons. Red letters refer to the mouse model. Black arrows are intragenic promoters. Red squares indicate exons mutated to generate the mouse models: ***Shank1 model****: **A**: Δ14-15* (Hung et al. 2008; Silverman et al. 2011; Sungur et al. 2014; Sungur, Schwarting, and Wöhr 2016; Sungur et al. 2017)*;* ***Shank2 model****: **B**: Δ16-17* (Won et al. 2012), ***C****: Δ17* (Schmeisser et al. 2012), ***D****: Δ24* (Pappas et al. 2017)*;* ***Shank3 model****: **E**: Δ4-7* (Peça et al. 2011), ***F****: Δ4-9B* (Bozdagi et al. 2010), ***G****: Δ4-9J (X. Wang et al., 2011,* ***H****: Δ4-9P* (Jaramillo et al. 2016), ***I****: Δ9* (J. Lee et al. 2015), ***J****: Δ11* (Schmeisser et al. 2012), ***K****: Δ13* (Jaramillo et al. 2017), ***L*** *: Δ13-16* (Peça et al. 2011), ***M****: Δ21P* (Kouser et al. 2013), ***N****: InsG21* (Speed et al. 2015), ***O****: InsG3680* (Zhou et al. 2016), ***P****: Δ4-22* (X. Wang et al. 2016), ***Q****: Δ4-22* (Drapeau et al. 2018).

Concerning communication, according to Won and colleagues (2012), *Shank2*Δ16-17-/- mice showed a decrease of call rate in males during mating behaviour. *Shank2*Δ17-/- displayed a decrease of the time spent in contact and a decrease of call rate during same-sex social interaction (Schmeisser et al. 2012; Ey et al. 2013). *Shank2*Δ24-/- mice displayed a decrease of time spent in contact compared to *Shank2*Δ24+/+ in the three-chambered test and dyadic social test (Pappas et al. 2017). Interestingly, Pappas and colleagues (2017) showed a decrease of bi-directional interaction during dyadic test. The social aspect seems to be perturbed in these models and can be related with *SHANK2* patients, who manifested mild social impairments (Leblond et al. 2014).

The second ASD core symptoms, stereotyped behaviours, is also analysed in *Shank2* mice. *Shank2*Δ16-17-/- mice displayed an increase of jumping behaviour in comparison with their wild-type

littermates, similarly to *Shank2*Δ17-/- mice (E.-J. Lee et al. 2015; Schmeisser et al. 2012; C.-S. Lim et al. 2017). Furthermore, *Shank2*Δ17-/- mice displayed an increase of duration of bouts of self-grooming behaviour in comparison with their wild-type littermates. Surprisingly, *Shank2*Δ24-/- mice displayed a decrease of self-grooming behaviour in comparison with their wild-type littermates (Pappas et al. 2017).

Model	***Shank1***	***Shank2***	***Shank2***	***Shank2***
Mutation	Δ14-15	Δ17	Δ16-17	Δ24
Reference	(Hung et al. 2008; Silverman et al. 2011; Wöhr et al. 2011; Sungur et al. 2014; Sungur, Schwarting, and Wöhr 2016; Sungur et al. 2017)	(Schmeisser et al. 2012; Ey et al. 2013; Ferhat et al. 2016)	(Won et al. 2012; E.-J. Lee et al. 2015; C.-S. Lim et al. 2017; Ha et al. 2016; Yoon et al. 2017; Ko et al. 2016)	(Pappas et al. 2017)
Remaining isoforms	None (predicted)	None (predicted)	None (predicted)	None (predicted)
Social interaction	Normal interaction	Disturbed socio-sexual interaction, reduced preference for novelty	*Reduced motivation	Reduced motivation
Communication observation	*Reduction of call rates (pups & adults)	*Reduction of call rates (female adult)	*Reduction of call rates (male adult mating behaviour)	-
Stereotyped behaviour	*↓ digging; ↑ self-grooming	↑ self-grooming	↑ jumping	↓ self-grooming
Locomotion	↓ in open-field	↑ in open-field	↑ in open-field; ↓ motor coordination	↑ in open-field & water maze
Memory	↑ in fear conditioning test; ↓ Object Recognition	-	↓ MWM	↓ MWM
Anxiety	*↑ in Dark/light	↑ in Dark/light	*↑ in EPM	-
Cellular Physiology	Abnormal PSD composition; ↓ spine density & size.	↓ mEPSP; ↑ NMDAR, Shank3, LTP; ↓ PSD, AMPAR	↓ NMDAR &LTP & GABAR & PSD	↓ NMDAR

Table 3: Behavioural, synaptic, and molecular phenotypes of Shank1 and Shank2 mutant mice*. All models represented are deleterious in whole brain and body Δ: deletion of exon; ↑: augmentation of phenotype compared to wild-type; ↓: reduction of phenotype compared to wild-type; *: Indicate different results between studies.*

Literature highlights an important comorbidity in *Shank2* mutant mice. First, the three models (*Shank2*Δ16-17-/-, *Shank2*Δ17-/- and *Shank2*Δ24-/-) showed an increase of the distance travelled in the open-field, revealing consistent hyperactivity in mice not reported in all human cases displaying a

mutation in *SHANK2* (Leblond et al. 2014). Furthermore, *Shank2*Δ16-17-/- mice displayed impairment in motor coordination (Ha et al. 2016). Pappas and colleagues (2017) suggested to relate the hyperactivity of *Shank2*Δ24-/- mice (and by extension of other complete *Shank2* models) with schizophrenia-like phenotype (Peykov et al. 2015) and manic-like behaviour seen in bipolar patients and models (Pappas et al. 2017). This observation is consistent with unpublished data, on *Shank2*Δ17-/-, revealing that the effect of methylphenidate on hyperactivity was similar between wild-type and mutant mice (Ey et al., n.d.). However, these observations were only based on hyperactivity and no analysis of others symptoms of manic-like behaviour were made. Then, several models exhibited impairments during the Morris water maze task, revealing cognitive impairment, which could be related with mild IQ in patients (Leblond et al. 2014). Anxiety-like behaviour had been reported in the dark/light test for *Shank2*Δ17-/- mice (Schmeisser et al. 2012) and in the elevated plus maze test for *Shank2*Δ16-17-/- mice (Won et al. 2012), but Lim and colleagues (2017) and Ha and colleagues (2016) did not observe any anxiety-like behaviours (C.-S. Lim et al. 2017; Ha et al. 2016). Furthermore, *Shank2*Δ24-/- mice showed an important dysregulation in circadian cycle (Pappas et al. 2017).

Concerning the conditional models, Peter and colleagues (2016) observed a reduction of social interest and social memory in c*Shank2*Δ17 mouse as well as reduction of motor learning and impairment in repetitive behaviours (Peter et al. 2016). Ha and colleagues (2016) only observed a decrease of motor coordination and increase of self-grooming behaviours in c*Shank2*Δ16-17 mouse (Ha et al. 2016). No impairment in social interaction, communication or olfaction was observed. Interestingly, Kim and colleagues (2018) associated reduction of social motivation, digging and increase of anxiety-like behaviour, through openfield and dark/light test, with the excitatory neurons on c*Shank2*Δe mouse and a reduction of vocalisations emitted and an increase of self-grooming with inhibitory neurons with the c*Shank2*ΔI mouse (Kim et al. 2018). Hyperactivity was found in both models.

IV.B.1.b. Neurobiology and electrophysiology

*Shank2*Δ16-17-/- mice displayed a decrease of Long-Term potentiation (LTP) as well as a decrease of NMDA/AMPA ratio in hippocampus, with an increase of the expression of GluN1 and a decrease of phosphorylation of GluA1 in comparison with their wild-type littermates (Won et al. 2012). Pappas and colleagues (2017) showed similar observation with a decrease of NMDA/AMPA ratio, and a decrease of GluN1 expression in comparison with control mice (Pappas et al. 2017). In contrast, Schmeisser and colleagues (2012) highlighted opposite results, with an increase of LTP and NMDA/AMPA ratio in comparison with wild-type mice. They also observed an increase of GluN1, GluN2 and, surprisingly, *Shank3* in striatum and hippocampus in comparison with wild-type mice.

This last observation can reveal an important compensatory mechanism between *Shank2* and *Shank3*. They also observed a decrease of the density of PSD in comparison with control mice (Schmeisser et al. 2012). Furthermore, Lim and colleagues (2017) highlighted a reduction of GABRA2, a GABA receptor sub-unit, in *Shank2*Δ16-17-/- mice, but not in *Shank2*Δ17-/- mice, in the hippocampus (C.-S. Lim et al. 2017). A reduction of the inhibitory strength in hippocampus, via GABAR, implies a dysregulation of activation of hippocampus and can be related to the E:I imbalance theory in ASD (see II.B). These observations were made at approximately the same age for all models and remain to be further investigated.

IV.B.1.c. Pharmacological studies

After highlighting the reduction of GABRA2 in the hippocampus, Lim and colleagues (2017) used a GABAR agonist, the L838.417, an anxiolytic drug. They were able to rescue impairment in spatial memory, but not in any other phenotypic aspects.

As we saw before (see III.A.2.e), the zinc ions are essential for Shank setting up. Lee and colleagues (2015) injected clioquinol, a zinc ions chelator, by intraperitoneal injection to *Shank2*Δ17-/- mice, and they observed an increase of social recognition with a ratio similar to wild-type mice as well as an increase of fEPSP slope similar to wild-type mice (E.-J. Lee et al. 2015).

Pappas and colleagues (2017) analysed the effects of two different drugs prescribed in human ASD patients for treatment of comorbidities, lithium (BPD) and valproic acid (VPA; epilepsy) (Pappas et al. 2017). With chronic lithium treatment (incorporated in chow alimentation), *Shank2*Δ24-/- mice demonstrated an improvement of circadian cycle that got similar to the one of *Shank2*Δ24+/+ mice. Furthermore, chronic lithium treatment or acute VPA treatment seemed to reduce the hyperactivity observed in *Shank2*Δ24-/- mice. These two drugs were used to treat mania in bipolar disorder and reduced the hyperactivity aspect in patients (Bowden 2000; Pope et al. 1991; Young and Newham 2006). Interestingly, a drug screening study on iPS cells from *SHANK3* patients revealed an increase of *SHANK3* expression in iPSC with lithium treatment (Darville et al. 2016). Therefore, the link between *SHANK2* and *SHANK3* seems to be an important clue in shankopathy and further investigation on the underlying mechanisms could reveal new treatment (Schmeisser et al. 2012).

IV.B.2. *Shank3*

Finally, *Shank3* is the most studied gene as a potential cause of ASD, both in cellular (genetic level and functional studies in human-derived cells) and in animal models. Seventeen independent animal models exist: thirteen with a mutation/deletion in one or more exon(s) in mice (Figure 13.E to Q); one in rats; two with a point mutation in mice and one study on *Shank3* over-expression in mice

(summarized in **Table 4**). For the majority of the models, the mutation targeted specific domains (ANK, SH3, PDZ, Pro or SAM) and two models proposed a complete deletion (exon 4 to 22) of *Shank3*.

As seen above (see III.A.4), *Shank3* displayed several isoforms, with their expression profiles depending on age and brain region (X. Wang et al. 2014). Because of deletion/mutation causing a frame shift, each model is expected to have different disruptions of different isoforms (Figure 8.C). While patients carrying a mutation in *SHANK3* showed haploinsufficiency, the majority of studied models showed impairment at the homozygous state. Furthermore, the majority of models is studied by several teams and displays different phenotypes according to the laboratory for the same model. Even if the expression of *Shank3* isoforms starts to be well-known, these discrepancies suggest that some gaps in the understanding of *Shank3* expression remain to be filled.

IV.B.2.a. Behavioural analysis

Complete behavioural analyses were performed, on both homozygous and heterozygous mutants. Overall, these results supported behavioural impairments, which were reminiscent of the phenotype displayed by *SHANK3* patients.

The social aspect was analysed in the majority of models and often showed a decrease of social interest (*Shank3*Δ**4-9B** (Bozdagi et al. 2010; M. Yang et al. 2012), *Shank3*Δ**4-9J** (X. Wang et al. 2011), *Shank3*Δ**4-9P** (Jaramillo et al. 2016), *Shank3*Δ**11** (Vicidomini et al. 2017), *Shank3*Δ**13** (Jaramillo et al. 2017), *Shank3*Δ**13-16** (Peça et al. 2011; J. Luo et al. 2017), *Shank3*Δ**21P** (Duffney et al. 2015; Qin et al. 2018), *Shank3*Δ**4-22J** (X. Wang et al. 2016), *Shank3***InsG3680** (Zhou et al. 2016)) or a reduction of interest in social novelty (associated with social memory) (*Shank3*Δ**4-7** (Peça et al. 2011), *Shank3*Δ**11** (Vicidomini et al. 2017), *Shank3*Δ**13** (Jaramillo et al. 2017), *Shank3*Δ**13-16** (Peça et al. 2011), *Shank3***InsG3680** (Zhou et al. 2016)). Interestingly, Drapeau and colleagues (2018) revealed a reduction of the latency of first contact, but not in the time spent in interaction in *Shank3*Δ**4-22B** (Drapeau et al. 2018). However, an important variability was present between studies on the same model. For example, Wang and colleagues (2011) showed a decrease of social interest on *Shank3*Δ**4-9J**, but not Kabitzke and colleagues (2017). Little information was gathered about the social communication, mainly olfactory and vocal communication. Studies on the models *Shank3*Δ**4-9B** (Bozdagi et al. 2010), *Shank3*Δ**4-9J** (Kabitzke et al. 2017), *Shank3*Δ**13-16** (Kabitzke et al. 2017), *Shank3*Δ**4-22J** (X. Wang et al. 2016, 2014), *Shank3*Δ**4-6 (rat)** (Berg et al. 2018) highlighted a decrease of ultrasonic vocalisations emitted during social interaction or playback test, and an increase of USVs emitted by male without social contact for *Shank3*Δ**4-9B** (X. Wang et al. 2011). As a neurodevelopmental disorder, social communication during development was mostly studied by examining the emission of ultrasonic vocalisations in pups (between PND1 and PND13). According to

Jaramillo and colleagues (2016), pups with *Shank3*Δ**4-9P** (Jaramillo et al. 2016) displayed an increase of the call rate during isolation compared to wild-type mice. It is the opposite for the transgenic mice with an **over-expression** of *Shank3* (Han et al. 2013), which emmited less ultrasonic vocalisations than wild-type mice., but this observation was not replicated for *Shank3*Δ**9** (J. Lee et al. 2015), and *Shank3***InsG3680** (Zhou et al. 2016).

Stereotyped behaviours appeared to be the trait most importantly impacted by the deletion in *Shank3* mutant mice (Ferhat et al. 2017). We observed an increase of self-grooming behaviour in *Shank3*Δ**4-9B** (M. Yang et al. 2012), *Shank3*Δ**4-9J** (X. Wang et al. 2011), *Shank3*Δ**4-9P** (Jaramillo et al. 2016), *Shank3*Δ**11** (Schmeisser et al. 2012; Vicidomini et al. 2017), *Shank3*Δ**13** (Jaramillo et al. 2017), *Shank3*Δ**13-16** (Peça et al. 2011), *Shank3*Δ**21P** (Kouser et al. 2013; Qin et al. 2018), *Shank3*Δ**4-22J** (X. Wang et al. 2016; Bey et al. 2018), *Shank3*Δ**4-22B** (Drapeau et al. 2018)**,** *Shank3***InsG3680** (Zhou et al. 2016). Only *Shank3*Δ**4-9B** displayed different phenotype according to the study. For Yang and colleagues (2012), mice displayed an increase of self-grooming behaviour, when Drapeau and colleagues (2014) did not observe significant difference between genotype. Only Drapeau and colleagues (2018) presented circling behaviour as a stereotyped behaviour for *Shank3*Δ**4-22B** (Drapeau et al. 2018). The digging and marble burying behaviour is often associated with stereotyped behaviour (Silverman et al. 2010; Deacon 2006). Surprisingly, *Shank3* mutants displayed a decrease of time spent in digging behaviour or marbling (*Shank3*Δ**13** (Jaramillo et al. 2017), *Shank3*Δ**13-16** (Kabitzke et al. 2017), *Shank3*Δ**21P** (Kouser et al. 2013), *Shank3***InsGex21** (Speed et al. 2015)). This observation can be due to the increase of time spent in other behaviour (i.e., self-grooming), or a reduction of exploratory behaviour. Indeed, the locomotion activity or the exploratory behaviour seems to be impacted, with a reduction of distance travelled in the open-field (*Shank3*Δ**4-9B** (M. Yang et al. 2012), *Shank3*Δ**4-9J** (X. Wang et al. 2011), *Shank3*Δ**13** (Jaramillo et al. 2017), **and** *Shank3*Δ**13-16** (Kabitzke et al. 2017)) or impairments in motor coordination (*Shank3*Δ**4-9B** (M. Yang et al. 2012), *Shank3*Δ**4-9J** (X. Wang et al. 2011), Δ**13** (Jaramillo et al. 2017)). In the opposite way, mouse with an **overexpression** of *Shank3* displayed hyperactivity (Han et al. 2013; B. Lee et al. 2017).

Other comorbidities were noticed in *Shank3* mouse models and can be related to comorbidities in *SHANK3* patients (see I.D). The most common comorbidity was cognitive defects, which can be paralleled with ID in patients. To test this aspect, several studies performed a spatial learning task, using the Morris water maze, and they identified a deficiency in this task for *Shank3*Δ**4-9B** (M. Yang et al. 2012), *Shank3*Δ**4-9J** (X. Wang et al. 2011), *Shank3*Δ**4-9P** (Jaramillo et al. 2016), *Shank3*Δ**11** (Vicidomini et al. 2017), *Shank3*Δ**21P** (Kouser et al. 2013), *Shank3*Δ**4-22J** (X. Wang et al. 2016), *Shank3***InsGex21** (Speed et al. 2015). No impairment in spatial learning was observed in *Shank3*Δ**9** (J. Lee et al. 2015), *Shank3*Δ**13-16** (Peça et al. 2011). No other cognitive impairment was reported except in touchscreen pairwise discrimination task in heterozygous *Shank3*Δ**13-16** (Copping et al. 2017). Among other comorbidities, an increase of anxiety-like behaviour was also reported in *Shank3*Δ**4-9B**

(Drapeau et al. 2014), *Shank3*Δ**4-9J** (Kabitzke et al. 2017), *Shank3*Δ**13-16** (Peça et al. 2011; Kabitzke et al. 2017), *Shank3*Δ**21P** (Kouser et al. 2013), *Shank3*Δ**4-22J** (X. Wang et al. 2016; Bey et al. 2018) and *Shank3*Δ**4-22B** (Drapeau et al. 2018) during the elevated plus maze test, elevated zero maze test, dark/light test or openfield test. However, several mouse models did not display anxiety-like behaviour, and this aspect was not observed in the previously cited models. It suggests an important impact of laboratory conditions during the test and, maybe, a kind of increase of sensibility in *Shank3*-/- mice.

Then, in a study on **over-expression** of *Shank3*, transgenic mice presented dysregulated circadian rhythm (Han et al. 2013). This can be related to the modulation of Shank3 expression, in striatum and hippocampus, along the circadian cycle (Sarowar et al. 2016).

Furthermore, Wei and colleagues (2017) showed a weaker intestinal barrier as well as a reduction of ZO-1 protein (associated with PDZ domain; see III.A.2.c) in *Shank3*Δ**21P** (Wei et al. 2017).

All findings from *Shank3* mutants were reminiscent to the observations in patients, even with the important variability and the behavioural inconsistency between studies. Many of the differences between models could be attributed to the different isoforms expressed and the transcriptional complexity of the gene. However, an impact of the laboratory, or the experimenter on the mouse behaviour cannot be excluded (Sorge et al. 2014).

IV.B.2.b. Neurobiology and electrophysiology

Different brain regions were analysed in different strains of mutant mice, including striatum, hippocampus and cortex. Overall, the data obtained from these studies support a general conclusion that synaptic function and proteins expression are impaired in mice with *Shank3* mutations.

In electrophysiology, the majority of models displayed a reduction of field EPSP slope (*Shank3*Δ**4-9B** (M. Yang et al. 2012), *Shank3*Δ**4-9J** (X. Wang et al. 2011), *Shank3*Δ**13-16** (Peça et al. 2011), *Shank3*Δ**21P** (Kouser et al. 2013), *Shank3***InsG21** (Speed et al. 2015), *Shank3*Δ**4-6-Rat** (Harony-Nicolas et al. 2017)) or mEPSP (*Shank3*Δ**11** (Vicidomini et al. 2017), *Shank3*Δ**21P** (Kouser et al. 2013), *Shank3*Δ**21G** (Bidinosti et al. 2016)**,** *Shank3*Δ**4-22J** (X. Wang et al. 2016), *Shank3***InsG3680** (Zhou et al. 2016)), revealing impairment in signal transduction in different brain structures caused by *Shank3* mutation. Furthermore, the model *Shank3*Δ**9** presented a synaptic imbalance with an increase of fIPSP (field Inhibitory Post Synaptic Potential) and a decrease of fEPSP (J. Lee et al. 2015), correlating with the synaptic E:I imbalance theory in autism (see II.B).

In parallel with electrophysiology studies, the expression of several proteins is deregulated in mutant mice. Ionotropic glutamatergic channels were under-expressed in mutant mice in comparison with wild-type mice; GluRA1-2-3 (*Shank3*Δ**4-9J** (X. Wang et al. 2011), *Shank3*Δ**13** (Jaramillo et al.

2017), *Shank3***InsG3680** (Zhou et al. 2016)); GluN1, GluN2A-B (*Shank3*Δ**4-9J** (X. Wang et al. 2011), *Shank3*Δ**11** (Schmeisser et al. 2012; Reim et al. 2017), *Shank3*Δ**13** (Jaramillo et al. 2017), *Shank3***InsG3680** (Zhou et al. 2016)). Similar effects were found for metabotropic glutamatergic receptors 5 (mGluR5) (*Shank3*Δ**11** (Schmeisser et al. 2012), *Shank3***InsG3680** (Zhou et al. 2016)). Surprisingly, Schmeisser and colleagues (2012) presented an increase of GluN2B, in opposite observation with other models (Schmeisser et al. 2012). However, a complete proteomic analysis on *Shank3*Δ**11** showed a decrease of GluN2B and potassium channel KCa1.1 in striatum, but also a decrease of Sapap2-3 and Homer1, scaffolding proteins associated with Shank (Reim et al. 2017). In the opposite, Kouser and colleagues (2013) and Wang and colleagues (2016) revealed an increase of mGLUR5. The expression of several proteins, directly interacting with Shank3, was altered, especially a decrease of Homer 1 was observed (see III.A.2.d; *Shank3*Δ**4-9J** (X. Wang et al. 2011), *Shank3*Δ**13** (Jaramillo et al. 2017)**,** *Shank3*Δ**11** (Schmeisser et al. 2012), *Shank3*Δ**4-22** (X. Wang et al. 2016), *Shank3***InsG3680** (Zhou et al. 2016)) and SAPAP3 was also reduced (see III.A.2.c; *Shank3*Δ**11** (Schmeisser et al. 2012), *Shank3***InsG3680** (Zhou et al. 2016)).

In parallel with the cellular physiology, brain circuit mechanisms were analysed. Kloth and colleagues (2015) presented abnormal response timing in delayed eye-blink conditioning, a behavioural test requiring cerebellar plasticity, in *Shank3*Δ**21P** model. They also show a reduced Purkinje-cell dendritic spine density (Kloth et al. 2015).

Another pathway seems to be relevant in *Shank3* mouse model: the mesocorticolimbic dopamine system (see II.C.1). First, Bariselli and colleagues (2016) highlighted a downregulation of excitatory transmission to GABAergic and dopaminergic neurons in the VTA and reduction of dopaminergic neuron activity in the VTA, in sh*Shank3* (Adeno-Associated Virus expressing shRNA targeting *Shank3*) models. Impairment of social interaction, compared to wild-type mice, correlated with these observations. Injection of mGluR1 agonist allowed a rescue of the phenotype (Bariselli et al. 2016). Furthermore, in *Shank3*Δ**13-16** mice, Wang and colleagues (2017) related a specific decrease of mEPSP of striatal D2-MSN, and a reduction of the spine density and alteration of calcium channel voltage-dependent, Cav1.3, in striatal D2-MSN, but not in striatal D1-MSN (W. Wang et al. 2017). However, the authors associated this alteration with the locomotor pathway (see II.C.2), and stereotyped behaviour pathway, and not with the mesocorticolimbic pathway. They reduced self-grooming behaviour targeting D2-MSN using the DREADD (designer receptor exclusively activated by designer drugs) technique, that allows the activation of specific cells via a designed receptor sensitive to a specific drug.

To corroborate the idea of impairment in striatal connection, Bey and colleagues proposed a *Shank3*Δ**4-22J** conditional mutant according to different cellular types, including Striatum specific mutant (Dlx5/6), Cortex-hippocampus specific mutant (NEX), D1-MSN specific mutant (Drd1) and D2-MSN specific mutant (Drd2) (Bey et al. 2018). Drd1 and Drd2 showed an increase of action potential and excitability, and a decrease of the expression of Homer1b/c in striatum compared to

controls. Surprisingly, these animals did not display impairment in social interaction, stereotyped behaviours or locomotion. The NEX mutants displayed an increase of NMDAR currents and an increase of expression of glutamatergic receptor GluN1-2B. In parallel, they showed an increase of self-grooming behaviour, hyperactivity and a reduction of coordination. The Dlx5/6 mutants showed a decrease of Homer1b/c in the striatum.

Overall, even with conflicting evidence between studies, we can observe impairment in excitatory synapses, with modification of EPSP or glutamate receptor expression, but also a possibility of impairment in inhibitory neurons, with the modulation of MSN or IPSP. The E:I theory could explain behavioural impairment in mice, in social or stereotyped behaviour.

IV.B.2.c. Pharmacological studies

Two different approaches were used for treatment trials in *Shank3* mutant mice: biological and molecular tools and well-known drugs. As we already mentioned above, Wang et al. (2017) used DREADD technique, based on the incorporation of designed-G-Protein-Coupled-Receptor (GPCR) exclusively activated by a designed-drugs (W. Wang et al. 2017). With this technique, they showed the implication of D2-MSN in stereotyped behaviours. However, the implication of dopamine more specifically in D2-MSN was already demonstrated, as well as a reduction of stereotyped behaviours with D2 agonist (F. Sams-Dodd 1996; Frank Sams-Dodd 1998), but this technique has several limitations because of its invasiveness. In 2016, Mei and colleagues proposed a *Shank3* mouse model floxed around the exon of PDZ domain with an activation of *cre* function after tamoxifen administration. This technique allowed a restoration of the Shank3 normal expression after tamoxifen administration in adult. They observed a restoration of electrophysiological and physiological impairment (mEPSC frequency and spine density), but also of behaviours (self-grooming behaviour, social motivation), but not of the locomotion in adult mice (Mei et al. 2016).

Recently, Luo and colleagues (2017) showed a rescue of social deficit using social training with optogenetic activation of neurons in the midbrain dorsal raphe nucleus (DRN) (J. Luo et al. 2017). Optogenetic activation of DRN allows a direct activation of reward circuit as a substitute of behavioural therapies. With this study, they highlighted the importance of behavioural therapies such ABA (see I.E).

Surprisingly, the use of well-known drugs is not really common in *Shank3* studies. In the model **over-expressing** *Shank3*, Han and colleagues (2013) tried valproic acid, usually used for epilepsy, and lithium, usually used for bipolar disorders, but also used for autism (Egger et al. 2017). Valproic acid rescued the hyperactivity phenotype (see IV.B.2.a), but not the lithium (Han et al. 2013). Recently, Qin and colleagues (2018) associated an over-regulation of a class I HDAC2 with *Shank3*Δ**21P** mutant mice (Qin et al. 2018). An increase of HDAC2 revealed epigenetic modulation in

this mouse model. Treatment with romidepsin, a specific HDAC2 inhibitor, induced a rescue of observed social deficit without rescuing the increased self-grooming behaviour

---

Table 4: Behavioural, synaptic and molecular phenotype of Shank3 mutant mice. *All models represented are deleterious in whole brain and body. Δ: deletion of exon; ↑: augmentation of phenotype compares to wild-type; ↓: reduction of phenotype compares to wild-type; *: Indicate different results between studies; Remaining isoforms based on* (X. Wang et al. 2014)

Mutation	Δ4-7	Δ4-9B	Δ4-9J	Δ4-9P	Δ9	Δ11	Δ13	Δ13-16	Δ21P	Δ4-22	Δ4-22	InsGex21	InsG3680	Over-expression	Δ4-6 (rat)
References (first article)	(Peça et al., 2011)	(Bozdagi et al., 2010)	(X. Wang et al., 2011)	(Jaramillo et al., 2016)	(J. Lee et al., 2015)	(Schmeisser et al., 2012)	(Jaramillo et al., 2017)	(Peça et al., 2011)	(Kouser et al., 2013)	(X. Wang et al., 2016)	(Drapeau et al., 2018)	(Speed et al., 2015)	(Zhou et al., 2016)	(Han et al., 2013)	(Harony-Nicolas et al., 2017)
Domain targeted	ANK	ANK	ANK	ANK	ANK	SH3	PDZ	PDZ	Proline	All	All	Proline	Proline	All	All
Remaining isoforms	c,d,e,f	c,d,e,f	c,d,e,f	c,d,e,f	c,d,e,f	d,e,f	e,f	e,f	None	None	None	-	-	a,b,c,d,e,f	a,b,c,d,e,f
Social behaviour	↓preference for novelty	* ↓male/ female interaction & juvenile	* ↓ preference for conspecific	↓interaction in adult	NS	* ↓ preference for conspecific and novelty	↓ preference for conspecific and novelty	* ↓ preference for conspecific and novelty	* ↓p reference for conspecific and novelty	*↑ non-reciprocal interaction	↓latency to first interaction	NS	* ↓ preference for conspecific and novelty	-	↓j uvenile interaction
Communication	-	* ↓USV emitted	↓call complexity and duration	↑pups call rate	NS	-		NS	NS	↓number and duration	NS	-	NS	-	↓long term social memory
Stereotyped behaviour	NS	* ↑SG	↑SG	↑SG	NS	↑SG	↑SG; ↓digging	↑SG; ↓digging	↑SG; ↓digging	↑SG	↑SG & rotation	↓digging	↑SG	-	↓number of USV
Locomotion & exploration	-	-	↓motor coordination and locomotion	↓motor coordination	↑exploration rearing	-	↓motor coordination & locomotion	↓locomotion	NS	NS	↓motor coordination & locomotion	-	-	↑locomotion	-
Learning & Memory	-	↓OR; NS: MWM, YM	*↑MWM	↓MWM	NS: MWM	↓MWM	↓MWM	NS: MWM	↓MWM	↓MWM	↓Fear conditioning	↓MWM	-	-	-
Anxiety-like behaviour	NS: EPM	↑EPM	↑EPM	NS: EPM, OF, DL	NS: OF	NS: EPM	NS: EPM, OF, DL	↑EPM	*↑DL	↑DL, OF ↓EZM	↑EZM	NS: EPM, OF, DL	-	NS	-
Electro-physiology	NS	↓mEPSP & fEPSP slope	↓fEPSP slope& LTP & PSD	CA1: ↓fEPSP slope & NMDA/AMPA ratio	CA1: ↑frequency fIPSP; ↓fEPSP slope	↓EPSP & calcium released	↓fEPSP slope& LTP a NMDA/AMPA ratio	↓fEPSP slope & LTP & PSD; ↑D2msn EPSC	↓mEPSP & fEPSP slope & LTP;	↓EPSP & PSD; ↑spike frequency	-	↓LTD & fEPSP slope & NMDA/AMPA ratio & EPSC frequency	↓mEPSP frequency and amplitude	Seizure	↓fEPSP slope
Protein expression	NS	↓GluA1	↓GluA1 GluN2A homer1b/c	-	-	↓mGluR5 ; ↑GluN2B, Shank2	↓GluA2, GluA3, GluN2A-B, Homer1, PSD-95	-	↑mGluR5 & immature neuron	↓homer1; ↑mGluR5	-	-	↓homer1 SPAP3 GluN 1 GluA2 mGluR5	↓Gad	-

V. Aims

As we saw in the different parts of this introduction, *Shank3* is strongly associated with ASD. Patients with ASD carrying a mutation in *SHANK3* displayed important phenotypic variability (Leblond et al. 2014) and 65% these patients displayed a regression of the phenotype at puberty (Guilmatre et al. 2014; De Rubeis et al. 2018). Furthermore, little is known about the impact of *SHANK3* mutation on gene expression in the different brain structures.

The aim of this thesis is to understand the impact of *Shank3* mutation on the behaviour, especially on the evolution of the phenotype in mouse model, and the relation with other Shanks, especially with *Shank2*. The characterisation of the brain transcriptome following *Shank3* mutation is also crucial to understand the mechanisms underlying the genetic mutation.

Several questions will be tackled:

- What is the behavioural trajectory of the *Shank3*-/- mice?
- What is the relation between *Shank2* and *Shank3* at the behavioural level in mice?
- What is the brain transcriptomic profile of adult *Shank3*-/- mice?

We are expecting genotype-related variations in the behaviours associated with ASD between wild-type and mutant mice, as well as differences in the behavioural trajectories within *Shank3*-/- mice. We hope to explain these differences by a differential gene expression between genotypes and between trajectories. Furthermore, we make the hypothesis that compensatory mechanisms exist between *Shank2* and *Shank3* to modulate the behaviour and the RNA expression.

To study these different aspects, we use the *Shank2* and *Shank3* mouse models previously described by Schmeisser and colleagues (Schmeisser et al. 2012). The *Shank2* mutants display a complete deletion of the exon 17, Δ17, and the *Shank3* mutants display a complete deletion of the exon 11, Δ11. These two mutations were reported in patients with ASD.

MATERIAL & METHODS

I. Mouse cohorts

I.A. *General*

The behavioural studies involved several cohorts of mice, with both males and females tested. All procedures were performed according to the welfare of experimental animals of the Ministry of agriculture of France and they were approved the ethical committee CETEA n°89 (Institut Pasteur, Paris, France).

Shank2 mice were generated from 129SV ES cells and implanted in C57Bl/6J mouse, with at least 12 backcrosses on C57Bl/6J background (Schmeisser et al. 2012). *Shank2* mice displayed a deletion in exon 17, which generated a complete deletion of the protein Shank2 (Figure 14.A-B). *Shank3*Δ11 mice, generated by Genoway (Lyon, FRANCE), (Schmeisser et al. 2012) were raised on a C57Bl/6J background (more than 15 backcrosses). The *Shank3*Δ*11* mice displayed a deletion in exon 11 (Figure 14.C-D). In this model, only 3 isoforms remained expressed, *Shank3-d*, *Shank3-e* and *Shank3-f* (Figure 8). We bred *Shank3*Δ*11* heterozygous males and females to generate cohort 1, with 13 males and 10 females *Shank3*Δ*11*+/+, 19 males and 16 females *Shank3*Δ*11*+/- and 12 males and 12 females *Shank3*Δ*11*-/- mice (Table 5.A). Cohort 1 underwent a longitudinal behavioural study, with tests of the same animals at three, eight and twelve months of age. After the tests at three months of age, males were housed individually. Cohort 2 was also generated using *Shank3*Δ11 heterozygous mice, with 15 males and 5 females *Shank3*Δ11+/+, 15 males and 11 females *Shank3*Δ11+/- and 13 males and 7 females *Shank3*Δ11-/- mice (Table 5.A). We crossed double heterozygous mice to generate the double mutant *Shank2*/*Shank3* cohort (cohort 3). These parents were obtained by breeding mice heterozygous for *Shank2* with mice heterozygous for *Shank3*Δ*11* (both strains described above; Table 5.B).

All mice were kept in pathogen-free animal facilities. We provided food and water ad libitum. All mice from cohort 1 were housed under constant temperature (22 ± 1 °C) with a 12:12 light/dark cycle (7h-19h) and cohort 2 and cohort 3 with a 14:10 light/dark cycle (7h-21h). The experimenters were blind of the genotype of the tested animals for data collection and analyses.

I.A. *Weaning*

Weaning was performed at 22 +/-1 days of age. We measured weight and observed hind limb clasping. Just after weaning, mice were housed from three to five per cages, except when otherwise specified.

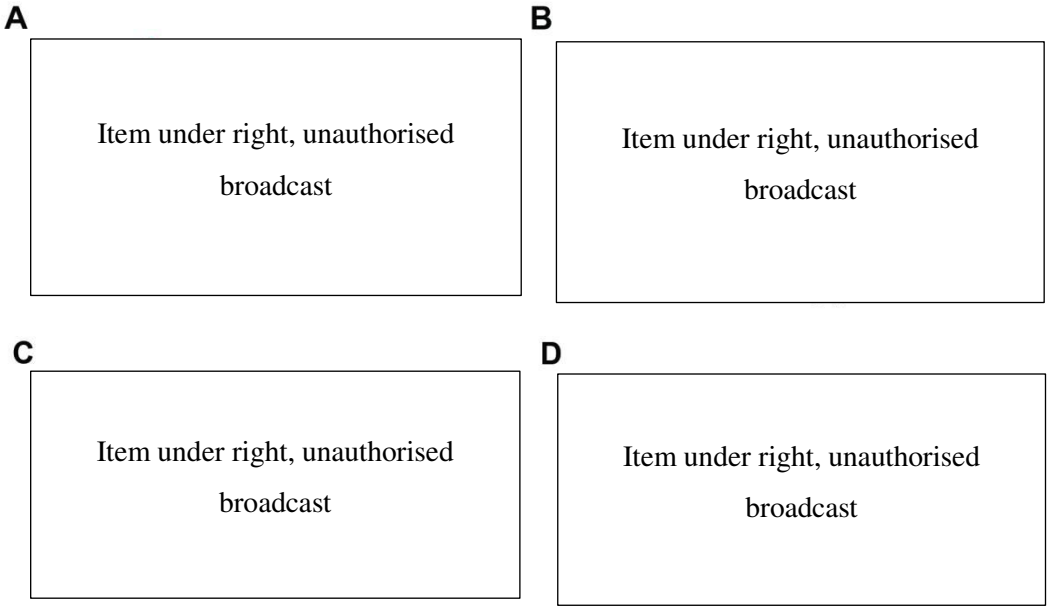

Figure 14: Generation of ProSAP1/Shank2 (A & B) and ProSAP2/Shank3 (C & D) mutant mice. *(A; C) ProSAP1/Shank2 (A; in red: ProSAP1E/Shank2E and blue: ProSAP1A/Shank2A.) and ProSAP2/Shank3 (C) structures. Ank = Ankyrin repeats, SH3 = SH3 domain, PDZ = PDZ domain, PRC, ppI = proline-rich clusters and ppI motif, SAM = sterile alpha motif domain. The deleted exon within the sequence of the PDZ domain (Shank2) or SH3 domain (Shank3) is marked by an empty triangle; the cDNA sequence around the deleted exon of homozygous ProSAP1/Shank2-/- mice is highlighted as is the frameshift caused by the deleted exon leading to a translational stop. (B; D) Targeting strategy. 5'HR and 3'HR mark the probes used for Southern Blot analysis, S and AS the primers used for genotyping. HR = homologous recombination, S = sense, AS = antisense. From* (Schmeisser et al. 2012)

I.A. *Behavioural procedures*

To examine adult behaviour, mice from Cohort 1 of both sexes were tested in the following order at 3 months, 8 months and 12 months of age: Y-maze working memory test; dark/light anxiety test; open field; three-chambered social test; stereotyped behaviour observation; occupant/new-comer social test with ultrasonic vocalisations (USV) recording; male behaviour in presence of an oestrus female with USV recording; observation of barbering and allo-grooming. Dark/light anxiety test, Y-maze and three chambered social tests were not performed on mice at eight and twelve months of age. The animals were weighted at 3 and 12 months of age and the physical aspect was noted at 8 months of age. Five females (two heterozygous and three knock-out mice) and three males (one heterozygous and two knock-outs) were euthanatized before the end of the experiment due to important self-inflicted injuries. We tested Cohort 2 and *Shank2*/*Shank3* cohort with dark/light anxiety test; elevated plus-maze; open field; stereotyped behaviour observation; occupant/new-comer social test with ultrasonic vocalisations (USV) recording; male behaviour in presence of an oestrus female with USV recording; rotarod.

A.

		+/+		+/-		-/-	
		♂	♀	♂	♀	♂	♀
Cohort 1	**3 months**	13	10	19	16	12	12
	8 months	13	10	18	14	12	11
	12 months	13	10	18	14	10	9
Cohort 2	**3 months**	15	5	15	11	13	7

B.

Shank2	**+/+**	**+/+**	**+/+**	**+/-**	**+/-**	**+/-**	**-/-**	**-/-**	**-/-**
Shank3	**+/+**	**+/-**	**-/-**	**+/+**	**+/-**	**-/-**	**+/+**	**+/-**	**-/-**
♂	6	11	3	7	14	6	1	2	1
♀	3	12	4	1	15	5	2	3	2
Total	9	23	7	8	29	11	3	5	3

Table 5: Number of individuals for each cohort. *(A) Number of mice from Shank3 cohort 1 at 3, 8 and 12 months of ages and cohort 2 at 3 months of age. (B) Number of mice for each genotype for the double mutant Shank2/Shank3 cohort.*

II. Behavioural tests

II.A. *General health*

We noticed the weight and the physical aspect (fur of animal, injury, or malformation) of all mice at weaning and in adulthood (for cohort 1: three and twelve months of age). The physical aspect of the animals was also evaluated before each behavioural test and any specificity was written down (change in the fur aspect, injuries).

II.B. *Dark/light anxiety-like test*

Initial condition:

- 1300 lux for bright side, 3 lux for the dark side
- 2-chambered cage

Protocol:

- Free exploration during 5min

Tested aspects of behaviour: Anxiety-like

The test cage was separated into two compartments connected by a small door (5x5 cm). The first was white and brightly illuminated (1300 lux), the second was dark with low light level (3 lux). The mouse was placed into the light compartment and freely explored the set up for 5 min. Video analysis was performed using Ethovision (Noldus Information Technology, Wageningen, The Netherlands). The latency to enter the dark compartment and the time spent in each compartment were measured.

II.C. *Elevated Plus-maze anxiety-like test*

Initial condition:

- 100 lux
- Plus-maze at a height of 50 cm

Protocol:

- Free exploration during 10 min

Tested aspects of behaviour: Anxiety-like

The elevated plus maze (four arms of 7 cm by 30 cm) consisted of two open arms (no walls), and two closed arms (with walls), all connected by a neutral zone in the centre. The apparatus was elevated at 50 cm above the floor and light was set at 100 lux. The animal was allowed to freely explore the set up for 10 min. The two open arms were supposed to be anxiogenic, while the two closed arms were supposed to be less anxiogenic. We therefore expected that the time spent in the closed arms reflects the level of anxiety of the mice.

II.D. *Locomotion and exploratory test in Open field*

Initial condition:

- 100 lux (for non-anxiety test)
- 1 m diameter round arena

Protocol:

- Free exploration during 30 min

Tested aspects of behaviour: Locomotion, motor capacities

The tested mouse was allowed to freely explore for 30 min a round open field arena of 1 m in diameter (100 lux in the centre of the arena). Automatic detection of the mouse using Ethovision (Noldus Information Technology, Wageningen, Netherlands) recorded the total distance travelled.

II.E. *Stereotyped behaviour observation*

Initial condition:

- 100 lux, soundproof box, 50x25x30 cm cage

Protocol:

- 10 min free exploration for habituation
- 10 min videotaped, several behaviours analysed: circling, digging, self-grooming, jumping.

Tested aspects of behaviour: Presence of stereotyped behaviours

The tested mouse was placed in a new test cage (Plexiglas, 50 x 25 x 30 cm; 100 lux; clean sawdust bedding) in a sound proof chamber. After 10 min habituation, we recorded its behaviour for 10 min (camera Logitech C920). We manually scored the time spent self-grooming, digging, jumping or circling using the software The Observer (Noldus Information Technology, Wageningen, The Netherlands). Behaviours were annotated manually and live with the same software. Total duration and average duration of each behavioural category were calculated.

II.F. *Occupant/new-comer social test with vocalisation recording*

Initial condition:

- 100 lux, soundproof box, 50x25x30 cm cage
- Marked different animals (especially newcomer) (2 or 3 lines on tail)
- Isolation: 3 days (females) or 3 weeks (males)

Protocol:

- 1st phase: tested mouse was allowed to freely explore the test cage during 20 min for habituation period.
- 2nd phase: introduction of an unknown mouse (newcomers 1, NC1). Free exploration and interaction during 4 min

Tested aspects of behaviour: Social interest

The tested animal was isolated socially for three days (females) or three weeks (males) to increase motivation for affiliative social contacts (Ferhat et al. 2016). After this test at 3 months of age, males stayed isolated for the remaining time of the experiment. During the first phase, the tested mouse was left during 20 min for habituation in the test cage, inside a soundproof box (Plexiglas, 50 x 25 x 30 cm; 100 lux; clean sawdust bedding). After this time, an unfamiliar C57Bl/6J mouse (New-comer 1, NC1) of the same sex and age was introduced into the test cage. The two animals were allowed to freely interact for 4 min. Social interactions were recorded using (Logitech C920). Videos were analysed using the semi-automated 2D tracking software, Mice Profiler module (de Chaumont,

Coura, et al. 2012) from the ICY platform (de Chaumont, Dallongeville, et al. 2012) (ICY Platform; Institut Pasteur, Paris, France). Using Mice Profiler, we quantified for both the occupant and the new-comer: the time in contact; the types of contact (oral-oral contact, oro-genital contact); approach/escape sequences; follow behaviour; the time spent in the vision field of the congener (Figure 15.A). At the same time, ultrasonic vocalisations were recorded with a Condenser ultrasound microphone Polaroid/CMPA, the interface UltraSoundGate 416-200, and the software Avisoft SASLab Pro Recorder from Avisoft Bioacoustics (Glienicke, Germany; sampling frequency: 300 kHz; FFT-length: 1024 points; 16-bit format).

Vocalisation files were manually annotated using the software Avisoft SASLab Pro Recorder from Avisoft Bioacoustics by an experienced worker. Different types of vocalisations were annotated according to the duration, frequency modulation and frequency jumps. Each call was classified into one category adapted from Scattoni et al (2011) (Scattoni, Ricceri, and Crawley 2011; Ey et al. 2013) (Figure 15.B):

- Short: duration shorter than 5 ms; frequency range ≤6.25 kHz.
- Flat: duration longer than 5 ms and frequency range ≤6.25 kHz.
- Upward: increase in frequency; frequency range >6.25 kHz with only one direction of frequency modulation.
- Downward: decrease in frequency; frequency range >6.25 kHz with only one direction of frequency modulation.
- Modulated: frequency modulations in more than one direction; frequency range >6.25 kHz.
- Complex: addition of one or more frequency component(s) (not necessarily harmonic).
- One frequency jump: inclusion of one jump in frequency without time gap between the two frequency components.
- Frequency jumps: inclusion of more than one jump in frequency without time gaps between the two consecutive frequency components.
- Mixed: inclusion of a noisy (“unstructured”) part within a pure tone call.
- Unstructured: no pure tone component identifiable; “noisy” calls.
- Others: include all the calls that did not fit in any of the preceding categories (e.g., calls combining features of several of the previous call types).

Using USV data and the behavioural events extracted by Mice Profiler, we analysed the proportion of vocalisations emitted in each behavioural context.

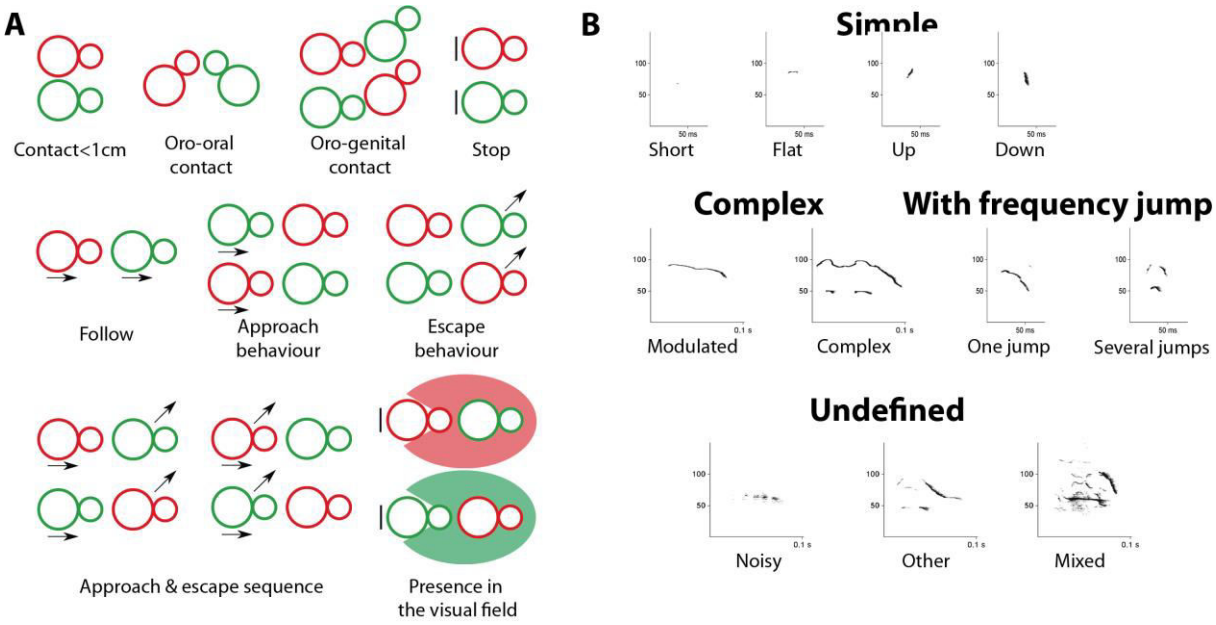

Figure 15: Representation of types of behavioural events and USVs observed during free-social interaction. *(A) Behavioural events detected by Mice Profiler during social interactions between the occupant (red) and the new-comer (green). (B) Spectrograms of the different call types used in the present call type classification*

II.G. *Male behaviour in presence of an oestrus female*

Initial condition:

- 100 lux, soundproof box, 50x25x30 cm cage
- put male in presence of female during 48 h one day before the test
- Isolation: 1 day for males

Protocol:

- 1st phase: the tested mouse was allowed to freely explore the test cage during 10 min for habituation period.
- 2nd phase: introduction of an unknown female in oestrus. Free exploration and interaction during 4 min.

Tested aspects of behaviour: Socio-sexual interest

The tested male was placed in the presence of a female during 48 hours. Then, they were isolated again during one day. During the test, the male was placed in the test cage (Plexiglas, 50 x 25 x 30 cm; 100 lux; with clean sawdust bedding) during 10 min for habituation (Ferhat et al. 2015). After this time, an unknown female in oestrus (tested through vaginal smears in the morning) was introduced into the test cage for 4 min. Both mice were allowed to freely interact. Social interactions as well as ultrasonic vocalisations were recorded, as described for the occupant-newcomer test.

II.H. *Three-chambered social test*

Initial conditions:

- Central compartment: 140 lux; outer compartment: 150 lux

Protocol:

- 1st phase: the tested mouse was allowed to freely explore the three chambers during 10 min for habituation period.
- 2nd phase: One mouse was placed under a wired cup in one of the outer compartments. Free exploration by the tested mouse during 10 min.
- 3rd phase: Another mouse was placed in the opposite outer compartment. Free exploration by the tested mouse during 10 min.

Tested aspects of behaviour: Social interest and social recognition

A Plexiglas cage was divided in three connected compartments as previously described (Nadler et al, 2004). Both side compartments contained an empty wire cup (side compartments: 150 lux; central compartment: 140 lux). First, the tested mouse was allowed to freely explore the setting, with doors open for 10 min (phase 1) for habituation. Then, the mouse was restricted in the central compartment, while an unfamiliar C57Bl/6J mouse of the same sex (stranger 1) was placed under one of the cups (sides alternated between each test). The tested mouse was then allowed to explore the apparatus for 10 min (phase 2). Then, it was restricted to the central compartment while another unfamiliar C57Bl/6J mouse of the same sex (stranger 2) was placed under the other cup. The tested mouse could then again freely explore the apparatus for 10 min (phase 3). In all three phases, the time spent in each compartment and the numbers of transitions between compartments were automatically recorded. The time spent in contact with the cup containing the mouse (stranger 1) and the time spent in contact with the empty cup were manually measured in phase 2 to evaluate social interest. The time spent in contact with the cup containing the unfamiliar mouse (stranger 2) and the time spent in contact with the cup containing the familiar mouse (stranger 1) were manually measured in phase 3 to evaluate social recognition.

II.I. *Behavioural statistics*

All group data are represented as mean ± standard error of the mean (S.E.M.), as well as the individual points. All statistics were performed with R software (R Core Team (R Foundation for Statistical Computing, Vienna,Austria) 2014). Between genotypes, the comparison was performed with Mann-Whitney tests. Between age points, the comparison was performed using paired Wilcoxon signed-rank tests. To analyse the variability within groups, the variances were compared using Ansari-

Bradley tests. If required, a Bonferroni correction was performed. Differences between groups were considered significant when $p<0.05$.

III. Biochemical & molecular biology test

III.A. *Tissue collection*

During the light phase, specifically between 9:00 and 11:00 AM, the mice were killed by CO_2 intoxication, followed by a cervical dislocation, at 12 months of age for the cohort 1 and at 4 months for the cohort 2 and *Shank2*/*Shank3* cohort. The brain was extracted and macro-dissected on ice (4°C) into HBSS solution by an experimented practitioner. We separated the hemispheres and extracted six brain structures: whole cortex, hippocampus, whole striatum, cerebellum, diencephalon, and brainstem. We stored the samples in different tubes, snap freezed them in liquid nitrogen and stored them at -80°C. These structures were used to perform RNAseq transcriptomic analysis and PCR validation.

III.B. *Total RNA extraction*

Total RNA was extracted from brain tissues using the miRNeasyPlus Micro Kit (Qiagen, Hamburg, Germany), following the manufacturer's instructions, including DNAse digestion. After first quality assessment using the Nanodrop spectrophotometer ND-1000 (Nanodrop, Thermoscientific, USA), the samples were analysed by the CNRGH (Centre National de Recherche en Génomique Humaine, CEA, Evry, France) testing the RNA integrity number (RIN) using bioanalzer2100 Agilent and RNA6000 Nano LabChip analysis on Bioanalyzer (Agilent Technologies, Santa Clara, California, USA). Then, an oriented mRNA sequencing was performed on samples with a RIN larger than eight.

III.C. *RNA-Seq samples*

Fifteen 12-months old male mice were used for the differential expression analysis: seven *Shank3*Δ*11*+/+, and eight *Shank3*Δ*11*-/- mice. Each of these mice had samples from four different brain regions (cerebellum, cortex, hippocampus, and striatum) except for one mouse in each group for which one sample was flagged by the Bioanalyzer QC step and discarded. These data were obtained from two batches of sequencing. RNA extraction was performed during the same day for the first batch and at two different days for the second sequencing batch. We refer to this variable containing three levels as the batch variable. Each sequencing run included two flow cells. The oriented mRNA

sequencing was performed on samples with a RIN larger than eight by CNRGH and sequenced in paired-end 100 bp.

III.D. *Mapping and reference genome*

The RNA-Seq reads were mapped to the genome with the STAR aligner v2.5.3a (Dobin et al. 2013) in 2-pass mode to a masked version of the *Mus Musculus* GRCm38 genome. During a first round of the differential gene expression analysis, we observed enrichment of the differentially expressed genes in genes located on the same arm of the chromosome 15 as Shank3. The potential difference of local genetic backgrounds of the *Shank3Δ11*-/- mice (129S1/SvImJ x C57Bl/6J) compared to the *Shank3Δ11*+/+ mice (C57Bl/6J) could affect the mapping by increasing the number of unmapped reads for the former in region with 129S1/SvImJ-specific variants. To avoid this bias, we masked the GRCm38 genome for variants of the 129S1/SvImJ mouse strain before mapping the sequencing reads. Variants were extracted from the VCF file provided by The Mouse Genome Project (Yalcin et al. 2012) (ftp://ftp-mouse.sanger.ac.uk/REL-1505-SNPs_Indels/mgp.v5.merged.snps_all.dbSNP142.vcf) and masked in the reference genome using the SNPsplit software (Krueger and Andrews 2016).

III.E. *Calling variants from the RNAseq data*

We followed the Gatk Best Practices (Van der Auwera et al. 2002) workflow for SNP and *indel* calling on RNA-Seq data (https://software.broadinstitute.org/gatk/guide/article?id=3891) which includes the following steps: (i) map to the reference genome with STAR in multi-sample 2-pass mode to get the most sensitive novel junction discovery; (ii) add read groups, sorting, marking duplicates, and create index, using Picard's tools (http://broadinstitute.github.io/picard); (iii) split reads into exon segments (removing Ns, but maintaining grouping information) and hardclipping sequences overhanging into the intronic regions, using the SplitNCigarReads Gatk tool; (iv) realign *indels* and recalibrate Base quality; (v) call variant with HaplotypeCaller, and finally filter the variants with VariantFiltration.

The last step was adapted to our project where several samples coming from the same mouse were available. HaplotypeCaller (with parameter -ERC BP_RESOLUTION) was called for each mouse individually using as input the processed BAM files coming from different brain tissues of the same mouse. Mice with the same *Shank3* status were then genotyped together by inputting the GVCF files to the Gatk tool GenotypeGVCFs. The *Shank3Δ11*+/+ and *Shank3Δ11*-/- specific VCF files were finally combined with the Gatk tool CombineVariants, which output allele frequency and specificity

of the variants to *Shank3Δ11*+/+ or *Shank3Δ11*-/- mouse populations. The resulting VCF file was filtered using the Gatk tool VariantFiltration using the parameters recommended in the Gatk workflow.

III.F. *Differential Expression Analysis*

The 18,194 genes with at least one count-per-million (CPM) in two samples were selected. The samples flagged by the QC Analyzer were filtered out. MDS plots showed separation of the samples according to brain regions, batches, and flow cells (Figure S10).

Differential gene expression (DGE) analysis was performed with limma-voom v3.34.8 (Law et al. 2014), and the version of *Voom* using sample-quality weights (Liu et al. 2015) (function *voomWithQualityWeights*) was used in order to take into account the sample heterogeneity observed within and across brain regions. The Trimmed Mean of *M*-values (TMM) method was used to calculate normalization factors between samples (Figure S 7). Four factors were included in the design matrix: the batch, the flow cell, the brain tissue and *Shank3* status combined into one factor of eight levels (Figure S 11). Since we were making comparisons both within and between mice, we treated the mouse as a random effect to adjust for baseline differences between subjects. To do so, the mouse was used as a blocking factor and the correlation between measurements made on the same mouse was computed using the function *duplicateCorrelation* and was input into the linear model fit; as suggested in the section "Multi-level Experiments" of the limma user guide. For each contrast of interest, the linear model was fit for each gene using the function *lmFit*, and empirical Bayes smoothing was applied to the standard errors using the function *eBayes* with robust mode set to TRUE. Plots were made in R with help of ggplot2 (Wickham 2009) and upsetR packages (Lex et al. 2014).

III.G. *Gene set analysis*

The ensemble of genes set enrichment analyses (EGSEA) (Alhamdoosh et al. 2017) available in the Bioconductor R package EGSEA v1.6.1 was used to combine the results of six methods of gene set enrichment analysis: camera, fry, and roast from the *limma* package (Ritchie et al. 2015), safe (Barry, Nobel, and Wright 2005) and gage (W. Luo et al. 2009) from the safe R package v3.18.0, globaltest R package v5.32.0 (Goeman et al. 2004), and over-representation analysis (ORA). The limma-voom output and the same contrasts as the one used for the differential expression analysis were input to the egsea function. The seven gene sets available for the mouse species were used: collections h, c1 to c7 of the MSigDB database (Subramanian et al. 2005) and KEGG (Kanehisa et al. 2012). Gene sets were ranked by their average ranks obtained across methods.

III.H. *RNA isolation and dd-PCR*

We selected several genes for validation by cross-checking list of DEG, EGSEA (gene ontology – GO – and Kyoto encyclopaedia of genes and genomes – KEGG), and data from the literature. To validate the genes of interest, a droplet digital Polymerase Chain Reaction (dd-PCR) was performed. First, total RNA of each sample was extracted following the previous protocol. Then cDNA-bank was generated using the kit iScript advanced cDNA (Bio-Rad, France) and following the manufacturer's instructions.

The cDNA of the samples were added into the dd-PCR supermix for probes (no dUTP) with primer – housekeeping primer dye was HEX and interesting primer dye was FAM –, mixed thoroughly and centrifuged. The housekeeping gene used was GAPDH. Next, samples were partitioned into, at least, 12000 droplets with c-DNA randomly distributed. Then, samples were transferred to a 96-well PCR plate and heat-sealed with a tinfoil sheet. PCR was conducted with the QX100 droplet digital PCR system (Bio-Rad). The thermo-cycling conditions were as follow: pre-incubation at 95°C for 5 min, amplification (denaturation: 95°C for 30 s; annealing: 52°C for 30 s; extension: 72°C for 45 s) for 40 cycles, followed by 72°C extension for 7 min. Results were analysed by the QuantaSoft Software according to the instructions. All statistics were performed with R software (R Core Team (R Foundation for Statistical Computing, Vienna,Austria) 2014). Between genotypes, the comparison was performed with Mann-Whitney tests.

III.I. *Protein-protein interaction network analysis*

Based on BioGRID database for *Mus Musculus* (https://thebiogrid.org/) (Chatr-aryamontri et al. 2017), we analysed the protein-protein interaction (PPI) network for DEGs for all brain structures independently. A randomisation of interactome using all genes detecting by RNAseq were performed to determine the p value. Cystoscape v3.6.1 was used to visualize the protein-protein interaction network to find out key genes. A randomisation of interaction of gene was performed to determine the probability of finding a network.

RESULTS

I. Molecular and behavioural characterisation of *Shank3Δ11* mutant mice

I.A. *Context*

As we saw in the introduction (see III.B.1), patients with a mutation in *SHANK3* display a large spectrum of phenotypes with a regression in adolescence and adulthood (De Rubeis et al. 2018; Guilmatre et al. 2014). However, little is known about the causes of this phenotypic worsening. Based on this observation in humans, we hypothesise the presence of different behavioural trajectories in mouse models. Testing this hypothesis will allow a better understanding of the correlation between *Shank3* expression and phenotype.

Here, we propose to characterise the *Shank3*Δ11 mouse model in a longitudinal study to observe the evolution of the phenotype. To examine the molecular bases of phenotypic differences and evolution between genotype and individuals, we realised a transcriptomic characterisation over four brain structures. The results are presented as an article manuscript.

I.B. *Article manuscript*

Atypical expression profile in the striatum of *Shank3Δ11* mutant mice might explain behavioural impairments

Allain-Thibeault Ferhat 1,2,3, Anne Biton 5, Anne-Marie Le Sourd 1,2,3, Anne Boland 6, Bertrand Fin 6, Elodie Ey 1,2,3 &Thomas Bourgeron 1,2,3

1 Unit of Human Genetics and Cognitive Functions, Institut Pasteur, Paris, France
2 CNRS UMR 3571 'Genes, synapses and cognition', Institut Pasteur, Paris, France
3 University Paris Diderot, Sorbonne Paris Cité, Human Genetics and Cognitive Functions, Paris, France
5 Centre de Bioinformatique, Biostatistique et Biologie Intégrative (C3BI, USR 3756 Institut Pasteur et CNRS), Paris, France
6 Centre National de Génotypage, Institut de Génomique, CEA, Evry, France

Correspondence

Pr. Thomas Bourgeron,
Human Genetics and Cognitive Functions Unit, Institut Pasteur,
25 rue du Docteur Roux, 75015, Paris, France,
thomasb@pasteur.fr,
+33 1 40 61 32 16

Running Title

Behavioural and transcriptomics impairment of *Shank3Δ11*-/- mice

Introduction

Autism Spectrum Disorders (ASD) are a group of psychological neurodevelopmental disorders based on two main criteria: an alteration of social communication and interaction associated with stereotyped behaviours and restricted interests (American Psychiatric Association 2013). ASD are strongly associated with genetic features and over 800 genes were associated with a higher risk for ASD. An important part of these genes encodes proteins expressed in the synaptic area of excitatory or inhibitory neurons, for example *Neuroligin* (*NLGN), Neurexin (NRXN)*, or the *SHANK* family. The *SHANK* gene family is composed by three genes: *SHANK1, SHANK2/PROSAP1* and *SHANK3/PROSAP2*. Around 1% of patients with ASD show a mutation in one of these genes, and more than 1% of patients with ASD and intellectual disabilities (ID) carry a mutation in *SHANK3* (Leblond et al. 2014)**.** The *Shank* gene family encodes proteins located in postsynaptic density (PSD) of glutamatergic synapses. These proteins are composed by several interaction domains that interact with other synaptic proteins (Monteiro and Feng 2017).

Several studies showed an important variability in patients carrying a mutation in *SHANK3,* ranging from ASD to other psychiatric disorders such as schizophrenia or bipolar disorders (Guilmatre et al. 2014). Furthermore, several studies revealed a regression of the patient during the adolescent and the adulthood (Guilmatre et al. 2014; De Rubeis et al. 2018). However, no study explored the bases of this variability or regression.

To evaluate and understand the behavioural consequences of the deletion of *Shank3*, we use the mouse model previously described carrying a mutation in exon eleven (Schmeisser et al. 2012; Vicidomini et al. 2017). This mutation allows the expression of 3 among the 6 Shank3 main isoforms: Shank3 d, e and f (Figure 8) (X. Wang et al. 2014). In previous analysis of this model, impairment in social interaction and stereotyped behaviour were revealed with dysregulation in the expression of synaptic proteins (Schmeisser et al. 2012; Vicidomini et al. 2017)

In this study, we characterised the behaviour of this model with a focus on social communication and interaction. We furthermore compared the behavioural results to the RNA expression.

Methods Summary

Experimental procedures

A full description of the methods used (behavioural test, tissue and RNA acquisition and processing, data generation, validation, analyses and statistics) is provided in the material and methods section of the present thesis.

Animals

All procedures were performed according to the guidelines for the welfare of experimental animals of Ministry of agriculture of France and they were approved by the ethical committee CETEA n°89 (Institut Pasteur, Paris, France). *Shank3* mice were generated by Genoway (Lyon, FRANCE) (Schmeisser et al. 2012). They were raised on a C57Bl/6J background (more than 15 backcrosses). The *Shank3* mice displayed a deletion in exon 11. In this model, only 3 isoforms remained expressed, *Shank3-d*, *Shank3-e* and *Shank3-f.* All analyses were performed on mice whose genotype was unknown to the experimenter.

Behavioural assays

Behavioural tests were performed on homozygous *Shank3*+/+, heterozygous *Shank3*+/- and homozygous *Shank3*-/- male and female mice at three, eight and twelve months of age. The behavioural characterisation included Y-maze working memory test, dark/light anxiety test, open field, three-chambered social test, stereotyped behaviour observation, occupant/new-comer social test with ultrasonic vocalisations (USV) recording, male behaviour in presence of an oestrus female with USV recording, and observation of barbering and allo-grooming.

RNA analysis and validation

Brains were extracted from 12 months old male mice and were dissected to collect whole cortex, whole striatum, hippocampus and cerebellum. Total RNA of each structure was extracted using miRNeasyPlus Micro Kit (Qiagen, Hamburg, Germany). The cDNA and oriented mRNA sequencing were performed on samples with a RIN larger than eight by CNRGH (Centre National de Recherche en Génomique Humaine) and sequenced in paired-end 100bp . The gene validation was performed using a droplet digital Polymerase Chain Reaction (dd-PCR) (Bio-Rad, France).

Data analysis

All group data of behaviour were presented as mean ± standard error of the mean (S.E.M.), as well as the individual points. The RNA-Seq reads were mapped to the genome of the *Mus Musculus* GRCm38 genome. Differential analysis and gene set analysis were performed using R software. Protein-protein interaction (PPI) analysis is based on BioGRID database (Chatr-aryamontri et al. 2017). All statistics were performed with R software (R Core Team (R Foundation for Statistical Computing, Vienna,Austria) 2014). Between genotypes, the comparison was performed with Mann-Whitney tests. Between age points, the comparison was performed using paired Wilcoxon signed-rank tests. To analyse the variability within groups, the variances were compared using Ansari-Bradley tests. Differences between groups were considered significant when $p<0.05$.

Results

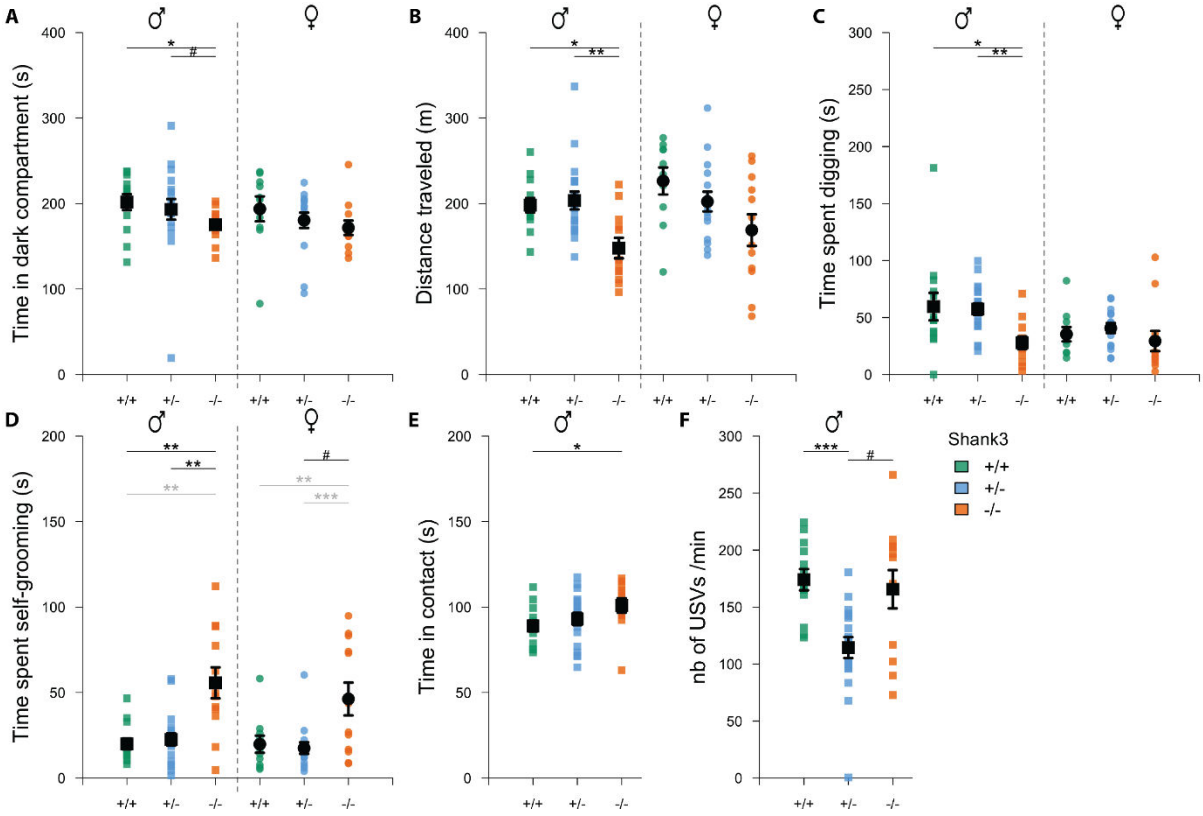

Figure 16: Shank3-/- mice displayed reduced activity and increased stereotyped behaviour at three months of age. *(A) Total time spent in the dark compartment in a 5-min dark-light anxiety test in Shank3+/+ (green), Shank3+/- (blue) and Shank3-/- (orange) mice, for males (left panel) and females (right panel). (B) Total distance travelled during 30 min of free exploration of an open-field in males (left panel) and females (right panel). (C) Total time spent digging, i.e. moving the bedding with front and/or hind legs, during 10 min observation in a test cage (after 10 min habituation) for males (left panel) and females (right panel). (D) Total time spent self-grooming during 10 min observation in a test cage with fresh bedding (after 10 min habituation), for males (left panel) and females (right panel). (E-F) Total time spent in contact (E) and rate of ultrasonic vocalisations emitted (F) during free male-female social interaction. Mann–Whitney U test, with Bonferroni correction for multiple testing (in black): #p<0.1, *p<0.05, **p<0.01, ***p<0.001; Ansari-Bradley test, with Bonferroni correction for multiple testing (in grey): #p<0.1, *p<0.05, **p<0.01, ***p<0.001; data are presented as mean ± s.e.m. (black squares and circles); 12–14 mice per group.*

Mild behavioural differences at three months of age:

At three months of age, *Shank3*-/- males and females did not display a significantly different weight between genotypes (Figure S 3.A). In the dark-light anxiety-like test, *Shank3*-/- male mice spent a slightly shorter time in the dark compartment of the test box in comparison with their wild-type littermates (W=122, p=0.048; Figure 16.A), suggesting that *Shank3*-/- male mice are less anxious than *Shank3*+/+ and *Shank3*+/- mice. No significant difference was observed between *Shank3*+/+ and *Shank3*+/- females. No significant difference was observed between *Shank3*+/+, *Shank3*+/- and *Shank3*-/- mice of both sexes in the latency to enter the dark compartment (Figure S 3.B). In the second cohort, no significant difference was observed in the elevated-plus maze or in the dark-light anxiety-like test (Figure S 4.A-B). In the Y-maze test to evaluate working memory, contrary to our expectations, *Shank3*-/- female mice displayed a tendency of higher proportion of perfect alternations

in comparison with *Shank3*+/+ female mice (W=24.5, p=0.063, Figure S 3.C). However, this might be explained by the level of alternations close to chance level (50 %) of Shank3+/+ mice.

Hypoactivity is one of the major and stable deficits found in *Shank3*-/- mouse models (M. Yang et al. 2012; X. Wang et al. 2011; Jaramillo et al. 2017; Kabitzke et al. 2017). In our study, during 30 min free exploration of an open-field, *Shank3*-/- males also travelled a significantly shorter distance in comparison with *Shank3*+/+ males (W=130, p=0.011) and *Shank3*+/- males (W=187, p=0.007; Figure 16.A, left panel). There were no significant genotype-related differences in the distance travelled by females, despite a trend for lower activity in Shank3-/- mice (W=92, p=0.107; Figure 16.A, right panel). We replicated these results in a second cohort, where both Shank3-/- males (W=151, p=0.039) and *Shank3*-/- females (W=35, p=0.008) displayed a reduced activity in comparison with *Shank3*+/+ mice of the same sex (Figure S 4.C). Since the performance of *Shank3*-/- mice in the rotarod test did not differ significantly from other genotype (Figure S 4.F), the reduced activity of *Shank3*-/- mice in the open-field could not be explained by an impaired motor coordination and could reflect a reduced interest in exploration.

As a parallel to the reduction of exploratory activity, *Shank3*-/- male mice spent less time digging in the bedding in comparison with Shank3+/+ (W=123, p=0.041) and *Shank3*+/- male mice (W=194, p=0.002; Figure 16.C). This observation was validated by the analysis of the second cohort, with a decrease of digging behaviour for *Shank3*-/- male compared to *Shank3*+/+ (W=173, p=0.001) and *Shank3*+/- male mice (W=150, p=0.001; Figure S 4.E).

Stereotyped behaviour is one of the major diagnosis criteria in ASD. In mice, we evaluated it by measuring the time spent in self-grooming behaviour. In an observation cage with fresh bedding, *Shank3*-/- male mice displayed a significant increase in the time spent self-grooming in comparison with *Shank3*+/+ males (W=21, p=0.004) and *Shank3*+/- males (W=40, p=0.006; **Figure 16**.D). A similar trend was observed in females, with *Shank3*-/- female mice spending more time self-grooming in comparison with *Shank3*+/+ females (W=29, p=0.128) and Shank3+/- females (W=45, p=0.084; Figure 16.D). Interestingly, a subset of *Shank3*-/- males and females increased their self-grooming behaviour to such an extent that it leads to hair removal. The inter-individual variability in the time spent self-grooming was indeed significantly higher in *Shank3*-/- mice in comparison with *Shank3*+/+ mice (male: AB=111, p=0.036; female: AB=82, p=0.009; Figure 16.D) and *Shank3*+/- mice (female: AB=144, p=0.001). In the second cohort, *Shank3*-/- males still displayed an increased time spent self-grooming in comparison with *Shank3*+/+ males (W=43, p=0.033), but this was not verified in females anymore (Figure S 4.D).

Atypical social interaction is the other major diagnosis criterion in ASD. As a standardised test to evaluate the interest in social interactions, we performed the three-chambered test. We did not reveal any significant impairment since mice of all three genotypes displayed a significant preference for sniffing the inverted cup containing a conspecific in comparison with the empty cup (males: Shank3+/+: W=156, p<0.001; Shank3+/-: W=350, p<0.001; Shank3-/-: W=128, p<0.001; females:

Shank3+/+: W=89, p=0.002; Shank3+/-: W=233, p<0.001; Shank3-/-: W=144, p<0.001; **Figure S 4**.C-F).

To analyse social communication at a finer level of details, we tested free same-sex social interactions. During male-male or female-female social interactions at three months of age, the time spent in contact, the latency of first contact and the time spent in the different types of contacts and social events did not differ significantly between *Shank3*+/+, *Shank3*+/- and *Shank3*-/- mice (Figure S 5.D & G).

In contrast, when we tested the interaction of a male with a C57Bl/6J female in oestrus, we observed a significant increase of the total time in contact for *Shank3*-/- mice in comparison with *Shank3*+/+ mice (W=32, p=0.034; Figure 16.E). A part of this increase may be explained by an increase of the time spent in oro-oral contact (W=22, p=0.008; Figure S 5.A). Moreover, we observed a decrease of the time spent by the female in the visual field of a *Shank3*-/- male in comparison with the time spent by the female in the visual field of a *Shank3*+/+ male (W=133, p=0.009). The total number of ultrasonic vocalisations recorded did not differ significantly between interactions involving *Shank3*+/+, *Shank3*+/- or *Shank3*-/- male mice (Figure 16.F). However, we quantified the proportion of ultrasonic vocalisations emitted during social events. We observed a significant increase of ultrasonic vocalisations emitted during oro-oral contact for *Shank3*-/- mice in comparison with *Shank3*+/+ mice (Figure S 5.H) but no significant difference between the type of USVs emitted (Figure S 5.I).

Longitudinal study of the deficits observed at 3, 8 and 12 months of age

We followed longitudinally the same cohort of *Shank3* mutant mice to describe the evolution of the phenotype with increasing age. We focused on exploratory activity (open-field free exploration), stereotyped behaviours as well as social interactions and communication.

In the openfield test, *Shank3*+/+ and *Shank3*+/- mice reduced their activity with increasing age (Figure 17.A). In contrast, Shank3-/- mice were already travelling short distances at three months of age, and did not change their activity levels with increasing age (Figure 17.A). Because of these two different trajectories, the hypoactivity of Shank3-/- mice remained significant only at three (see above) and eight months of age (males: W= 132, p= 0.007) when compared to *Shank3*+/+ mice. At twelve months of age, the levels of activity of *Shank3*+/+, *Shank3*+/- and *Shank3*-/- mice were similarly low.

Digging behaviour was not affected by increasing age in the same way as activity levels. Indeed, the profiles of *Shank3*+/+, *Shank3*+/- and *Shank3*-/- mice evolved in parallel. Digging behaviour remained reduced in *Shank3*-/- male mice in comparison with *Shank3*+/+ males (eight months: W= 140, p= 0.001; twelve months: W=107, p=0.024) and Shank3+/- males (eight months: W= 189, p= 0.002; twelve months: W=189, p=0.022; Figure 17.B). In contrast, only eight-months old Shank3-/- females dug for significantly shorter times than *Shank3*+/+ age-matched females (W=91, p=0.030).

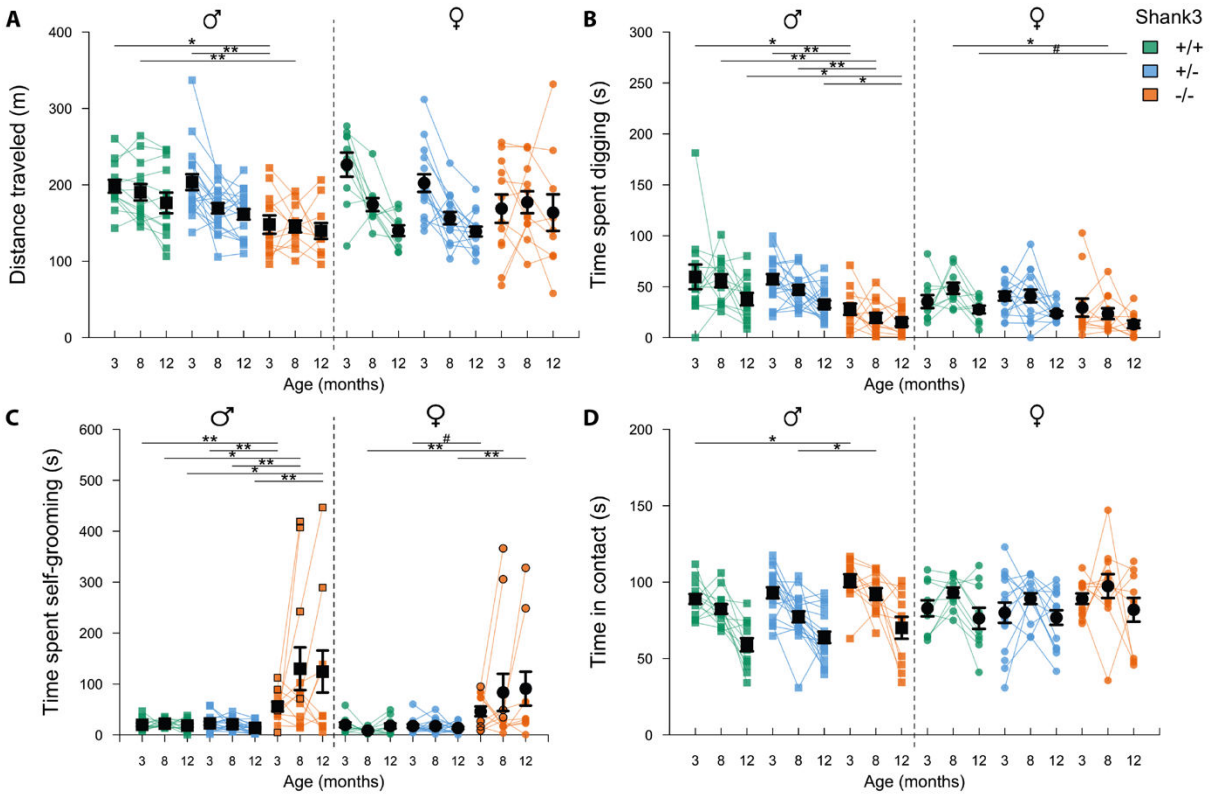

Figure 17 Shank3-/- mice displayed a significant worsening of self-grooming abnormalities with increasing age, while locomotion and exploration were mildly affected. *(A) Total distance travelled during 30 min of free exploration of an openfield in Shank3+/+ (green), Shank3+/- (blue) and Shank3-/- (orange) mice, at three, eight, and twelve months of age, for males (left panel) and females (right panel). (B) Total time spent digging during 10 min observation in a test cage, at three, eight, and twelve months of age, for males (left panel) and females (right panel). (C) Total time spent self-grooming during 10 min observation in a test cage with fresh bedding, at three, eight, and twelve months of age, for males (left panel) and females (right panel). (D) Total time spent in contact during free male/female social interaction (left panel) or female/female social interact (right panel), at three, eight, and twelve months of age. Mann–Whitney U test, with Bonferroni correction for multiple testing: #p<0.1, *p<0.05, **p<0.01, ***p<0.001; data are presented as mean ± s.e.m. (black squares and circles); 12–14 mice per group.*

The evolution with increasing age of the time spent self-grooming differed between *Shank3*+/+, *Shank3*+/- and *Shank3*-/- mice. Indeed, the level of self-grooming remained stable over ages in *Shank3*+/+ and *Shank3*+/- mice (Figure 17.C). In contrast, the level of self-grooming tended to increase with age in *Shank3*-/- mice. In line with the observation at three months of age, Shank3-/- male groomed themselves for significantly longer time in comparison with *Shank3*+/+ mice (eight months: W= 27, p= 0.014; twelve months: W=25, p=0.062) and Shank3+/- mice (eight months: W= 30, p= 0.003; twelve months: W=26, p=0.004). Interestingly, the inter-individual variability was significantly increased in Shank3-/- mice compared to *Shank3*+/+ and *Shank3*+/- mice (*Shank3*-/- vs *Shank3*+/+ at eight months for males: AB=118, p=0.002; and females: AB=75, p=0.044; at twelve months for males: AB=102, p<0.001; *Shank3*-/- vs *Shank3*+/- at eight months for males: AB=181, p=0.005; at twelve months: males: AB=180, p<0.001). Four *Shank3*-/- males and four Shank3-/- females showed an impressive worsening of the phenotype, displaying at eight and/or twelve months of age a level of self-grooming equivalent to three times more the level displayed at three months of

age (Figure 17.C). Among these over-groomed animals, two males and two females had to be killed before the end of the experiment at eight months of age because of self-inflicted injuries.

Social interactions during female-female encounters did not differ significantly between age classes in any genotype, and therefore, similarly to the results at three months of age, no genotype-related significant differences were observed at eight and twelve months of age in any variable measured (Figure 17.D, right panel, & Figure S 5.E & F). In contrast, during male/female social interactions, we observed an increase in the duration of nose-to-nose sniffing at eight months of age in *Shank3*-/- compared to *Shank3*+/+ mice (W=29, p=0.025) and *Shank3*+/- (W=48, p=0.035), similarly to what we found at three months of age (Figure S 5.B). These differences were not significant any more at twelve months of age (Figure S 5.C). Nevertheless, we detected an increase of approach/escape behaviour of C57Bl/6J females toward the *Shank3*-/- male in comparison with C57Bl/6J females toward the *Shank3*+/+ male (W=15.5, p=0.007, Figure S 5.C).

Major effects of the Shank3 mutation in the striatum

We dissected the brains of the mice after they completed the behavioural tests at twelve months of age. We generated RNA-Seq data from four brain structures (whole cortex, striatum, hippocampus and cerebellum) of seven *Shank3*-/- mice and eight *Shank3*+/+ mice (Table S 1)

First, as expected, *Shank3* expression level was significantly reduced in Shank3-/- mice in comparison with *Shank3*+/+ mice in all four brain structures (whole cortex: B=7.6, p<0.001; striatum: B=12.2, p<0.001; hippocampus: B=12.6, p<0.001; cerebellum: B=19.4, p<0.001; Suppl. Fig. S8A). The *Shank3* expression level was not null since *Shank3*-/- mice are deleted for exon 11 and still expressed some Shank3 isoforms (Figure S 9.A &D). Expression levels of *Shank1* and *Shank2* in the cortex, hippocampus, and cerebellum were not significantly impacted by the reduced expression of *Shank3* since no significant variations were found between *Shank3*+/+ and *Shank3*-/- mice (Figure S 9.B & C) as previously reported (Boeckers et al. 2005; Peça et al. 2011). Contrary to a previous study (Peça et al. 2011), we detected *Shank1* and *Shank2* transcripts in the striatum. We observed no link between the expression level of *Shank1*, *Shank2* or *Shank3* and the behavioural variability (Figure S 9).

Second, we studied the genes that were differentially expressed between *Shank3*+/+ and *Shank3*-/- mice (with an adjusted p-value <0.05) across and within structures (Tables S 3). *Shank3* was one of the top differentially expressed genes (DEG) in all comparisons. In the comparisons across all structures, 24 out of 69 DEG were located in the vicinity of the *Shank3* locus on chromosome 15 (Figure 18.A; Figure S 10.A). The local genetic background differs between *Shank3*-/- (129S1/SvImJ x C57Bl/6J) and *Shank3*+/+ (C57Bl/6J) mice. This can explain the presence of DEG around *Shank3* position revealed by RNA-Seq (see Methods). In the region spanning between 10.4 Mb upstream and 7.5 Mb downstream of *Shank3*, many single nucleotide polymorphisms (SNP) differing from the reference genome of C57Bl/6J mice were found in *Shank3*-/- mice, but not in *Shank3*+/+ mice (Figure S 10.B-C). Given that this increased number of SNP in chromosome 15 might be related to the

residues of the 129S1/SvImJ genome (due to the genetic construction of the *Shank3* mutant mice), all genes from this region were considered separately in the following analyses.

We next examined the DEG within each of the four brain structures. The striatum included 186 DEG (adjusted p-value <0.05; including 23 genes from chromosome 15), with 88 genes overexpressed in *Shank3*-/- mice (log-Fold-Change>1) and 98 genes underexpressed in *Shank3*-/- mice (logFC<1; Figure 18.A, left panel) in comparison with wild-type mice. By comparison, the hippocampus displayed 33 DEG (logFC>1: 18; logFC<1: 15), the cortex 22 DEG (logFC>1: 8; logFC<1: 14) and the cerebellum 24 DEG (logFC>1: 5; logFC<1: 19; Figure 18.A, left panel). DEGs with a log-fold-change larger than one in absolute value are shown in Figure S 8.A. A large majority of the DEG found in the striatum (163 over 186) was specific to this structure and was not found in any other brain structure (Figure 18.A, right panel). Only a few genes were found differentially expressed in all or at least three brain regions, most of them being located around *Shank3* locus except for two of them (Rpl3-ps1 and Gm12906). The DEG in the striatum displayed an increased dispersion compared to the other structures, indicating an increased variability of response between animals (Figure S 8.B, panel up-right).

Impairments of striatal pathways in *Shank3*-/- mice

We used the ensemble of gene set enrichment analyses (EGSEA) method (Alhamdoosh et al. 2017) to annotate the functions of the DEG and performed a pathway analysis over all brain structures. We selected pathways associated with cellular mechanisms and pathways involved in the brain, with an adjusted p-value above 0.05 and at least one DEG selected Figure 18.B). We found no significant pathway in the cortex and only few pathways in the cerebellum ("PI3K signalling") and in the hippocampus ("Tryptophan metabolism"). From here now, we focus on the striatum that revealed several sub-cellular pathways impacted by the *Shank3* mutation revealed by the EGSEA method (Figure 18.B; see hereafter).

First, we found enrichment in gene sets associated with the dopaminergic pathway (Figure 18.B). The DEG in the striatum were enriched (Fisher test p-value < 0.02) in five clusters of genes previously identified from scRNA-Seq data as markers of GABAergic medium spiny neurons (MSN) in the striatum (Gokce et al. 2016): D1-MSN, D1-Cxcl4-MSN, D1-Tacr1-MSN, D2-MSN, and D2-Htr7-MSN. Almost all genes with an adjusted p-value above 5% associated with D1-MSN were under-expressed in *Shank3*-/- mice in comparison with *Shank3*+/+ mice (Figure 19.A). In contrast, almost all genes associated with D2-MSN were overexpressed in *Shank3*-/- mice (Figure 19.A), like Tropomyosin 1 (TPM1), a gene strongly associated with D2-MSN and displaying an important increase in *Shank3*-/- mice in comparison with *Shank3*+/+ mice (logFC: -0.25; adj.p=0.011). Then, the D1 and D2 MSN are GABAergic neurons that generate GABA from glutamate with the glutamate decarboxylase (Gad). The *Shank3*-/- mice display an increase of gene expression of Gad2 in striatum

(Figure S 12). Glutamatergic pathways in striatum were also impacted according to EGSEA analysis. The expression of glutamatergic receptors and associated proteins is impacted in *Shank3*-/- mice.

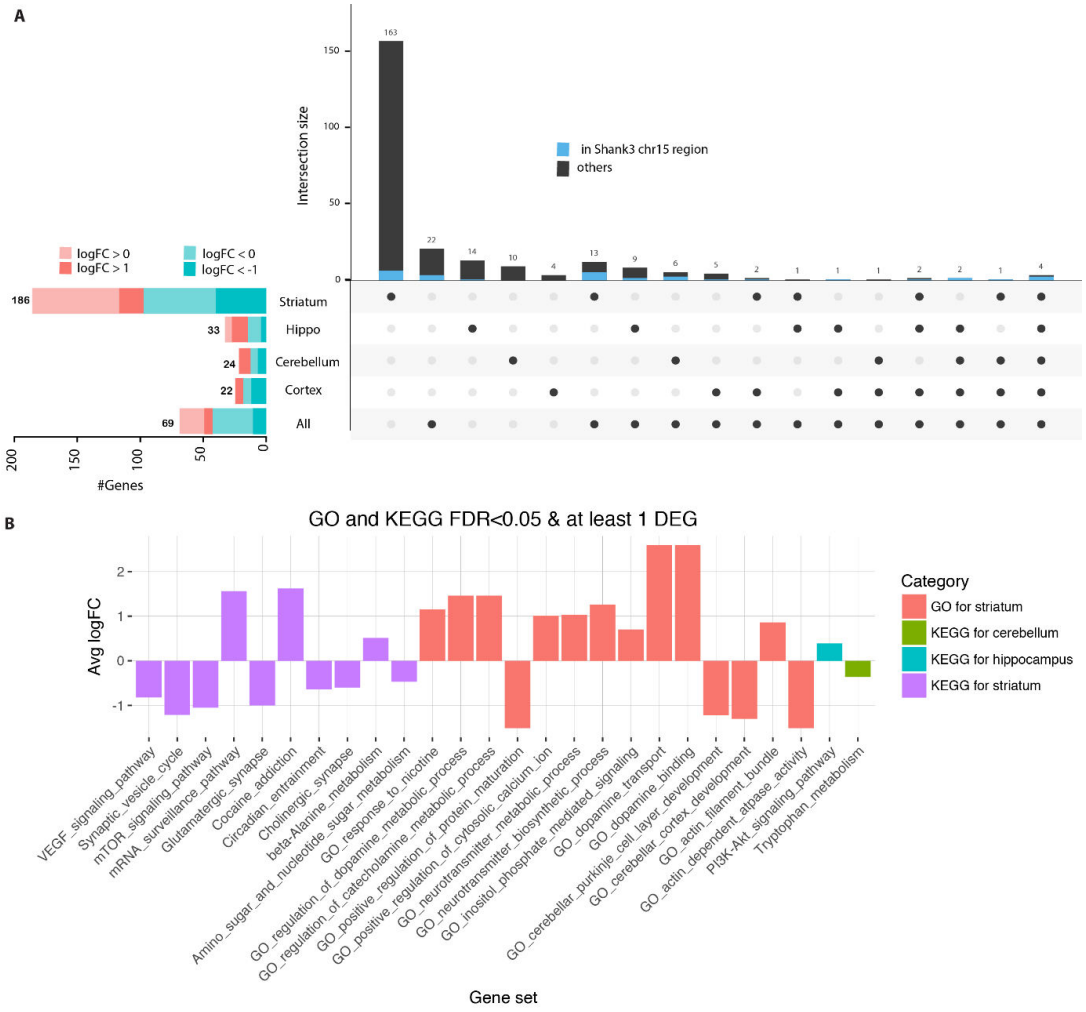

Figure 18: The striatum displayed the largest gene expression differences between Shank3+/+ and Shank3-/- mice and the largest number of impacted pathways. *(A) Upset plot displaying the intersection between brain structures for the genes differentially expressed between Shank3-/- and Shank3+/+ mice (adjust p-value < 5%; determined by limma-voom using observation quality weights). Genes located around the Shank3 region in chromosome 15 are shown in blue. The horizontal bar plots on the left show the number of differentially expressed genes in the different brain regions according to the value of their log-fold changes. (B) Average logarithmic fold change (avg logFC) of GO or KEGG pathways with an adjusted p-value < 0.05 and at least one differentially expressed gene in the striatum (GO: red; KEGG: purple), cerebellum (KEGG: green) and hippocampus (KEGG: blue); the white number indicate the number of DEG in the pathway.*

The metabotropic glutamate receptor 2 (Grm2; logFC: -1.66; adj.p=0.015) and protein kinase c type g (Prkcg; logFC:-0.67; adj.p=0,016) are both under-expressed, while the Glutamate Ionotropic Receptor Kainate (Grik2; logFC: 0.49; adj.p=0.042) is overexpressed. Interestingly, Cornichon Family AMPA Receptor Auxiliary Protein 3 (Cnih3; logFC: -1.19; adj.p=0.002), a protein modulating the activation of glutamate AMPA receptor, are under-expressed.

Protein-protein interaction analysis

The PPI analysis was performed on all brain structures. The majority of DEG for each structure was not annotated in BioGRID database (striatum: 71/186 DEGs; hippocampus: 7/33 DEGs, cerebellum: 4/24 DEGs, cortex: 3/22 DEGs). The proteins annotated in hippocampus, cortex and cerebellum did not reveal any known network. However, two networks were highlighted by PPI analysis in the striatum (p-value: 0,029) (Figure 19.B). They were composed by eight proteins directly or indirectly interacting with *Shank3*, including Grm2, Slk, Camk2g, Dlgap1 (GKAP), Prkcg, Lnx1, Srgap1 and Unc13band as well as two proteins associated with G-proteins (Gnal and Ric8b). These proteins are involved in the signalling transduction in post-synaptic glutamatergic synapses. This analysis revealed impairment in signalling pathway in striatum.

Discussion & conclusion

Shank family, and especially *Shank3*, are some of the most expressed proteins in PSD of glutamatergic synapses (Sheng and Hoogenraad, 2007). Furthermore, several studies showed *Shank3* is also expressed in nucleus and is implicated in DNA regulation via HDAC2 (X. Wang et al. 2014; Qin et al. 2018).

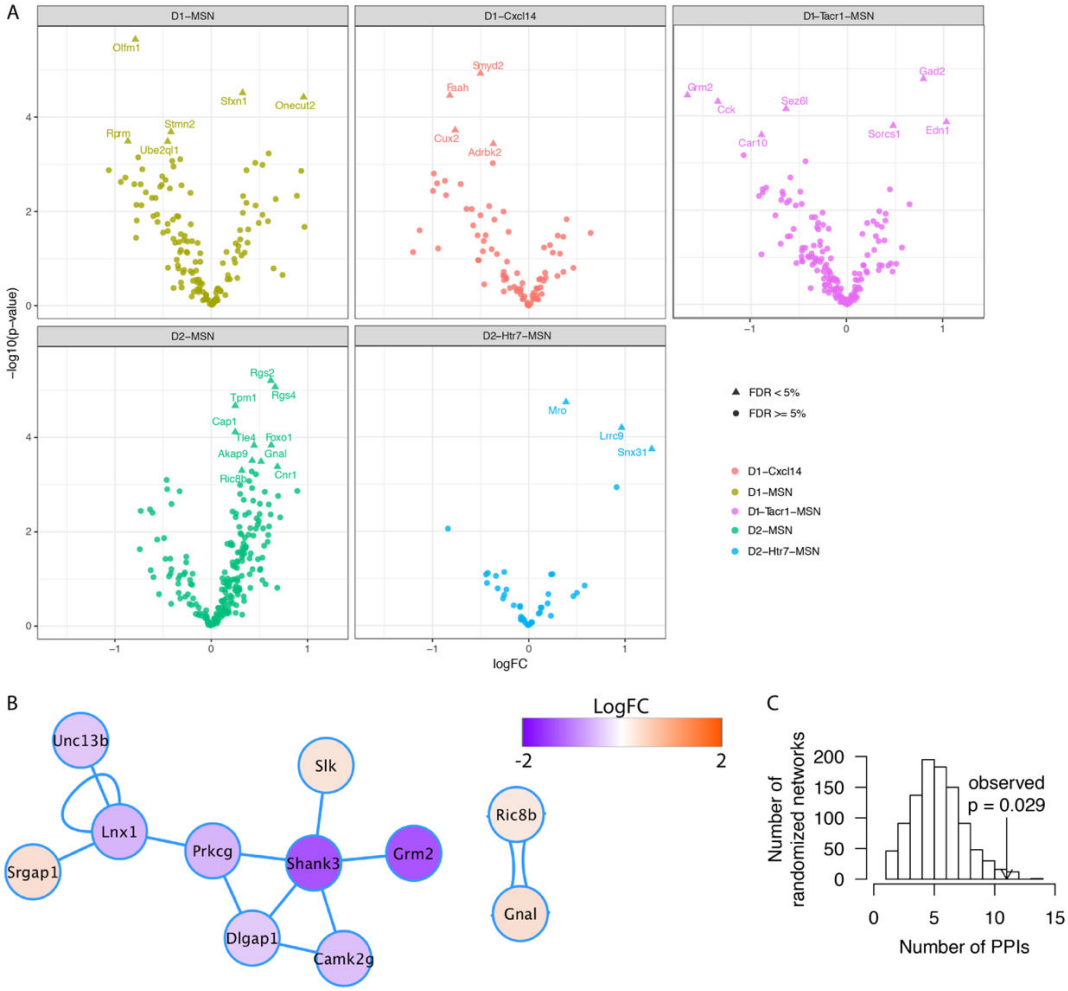

Figure 19: Genes were overexpressed in D2-MSN and underexpressed in D1-MSN in the striatum. *(A) Based on specific gene expression in D1-MSN (D1-MSN in yellow; D1-Cxcl14 in red; Tacr1-MSN in purple) and D2-MSN (D2-MSN in green and Htr7-MSN in blue). Logarithmic p-value and logarithmic fold change were presented. Annotated genes have an adjust p-value < 5%. (B) Protein-protein interaction network for the differentially expressed genes (DEGs). Node represents protein, edge represents interaction between proteins. The colour of the node represents the LogFC of DEG: Red means up-regulation and blue means down-regulation in Shank3-/-. C. Number of randomized networks based of proteins in B*

Our analysis on behaviour and transcriptomic revealed some interesting molecular bases of the impairment generated by a *Shank3*Δ11 mutation.

In our study, we revealed impairments in ASD core symptoms for *Shank3*-/- mice. The mice displayed stereotyped behaviours, via an increase of self-grooming behaviour, and increase of socio-sexual interaction compared to *Shank3*+/+ mice. We also observed impairment in exploratory behaviour, via the distance travelled in the openfield as well as in digging behaviour, but not in locomotor capacity. Interestingly, we observed a worsening of the phenotype represented by an increase of self-grooming behaviour over the different time points. This aspect can be related with observed regression in patients and can be linked to altered gene expression in the striatum at a later age (De Rubeis et al. 2018).

Then, using RNA sequencing, we detected an imbalance between D1-MSN and D2-MSN in the striatum. A previous analysis of MSN showed a reduction of synaptic strength in D2-MSN in *Shank3*Δ13-16 model (W. Wang et al. 2017), which could support our results. The D1-MSN and D2-MSN are involved in two behavioural circuits: the reward system and the locomotor control. However, in the present work, we cannot define the implication of the dorsal or ventral striatum, as well as the modulation of synaptic strength of D1-MSN or D2-MSN. Further behavioural analyses will provide complementary information. We would suggest to use social reward test and addiction test, associated with *Shank3* mouse models conditionally mutated in the striatum and especially in D1-MSN or D2-MSN.

Furthermore, RNA sequencing revealed a decrease of G-protein-coupled receptors and proteins involving in signaling pathway. This modulation of the signalling will impair the expression of several genes, particularly in the striatum. Considering the antagonist mechanisms for D1-MSN and D2-MSN and the relation between dopamine and glutamatergic receptors, impairments in glutamatergic synaptic signalling may have opposite effect for both types of striatal neurons (Beaulieu and Gainetdinov 2011).

Based on all observations, mutations in Shank3 PDZ domains, and likely the loss of Shank3a-b-c, seem to impair the gene expression of synaptic signalling proteins. Two hypotheses can be drawn. First, the suppression of *Shank3* dysregulates the expression of proteins, mainly those involved in cell signalling (X. Wang et al. 2014; Qin et al. 2018). Second, the suppression of the ANK, SH3 and PDZ domains does not allow the recruitment of signalling proteins, leading to a reduction of those proteins. In both cases, the reduction of signalling proteins generates impairment in signal transduction, especially in striatum. This impairment in cell signalling has an opposite effect between D1-MSN and

D2-MSN that will impair controlled locomotor activities, generating stereotyped behaviour, or affect the reward circuit, generating unusual social interaction.

A deeper analysis of striatum and MSN could provide new pharmaceutical approach targeting the imbalance in MSN. It might also provide complementary information on the worsening of the phenotype observed in mice to better understand the evolution of the patient phenotype and probably identify new therapeutic pathways or validate already used treatment, such as lithium.

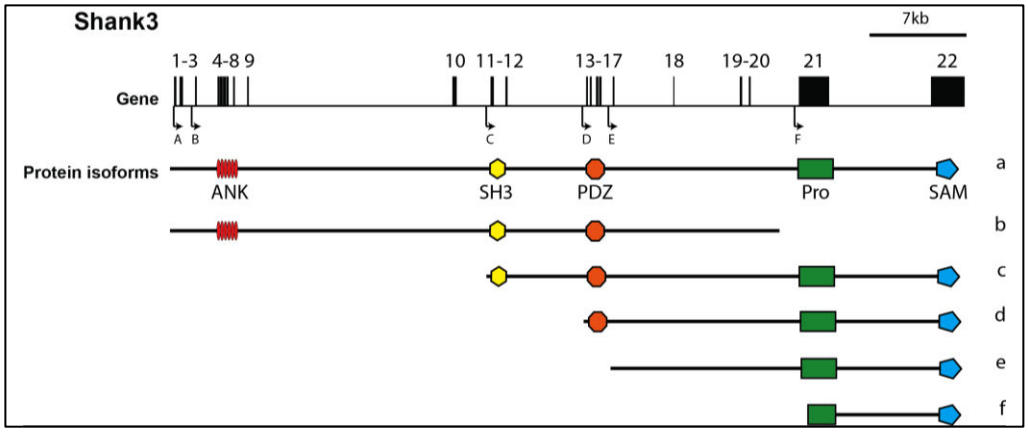

Figure S 1: Schematic representations of Shank3 gene in mouse genome and corresponding protein isoforms*. The protein domains are aligned with the corresponding exons. Gene: Black squares are exons. Black arrows are intragenic promoters. Protein: black lines are amino acids sequences; geometrical figures are domains. The diagram was drawn on the basis of the information contained at the National Centre for Biotechnology Information (NCBI) and Uniprot database.*

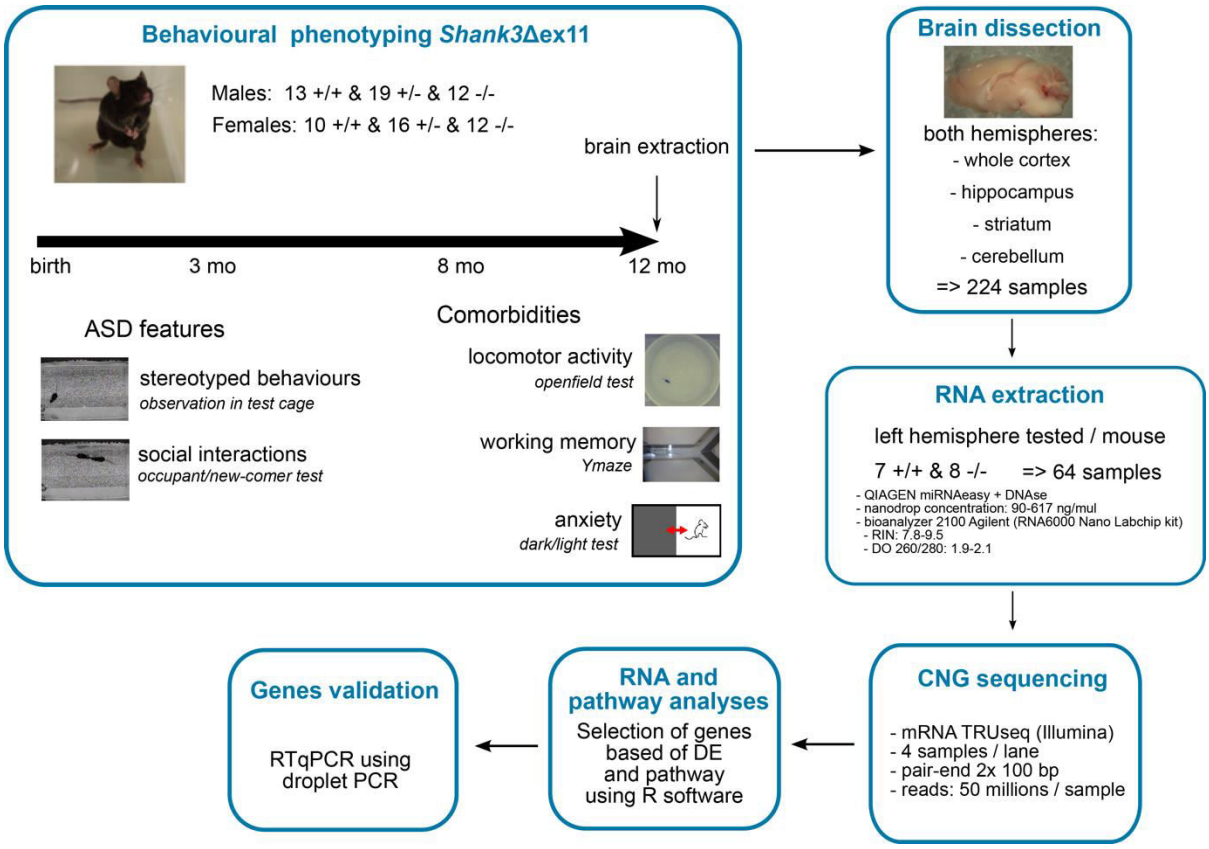

Figure S 2: Pipeline of testing and analyses used to characterise the Shank3 mutant mice. *The behavioural characterisation included tests to evaluate ASD core symptoms (social communication, stereotyped behaviours) and comorbidities (activity, exploration, memory, anxiety). After the longitudinal study of the same animals at three time points (3, 8 and 12 months of age), their brains were extracted and four brain regions were dissected for each animal. RNA sequencing was performed on the left hemispheres of a subset of these samples. Gene sequencing was performed at the CNRGH (Centre National de Recherche en Génomique Humaine). Data were analysed using R software. Selected genes were validated using droplet digital PCR (Bio-Rad).*

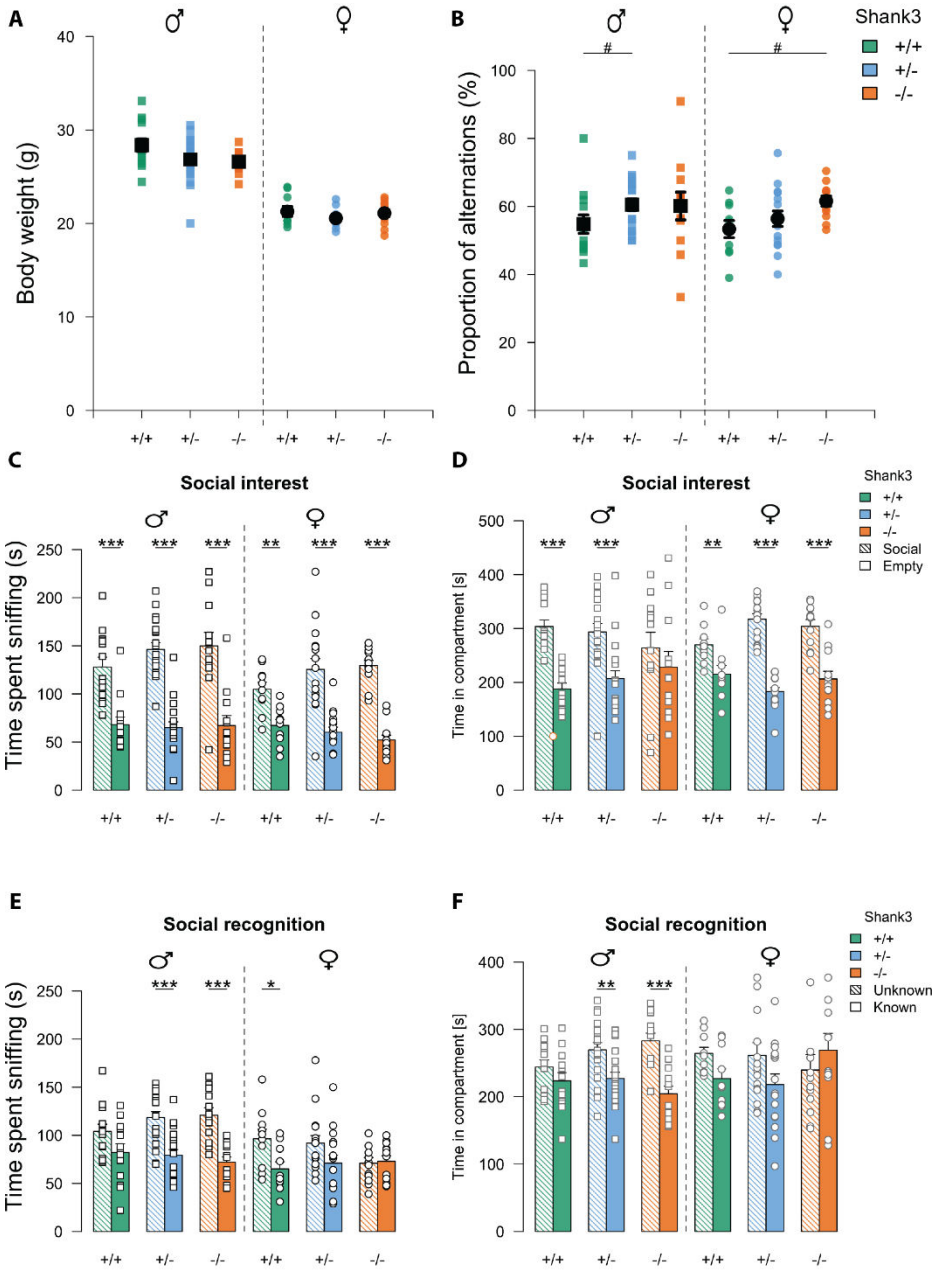

Figure S 3: Shank3-/- mice displayed subtle genotype-related differences in weight, working memory and social behaviour at three months of age. *(A) Body weight of male (left panel) and female (right panel) Shank3+/+ (green), Shank3+/- (blue) and Shank3-/- (orange) mice aged of three months. (B) Proportion of alternations between the three arms of a Y-maze. Mann–Whitney U test, with Bonferroni correction for multiple testing (in black): #p<0.1, *p<0.05, **p<0.01, ***p<0.001; Ansari-Bradley test, with Bonferroni correction for multiple testing (in grey): #p<0.1, *p<0.05, **p<0.01, ***p<0.001; data are presented as mean ± s.e.m.; 12–14 mice per group. (C-D) Social preference measured in the three-chambered test. First phase of three-chambered test with the time spent in sniffing (C) or time spent in the compartment (E) containing a caged same-sex conspecific (hashed bars) and in the compartment containing the empty wired cup (non-social stimulus; solid bars) for Shank3+/+ (green), Shank3+/- (blue) and Shank3-/- (orange) mice, with males (left panel) and females (right panel). Second phase of three-chambered test with the time spent in sniffing (E) or in the compartment (F) containing an unfamiliar caged same-sex conspecific (hashed bars) and in the compartment containing a familiar caged same-sex conspecific (solid bars) for Shank3+/+ (green), Shank3+/- (blue) and Shank3-/- (orange) mice, with males (left panel) and females (right panel). Mann–Whitney U test, with Bonferroni correction for multiple testing: #p<0.1, *p<0.05, **p<0.01, ***p<0.001; data are presented as mean ± s.e.m. (black squares and circles); 12–14 mice per group.*

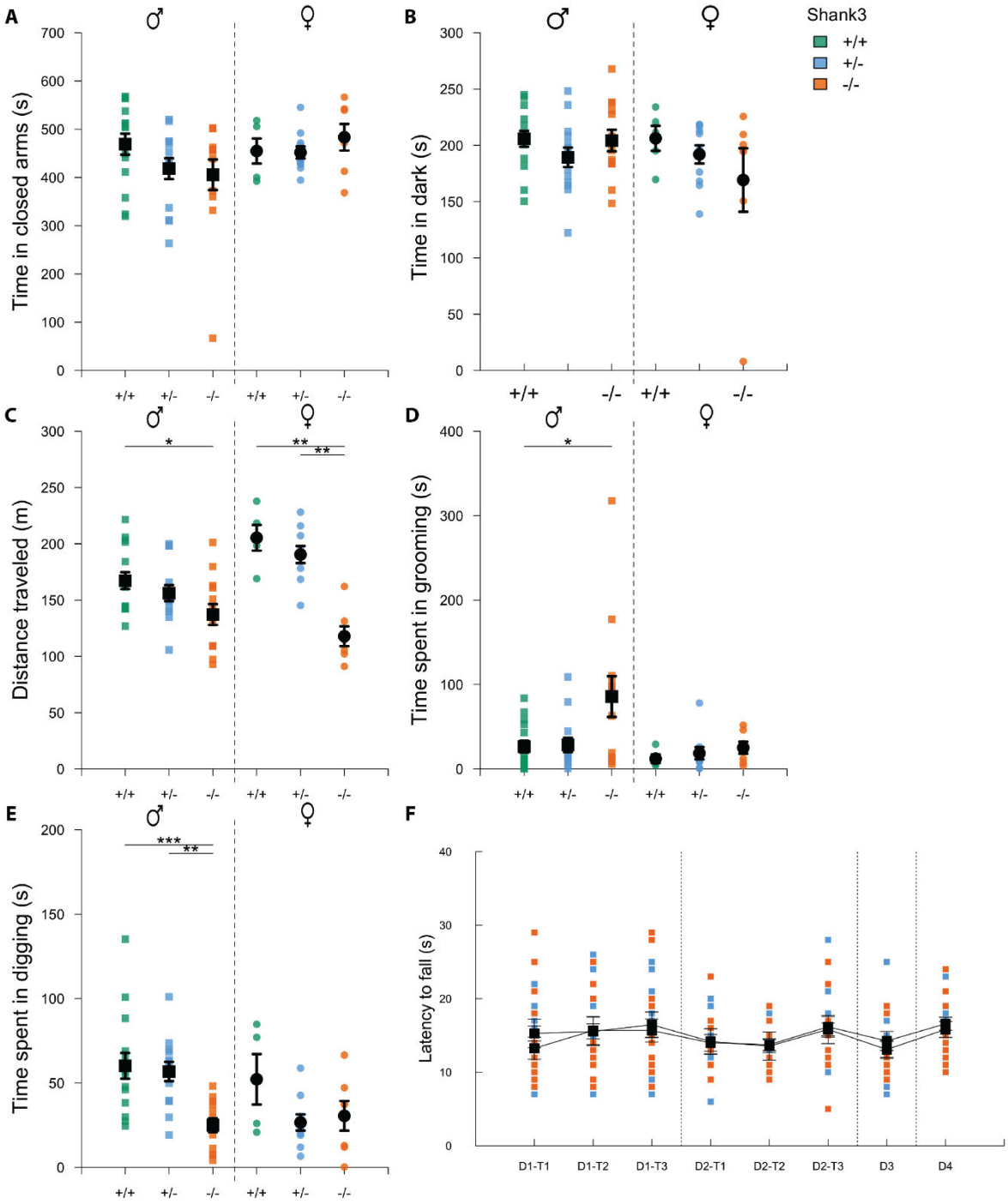

Figure S 4: Shank3-/- mice of a second cohort displayed decreased activity and increased stereotyped behaviour. *(A) Time spent in open arm in EPM during 10 min in Shank3+/+ (green), Shank3+/- (blue) and Shank3-/- (orange) mice, for males (left panel) and females (right panel). (B) Time spent in the dark compartment in dark/light test during 5 min. (C) Total distance travelled during 30 min of free exploration of an open-field. (D) Total time spent self-grooming during 10 min observation in a test cage with fresh bedding (after 10 min habituation), for males (left panel) and females (right panel). (E) Total time spent digging, i.e. moving the bedding with front and/or hind legs, during 10 min observation in a test cage (after 10 min habituation) for males (left panel) and females (right panel). (F) Latency to fall in the rotarod test. Three trials were conducted on day 1 and 2, and only one trial was performed on day 3 and 4. Mann–Whitney U test, with Bonferroni correction for multiple testing (in black): *P<0.05, **P<0.01, ***P<0.001; Ansari-Bradley test, with Bonferroni correction for multiple testing (in grey): *P<0.05, **P<0.01, ***P<0.001; data are presented as mean ± s.e.m. (black squares and circles); 12–14 mice per group.*

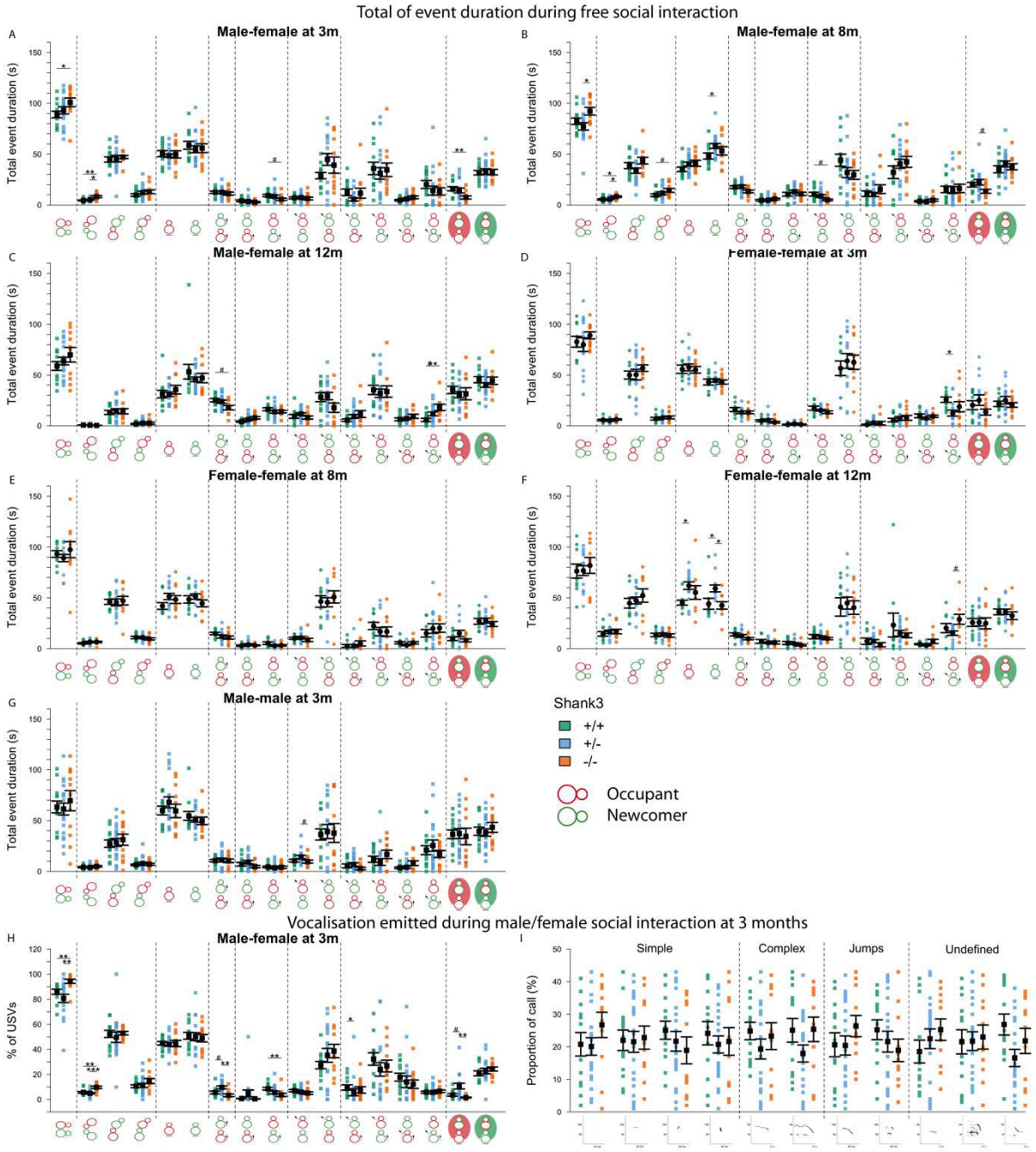

Figure S 5: Shank3-/- mice displayed limited genotype-related difference in social events at eight and twelve months of age. *Time spent in the different types of social events during 4-min male/female (A-B-C), female/female (D-E-F) and male/male (G) social interactions of Shank3 s with a female C57Bl/6J conspecific for Shank3+/+ (green), Shank3+/- (blue) and Shank3-/- (orange) mice. USVs rate in the different types of social events (H) and types of USVs emitted (I) during 4-min male/female interactions. Mann–Whitney U test, with Bonferroni correction for multiple testing (in black): #p<0.1, *p<0.05, **p<0.01, ***p<0.001; data are presented as mean ± s.e.m (black squares and circles).; 12–14 mice per group.*

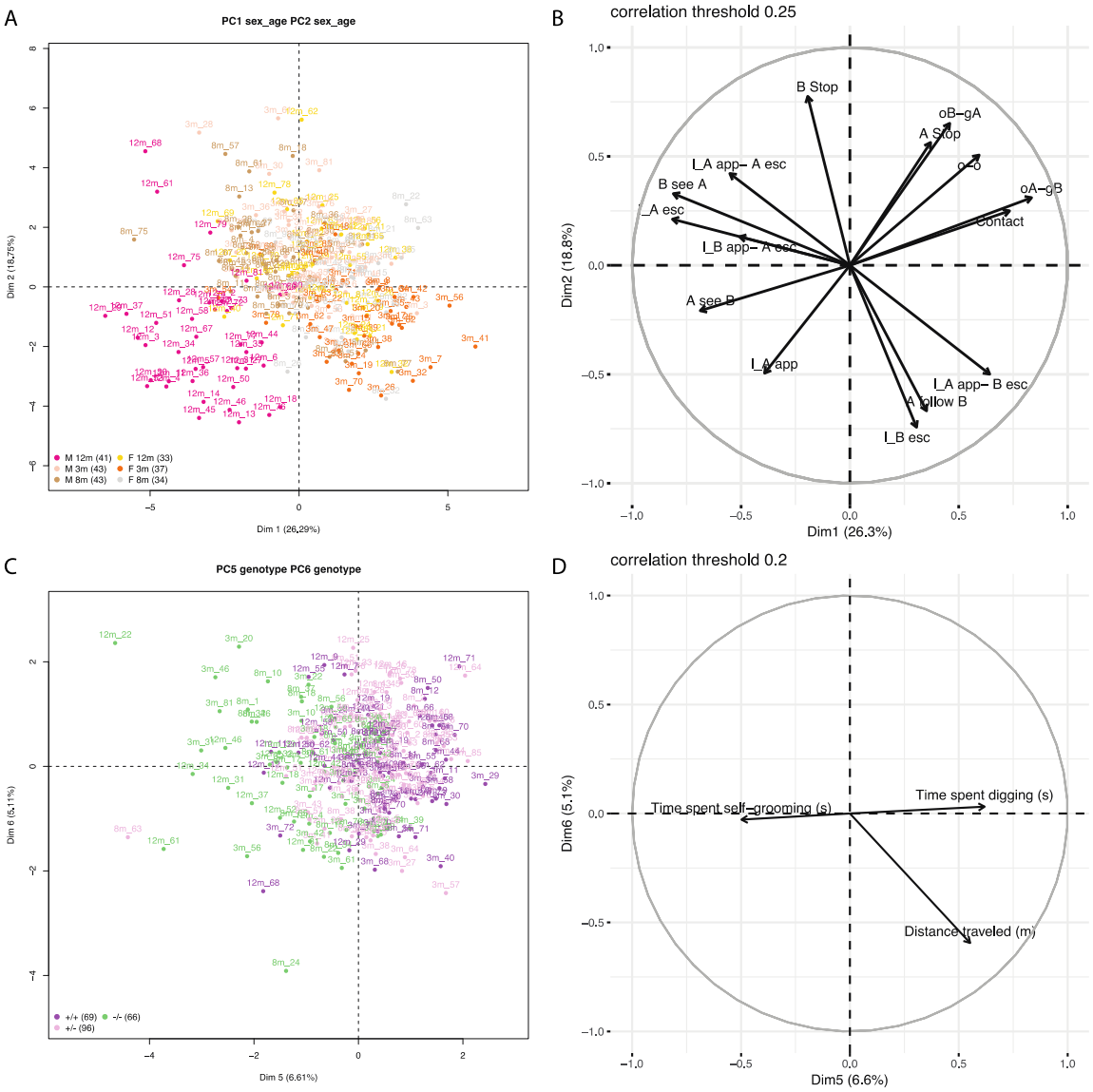

Figure S 6: Principal component analysis of the behaviour of Shank3 cohort 1. *(A-B) Dimensions 1 & 2 separate individuals according to their sex and age, in particular the 12m old males are separated from the others. The separation is mainly based on the type of social interaction. (C-D) Dimensions 5 & 6 separate individuals according to the genotype. The separation is based on the time spent in grooming and digging and the distance travelled.*

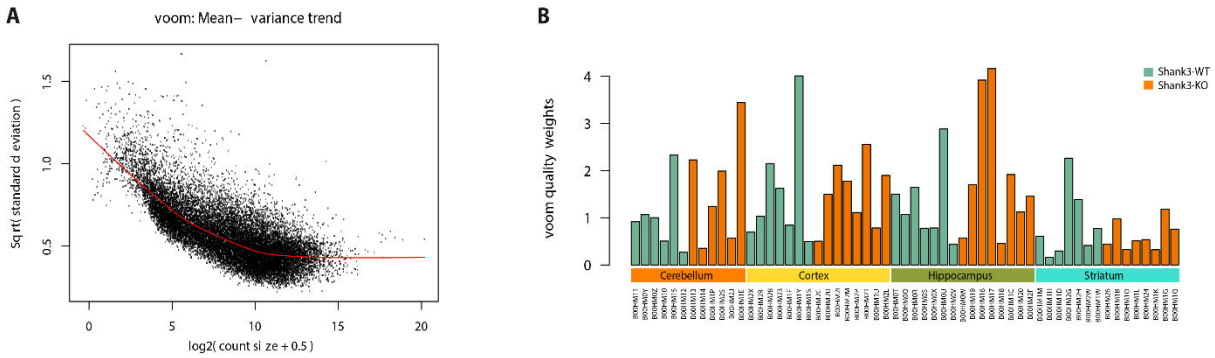

Figure S 7: Mean-variance relationship. *(A) Voom mean-variance trend output for the RNA-Seq data. Gene-wise means and variances of the RNA-Seq data are represented by black points with a LOWESS trend. (B) 'Voom' sample-specific weights, each bar plot represents the weight of one sample used to model variability between different samples.*

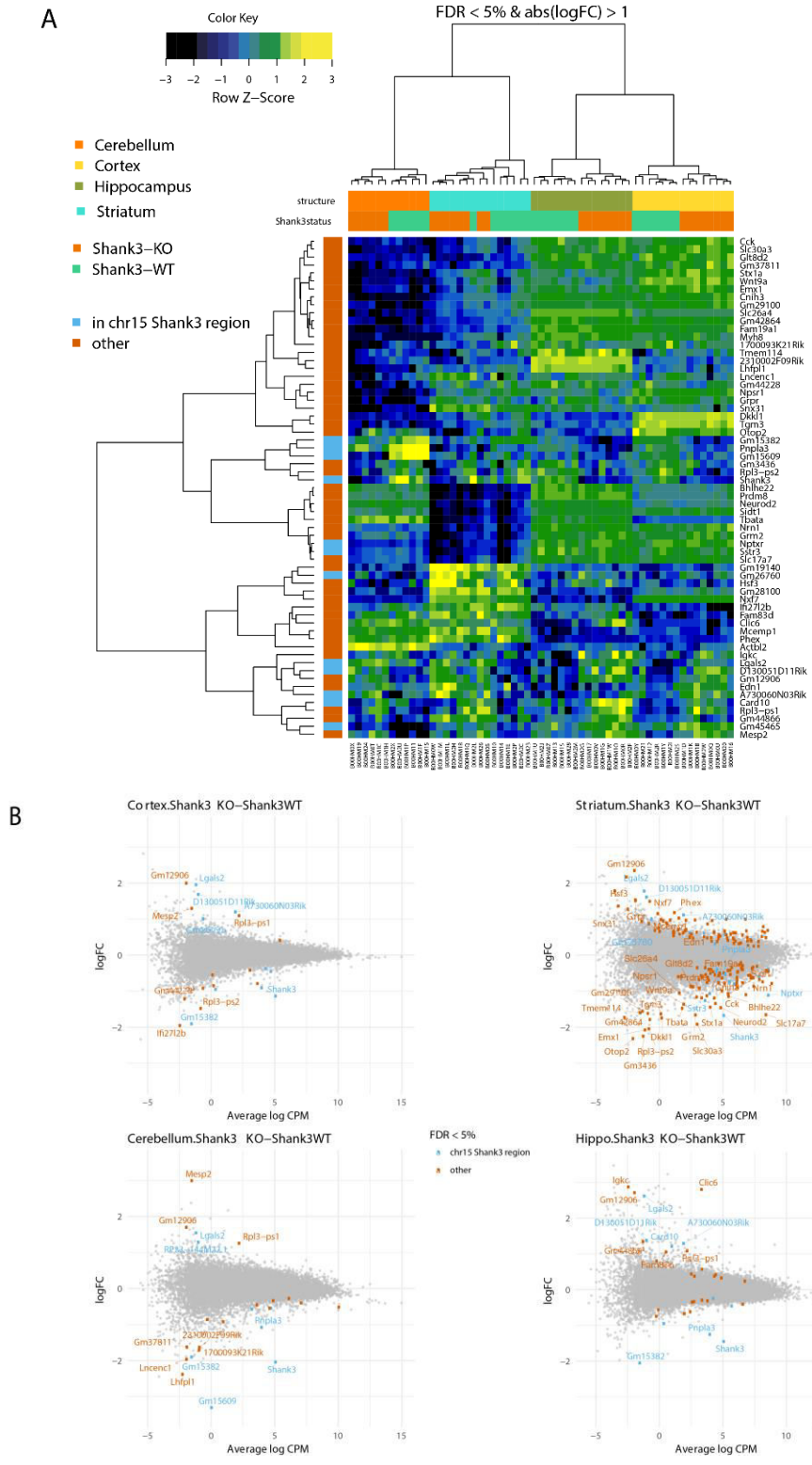

Figure S 8: Gene expression differences associated with the mutation in Shank3 in four brain regions of Shank3 mutant mice. *(A) Heat map of the average gene expression (logarithmic count per million; logCPM) of the differentially expressed genes (adjust p-value < 5%; determined by limma-voom using observation quality weights; absolute logFC value larger than 1). (B) Mean-difference plots showing logFC between Shank3-/- and Shank3+/+ samples as a function of logCPM in the cortex (upper left), the striatum (upper right), the cerebellum (lower left) and the hippocampus (lower right). Genes with a FDR lower than 5% are coloured in orange; genes with a FDR lower than 5%, located around the Shank3 region in chromosome 15, are displayed in blue. Only names of the genes with an absolute log fold-change value larger than 1 are shown.*

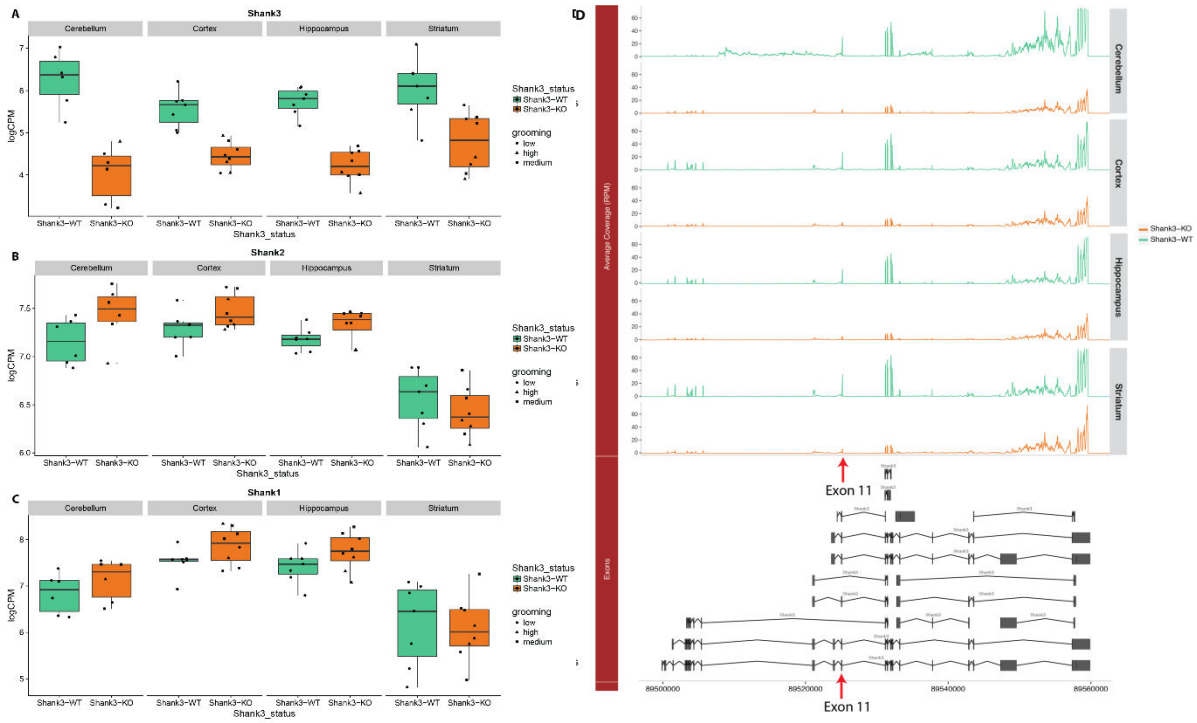

Figure S 9: RNA sequencing-based expression levels of Shank3, Shank2 and Shank1 in four brain regions. *(A- B- C). Log counts of reads per million of (A) Shank3, (B) Shank2 and (C) Shank1 in the cerebellum, cortex, hippocampus and striatum for Shank3+/+ (green) and Shank3-/- (orange) mice. Data are presented as box-plots (median and first and third quartiles) and sample points (black points). (D) Reads expression profiles of the different Shank3 (upper panel) related with exon and Shank3 isoforms (lower panel) in the cerebellum, cortex, hippocampus and striatum for Shank3+/+ (green) and Shank3-/- (orange) mice. Reads expression profiles of the different Shank3 (upper panel) related with exon and Shank3 isoforms (lower panel) in the cerebellum, cortex, hippocampus and striatum for Shank3+/+ (green) and Shank3-/- (orange) mice. Red arrow indicates the position of exon 11 according to National Centre for Biotechnology Information (NCBI).*

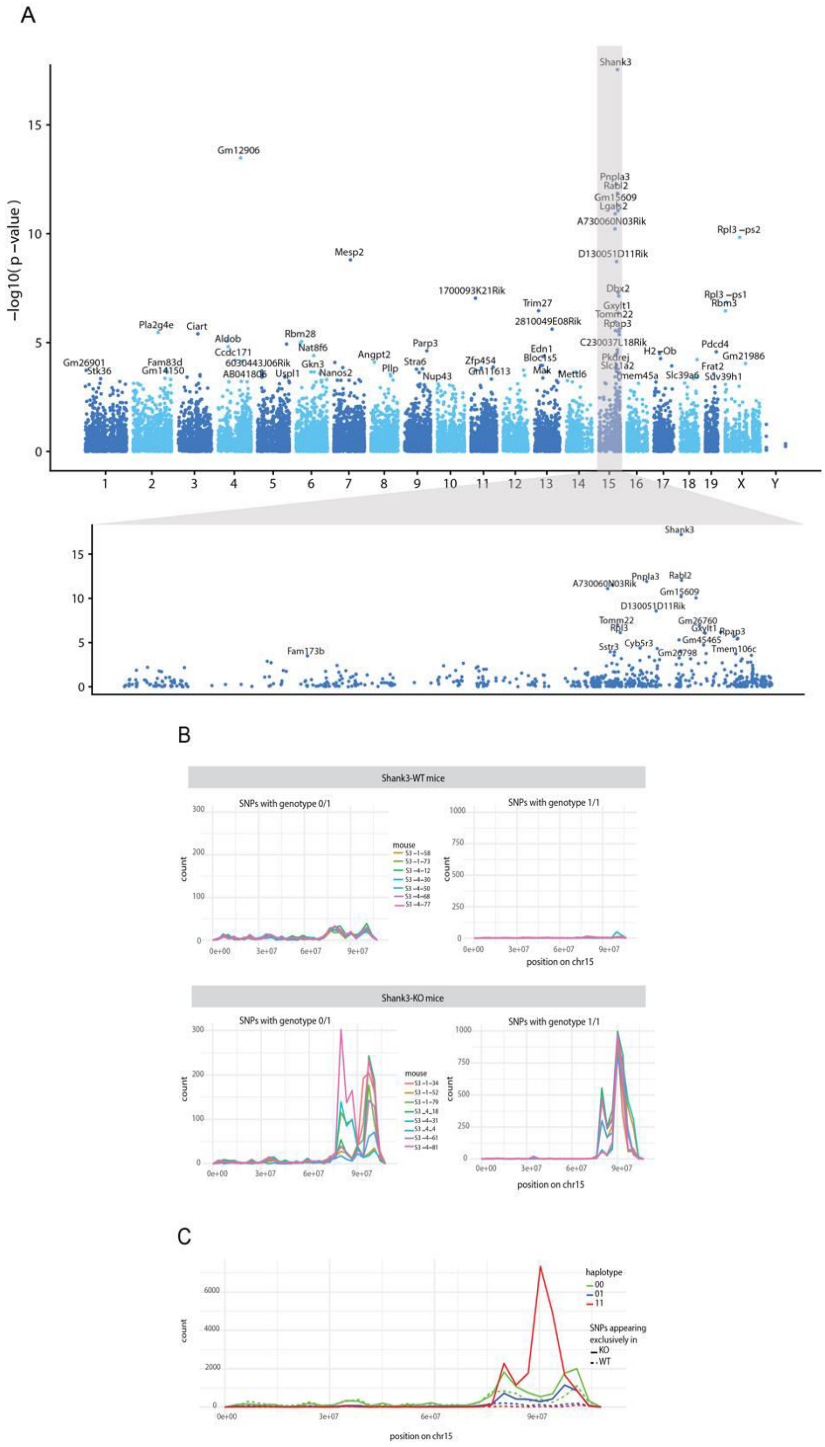

Figure S 10: An increased number of SNP around the Shank3 position suggests a construct bias. *(A) Manhattan plot showing the negative log10-transformed p-value of the comparison (across all brain structures) of gene expression between Shank3+/+ and Shank3-/- mice for each read on the whole genome (upper panel) and a close-up on the chromosome 15. (B) Distribution over the chromosome 15 of the number of heterozygous variant genotypes (0/1; right panel) and homozygous variant genotypes (1/1; left panel) that are specific to either Shank3+/+ mice (upper panels) or Shank3+/+ mice (lower panels). Data are presented as the counts of variants as a function of the genomic position on chromosome; each line represents an individual, with samples from all brain regions pooled together. (C) Distribution of the number of homozygous and heterozygous variants counted across individuals of the same genotype. Data are presented as the counts of variants as a function of the genomic position on chromosome 15. Homozygous (resp. heterozygous) variant genotypes are shown in red (resp. green). Plain (resp. dotted) lines represent variants specific to the Shank3-/- (resp. Shank3+/+) mice.*

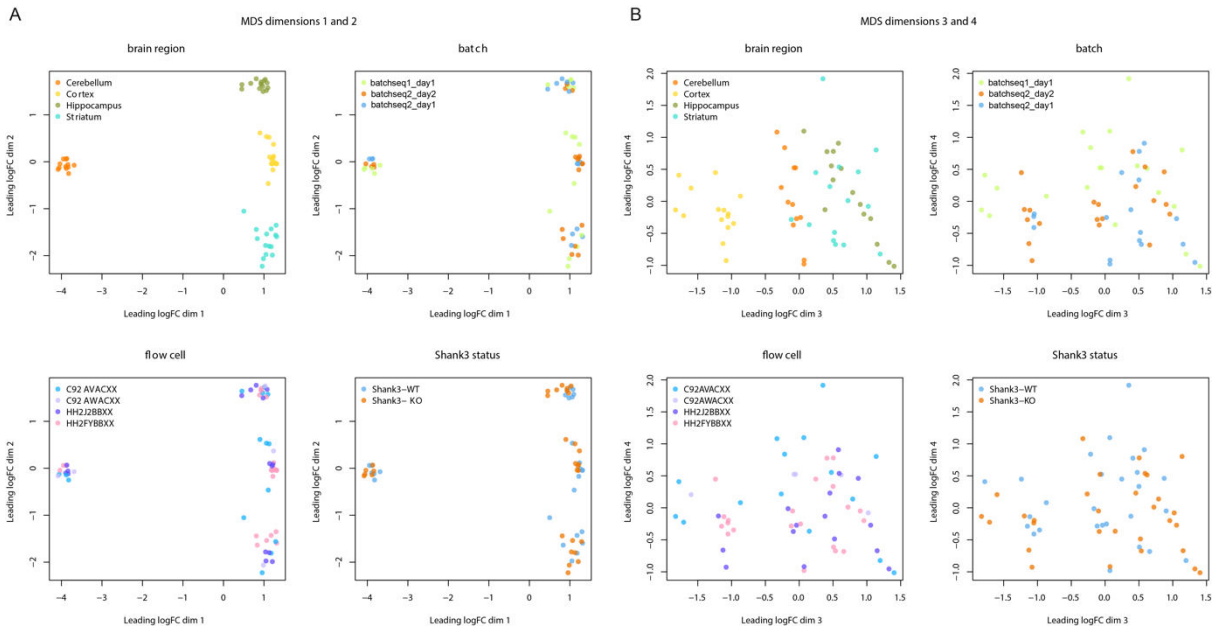

Figure S 11: Multi-dimensional scaling (MDS) plots of the gene log counts-per-million (logCPM) data showing the positions of the samples in the space spanned by the first and second MDS dimensions*. Samples are coloured with respect to brain region (upper left), batch of sequencing and RNA extraction (upper right), flow cell (lower left) and genotype (lower right). (B) Multi-dimensional scaling (MDS) plots of the gene log counts-per-million (logCPM) data showing the positions of the samples in the space spanned by the third and fourth MDS dimensions. Samples are coloured with respect to brain structure (upper left), batch of sequencing and RNA extraction (upper right), flow cell (lower left) and genotype (lower right).*

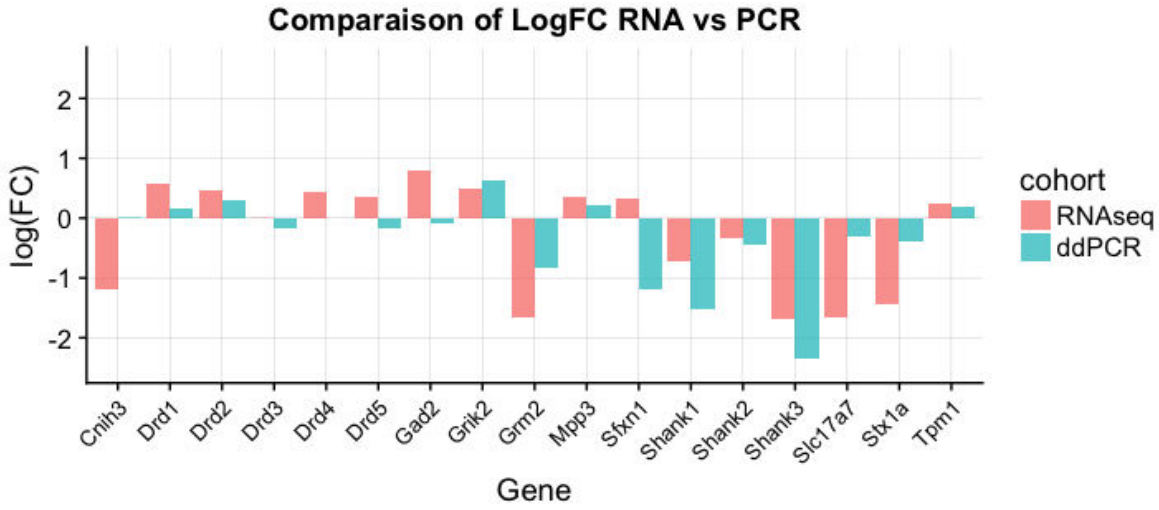

Figure S 12: Log FC of selected genes for PCR validation compared to RNAseq*. In pink Log FC based of RNAseq analysis, in blue LogFC based of dd-PCR validation.*

All supplementary tables (Table S1-5) are present in the following repository:

https://www.dropbox.com/sh/bz2hqg38hvlsy66/AAD0Jm2ioVFAfTHrSOcx_Rj8a?dl=0

Tables S 1: Statistical analyses of behavioural tests

Table S 2: RNAseq annotations

Tables S 3: Results of differential analysis based on RNA sequencing

Tables S 4: GSEA tables

Table S 5: Selected genes for validation

II. Behavioural characterisation of *Shank2*/*Shank3* double mutant mice

II.A. Context

In the study in 2012, Schmeisser and colleagues studied expressions of Shank protein in *Shank2*Δ17 and *Shank3*Δ11 mice. They revealed an increase of Shank2 protein expression in *Shank3*Δ11 mice and an increase of Shank3 protein expression in *Shank2*Δ17 mice in the striatum at p70 (≈ 2 months of age).

Furthermore, from unpublished data from the "Human genetic and cognitive functions" lab, E. Ey revealed an increase of Shank3 protein expression in a sub-group of *Shank2*Δ17 mice. Indeed, during a male/female social interaction, two sub-groups of *Shank2*Δ17-/- mice were identified: one displaying low levels of social interaction and vocal communication with oestrus female and the other one displaying levels of social communication similar to that of *Shank2*Δ17+/+ mice. They observed an increase of Shank3 in this second sub-group and not in the first one.

Based on these observations, we hypothesise that Shank2 and Shank3 can compensate each other to reduce the behavioural outcome of the mutation. Therefore, to improve the understanding of the balance between Shank2 and Shank3 expression, we generated a double mutant cohort with all possible combination of gene dosage between *Shank2* and *Shank3* and characterised the behavioural phenotype of the mice.

II.B. Results

First, based on the number of individuals in each group (Table 5.B) and the expected number of individuals, our cohort did not follow a Mendelian distribution (X^2 test: p=0.008) with a decreased number of animals with a homozygous mutation in *Shank2* (Table 6). This observation suggests that deleting *Shank2* is more severe than deleting *Shank3* in mice.

Due to the small number of individuals for several groups and the low statistical power, we will only describe the behavioural phenotype without statistics.

To facilitate the understanding of the figures due to the important number of genotypes, we simplify the nomenclature (Table 7).

Shank2	+/+	+/-	-/-	-/-	+/+	-/-	+/-	+/+	+/-
Shank3	+/+	+/-	-/-	+/+	-/-	+/-	-/-	+/-	+/+
Expected	6.13	24.5	6.13	6.13	6.13	12.25	12.25	12.25	12.25
Proportion	1/16	4/16	1/16	1/16	1/16	2/16	2/16	2/16	2/16
Observed	9	29	3	3	7	5	11	23	8

Table 6: Abnormal Mendelian distribution

Genotype	$S2^{+/+}S3^{+/+}$	$S2^{+/-}S3^{+/-}$	$S2^{-/-}S3^{-/-}$	$S2^{-/-}S3^{+/+}$	$S2^{+/+}S3^{-/-}$	$S2^{-/-}S3^{+/-}$	$S2^{+/-}S3^{-/-}$	$S2^{+/+}S3^{+/-}$	$S2^{+/-}S3^{+/+}$
Shank2	+/+	+/-	-/-	-/-	+/+	-/-	+/-	+/+	+/-
Shank3	+/+	+/-	-/-	+/+	-/-	+/-	-/-	+/-	+/+
Males	**6**	**14**	**1**	**1**	**3**	**2**	**6**	**11**	**7**
Females	**3**	**15**	**2**	**2**	**4**	**6**	**5**	**12**	**1**

Table 7: Corresponding table between genotype and annotation on the graphics. In green: homozygous wild-type; in blue: heterozygous mutant; in orange: homozygous mutant for Shank2 or Shank3.

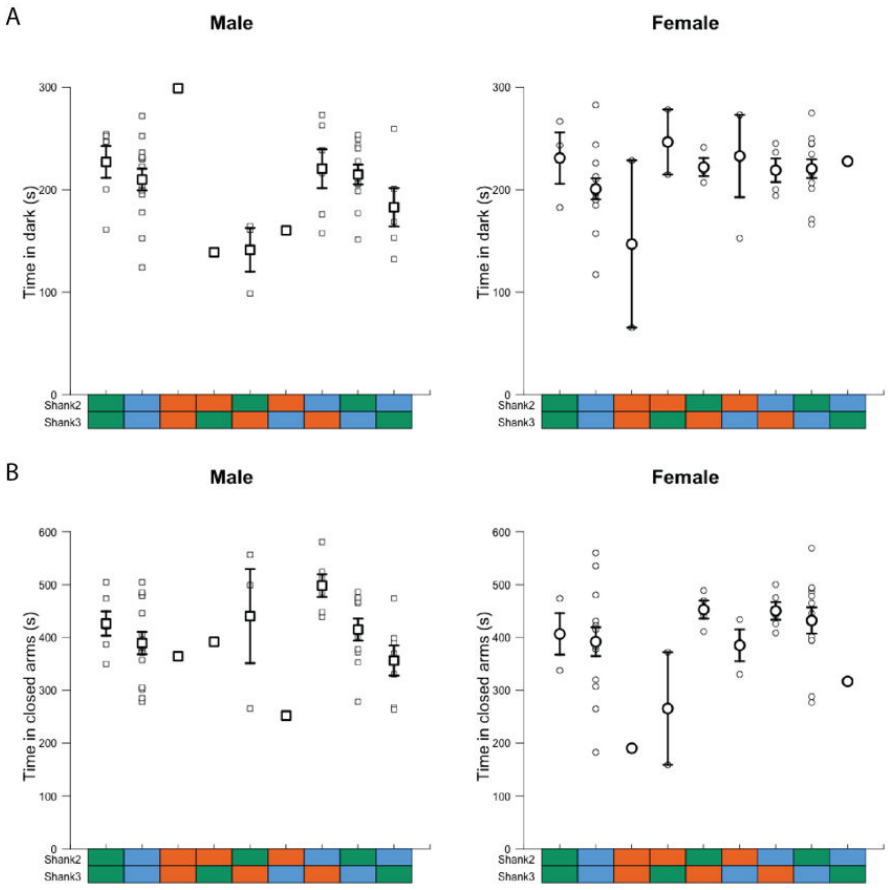

Figure 20: Anxiety-like tests in Shank2/Shank3 double mutant mice*. (A) Total time spent in the dark compartment in a dark-light test during 5 min, for males (left panel) and females (right panel). (B) Total time spent in the closed arms in a plus-maze test during 10 min, for males (left panel) and females (right panel).*

Anxiety-like

We analysed the anxiety-like behaviour through two tests, dark/light test and elevated plus maze. In the dark/light test, $S2^{+/+}S3^{+/+}$, $S2^{+/-}S3^{+/-}$, $S2^{+/-}S3^{-/-}$, $S2^{+/+}S3^{+/-}$, $S2^{+/-}S3^{+/+}$ males displayed similar time spent in the dark compartment, suggesting no anxiety-like behaviour. However, $S2^{-/-}S3^{+/+}$, $S2^{+/+}S3^{-/-}$, $S2^{-/-}S3^{+/-}$ males seemed to display a reduction of time spent in dark compartment while $S2^{-/-}S3^{-/-}$ mice spent more time in dark compartment revealing an increase of anxiety-like behaviour. Concerning females, no difference seemed to be present between genotypes in the time spent in the dark compartment. However, $S2^{+/-}S3^{+/-}$ and $S2^{-/-}S3^{-/-}$ females presented an important inter-individual variability compared to other genotypes in the time spent in the dark compartment. In the elevated plus maze, there seemed to be no difference between genotypes in the time spent in close arms for males, except a slight reduction for $S2^{-/-}S3^{+/-}$ mice, but there was only one animal (Figure 20.B). $S2^{-/-}S3^{-/-}$ and $S2^{-/-}S3^{+/+}$ females seemed to show a decrease of time spent in close arms compared to other genotypes.

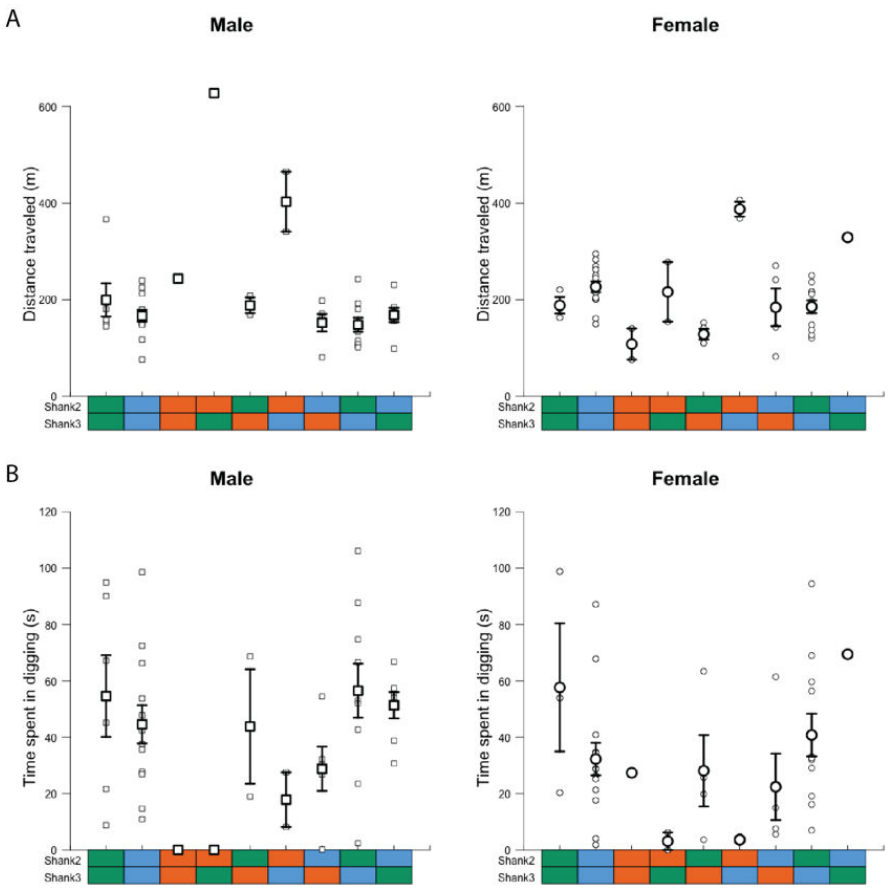

Figure 21: Locomotor activity and exploratory behaviour in Shank2/Shank3 double mutant mice. *(A) Total distance travelled during 30 min of free exploration of an open-field in males (left panel) and females (right panel). (B) Total time spent digging during 10 min observation in a test cage with fresh bedding (after 10 min habituation), for males (left panel) and females (right panel).*

Locomotion

In this cohort, the activity was measured by the distance travelled in the openfield during 30 min (Figure 21.A). Mice of most genotypes displayed similar distance travelled for males and females, around 200 meters. Interestingly, only $S2^{-/-}S3^{+/+}$ and $S2^{-/-}S3^{+/-}$ males and $S2^{-/-}S3^{+/-}$ females displayed an increase of the distance travelled compared to other genotypes, suggesting a hyperactivity linked to the homozygous deletion of *Shank2*. Surprisingly, the $S2^{+/-}S3^{+/+}$ mice also displayed an increase of the distance travelled probably due to the heterozygous mutation in *Shank2*. This observation is consistent with the initial characterisation of *Shank2*-/- mice (Schmeisser et al. 2012). Furthermore, $S2^{-/-}S3^{-/-}$ and $S2^{+/+}S3^{-/-}$ females displayed a reduction of the distance travelled. This could be associated with the homozygous deletion of *Shank3*.

The digging behaviour could be considered an exploratory behaviour (Belzung 1999). This behaviour presented an important variability is present for each genotype. (Figure 22.B). Interestingly, individuals with homozygous mutation in *Shank2* or *Shank3*, $S2^{-/-}S3^{-/-}$, $S2^{-/-}S3^{+/+}$, $S2^{+/+}S3^{-/-}$, $S2^{-/-}S3^{+/-}$ and $S2^{+/-}S3^{-/-}$ seemed to display a reduction of the time spent digging in comparison with $S2^{+/+}S3^{+/+}$ mice.

Social interaction

Concerning the motivation to interact socially, we analysed the time spent in contact during the interaction of a male with a C57Bl/6J oestrus female and during the interaction of a female with a C57Bl/6J female (Figure 21.B).

Regarding the socio-sexual interaction, $S2^{+/+}S3^{+/+}$, $S2^{-/-}S3^{+/+}$, $S2^{+/+}S3^{-/-}$, $S2^{+/-}S3^{-/-}$, $S2^{+/+}S3^{+/-}$, $S2^{+/-}S3^{+/+}$ individuals displayed similar time spent in contact with an oestrus female. Surprisingly, $S2^{+/-}S3^{+/-}$ mice seemed to spend more time in contact with the oestrus female than mice of other genotypes. $S2^{-/-}S3^{-/-}$ and $S2^{-/-}S3^{+/-}$ mice displayed a reduction of time spent in contact with the oestrus female in comparison with other mice. For females during same-sex social interactions, $S2^{-/-}S3^{+/+}$, $S2^{+/+}S3^{-/-}$, $S2^{-/-}S3^{+/-}$, $S2^{+/-}S3^{-/-}$, $S2^{+/+}S3^{+/-}$, $S2^{+/-}S3^{+/+}$ individuals spent less time in social contact than $S2^{+/+}S3^{+/+}$ and $S2^{+/-}S3^{+/-}$ mice.

Stereotyped behaviour

We observed two types of stereotyped behaviours: jumping and self-grooming behaviour. Interestingly, the time spent in self-grooming behaviour is relatively low for the majority of genotypes (Figure 22.A). Indeed, only individuals with homozygous mutation of *Shank3*, $S2^{+/+}S3^{-/-}$ and $S2^{+/-}S3^{-/-}$, displayed an increase of time spent in self-grooming with an important inter-individual variability. This observation was consistent with the previous analysis of this manuscript. Surprisingly, the double mutant mice did not display increased self-grooming, neither in males nor in females.

The jumping behaviour is mainly observed in mice with a mutation in *Shank2*, namely in $S2^{-/-}S3^{-/-}$ and $S2^{-/-}S3^{+/+}$ males and for $S2^{+/-}S3^{+/-}$, $S2^{-/-}S3^{+/+}$, $S2^{-/-}S3^{+/-}$ and $S2^{+/-}S3^{+/+}$ females (Figure 22.C).

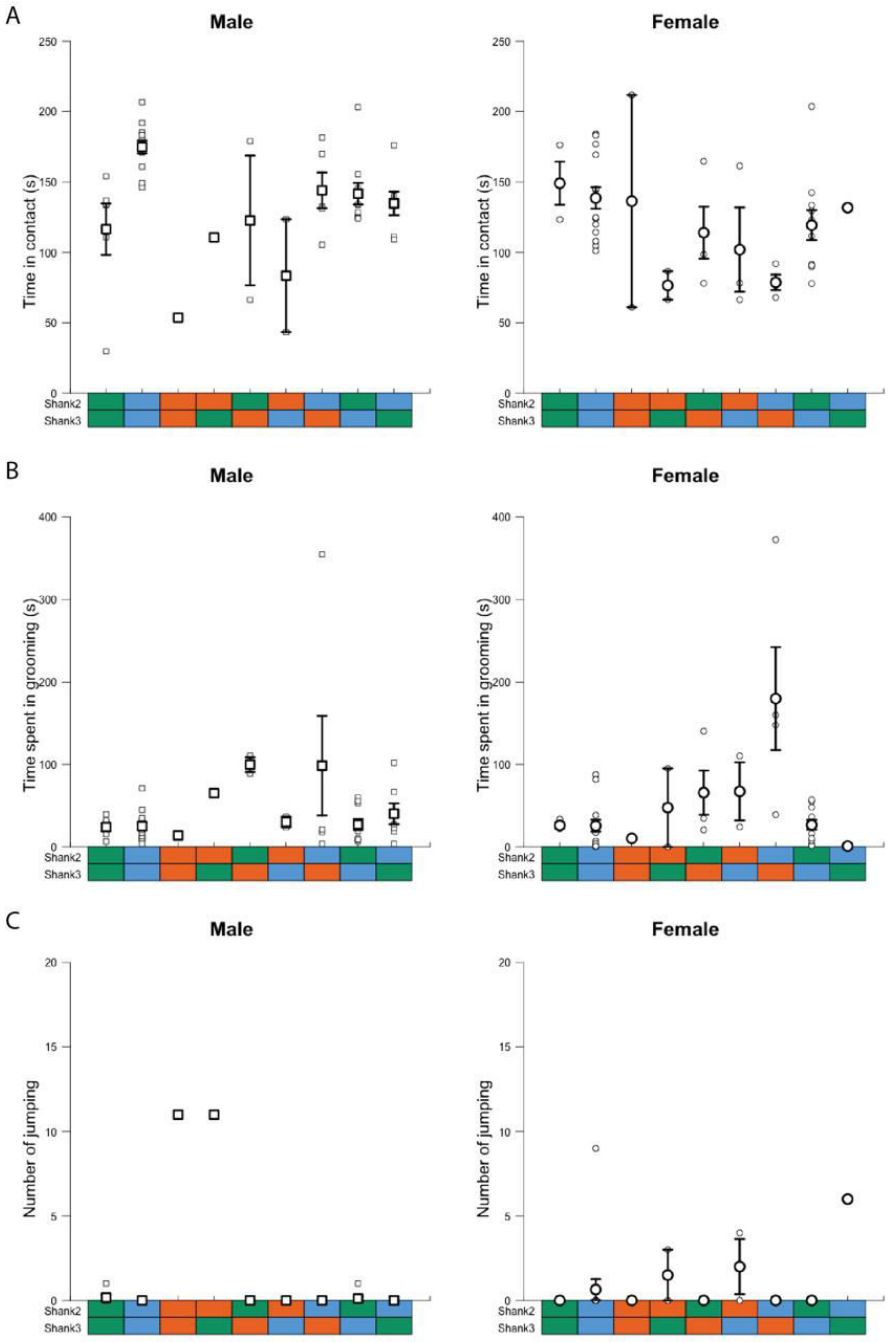

Figure 22: Social interaction and stereotyped phenotype according to the genotype. *(A) Total time spent in contact during free male-female social interaction (left panel) and free female/female social interaction (right panel). (B) Total time spent self-grooming during 10 min observation in a test cage with fresh bedding (after 10 min habituation), for males (left panel) and females (right panel). (C) Total number of jumping, i.e. jump against the cage wall, during 10 min observation in a test cage (after 10 min habituation) for males (left panel) and females (right panel).*

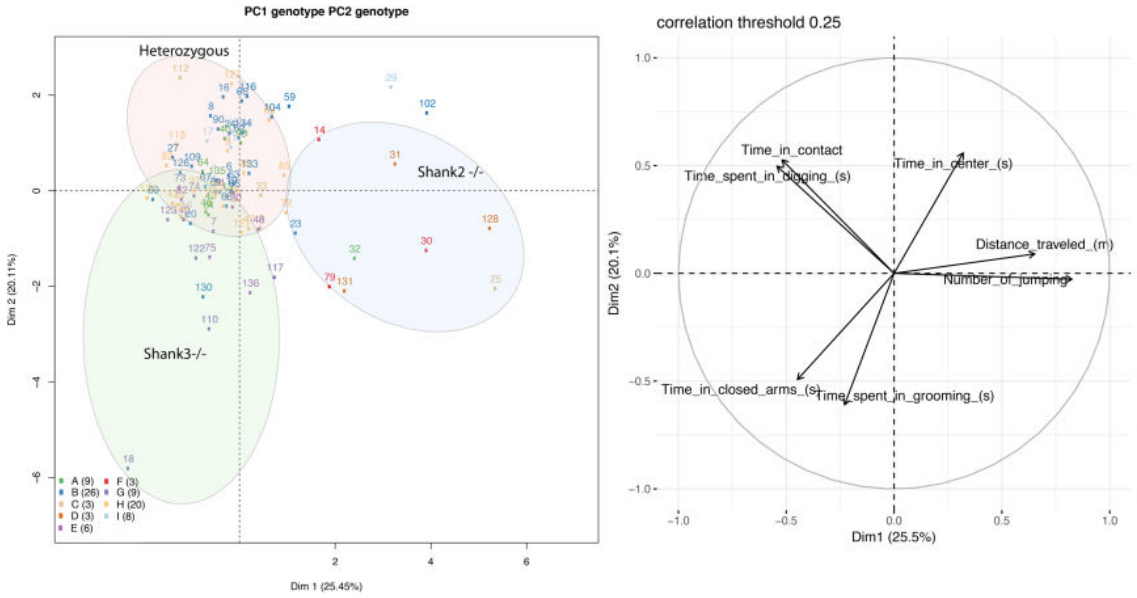

Figure 23: Principal component analysis of the behaviour of double mutant cohort. *Dispersion of the different individuals (Right panel) according to the contribution of behaviour (Left panel)*

Principal component analysis of the behaviour

In a principal component analysis (PCA) on all behavioural variables, we observed independent groups. Here, we present the two first dimensions of the PCA driving 25.5% (dimension 1) and 20.1% (dimension 2) of the total variability (Figure 23). In the first eight dimensions, none separated the animals by sex. First, $S2^{+/+}S3^{+/+}$ mice and simple or double heterozygous mutant seemed to be homogenous, except for two animals ($S2^{+/-}S3^{+/-}$ and $S2^{+/-}S3^{+/+}$). This group was driven by an important time spent in contact during social interaction (male/oestrus female or female/female) and in digging. Surprisingly, the two double homozygous mutant females were in this group, which revealed little impairment for these animals. A second group can be observed containing animals carrying homozygous mutation of *Shank3* except for the double mutant (E and G). This group was characterised by an increase of anxiety-like behaviour in the plus-maze as well as a long time spent in self-grooming behaviour. This last aspect is common with the majority of *Shank3* mouse models (See Intro XXX). The last group included mice displaying homozygous mutation in *Shank2*, $S2^{-/-}S3^{+/+}$ and $S2^{-/-}S3^{+/-}$, and the double homozygous mutant male. This group is characterised by an increase of the number of jumping behaviour and by hyperactivity. Interestingly, hyperactivity was a phenotype related to the homozygous *Shank2* mutation.

DISCUSSION

I. Comparison between studies

Variability between *Shank3* mouse models

When considering all studies on *Shank3* models, we found behavioural phenotypes that were strongly associated with any *Shank3* mutation. The most stable phenotypes seemed to be the increase of stereotyped behaviour via self-grooming and the reduction of locomotor activity. All other phenotypes (anxiety, memory, social interactions) seemed to vary without a real impact of isoforms expression.

As reported in the introduction, (see III.B.1), we noticed an important variability between the models and also between studies on the same model with, as a main phenotype, stereotyped behaviour and locomotor impairment (Ferhat et al. 2017). For example, the two complete *Shank3*-/- mice displayed different behavioural phenotypes. Wang and colleagues (2016) showed impairment in social communication and no impairment in locomotion while Drapeau and colleagues (2018) showed opposite observation. Our study showed different results in the behavioural and biochemical parts compared to the previous studies (Schmeisser et al. 2012; Vicidomini et al. 2017). Vicidomini and colleagues (2017) revealed a reduction of social interaction and social recognition, and a reduction of mGlu5 in the cortex and homer1b/c that we did not find with RNAseq. Two main hypotheses can be drawn to explain this divergence between studies.

Hypothesis 1 for divergence between studies: differences in the protocols

The first one, especially for behavioural tests, is the use of different protocols to quantify similar phenotypes. Consequently, different interpretations and conclusions can be made. Indeed, the social motivation tests, direct social interaction or three-chambered test for example, illustrate well the situation. For instance, Yang and colleagues (2012) found a reduction of social interaction during free social interaction, but not during the three-chambered social test (M. Yang et al. 2012). This observation reveals that each test analyses different aspect of social behaviour grouped under the name “social interaction”. The different conditions and the experimenter could also impact the observable phenotype during the tests (Sorge et al. 2014).

The diagnostic in human patients is very structured and based on standardised tests and procedures like ADOS (see I.E). Integrating standardised tests for all possible phenotypes and, consequently, developing a kind of rodent ADOS-like, could reduce this variability. This standardised test should avoid all anthropomorphic interference (Holmes 2003), incorporate new approaches and, as much as possible, avoid human intervention during all steps in the test. Drapeau and colleagues (2018) performed a complete behavioural analysis, on adults and pups, noting the majority of behavioural phenotypes associated with ASD-like traits in mice (Drapeau et al. 2018). A

standardisation of this study could be an important first step for a standardisation of behavioural tests allowing a comparison between studies.

Furthermore, concerning results interpretation, the majority of studies on animal models did not reveal variability between individuals and stay close to the mean and standard deviation. A meta-analysis of *Shank3* mouse model collecting all raw data could improve the understanding of impact of *Shank3* mutation, and remaining isoforms, and go deeper on the analysis.

Hypothesis 2 for divergence between studies: genetic and epigenetic factors

The second reason that could explain this variability is the genetic and epigenetic basis. We noticed that the majority of mouse models displayed different genetic backgrounds, even if almost all of them presented several C57Bl/6 backcrosses before testing. Drapeau and colleagues (2014) studied *Shank3* mutation in different genetic backgrounds (C57Bl/6N; 129S6/SvEvTac and FVB/NTac) and observed different phenotypes between strains for mutated mice and also control mice (Drapeau et al. 2014). Consequently, this study shows the importance and the impact of the mouse strain on the phenotype.

Furthermore, in our mouse model, even with at least 15 backcrosses on C57Bl/6J background, we observe a higher number of SNP around the *Shank3* position compared to other regions of the genome. We associated this increase of SNP with the remaining 129 strain background linked to the genetic construction of the model. In all analyses, we consider genes present in this area apart. However, several genes that are associated with ASD and PMS in humans are located in this area in the mouse genome, due to the homology of gene position, for instance TCF20 (SFARI category2) or ADLS and CHKB (associated with syndromic ASD) (see Introduction III.B.2.b). Consequently, these genes could have an impact on the expression of other genes and on the phenotype. No such observation was reported before.

Benefit of variability

Even with behavioural phenotypes in common between studies, this variability can hinder a good comparison to highlight similar impairments and pharmacological pathways. An interesting way to exploit and understand this variability is to perform extensive analysis of gene expression, protein expression or methylation profiles. This type of analyses will provide a better understanding of the mechanisms leading gene mutations to atypical phenotypes in mice for each model. These will also provide clues for new pathways and *in fine* new pharmaco-therapeutic pathways.

II. Behaviour & transcriptomics

Even with the differences between studies, our analysis validated observations made by previous studies, especially at the behavioural level.

Hypoactivity linked with other behaviours

First of all, our model displayed phenotypes similar to other *Shank3* mouse models (see Introduction IV.B.2). Shank3-/- mice displayed an increase of self-grooming, a repetitive-like behaviour (Silverman et al. 2010), as well as a reduction of the distance travelled in the openfield in comparison with their wild-type littermates. Three possibilities can explain this reduced activity: an increase of self-grooming behaviour, a hypoactivity or hypotonicity, or a reduction of the exploratory behaviour. First, a mouse with a high self-grooming score spends less time expressing other behaviours like exploration. Indeed, in a principal component analysis, there was a negative correlation between the time spent in self-grooming behaviour and the distance travelled by each animal (see Results 0). Then, a hypoactivity or hypotonicity could explain this reduction. Indeed, Raab and colleagues (2010) showed the presence of *Shank3* in PSD of neuromuscular synapses, which could reduce the synaptic transmission to the muscles and reduce tonicity (Raab, Boeckers, and Neuhuber 2010). However, we did not observe a reduction of tonicity or motor coordination in the rotarod test. The absence of impairment in rotarod suggested intact cerebellar functions (Goddyn et al. 2006), and actually we did not find noteworthy impairment in cerebellum by RNAseq. Finally, this reduction can be linked to a lack of interest in exploration. The reduction of distance travelled is correlated with the reduction of digging behaviour, a classic exploratory behaviour (Belzung 1999). This can reveal a reduction of the exploratory behaviour not necessarily linked to self-grooming or hypoactivity.

Link between social impairments and reward circuit

In our analysis, no significant differences were observed between genotypes during same-sex social interaction, but, surprisingly, an increase of the time spent in contact was present for *Shank3-/-* males as occupant during socio-sexual interactions. It is difficult to conclude with this observation because no other study revealed this aspect. However, based on the implication of brain structure on social motivation, the implication of social reward can be an interesting hypothesis. Indeed, several studies showed the implication of structures from the mesocorticolimbic system, reward circuit (see Introduction II.C.1.c), like the VTA (Bariselli and Bellone 2017; Bariselli et al. 2016) or the striatum (W. Wang et al. 2017; Bey et al. 2018). To support the implication of mesocorticolimbic system in social impairment, Bariselli and colleagues (2016-2017) associated Shank3 with the maturation of dopaminergic neurons in the VTA and showed the impact of *Shank3* mutation on the social reward circuit (Bariselli et al. 2016; Bariselli and Bellone 2017). However, no study was made between NAcc, Shank3 mutation and the social reward aspect. Concerning the striatum, Wang and colleagues (2017) and Bey and colleagues (2018) studied the striatum in *Shank3* mutant mice and they revealed

impairments in synaptic transduction in striatum and especially a reduction of synaptic strength in D2 receptors (W. Wang et al. 2017; Bey et al. 2018). They connected impairments in striatal neurons with the presence of stereotyped behaviours and showed the implication of corticostriatal connection.

Validating these observations, our findings showed that the mutation of *Shank3* had opposite effects on gene expression in D1-MSN and D2-MSN, with an increase of gene expression in D2-MSN and a decrease of gene expression in D1-MSN, based on genes expressed in specific striatal cell types (Gokce et al. 2016). An increase of self-grooming behaviour might be associated with observed impairment in MSN and in particular in the dorsal striatum and locomotor activities. However, our results are performed on the whole striatum and we cannot determine if the impairments in MSN are linked to the cognitive aspect, via the NAcc, or locomotor aspect, via the dorsal striatum. An interesting future analysis will be to dissociate the ventral and dorsal striatum and to separate social cognition and locomotor activities. Interestingly, based on our RNAseq analysis, the implication of MSN and dopamine pathway, in *Shank3*Δ11, is accentuated by the increase of glutamate acid decarboxylase 2 (*Gad2)* in striatum, suggesting an increase of GABA formation and release. Based on KEGG analysis, we also observed correlations with *Shank3* mutation and the pathway associated with addiction and reward circuit (see Results 0). Recently, Rothwell and colleagues found common impaired pathways between ASD and drug addiction disorders (Rothwell 2016). An interesting behavioural validation of impairment in mesocorticolimbic pathway could be to test addiction of substance of abuse by conditioned place preference or drug self-administration procedure.

All this information suggested impairment in the striatum in *Shank3*-/- mice and especially in NAcc which will impair reward circuit and socio-sexual behaviour. This aspect was tested with social conditioned place preference using cotton soaked with female smell as a stimulus. However, social scent and interaction are a very subtle stimulus for induction and no significant difference were observed in wild-type or knock-out *Shank3* mice (data not shown). Furthermore, a deeper analysis of free social interaction with same genotype or modifying genotype for the "new-comer" could be interesting to detect subtle modulations of social interactions (Chaumont et al. 2018).

Home cage social behaviour

We observed another surprising behaviour. Indeed, in cages, with at least three females (*Shank3*$^{+/+}$ or *Shank3*$^{+/-}$) and only one *Shank3*-/- mouse, we observed that the *Shank3*-/- female was the only one to present intact fur and whiskers, suggesting that the *Shank3*$^{-/-}$ mouse performed barbering on its cage mates. This behaviour might reflect dominant traits in *Shank3*-/- females over *Shank3*$^{+/+}$ and *Shank3*$^{+/-}$ females (Kalueff et al. 2006). Based on the social brain aspect of hierarchy and dominance, it possibly revealed impairment in dorsomedian prefrontal cortex (see Introduction II.C.1.d). However, the dominance test, based on the dominance tube test, was not efficient to validate this observation (data not shown). Two potential reasons might explain this failure: (i) we tested females and the test is designed for males; (ii) the tube test reflects the immediate physical dominance

while dominance in the home cage might involve a combination of events. Since our males were housed in social isolation from three months of age on, we could not observe this dominance specificity on males.

Isoform expression

In our analysis, we observed a significant reduction of *Shank3* expression and no modification of *Shank1* and *Shank2*. Even with little information on expressed isoforms, we only observed the global expression of *Shank*s. However, the expression of *Shank1* and *Shank2* was not modified between *Shank3*+/+ and *Shank3*-/- mice. Very little information can be extracted about the different isoforms expressed, mainly because of the type of RNAsequencing used and the small size of the reads generated. Ususally, long-read RNAsequencing is used for this kind of analaysis. Future analyses should perform a quantification of different *Shank* (1-2-3) isoforms expression in different brain structures for each genotype (in *Shank3* cohort and *Shank2*/*Shank3* cohort) using qPCR analysis.

Interaction between Shank2 and Shank3

Schmeisser and colleagues (2012) revealed an increase of *Shank2* expression in *Shank3* mutant mouse and vice versa for *Shank2* mouse model (Schmeisser et al. 2012). Furthermore, in unpublished data from E. Ey, compensation between *Shank2* and *Shank3* seemed to be present in a subgroup of *Shank2*-/- mice performing similar social interaction and communication than *Shank2*+/+ mice. Unfortunately, when we analysed the behaviour of mice mutated in *Shank2* and/or *Shank3*, little information could be extracted due to the low number of individuals of each genotype.

In our characterisation of the *Shank2*/*Shank3* double mutant, mice carrying *Shank2* homozygous deletion displayed hyperactivity like *Shank2*-/- mice previously described (Schmeisser et al. 2012; Won et al. 2012; Pappas et al. 2017), while mice carrying *Shank3* homozygous deletion displayed an increase of self-grooming like *Shank3*-/- mice previously described. Surprisingly, the double homozygous mutants did not seem to display *Shank2* hyperactivity or *Shank3* self-grooming and males and females displayed different phenotypes. The behavioural phenotype did not seem to be impacted by the presence or not of the other *Shank*. A complementary study with more animals as well as RNA or proteins expression analysis will improve the understanding of *Shank2*/*Shank3* interaction and document any potential compensation between *Shank2* and *Shank3*.

Heterogeneity in patients and mice

As we saw in a previous part of this manuscript, different factors, genetic, environmental and epigenetic, impact gene expression (see Introduction III.B.1). These factors cause an important phenotypic heterogeneity in observable phenotype between patients. This is especially true for the gene *SHANK3*. Several analyses of phenotype and genotype of S*HANK3* patients highlighted this heterogeneity, with an implication in different neurological and psychiatric disorders (Guilmatre et al.

2014). In addition, there exists also an important variability between patients with ASD carrying a mutation in *SHANK3* (Leblond et al. 2014). To understand the mechanisms underlying *SHANK3* mutations in humans, several mouse models were generated. However, the aspect of inter-individual variability in patients is not studied in mouse models.

In our study, we highlighted an important variability between *Shank3*-/- mice, especially in self-grooming behaviour. We compared, for the first time, this variability with the observation in patients and we tried to exploit this aspect to understand the underlying pathways. This important variability between individuals is already present in young adults (three months of age), with some animals displaying a level of self-grooming similar to *Shank3*+/+ mice, and others expressing an already high level of self-grooming. Based on RNA-Seq, we tried to find specific genes and cellular pathways in different brain structures explaining the self-grooming variability for *Shank3*-/- mice. Surprisingly, we did not find significant explanation for the variability at 12 months, due to the low statistical power. A similar study with a larger cohort or a study on selected genes should be performed. Other levels need to be investigated like proteomic or epigenetic analyses. Indeed, Wang and colleagues (2014) showed the presence of the isoform Shank3b in the nucleus, suggesting an impact of Shank3 on gene expression without proposing a mechanism of action (X. Wang et al. 2014). Furthermore, Qin and colleagues (2018) promoted the implication of Shank3 in the regulation of a HDAC, which regulate the opening of DNA strain and DNA expression (Qin et al. 2018). Consequently, Shank3 seemed to have an impact at the epigenetic level. However, the relation between HDAC and Shank3 could depend on the isoform expressed because this observation was only made on *Shank3*Δ**21P** and not on the models expressing more isoforms, especially in mouse *Shank3*Δ**11** via proteomic (Reim et al. 2017) and transcriptomic (this study) or mouse with **over-expression** via proteomic (Y. Lee, Kim, et al. 2017).

Our study gives some clues to explain the inter-individual variability and the behavioural trajectories. Unfortunately, due to the small number of individuals, we cannot propose a likely explanation of inter-individual variability, based on RNA sequencing. To better understand the impact of gene or protein expression explaining the evolution of the phenotype in mice, and potentially in patients, future studies should investigate the proteomics and transcriptomics including microRNA analysis in a larger cohort.

Behavioural worsening with age

Interestingly, the phenotypic variability between animals increased while ageing. In several *Shank3*-/- individuals, we observed a worsening of the phenotype with increasing age that was not present in *Shank3*+/+ and *Shank3*+/- mice, especially for self-grooming behaviour. Interestingly, patients with *SHANK3* mutation or deletion often displayed similar decline at adolescence (De Rubeis et al. 2018). However, all *Shank3*-/- mice did not display this worsening of the phenotype and revealed different behavioural trajectories while ageing. This worsening of the phenotype, or regression, is

observed in several patients at adolescence or young adulthood, and a lithium treatment is proposed to reduce some aspects of this regression (Serret et al. 2015; Guilmatre et al. 2014; De Rubeis et al. 2018). Lithium is usually used as a mood stabiliser in *Shank3* patients. Study of lithium treatment on mouse models, displaying worsening of the phenotype, will validate the phenotype and allow a better understanding of cellular interaction.

In future studies, we will analyse the expression of genes in different parts of the brain for mice at three months of age. The aim of this analysis is to confirm the gene expression at different ages and to provide a time course for the modification of the gene expression. Further investigation should be performed to assess relations between regressions of phenotype, gene expression and protein expression in this model.

III. Specific gene expression impaired

In previous studies, *Shank3* seemed to have an impact on the nucleus and gene expression (X. Wang et al. 2014; Qin et al. 2018). In the present thesis, we analysed the general gene expression to determine the impact of mutation at the cellular level. Comparing our analysis with the different omics analyses on our model (Δ11; (Reim et al. 2017)) and over-expressing model (Y. Lee, Kim, et al. 2017), we did not notice any crossed gene/protein in common with an adjusted p.value ≤0.05. Two main reasons can explain this observation. The first is related to the variability of the phenotype (behaviour and electrophysiology), as explained above. Indeed, as we observed a variability of the behavioural phenotype between studies on the same model, we hypothesise similar variability at the molecular level. The second reason is the presence of impairment in pre/post-traductional regulation and, by extension, the direct or indirect implication of Shank3 in this regulation. Indeed, no study was made on the regulation of protein expression from RNA. Further investigations on the pre/post traductional regulation could improve the understanding of the difference between the results from the proteomic and the results of transcriptomic analysis.

We studied the differential gene expression between *Shank3*+/+ and *Shank3*-/- *mice*. Surprisingly, the whole striatum seemed to be the most impacted among all brain structures and several differentially expressed genes encode for neuronal and synaptic proteins. As we saw in the introduction, the striatum is a key structure involved in different aspects of social interaction as well as stereotyped behaviours (see Introduction II.C).

First, we showed an implication of different glutamate receptors. Previous studies on *Shank3* mouse mutants showed a decrease of some ionotropic glutamate receptors, more specifically GluA (*Shank3*Δ4-9J (X. Wang et al. 2011), *Shank3*Δ13 (Jaramillo et al. 2017), *Shank3*InsG3680 (Zhou et al. 2016)); GluN1, GluN2A-B (*Shank3*Δ4-9J (X. Wang et al. 2011), *Shank3*Δ11 (Schmeisser et al. 2012; Reim et al. 2017), *Shank3*Δ13 (Jaramillo et al. 2017), *Shank3*InsG3680 (Zhou et al. 2016)), and

metabotropic receptors, more specifically mGluR5 (*Shank3*Δ11 (Schmeisser et al. 2012), *Shank3*InsG3680 (Zhou et al. 2016)). Surprinsingly, we did not observed similar impairment for GluA, GluN or mGluR5 by RNA-seq. We found a decrease of mGluR2 (Grm2) expression and an increase of GluR6 (Grik2). The gene *Grik2* encodes an ionotropic kainate glutamate receptor sub-unit, which participates postsynaptically in transmission with NMDAR and AMPAR (Huettner 2003; Lerma 2003). Recently, this gene has been associated with ataxia and intellectual disabilities in patients (Guzmán et al. 2017). Interestingly, ionotropic kainate receptors have a non – canonical impact on the cellular signalisation by connexion with Gq-protein (Rodrigues and Lerma 2012). The gene *Grm2* (mGluR2) encodes a G-protein coupled receptor linked to the Pro *Shank3* domain (see Introduction III.A.2.d). This protein negatively modulates the adenylate cyclase and reduces the production of cAMP and protein kinase A (Conn and Pin 1997; Anwyl 1999a, 1999b). Interestingly, Grm2 and Grm3 are target for schizophrenia treatment (Muguruza, Meana, and Callado 2016; Conn and Jones 2009) and a decrease of mRNA and protein expression of Grm2 was observed in valproate-induced rat model of autism (Y.-W. Chen et al. 2014). However, up to now, no modification of this protein expression has been reported in other *Shank3* mouse models.

Furthermore, cornichon family AMPA receptor auxiliary protein 3 (Cnih3) is a protein binding AMPAR, promotes receptor traffiking and AMPAR sub-unit assembly and slows down AMPAR deactivation (Herring et al. 2013). The protein is associated with dependence behaviour especially for opioid (E. C. Nelson et al. 2016). We found a decrease of *Cnih3* gene expression in *Shank3-/-* mice that could reveal impairments in AMPAR activation. However, we did not test the addiction to drugs on our mouse model. This observation indicates a possible impairment on ionotropic glutamatergic receptors without a reduction of the ionotropic receptors expression.

Finally, the expression of GKAP/SAPAP is significantly reduced in striatum. This is a scaffolding protein connecting PDZ domain with AMPAR and NMDAR (see III.A.2.c).

All these observations indicate impairment in signal induction at glutamatergic synapses in *Shank3-/-* mice. This aspect is reinforced by the PPI analysis. This last analysis revealed dysregulation of the expression of several genes related to cellular signalisation in striatum. Impairment in post-synaptic processing in glutamatergic synapses provokes dysregulation of gene expression, which is, apparently, specifically associated with striatum and MSN.

However, these findings should also be interpreted with caution due to the difference observed between RNAseq analysis and ddPCR validation. Indeed, an important variability is present in PCR validation results, preventing a robust validation of these genes, likely due to the different techniques used.

IV. Perpectives and conclusion

To conclude, due to the variability between studies, new approaches of mouse models study should be generated to allow a better characterisation and a better understanding over the age of the observed phenotype of models and by extension in humans. These new approaches will improve the understanding of the phenotypic evolution that we observed in mice.

Our analysis on behaviour and transcriptomic revealed some interesting molecular bases of the impairment generated by a *Shank3*Δ11 mutation. We revealed impairments in self-grooming behaviour, socio-sexual interaction and locomotion at different time points, which can be related with observed impairment in gene expression in striatum at a later age. In our study, we noticed especially an impairment of the balance between D1-MSN and D2-MSN (see Results 0). However, we cannot define the implication of dorsal or ventral striatum as well as the modification of synaptic strength of D1-MSN or D2-MSN. Complementary behavioural analyses will be interesting, especially social reward test and addiction test. These behavioural studies can be complemented by a conditional knock-out *Shank3* mice in the striatum and especially in D1-MSN or D2-MSN. This study on striatal conditional knock-out mice can be associated with the analysis of other conditional mice, in cerebellar granule cells or cortex. An electrophysiological study would be recommended to determine these aspects and elucidate the impact of *Shank3*Δ11 in sub-level of our transcriptome analysis in all brain structures to determine impairment.

One of the important bias in our study is the age of the mice used for RNAseq. The majority of studies used adult animal of three to four months of age. We are currently analysing the brains of three-months old mice from a second cohort to validate the RNA expression results observed in old animals. This complementary study will allow us to determine the impact of *Shank3* mutation in younger animals and to understand the evolution of the phenotype based on RNA expression. However, as we said previously, a possible post-transcriptomic regulation can be present. Complementary analysis of RNA expression, including miRNA, protein expression and expression regulation could provide more details on the mechanisms underlying *Shank3* mutation.

Furthermore, we did not determine the expression of the different isoforms of *Shank1, Shank2* and *Shank3*. We are currently trying to quantify by qPCR the expression of the different isoforms of the three Shanks in the different brain structures in different cohorts. Then, we will study the correlation between *Shank* expression and behaviours.

Based on all observations, mutation on Shank3 PDZ domains, and likely the loss of Shank3a-b-c, seems to impair the gene expression of synaptic signalisation proteins. Two hypotheses can explain this reduction. The suppression of *Shank3* generates dysregulation of expression of proteins mainly involved in cell signalling (X. Wang et al. 2014; Qin et al. 2018). Or the suppression of ANK SH3 and PDZ domains does not allow recruitment of signalling proteins, provoking a reduction of those proteins. In both cases, reduction of signalling proteins generates impairment in signal transduction, especially in striatum over the long term. In view of antagonist mechanisms for D1-MSN and D2-MSN and the relationship between dopamine and glutamatergic receptors, impairment in

glutamatergic synaptic signalisation have opposite effect for both types of striatal neurons (Beaulieu and Gainetdinov 2011). This imbalance will impair controlled locomotor activities, generating stereotyped behaviour, or impair reward circuit, generating unusual social interaction.

Finally, this study gives good understanding of the level of impairment generated by *Shank3* and the pathway and brain structure implicated. Our data corroborate previous studies. A deeper analysis of striatum and MSN could suggest new pharmaceutical approach for patients, targeting the imbalance in MSN. Furthermore, complementary study on the worsening of the phenotype observed in mice will give new knowledge about the evolution of the patient phenotype. A better understanding will give new therapeutic pathways, using mGluR2 agonist (Muguruza, Meana, and Callado 2016; Conn and Jones 2009), or validate already used treatment, for instance lithium (Serret et al. 2015), to avoid or reduce this variability.

REFERENCES

Alexander, G E, M R DeLong, and P L Strick. 1986. “Parallel Organization of Functionally Segregated Circuits Linking Basal Ganglia and Cortex.” *Annual Review of Neuroscience* 9 (1). Annual Reviews 4139 El Camino Way, P.O. Box 10139, Palo Alto, CA 94303-0139, USA : 357–81. https://doi.org/10.1146/annurev.ne.09.030186.002041.

Alhamdoosh, Monther, Milica Ng, Nicholas J. Wilson, Julie M. Sheridan, Huy Huynh, Michael J. Wilson, and Matthew E. Ritchie. 2017. “Combining Multiple Tools Outperforms Individual Methods in Gene Set Enrichment Analyses.” *Bioinformatics* 33 (3): 414–24. https://doi.org/10.1093/bioinformatics/btw623.

American Psychiatric Association. 1980. *Diagnostic and Statistical Manual of Mental Disorders, Third Edition, Text Revision (DSM-III-TR)*. Vol. 1. Arlington, VA: American Psychiatric Association. https://doi.org/10.1176/appi.books.9780890423349.

———. 2000. *Diagnostic and Statistical Manual of Mental Disorders, Fourth Edition, Text Revision (DSM-IV-TR)*. Vol. 1. Arlington, VA: American Psychiatric Association. https://doi.org/10.1176/appi.books.9780890423349.

———. 2013. *Diagnostic and Statistical Manual of Mental Disorders*. American Psychiatric Association. https://doi.org/10.1176/appi.books.9780890425596.

Amiet, Claire, Isabelle Gourfinkel-An, Anissa Bouzamondo, Sylvie Tordjman, Michel Baulac, Philippe Lechat, Laurent Mottron, and David Cohen. 2008. “Epilepsy in Autism Is Associated with Intellectual Disability and Gender: Evidence from a Meta-Analysis.” *Biological Psychiatry* 64 (7): 577–82. https://doi.org/10.1016/j.biopsych.2008.04.030.

Amir, Ruthie E., Ignatia B. Van den Veyver, Mimi Wan, Charles Q. Tran, Uta Francke, and Huda Y. Zoghbi. 1999. “Rett Syndrome Is Caused by Mutations in X-Linked MECP2, Encoding Methyl-CpG-Binding Protein 2.” *Nature Genetics* 23 (2): 185–88. https://doi.org/10.1038/13810.

Anwyl, R. 1999a. “Metabotropic Glutamate Receptors: Electrophysiological Properties and Role in Plasticity.” *Brain Research. Brain Research Reviews* 29 (1): 83–120. http://www.ncbi.nlm.nih.gov/pubmed/9974152.

———. 1999b. “Metabotropic Glutamate Receptors: Electrophysiological Properties and Role in Plasticity.” *Brain Research. Brain Research Reviews* 29 (1): 83–120. http://www.ncbi.nlm.nih.gov/pubmed/11239574.

Arriaga, Gustavo, and Erich D. Jarvis. 2013. “Mouse Vocal Communication System: Are Ultrasounds Learned or Innate?” *Brain and Language* 124 (1). Academic Press: 96–116. https://doi.org/10.1016/j.bandl.2012.10.002.

Arriaga, Gustavo, Eric P. Zhou, and Erich D. Jarvis. 2012. “Of Mice, Birds, and Men: The Mouse Ultrasonic Song System Has Some Features Similar to Humans and Song-Learning Birds.” Edited by Charles R. Larson. *PLoS ONE* 7 (10). Public Library of Science: e46610. https://doi.org/10.1371/journal.pone.0046610.

Asperger, Hans. 1944. “Die „Autistischen Psychopathen” Im Kindesalter.” *Archiv Für Psychiatrie Und Nervenkrankheiten* 117 (1). Springer-Verlag: 76–136. https://doi.org/10.1007/BF01837709.

August, G. J., M. A. Stewart, and L. Tsai. 1981. “The Incidence of Cognitive Disabilities in the Siblings of Autistic Children.” *The British Journal of Psychiatry* 138 (5). Cambridge University Press: 416–22. https://doi.org/10.1192/bjp.138.5.416.

Auwera, Geraldine A. Van der, Mauricio O. Carneiro, Christopher Hartl, Ryan Poplin, Guillermo del Angel, Ami Levy-Moonshine, Tadeusz Jordan, et al. 2002. “From FastQ Data to High-Confidence Variant Calls: The Genome Analysis Toolkit Best Practices Pipeline.” In *Current Protocols in Bioinformatics*. John Wiley & Sons, Inc.

Bachevalier, Jocelyne. 1996. “Brief Report: Medial Temporal Lobe and Autism: A Putative Animal Model in Primates.” *Journal of Autism and Developmental Disorders* 26 (2). Kluwer Academic Publishers-Plenum Publishers: 217–20. https://doi.org/10.1007/BF02172015.

Bailey, A, A Le Couteur, I Gottesman, P Bolton, E Simonoff, E Yuzda, and M Rutter. 1995. “Autism as a Strongly Genetic Disorder: Evidence from a British Twin Study.” *Psychological Medicine* 25 (1): 63–77. http://www.ncbi.nlm.nih.gov/pubmed/7792363.

Baio, Jon, Lisa Wiggins, Deborah L. Christensen, Matthew J Maenner, Julie Daniels, Zachary Warren, Margaret Kurzius-Spencer, et al. 2018. “Prevalence of Autism Spectrum Disorder Among Children Aged 8 Years — Autism and Developmental Disabilities Monitoring Network, 11 Sites, United States, 2014.” *MMWR. Surveillance Summaries* 67 (6): 1–23. https://doi.org/10.15585/mmwr.ss6706a1.

Bariselli, Sebastiano, and Camilla Bellone. 2017. “VTA DA Neuron Excitatory Synapses in Shank3 Δex4–9mouse Line.” *Synapse* 71 (6): 1–5. https://doi.org/10.1002/syn.21955.

Bariselli, Sebastiano, Stamatina Tzanoulinou, Christelle Glangetas, Clément Prévost-Solié, Luca Pucci, Joanna Viguié, Paola Bezzi, et al. 2016. “SHANK3 Controls Maturation of Social Reward Circuits in the VTA.” *Nature Neuroscience* 19 (7): 926–34. https://doi.org/10.1038/nn.4319.

Barry, William T., Andrew B. Nobel, and Fred A. Wright. 2005. “Significance Analysis of Functional Categories in Gene Expression Studies: A Structured Permutation Approach.” *Bioinformatics* 21 (9): 1943–49. https://doi.org/10.1093/bioinformatics/bti260.

Beaulieu, J.-M., and Raul R Gainetdinov. 2011. “The Physiology, Signaling, and Pharmacology of Dopamine Receptors.” *Pharmacological Reviews* 63 (1): 182–217. https://doi.org/10.1124/pr.110.002642.

Belmonte, Matthew K, Greg Allen, Andrea Beckel-Mitchener, Lisa M Boulanger, Ruth A Carper, and Sara J Webb. 2004. “Autism and Abnormal Development of Brain Connectivity.” *The Journal of Neuroscience : The Official Journal of the Society for Neuroscience* 24 (42). Society for Neuroscience: 9228–31. https://doi.org/10.1523/JNEUROSCI.3340-04.2004.

Belzung, Catherine. 1999. “Chapter 4.11 Measuring Rodent Exploratory Behavior.” *Techniques in the Behavioral and Neural Sciences* 13 (January). Elsevier: 738–49. https://doi.org/10.1016/S0921-0709(99)80057-1.

Berchtold, Nicole C, David H Cribbs, Paul D Coleman, Joseph Rogers, Elizabeth Head, Ronald Kim, Tom Beach, et al. 2008. “Gene Expression Changes in the Course of Normal Brain Aging Are Sexually Dimorphic.” *Proceedings of the National Academy of Sciences of the United States of America* 105 (40). National Academy of Sciences: 15605–10. https://doi.org/10.1073/pnas.0806883105.

Berg, Elizabeth L., Nycole A. Copping, Josef K. Rivera, Michael C. Pride, Milo Careaga, Melissa D. Bauman, Robert F. Berman, et al. 2018. “Developmental Social Communication Deficits in the Shank3 Rat Model of Phelan-Mcdermid Syndrome and Autism Spectrum Disorder.” *Autism Research : Official Journal of the International Society for Autism Research*, January. https://doi.org/10.1002/aur.1925.

Berger, Brynn E, Ann Marie Navar-Boggan, and Saad B Omer. 2011. “Congenital Rubella Syndrome and Autism Spectrum Disorder Prevented by Rubella Vaccination - United States, 2001-2010.” *BMC Public Health* 11 (1): 340. https://doi.org/10.1186/1471-2458-11-340.

Beri, Silvana, Noemi Tonna, Giorgia Menozzi, Maria Clara Bonaglia, Carlo Sala, and Roberto Giorda. 2007. “DNA Methylation Regulates Tissue-Specific Expression of Shank3.” *Journal of Neurochemistry* 101 (5). Wiley/Blackwell (10.1111): 1380–91. https://doi.org/10.1111/j.1471-

4159.2007.04539.x.

Bertone, Armando, Laurent Mottron, Patricia Jelenic, and Jocelyn Faubert. 2005. "Enhanced and Diminished Visuo-Spatial Information Processing in Autism Depends on Stimulus Complexity." *Brain* 128 (10): 2430–41. https://doi.org/10.1093/brain/awh561.

Bey, Alexandra L., Xiaoming Wang, Haidun Yan, Namsoo Kim, Rebecca L. Passman, Yilin Yang, Xinyu Cao, et al. 2018. "Brain Region-Specific Disruption of Shank3 in Mice Reveals a Dissociation for Cortical and Striatal Circuits in Autism-Related Behaviors." *Translational Psychiatry* 8 (1). Nature Publishing Group: 94. https://doi.org/10.1038/s41398-018-0142-6.

Bidinosti, Michael, Paolo Botta, Sebastian Krüttner, Catia C. Proenca, Natacha Stoehr, Mario Bernhard, Isabelle Fruh, et al. 2016. "CLK2 Inhibition Ameliorates Autistic Features Associated with SHANK3 Deficiency." *Science* 351 (6278). American Association for the Advancement of Science: 1199–1203. https://doi.org/10.1126/science.aad5487.

Bird, Adrian. 2002. "DNA Methylation Patterns and Epigenetic Memory." *Genes & Development* 16 (1). Cold Spring Harbor Laboratory Press: 6–21. https://doi.org/10.1101/gad.947102.

Bishop, D V. 1998. "Development of the Children's Communication Checklist (CCC): A Method for Assessing Qualitative Aspects of Communicative Impairment in Children." *Journal of Child Psychology and Psychiatry, and Allied Disciplines* 39 (6): 879–91. http://www.ncbi.nlm.nih.gov/pubmed/9758196.

Boat, Thomas F., Joel T. Wu, Committee to Evaluate the Supplemental Security Income Disability Program for Children with Mental Disorders, Board on the Health of Select Populations, Youth, and Families Board on Children, Institute of Medicine, Division of Behavioral and Social Sciences and Education, and Engineering, and Medicine The National Academies of Sciences. 2015. *Mental Disorders and Disabilities Among Low-Income Children*. *Mental Disorders and Disabilities Among Low-Income Children*. National Academies Press (US). https://doi.org/10.17226/21780.

Boccuto, Luigi, Maria Lauri, Sara M Sarasua, Cindy D Skinner, Daniela Buccella, Alka Dwivedi, Daniela Orteschi, et al. 2013. "Prevalence of SHANK3 Variants in Patients with Different Subtypes of Autism Spectrum Disorders." *European Journal of Human Genetics* 21 (3). Nature Publishing Group: 310–16. https://doi.org/10.1038/ejhg.2012.175.

Bodfish, J W, F J Symons, D E Parker, and M H Lewis. 2000. "Varieties of Repetitive Behavior in Autism: Comparisons to Mental Retardation." *Journal of Autism and Developmental Disorders* 30 (3): 237–43. http://www.ncbi.nlm.nih.gov/pubmed/11055459.

Boeckers, Tobias M., Carsten Inter, Karl Heinz Smalla, Michael R. Kreutz, Juergen Bockmann, Constanze Seidenbecher, Craig C. Garner, and Eckart D. Gundelfinger. 1999. "Proline-Rich Synapse-Associated Proteins ProSAP1 and ProSAP2 Interact with Synaptic Proteins of the SAPAP/GKAP Family." *Biochemical and Biophysical Research Communications* 264 (1): 247–52. https://doi.org/10.1006/bbrc.1999.1489.

Boeckers, Tobias M., Thomas Liedtke, Christina Spilker, Thomas Dresbach, Jürgen Bockmann, Michael R. Kreutz, and Eckart D. Gundelfinger. 2005. "C-Terminal Synaptic Targeting Elements for Postsynaptic Density Proteins ProSAP1/Shank2 and ProSAP2/Shank3." *Journal of Neurochemistry* 92 (3): 519–24. https://doi.org/10.1111/j.1471-4159.2004.02910.x.

Bonaglia, Maria Clara, Roberto Giorda, Silvana Beri, Cristina De Agostini, Francesca Novara, Marco Fichera, Lucia Grillo, et al. 2011. "Molecular Mechanisms Generating and Stabilizing Terminal 22q13 Deletions in 44 Subjects with Phelan/McDermid Syndrome." Edited by Nancy B. Spinner. *PLoS Genetics* 7 (7): e1002173. https://doi.org/10.1371/journal.pgen.1002173.

Bosch, Oliver J., and Inga D. Neumann. 2012. “Both Oxytocin and Vasopressin Are Mediators of Maternal Care and Aggression in Rodents: From Central Release to Sites of Action.” *Hormones and Behavior* 61 (3). Elsevier Inc.: 293–303. https://doi.org/10.1016/j.yhbeh.2011.11.002.

Bourgeron, T. 2007. “The Possible Interplay of Synaptic and Clock Genes in Autism Spectrum Disorders.” *Cold Spring Harbor Symposia on Quantitative Biology* 72 (January). Cold Spring Harbor Laboratory Press: 645–54. https://doi.org/10.1101/sqb.2007.72.020.

Bourgeron, Thomas. 2015. “From the Genetic Architecture to Synaptic Plasticity in Autism Spectrum Disorder.” *Nature Reviews Neuroscience* 16 (9). Nature Publishing Group: 551–63. https://doi.org/10.1038/nrn3992.

———. 2016. “Current Knowledge on the Genetics of Autism and Propositions for Future Research.” *Comptes Rendus Biologies* 339 (7–8): 300–307. https://doi.org/10.1016/j.crvi.2016.05.004.

Bowden, C L. 2000. “Efficacy of Lithium in Mania and Maintenance Therapy of Bipolar Disorder.” *The Journal of Clinical Psychiatry* 61 Suppl 9: 35–40. http://www.ncbi.nlm.nih.gov/pubmed/10826659.

Bozdagi, Ozlem, Takeshi Sakurai, Danae Papapetrou, Xiaobin Wang, Dara L Dickstein, Nagahide Takahashi, Yuji Kajiwara, et al. 2010. “Haploinsufficiency of the Autism-Associated Shank3 Gene Leads to Deficits in Synaptic Function, Social Interaction, and Social Communication.” *Molecular Autism* 1 (1). BioMed Central: 15. https://doi.org/10.1186/2040-2392-1-15.

Brennan, Peter a, and Keith M Kendrick. 2006. “Mammalian Social Odours: Attraction and Individual Recognition.” *Philosophical Transactions of the Royal Society of London. Series B, Biological Sciences* 361 (1476): 2061–78. https://doi.org/10.1098/rstb.2006.1931.

Brown, Steve D M, John M Hancock, and Hilary Gates. 2006. “Understanding Mammalian Genetic Systems: The Challenge of Phenotyping in the Mouse.” *PLoS Genetics* 2 (8): e118. https://doi.org/10.1371/journal.pgen.0020118.

Brückner, Katja, Juan Pablo Labrador, Peter Scheiffele, Anne Herb, Peter H. Seeburg, and Rüdiger Klein. 1999. “EphrinB Ligands Recruit GRIP Family PDZ Adaptor Proteins into Raft Membrane Microdomains.” *Neuron* 22 (3): 511–24. https://doi.org/10.1016/S0896-6273(00)80706-0.

Carper, Ruth A., and Eric Courchesne. 2005. “Localized Enlargement of the Frontal Cortex in Early Autism.” *Biological Psychiatry* 57 (2). Elsevier: 126–33. https://doi.org/10.1016/J.BIOPSYCH.2004.11.005.

Casanova, Manuel F., Daniel P. Buxhoeveden, Andrew E. Switala, and Emil Roy. 2002. “Neuronal Density and Architecture (Gray Level Index) in the Brains of Autistic Patients.” *Journal of Child Neurology* 17 (7): 515–21. https://doi.org/10.1177/088307380201700708.

Casanova, Manuel, and Juan Trippe. 2009. “Radial Cytoarchitecture and Patterns of Cortical Connectivity in Autism.” *Philosophical Transactions of the Royal Society of London. Series B, Biological Sciences* 364 (1522). The Royal Society: 1433–36. https://doi.org/10.1098/rstb.2008.0331.

Casey, Jillian P., Tiago Magalhaes, Judith M. Conroy, Regina Regan, Naisha Shah, Richard Anney, Denis C. Shields, et al. 2012. “A Novel Approach of Homozygous Haplotype Sharing Identifies Candidate Genes in Autism Spectrum Disorder.” *Human Genetics* 131 (4): 565–79. https://doi.org/10.1007/s00439-011-1094-6.

Cellot, Giada, and Enrico Cherubini. 2014. “GABAergic Signaling as Therapeutic Target for Autism Spectrum Disorders.” *Frontiers in Pediatrics* 2 (July). Frontiers: 70. https://doi.org/10.3389/fped.2014.00070.

Chatr-aryamontri, Andrew, Rose Oughtred, Lorrie Boucher, Jennifer Rust, Christie Chang, Nadine K. Kolas, Lara O'Donnell, et al. 2017. "The BioGRID Interaction Database: 2017 Update." *Nucleic Acids Research* 45 (D1): D369–79. https://doi.org/10.1093/nar/gkw1102.

Chaumont, Fabrice de, Renata Dos-Santos Coura, Pierre Serreau, Arnaud Cressant, Jonathan Chabout, Sylvie Granon, and Jean-Christophe Olivo-Marin. 2012. "Computerized Video Analysis of Social Interactions in Mice." *Nature Methods* 9 (4): 410–17. https://doi.org/10.1038/nmeth.1924.

Chaumont, Fabrice de, Stéphane Dallongeville, Nicolas Chenouard, Nicolas Hervé, Sorin Pop, Thomas Provoost, Vannary Meas-Yedid, et al. 2012. "Icy: An Open Bioimage Informatics Platform for Extended Reproducible Research." *Nature Methods* 9 (7): 690–96. https://doi.org/10.1038/nmeth.2075.

Chaumont, Fabrice de, Elodie Ey, Nicolas Torquet, Thibault Lagache, Stephane Dallongeville, Albane Imbert, Thierry Legou, et al. 2018. "Live Mouse Tracker: Real-Time Behavioral Analysis of Groups of Mice." *BioRxiv*, June. Cold Spring Harbor Laboratory, 345132. https://doi.org/10.1101/345132.

Chen, Lu, Dane M. Chetkovich, Ronald S. Petralia, Neal T. Sweeney, Yoshimi Kawasaki, Robert J. Wenthold, David S. Bredt, and Roger A. Nicoll. 2000. "Stargazin Regulates Synaptic Targeting of AMPA Receptors by Two Distinct Mechanisms." *Nature* 408 (6815): 936–43. https://doi.org/10.1038/35050030.

Chen, Yu-Wen, Hui-Ching Lin, Ming-Chong Ng, Ya-Hsin Hsiao, Chao-Chuan Wang, Po-Wu Gean, and Po See Chen. 2014. "Activation of MGluR2/3 Underlies the Effects of N-Acetylcystein on Amygdala-Associated Autism-like Phenotypes in a Valproate-Induced Rat Model of Autism." *Frontiers in Behavioral Neuroscience* 8 (June): 219. https://doi.org/10.3389/fnbeh.2014.00219.

Chevallier, Coralie, Gregor Kohls, Vanessa Troiani, Edward S. Brodkin, and Robert T. Schultz. 2012. "The Social Motivation Theory of Autism." *Trends in Cognitive Sciences* 16 (4). Elsevier Ltd: 231–38. https://doi.org/10.1016/j.tics.2012.02.007.

Chinwalla, Asif T., Lisa L. Cook, Kimberly D. Delehaunty, Ginger A. Fewell, Lucinda A. Fulton, Robert S. Fulton, Tina A. Graves, et al. 2002. "Initial Sequencing and Comparative Analysis of the Mouse Genome." *Nature* 420 (6915). Nature Publishing Group: 520–62. https://doi.org/10.1038/nature01262.

Choi, Su Yeon, Kaifang Pang, Joo Yeon Kim, Jae Ryun Ryu, Hyojin Kang, Zhandong Liu, Won Ki Kim, Woong Sun, Hyun Kim, and Kihoon Han. 2015. "Post-Transcriptional Regulation of SHANK3 Expression by MicroRNAs Related to Multiple Neuropsychiatric Disorders." *Molecular Brain* 8 (1). Molecular Brain: 1–12. https://doi.org/10.1186/s13041-015-0165-3.

Chow, Maggie L, Tiziano Pramparo, Mary E Winn, Cynthia Carter Barnes, Hai-Ri Li, Lauren Weiss, Jian-Bing Fan, et al. 2012. "Age-Dependent Brain Gene Expression and Copy Number Anomalies in Autism Suggest Distinct Pathological Processes at Young Versus Mature Ages." *PLoS Genet* 8 (3). https://doi.org/10.1371/journal.pgen.1002592.

Colantuoni, Carlo, Barbara K. Lipska, Tianzhang Ye, Thomas M. Hyde, Ran Tao, Jeffrey T. Leek, Elizabeth A. Colantuoni, et al. 2011. "Temporal Dynamics and Genetic Control of Transcription in the Human Prefrontal Cortex." *Nature* 478 (7370). Nature Publishing Group: 519–23. https://doi.org/10.1038/nature10524.

Collins, Sean M., Amogh P. Belagodu, Samantha L. Reed, and Roberto Galvez. 2017. "SHANK1 Is Differentially Expressed during Development in CA1 Hippocampal Neurons and Astrocytes." *Developmental Neurobiology*, December. https://doi.org/10.1002/dneu.22564.

Colvert, Emma, Beata Tick, Fiona McEwen, Catherine Stewart, Sarah R. Curran, Emma Woodhouse,

Nicola Gillan, et al. 2015. “Heritability of Autism Spectrum Disorder in a UK Population-Based Twin Sample.” *JAMA Psychiatry* 72 (5): 415. https://doi.org/10.1001/jamapsychiatry.2014.3028.

Conn, P. Jeffrey, and Jean-Philippe Pin. 1997. “PHARMACOLOGY AND FUNCTIONS OF METABOTROPIC GLUTAMATE RECEPTORS.” *Annual Review of Pharmacology and Toxicology* 37 (1): 205–37. https://doi.org/10.1146/annurev.pharmtox.37.1.205.

Conn, P Jeffrey, and Carrie K Jones. 2009. “Promise of MGluR2/3 Activators in Psychiatry.” *Neuropsychopharmacology* 34 (1). Nature Publishing Group: 248–49. https://doi.org/10.1038/npp.2008.156.

Constantino, J N, T Przybeck, D Friesen, and R D Todd. 2000. “Reciprocal Social Behavior in Children with and without Pervasive Developmental Disorders.” *Journal of Developmental and Behavioral Pediatrics : JDBP* 21 (1): 2–11. http://www.ncbi.nlm.nih.gov/pubmed/10706343.

Copping, Nycole A., Elizabeth L. Berg, Gillian M. Foley, Melanie D. Schaffler, Beth L. Onaga, Nathalie Buscher, Jill L. Silverman, and Mu Yang. 2017. “Touchscreen Learning Deficits and Normal Social Approach Behavior in the Shank3B Model of Phelan–McDermid Syndrome and Autism.” *Neuroscience* 345 (March): 155–65. https://doi.org/10.1016/j.neuroscience.2016.05.016.

Courchesne, Eric, Kathleen Campbell, and Stephanie Solso. 2011. “Brain Growth across the Life Span in Autism: Age-Specific Changes in Anatomical Pathology.” *Brain Research* 1380 (March). Autism Speaks manuscript submission: 138–45. https://doi.org/10.1016/j.brainres.2010.09.101.

Crawford, D C, J M Acuña, and S L Sherman. 2001. “FMR1 and the Fragile X Syndrome: Human Genome Epidemiology Review.” *Genetics in Medicine : Official Journal of the American College of Medical Genetics* 3 (5): 359–71. https://doi.org/10.109700125817-200109000-00006.

Crawley, Jacqueline N. 2012. “Translational Animal Models of Autism and Neurodevelopmental Disorders.” *Dialogues in Clinical Neuroscience* 14 (3): 293–305.

Darville, Hélène, Aurélie Poulet, Frédérique Rodet-Amsellem, Laure Chatrousse, Julie Pernelle, Claire Boissart, Delphine Héron, et al. 2016. “Human Pluripotent Stem Cell-Derived Cortical Neurons for High Throughput Medication Screening in Autism: A Proof of Concept Study in SHANK3 Haploinsufficiency Syndrome.” *EBIOM* 9 (July). Elsevier: 293–305. https://doi.org/10.1016/j.ebiom.2016.05.032.

Deacon, Robert M J. 2006. “Digging and Marble Burying in Mice: Simple Methods for in Vivo Identification of Biological Impacts.” *Nature Protocols* 1 (1): 122–24. https://doi.org/10.1038/nprot.2006.20.

DeLorey, Timothy M, Peyman Sahbaie, Ezzat Hashemi, Gregg E Homanics, and J David Clark. 2008. “Gabrb3 Gene Deficient Mice Exhibit Impaired Social and Exploratory Behaviors, Deficits in Non-Selective Attention and Hypoplasia of Cerebellar Vermal Lobules: A Potential Model of Autism Spectrum Disorder.” *Behavioural Brain Research* 187 (2): 207–20. https://doi.org/10.1016/j.bbr.2007.09.009.

Denayer, A, H Van Esch, T De Ravel, J.-P Frijns, G Van Buggenhout, A Vogels, K Devriendt, J Geutjens, P Thiry, and A Swillen. 2012. “Neuropsychopathology in 7 Patients with the 22q13 Deletion Syndrome: Presence of Bipolar Disorder and Progressive Loss of Skills.” *Mol Syndromol* 3: 14–20. https://doi.org/10.1159/000339119.

Dingledine, Raymond, and Chris J McBain. 1999. “Three Classes of Ionotropic Glutamate Receptor.” Lippincott-Raven. https://www.ncbi.nlm.nih.gov/books/NBK28270/.

Disciglio, Vittoria, Caterina Lo Rizzo, Maria Antonietta Mencarelli, Mafalda Mucciolo, Annabella Marozza, Chiara Di Marco, Antonio Massarelli, et al. 2014. “Interstitial 22q13 Deletions Not

Involving SHANK3 Gene: A New Contiguous Gene Syndrome." *American Journal of Medical Genetics. Part A* 164A (7): 1666–76. https://doi.org/10.1002/ajmg.a.36513.

Dobin, Alexander, Carrie A. Davis, Felix Schlesinger, Jorg Drenkow, Chris Zaleski, Sonali Jha, Philippe Batut, Mark Chaisson, and Thomas R. Gingeras. 2013. "STAR: Ultrafast Universal RNA-Seq Aligner." *Bioinformatics* 29 (1): 15–21. https://doi.org/10.1093/bioinformatics/bts635.

Dong, Hualing, Richard J. O'Brien, Eric T. Fung, Anthony A. Lanahan, Paul F. Worley, and Richard L. Huganir. 1997. "GRIP: A Synaptic PDZ Domain-Containing Protein That Interacts with AMPA Receptors." *Nature*. https://doi.org/10.1038/386279a0.

Drapeau, Elodie, Nate P. Dorr, Gregory A. Elder, and Joseph D. Buxbaum. 2014. "Absence of Strong Strain Effects in Behavioral Analyses of Shank3-Deficient Mice." *Disease Models & Mechanisms* 7 (6). The Company of Biologists Ltd: 667–81. https://doi.org/10.1242/dmm.013821.

Drapeau, Elodie, Mohammed Riad, Yuji Kajiwara, and Joseph D Buxbaum. 2018. "Behavioral Phenotyping of an Improved Mouse Model of Phelan-McDermid Behavioral Phenotyping of a Full Shank3 Knockout Mouse." *BioRxiv*. https://doi.org/10.1101/278622.

Du, Yunrui, Scott A Weed, W C Xiong, Trudy D Marshall, and J Thomas Parsons. 1998. "Identification of a Novel Cortactin SH3 Domain-Binding Protein and Its Localization to Growth Cones of Cultured Neurons." *Molecular and Cellular Biology* 18 (10). American Society for Microbiology: 5838–51. https://doi.org/10.1128/MCB.18.10.5838.

Duffney, Lara J., Ping Zhong, Jing Wei, Emmanuel Matas, Jia Cheng, Luye Qin, Kaijie Ma, et al. 2015. "Autism-like Deficits in Shank3-Deficient Mice Are Rescued by Targeting Actin Regulators." *Cell Reports* 11 (9). Cell Press: 1400–1413. https://www.sciencedirect.com/science/article/pii/S2211124715004969?via%3Dihub.

Durand, Christelle M, Catalina Betancur, Tobias M Boeckers, Juergen Bockmann, Pauline Chaste, Fabien Fauchereau, Gudrun Nygren, et al. 2007. "Mutations in the Gene Encoding the Synaptic Scaffolding Protein SHANK3 Are Associated with Autism Spectrum Disorders." *Nature Genetics* 39 (1): 25–27. https://doi.org/10.1038/ng1933.

Ecker, C., D. Andrews, F. Dell'Acqua, E. Daly, C. Murphy, M. Catani, M. Thiebaut de Schotten, et al. 2016. "Relationship Between Cortical Gyrification, White Matter Connectivity, and Autism Spectrum Disorder." *Cerebral Cortex* 26 (7). Oxford University Press: 3297–3309. https://doi.org/10.1093/cercor/bhw098.

Egger, Jos I M, Willem M A Verhoeven, Renske Groenendijk-Reijenga, and Sarina G Kant. 2017. "Phelan-McDermid Syndrome Due to SHANK3 Mutation in an Intellectually Disabled Adult Male: Successful Treatment with Lithium." *BMJ Case Reports* 2017 (September). BMJ Publishing Group Ltd: bcr-2017-220778. https://doi.org/10.1136/bcr-2017-220778.

Eichenbaum, Howard. 2017. "Prefrontal–Hippocampal Interactions in Episodic Memory." *Nature Reviews Neuroscience* 18 (9). Nature Publishing Group: 547–58. https://doi.org/10.1038/nrn.2017.74.

Eisenberg, L, and L Kanner. 1956. "Childhood Schizophrenia; Symposium, 1955. VI. Early Infantile Autism, 1943-55." *The American Journal of Orthopsychiatry* 26 (3): 556–66. http://www.ncbi.nlm.nih.gov/pubmed/13339939.

Ey, Elodie, Nicolas Torquet, Fabrice De Chaumont, Julie Levi-Strauss, Allain-Thibeault Ferhat, Anne-Marie Le Sourd, Tobias M. Boeckers, and Thomas Bourgeron. n.d. "Shank2 Mutant Mice Display Hyperactivity Insensitive to Methylphenidate and Reduced Flexibility in Social Motivation, but Normal Social Recognition."

Ey, Elodie, Nicolas Torquet, Anne-Marie Le Sourd, Claire S. Leblond, Tobias M. Boeckers, Philippe Faure, and Thomas Bourgeron. 2013. "The Autism ProSAP1/Shank2 Mouse Model Displays Quantitative and Structural Abnormalities in Ultrasonic Vocalisations." *Behavioural Brain Research* 256 (November): 677–89. https://doi.org/10.1016/j.bbr.2013.08.031.

Fayyad, John, Ron De Graaf, Ronald Kessler, Jordi Alonso, Matthias Angermeyer, Koen Demyttenaere, Giovanni De Girolamo, et al. 2007. "Cross-National Prevalence and Correlates of Adult Attention-Deficit Hyperactivity Disorder." *British Journal of Psychiatry* 190 (05): 402–9. https://doi.org/10.1192/bjp.bp.106.034389.

Ferguson, Jennifer N, Larry J Young, Elizabeth F Hearn, Martin M Matzuk, Thomas R Insel, and James T Winslow. 2000. "Social Amnesia in Mice Lacking the Oxytocin Gene." *Nature Genetics* 25 (3): 284–88. https://doi.org/10.1038/77040.

Ferhat, Allain-Thibeault, Sonja Halbedl, Michael J. Schmeisser, Martien J. Kas, Thomas Bourgeron, and Elodie Ey. 2017. "Behavioural Phenotypes and Neural Circuit Dysfunctions in Mouse Models of Autism Spectrum Disorder." In *Advances in Anatomy, Embryology and Cell Biology*, Advances i, 85–101. Springer, Cham. https://doi.org/10.1007/978-3-319-52498-6_5.

Ferhat, Allain-Thibeault, Anne Marie Le Sourd, Fabrice De Chaumont, Jean Christophe Olivo-Marin, Thomas Bourgeron, and Elodie Ey. 2015. "Social Communication in Mice - Are There Optimal Cage Conditions?" *PLoS ONE* 10 (3): 1–19. https://doi.org/10.1371/journal.pone.0121802.

Ferhat, Allain-Thibeault, Nicolas Torquet, Anne-Marie Le Sourd, Fabrice de Chaumont, Jean-Christophe Olivo-Marin, Philippe Faure, Thomas Bourgeron, and Elodie Ey. 2016. "Recording Mouse Ultrasonic Vocalizations to Evaluate Social Communication." *Journal of Visualized Experiments*, no. 112 (June). https://doi.org/10.3791/53871.

Fernández, Marta, Irene Mollinedo-Gajate, and Olga Peñagarikano. 2018. "Neural Circuits for Social Cognition: Implications for Autism." *Neuroscience* 370 (February): 148–62. https://doi.org/10.1016/j.neuroscience.2017.07.013.

Fisher, Robert S., Walter van Emde Boas, Warren Blume, Christian Elger, Pierre Genton, Phillip Lee, and Jerome Engel. 2005. "Epileptic Seizures and Epilepsy: Definitions Proposed by the International League Against Epilepsy (ILAE) and the International Bureau for Epilepsy (IBE)." *Epilepsia* 46 (4). Wiley/Blackwell (10.1111): 470–72. https://doi.org/10.1111/j.0013-9580.2005.66104.x.

Földy, Csaba, Robert C. Malenka, and Thomas C. Südhof. 2013. "Autism-Associated Neuroligin-3 Mutations Commonly Disrupt Tonic Endocannabinoid Signaling." *Neuron* 78 (3). Cell Press: 498–509. https://doi.org/10.1016/J.NEURON.2013.02.036.

Folstein, Susan, and Michael Rutter. 1977. "INFANTILE AUTISM: A GENETIC STUDY OF 21 TWIN PAIRS." *Journal of Child Psychology and Psychiatry* 18 (4). Wiley/Blackwell (10.1111): 297–321. https://doi.org/10.1111/j.1469-7610.1977.tb00443.x.

Frith, Uta. 1991. *Autism and Asperger Syndrome*. Cambridge University Press.

Frye, Richard E., Manuel F. Casanova, S. Hossein Fatemi, Timothy D. Folsom, Teri J. Reutiman, Gregory L. Brown, Stephen M. Edelson, John C. Slattery, and James B. Adams. 2016. "Neuropathological Mechanisms of Seizures in Autism Spectrum Disorder." *Frontiers in Neuroscience* 10 (May). Frontiers: 192. https://doi.org/10.3389/fnins.2016.00192.

Fuccillo, Marc V. 2016. "Striatal Circuits as a Common Node for Autism Pathophysiology." *Frontiers in Neuroscience* 10 (February). Frontiers: 27. https://doi.org/10.3389/fnins.2016.00027.

Fuster, Joaquín M. 2008. *Prefrontal Cortex*. *Zhurnal Eksperimental'noi i Teoreticheskoi Fiziki*. https://doi.org/10.1016/B978-0-12-373644-4.00010-4.

Gardener, Hannah, Donna Spiegelman, and Stephen L. Buka. 2009. "Prenatal Risk Factors for Autism: Comprehensive Meta-Analysis." *British Journal of Psychiatry* 195 (01): 7–14. https://doi.org/10.1192/bjp.bp.108.051672.

Gardener, Hannah, Donna Spiegelman, and Stephen L Buka. 2011. "Perinatal and Neonatal Risk Factors for Autism: A Comprehensive Meta-Analysis." *PEDIATRICS* 128 (2): 344–55. https://doi.org/10.1542/peds.2010-1036.

Gauthier, Julie, Nathalie Champagne, Ronald G Lafrenière, Lan Xiong, Dan Spiegelman, Edna Brustein, Mathieu Lapointe, et al. 2010. "De Novo Mutations in the Gene Encoding the Synaptic Scaffolding Protein SHANK3 in Patients Ascertained for Schizophrenia." *Proceedings of the National Academy of Sciences* 107 (17): 7863–68. https://doi.org/10.1073/pnas.0906232107.

Geschwind, Daniel H. 2009. "Advances in Autism." *Annual Review of Medicine* 60 (1): 367–80. https://doi.org/10.1146/annurev.med.60.053107.121225.

Ghaziuddin, Mohammad. 2010. "Brief Report: Should the DSM V Drop Asperger Syndrome?" *Journal of Autism and Developmental Disorders* 40 (9). Springer US: 1146–48. https://doi.org/10.1007/s10803-010-0969-z.

Ghaziuddin, Mohammad, and John Greden. 1998. "Depression in Children with Autism/Pervasive Developmental Disorders: A Case-Control Family History Study." *Journal of Autism and Developmental Disorders* 28 (2). Kluwer Academic Publishers-Plenum Publishers: 111–15. https://doi.org/10.1023/A:1026036514719.

Gladding, Clare M, Stephen M Fitzjohn, Elek Molnár, and S F Traynelis. 2009. "Metabotropic Glutamate Receptor-Mediated Long-Term Depression: Molecular Mechanisms." *Pharmacological Reviews* 61 (4). American Society for Pharmacology and Experimental Therapeutics: 395–412. https://doi.org/10.1124/pr.109.001735.

Goddyn, Hannelore, Sandra Leo, Theo Meert, and Rudi D'Hooge. 2006. "Differences in Behavioural Test Battery Performance between Mice with Hippocampal and Cerebellar Lesions." *Behavioural Brain Research* 173 (1). Elsevier: 138–47. https://doi.org/10.1016/J.BBR.2006.06.016.

Goeman, Jelle J., Van De Geer, Sara A, Floor de Kort, Van Houwelingen, and Hans C. 2004. "A Global Test for Groups of Genes: Testing Association with a Clinical Outcome." *Bioinformatics* 20 (1): 93–99. https://doi.org/10.1093/bioinformatics/btg382.

Gogolla, Nadine, Jocelyn J. LeBlanc, Kathleen B. Quast, Thomas C. Südhof, Michela Fagiolini, and Takao K. Hensch. 2009. "Common Circuit Defect of Excitatory-Inhibitory Balance in Mouse Models of Autism." *Journal of Neurodevelopmental Disorders* 1 (2). BioMed Central: 172–81. https://doi.org/10.1007/s11689-009-9023-x.

Gokce, Ozgun, Geoffrey M. Stanley, Barbara Treutlein, Norma F. Neff, J. Gray Camp, Robert C. Malenka, Patrick E. Rothwell, Marc V. Fuccillo, Thomas C. Südhof, and Stephen R. Quake. 2016. "Cellular Taxonomy of the Mouse Striatum as Revealed by Single-Cell RNA-Seq." *Cell Reports* 16 (4): 1126–37. https://doi.org/10.1016/j.celrep.2016.06.059.

Gonçalves, Joana, Inês R Violante, José Sereno, Ricardo A Leitão, Ying Cai, Antero Abrunhosa, Ana Paula Silva, Alcino J Silva, and Miguel Castelo-Branco. 2017. "Testing the Excitation/Inhibition Imbalance Hypothesis in a Mouse Model of the Autism Spectrum Disorder: In Vivo Neurospectroscopy and Molecular Evidence for Regional Phenotypes." *Molecular Autism* 8. https://doi.org/10.1186/s13229-017-0166-4.

Gong, Yuesong, Carol F Lippa, Jinghua Zhu, Qishan Lin, and Andrea L Rosso. 2009. "Disruption of Glutamate Receptors at Shank-Postsynaptic Platform in Alzheimer's Disease." *Brain Research*

1292 (October). NIH Public Access: 191–98. https://doi.org/10.1016/j.brainres.2009.07.056.

Grabrucker, Andreas M. 2014. "A Role for Synaptic Zinc in ProSAP/Shank PSD Scaffold Malformation in Autism Spectrum Disorders." *Developmental Neurobiology* 74 (2): 136–46. https://doi.org/10.1002/dneu.22089.

Groenewegen, Henk J. 2003. "The Basal Ganglia and Motor Control." *Neural Plasticity* 10 (1–2). Hindawi Limited: 107–20. https://doi.org/10.1155/NP.2003.107.

Guilmatre, Audrey, Guillaume Huguet, Richard Delorme, and Thomas Bourgeron. 2014. "The Emerging Role of SHANK Genes in Neuropsychiatric Disorders." *Developmental Neurobiology* 74 (2): 113–22. https://doi.org/10.1002/dneu.22128.

Gunaydin, Lisa A., Logan Grosenick, Joel C. Finkelstein, Isaac V. Kauvar, Lief E. Fenno, Avishek Adhikari, Stephan Lammel, et al. 2014. "Natural Neural Projection Dynamics Underlying Social Behavior." *Cell* 157 (7): 1535–51. https://doi.org/10.1016/j.cell.2014.05.017.

Guzmán, Yomayra F., Keri Ramsey, Jacob R. Stolz, David W. Craig, Mathew J. Huentelman, Vinodh Narayanan, and Geoffrey T. Swanson. 2017. "A Gain-of-Function Mutation in the *GRIK2* Gene Causes Neurodevelopmental Deficits." *Neurology Genetics* 3 (1): e129. https://doi.org/10.1212/NXG.0000000000000129.

Ha, Seungmin, D. Lee, Y. S. Cho, Changuk Chung, Ye-Eun Yoo, J. Kim, Jiseok Lee, et al. 2016. "Cerebellar Shank2 Regulates Excitatory Synapse Density, Motor Coordination, and Specific Repetitive and Anxiety-Like Behaviors." *Journal of Neuroscience* 36 (48). Society for Neuroscience: 12129–43. https://doi.org/10.1523/JNEUROSCI.1849-16.2016.

Haber, S N, J L Fudge, and N R McFarland. 2000. "Striatonigrostriatal Pathways in Primates Form an Ascending Spiral from the Shell to the Dorsolateral Striatum." *The Journal of Neuroscience : The Official Journal of the Society for Neuroscience* 20 (6): 2369–82. http://www.ncbi.nlm.nih.gov/pubmed/10704511.

Hallmayer, Joachim, Sue Cleveland, Andrea Torres, Jennifer Phillips, Brianne Cohen, Tiffany Torigoe, Janet Miller, et al. 2011. "Genetic Heritability and Shared Environmental Factors Among Twin Pairs With Autism." *Archives of General Psychiatry* 68 (11): 1095. https://doi.org/10.1001/archgenpsychiatry.2011.76.

Hammerschmidt, Kurt, Konstantin Radyushkin, Hannelore Ehrenreich, and Julia Fischer. 2012. "The Structure and Usage of Female and Male Mouse Ultrasonic Vocalizations Reveal Only Minor Differences." *PLoS ONE* 7 (7): 1–7. https://doi.org/10.1371/journal.pone.0041133.

Han, Kihoon, J. Lloyd Holder Jr, Christian P. Schaaf, Hui-Chen Lu, Hongmei Chen, Hyojin Kang, Jianrong Tang, et al. 2013. "SHANK3 Overexpression Causes Manic-like Behaviour with Unique Pharmacogenetic Properties." *Nature* 503 (7474). Nature Publishing Group: 72–77. https://doi.org/10.1038/nature12630.

Hansen, Stefan N., Diana E. Schendel, and Erik T. Parner. 2015. "Explaining the Increase in the Prevalence of Autism Spectrum Disorders." *JAMA Pediatrics* 169 (1). American Medical Association: 56. https://doi.org/10.1001/jamapediatrics.2014.1893.

Hardy, John, and Dennis J Selkoe. 2002. "The Amyloid Hypothesis of Alzheimer's Disease: Progress and Problems on the Road to Therapeutics." *Science (New York, N.Y.)* 297 (5580). American Association for the Advancement of Science: 353–56. https://doi.org/10.1126/science.1072994.

Harony-Nicolas, Hala, Maya Kay, Johann du Hoffmann, Matthew E Klein, Ozlem Bozdagi-Gunal, Mohammed Riad, Nikolaos P Daskalakis, et al. 2017. "Oxytocin Improves Behavioral and Electrophysiological Deficits in a Novel Shank3-Deficient Rat." *ELife* 6 (January). eLife Sciences Publications, Ltd: e18904. https://doi.org/10.7554/eLife.18904.

Harony-Nicolas, Hala, Silvia De Rubeis, Alexander Kolevzon, and Joseph D. Buxbaum. 2015. "Phelan McDermid Syndrome." *Journal of Child Neurology* 30 (14): 1861–70. https://doi.org/10.1177/0883073815600872.

Hazen, Eric P., Christopher J. McDougle, and Fred R. Volkmar. 2013. "Changes in the Diagnostic Criteria for Autism in *DSM-5* : Controversies and Concerns." *The Journal of Clinical Psychiatry* 74 (07): 739–40. https://doi.org/10.4088/JCP.13ac08550.

Hazlett, Heather Cody, Michele Poe, Guido Gerig, Rachel Gimpel Smith, James Provenzale, Allison Ross, John Gilmore, and Joseph Piven. 2005. "Magnetic Resonance Imaging and Head Circumference Study of Brain Size in Autism." *Archives of General Psychiatry* 62 (12). American Medical Association: 1366. https://doi.org/10.1001/archpsyc.62.12.1366.

Heckman, Jesse, Brigit McGuinness, Tansu Celikel, and Bernhard Englitz. 2016. "Determinants of the Mouse Ultrasonic Vocal Structure and Repertoire." *Neuroscience & Biobehavioral Reviews* 65 (June). Pergamon: 313–25. https://doi.org/10.1016/J.NEUBIOREV.2016.03.029.

Herbert, M. R., D. A. Ziegler, C. K. Deutsch, L. M. O'Brien, D. N. Kennedy, P. A. Filipek, A. I. Bakardjiev, et al. 2004. "Brain Asymmetries in Autism and Developmental Language Disorder: A Nested Whole-Brain Analysis." *Brain* 128 (1). Oxford University Press: 213–26. https://doi.org/10.1093/brain/awh330.

Herring, Bruce E., Yun Shi, Young Ho Suh, Chan-Ying Zheng, Sabine M. Blankenship, Katherine W. Roche, and Roger A. Nicoll. 2013. "Cornichon Proteins Determine the Subunit Composition of Synaptic AMPA Receptors." *Neuron* 77 (6): 1083–96. https://doi.org/10.1016/j.neuron.2013.01.017.

Hitti, Frederick L., and Steven A. Siegelbaum. 2014. "The Hippocampal CA2 Region Is Essential for Social Memory." *Nature* 508 (7494). Nature Publishing Group: 88–92. https://doi.org/10.1038/nature13028.

Holmes, Philip V. 2003. "Rodent Models of Depression: Reexamining Validity without Anthropomorphic Inference." *Critical Reviews in Neurobiology* 15 (2): 143–74. http://www.ncbi.nlm.nih.gov/pubmed/14977368.

Huettner, James E. 2003. "Kainate Receptors and Synaptic Transmission." *Progress in Neurobiology* 70 (5): 387–407. http://www.ncbi.nlm.nih.gov/pubmed/14511698.

Huguet, Guillaume, Elodie Ey, and Thomas Bourgeron. 2013. "The Genetic Landscapes of Autism Spectrum Disorders." *Annual Review of Genomics and Human Genetics* 14 (1): 191–213. https://doi.org/10.1146/annurev-genom-091212-153431.

Hung, Albert Y, Kensuke Futai, Carlo Sala, Juli G Valtschanoff, Jubin Ryu, Mollie A Woodworth, Fleur L Kidd, et al. 2008. "Smaller Dendritic Spines, Weaker Synaptic Transmission, but Enhanced Spatial Learning in Mice Lacking Shank1." *The Journal of Neuroscience : The Official Journal of the Society for Neuroscience* 28 (7). Society for Neuroscience: 1697–1708. https://doi.org/10.1523/JNEUROSCI.3032-07.2008.

Ikemoto, Satoshi, Chen Yang, and Aaron Tan. 2015. "Basal Ganglia Circuit Loops, Dopamine and Motivation: A Review and Enquiry." *Behavioural Brain Research* 290 (September): 17–31. https://doi.org/10.1016/j.bbr.2015.04.018.

Iossifov, Ivan, Brian J. O'Roak, Stephan J. Sanders, Michael Ronemus, Niklas Krumm, Dan Levy, Holly A. Stessman, et al. 2014. "The Contribution of de Novo Coding Mutations to Autism Spectrum Disorder." *Nature* 515 (7526): 216–21. https://doi.org/10.1038/nature13908.

Isaacson, Jeffry S., and Massimo Scanziani. 2011. "How Inhibition Shapes Cortical Activity." *Neuron* 72 (2): 231–43. https://doi.org/10.1016/j.neuron.2011.09.027.

Jaramillo, Thomas C., Haley E. Speed, Zhong Xuan, Jeremy M. Reimers, Christine Ochoa Escamilla, Travis P. Weaver, Shunan Liu, Irina Filonova, and Craig M. Powell. 2017. "Novel Shank3 Mutant Exhibits Behaviors with Face Validity for Autism and Altered Striatal and Hippocampal Function." *Autism Research* 10 (1): 42–65. https://doi.org/10.1002/aur.1664.

Jaramillo, Thomas C., Haley E. Speed, Zhong Xuan, Jeremy M. Reimers, Shunan Liu, and Craig M. Powell. 2016. "Altered Striatal Synaptic Function and Abnormal Behaviour in *Shank3* Exon4-9 Deletion Mouse Model of Autism." *Autism Research* 9 (3). Wiley-Blackwell: 350–75. https://doi.org/10.1002/aur.1529.

Jiang, Yong hui, and Michael D. Ehlers. 2013. "Modeling Autism by SHANK Gene Mutations in Mice." *Neuron* 78 (1): 8–27. https://doi.org/10.1016/j.neuron.2013.03.016.

Kabitzke, P.A. A., D. Brunner, D. He, P.A. A. Fazio, K. Cox, J. Sutphen, L. Thiede, et al. 2017. "Comprehensive Analysis of Two Shank3 and the Cacna1c Mouse Models of Autism Spectrum Disorder." *Genes, Brain and Behavior* 17 (1): 1–19. https://doi.org/10.1111/gbb.12405.

Kalueff, A.V., A. Minasyan, T. Keisala, Z.H. Shah, and P. Tuohimaa. 2006. "Hair Barbering in Mice: Implications for Neurobehavioural Research." *Behavioural Processes* 71 (1). Elsevier: 8–15. https://doi.org/10.1016/J.BEPROC.2005.09.004.

Kandel, Eric R., James H Schwartz, Thomas M Jessel, Steven A. Siegelbaum, and A.J. Hudspeth. 2013. *Principles of Neural Science*. Fifth edit. Mc Graw Hill. https://neurology.mhmedical.com/content.aspx?bookid=1049&sectionid=59138139.

Kanehisa, Minoru, Susumu Goto, Yoko Sato, Miho Furumichi, and Mao Tanabe. 2012. "KEGG for Integration and Interpretation of Large-Scale Molecular Data Sets." *Nucleic Acids Research* 40 (D1): D109–14. https://doi.org/10.1093/nar/gkr988.

Kang, Hyo Jung, Yuka Imamura Kawasawa, Feng Cheng, Ying Zhu, Xuming Xu, Mingfeng Li, André M M Sousa, et al. 2011. "Spatio-Temporal Transcriptome of the Human Brain." *Nature* 478 (7370): 483–89. https://doi.org/10.1038/nature10523.

Kanner, L. 1943. "Autistic Disturbances of Affective Contact." *Acta Paedopsychiatrica* 35 (4): 100–136. http://www.ncbi.nlm.nih.gov/pubmed/4880460.

Karimi, Padideh, Elahe Kamali, Seyyed Mohammad Mousavi, and Mojgan Karahmadi. 2017. "Environmental Factors Influencing the Risk of Autism." *Journal of Research in Medical Sciences : The Official Journal of Isfahan University of Medical Sciences* 22. Wolters Kluwer -- Medknow Publications: 27. https://doi.org/10.4103/1735-1995.200272.

Karten, Harvey J. 2015. "Vertebrate Brains and Evolutionary Connectomics: On the Origins of the Mammalian 'Neocortex'." *Philosophical Transactions of the Royal Society of London. Series B, Biological Sciences* 370 (1684). The Royal Society: 20150060. https://doi.org/10.1098/rstb.2015.0060.

Keverne, E B. 1999. "The Vomeronasal Organ." *Science (New York, N.Y.)* 286 (5440): 716–20. https://doi.org/10.2307/2899372.

Kim, Ryunhee, Jihye Kim, Changuk Chung, Seungmin Ha, Seungjoon Lee, Eunee Lee, Ye-Eun Yoo, Woohyun Kim, Wangyong Shin, and Eunjoon Kim. 2018. "Cell-Type-Specific Shank2 Deletion in Mice Leads to Differential Synaptic and Behavioral Phenotypes." *The Journal of Neuroscience : The Official Journal of the Society for Neuroscience* 38 (17). Society for Neuroscience: 4076–92. https://doi.org/10.1523/JNEUROSCI.2684-17.2018.

Kloth, Alexander D, Aleksandra Badura, Amy Li, Adriana Cherskov, Sara G Connolly, Andrea Giovannucci, M Ali Bangash, et al. 2015. "Cerebellar Associative Sensory Learning Defects in Five Mouse Autism Models." *ELife* 4 (July). eLife Sciences Publications Limited: e06085.

https://doi.org/10.7554/eLife.06085.

Ko, Hyoung Gon, Seog Bae Oh, Min Zhuo, and Bong Kiun Kaang. 2016. "Reduced Acute Nociception and Chronic Pain in Shank2−/−mice." *Molecular Pain* 12: 1–5. https://doi.org/10.1177/1744806916647056.

Kohls, Gregor, Martin Schulte-Rüther, Barbara Nehrkorn, Kristin Müller, Gereon R. Fink, Inge Kamp-Becker, Beate Herpertz-Dahlmann, Robert T. Schultz, and Kerstin Konrad. 2013. "Reward System Dysfunction in Autism Spectrum Disorders." *Social Cognitive and Affective Neuroscience* 8 (5): 565–72. https://doi.org/10.1093/scan/nss033.

Kolevzon, Alexander, Benjamin Angarita, Lauren Bush, A Wang, Yitzchak Frank, Amy Yang, Robert Rapaport, et al. 2014. "Phelan-McDermid Syndrome: A Review of the Literature and Practice Parameters for Medical Assessment and Monitoring." *Journal of Neurodevelopmental Disorders* 6 (1): 39. https://doi.org/10.1186/1866-1955-6-39.

Kouser, Mehreen, Haley E. Speed, Colleen M. Dewey, Jeremy M. Reimers, Allie J. Widman, Natasha Gupta, Shunan Liu, et al. 2013. "Loss of Predominant Shank3 Isoforms Results in Hippocampus-Dependent Impairments in Behavior and Synaptic Transmission." *Journal of Neuroscience* 33 (47). Society for Neuroscience: 18448–68. https://doi.org/10.1523/JNEUROSCI.3017-13.2013.

Kreienkamp, H. -J. 2008. "Scaffolding Proteins at the Postsynaptic Density: Shank as the Architectural Framework." In *Handbook of Experimental Pharmacology*, 365–80. https://doi.org/10.1007/978-3-540-72843-6_15.

Krueger, Felix, and Simon R. Andrews. 2016. "SNPsplit: Allele-Specific Splitting of Alignments between Genomes with Known SNP Genotypes." *F1000Research* 5 (July). https://doi.org/10.12688/f1000research.9037.2.

Kruk, Menno R, Thea P. De Vos-frerichs, and A.M. Van Der Poel. 1979. "The Induction of Aggressive Behaviour By Electrical Stimulation in the Hypothalamus of Male Rats." *Behaviour* 70 (3): 292–322. https://doi.org/10.1163/156853979X00106.

Kupchik, Yonatan M, Robyn M Brown, Jasper A Heinsbroek, Mary Kay Lobo, Danielle J Schwartz, and Peter W Kalivas. 2015. "Coding the Direct/Indirect Pathways by D1 and D2 Receptors Is Not Valid for Accumbens Projections." *Nature Neuroscience* 18 (9). Nature Publishing Group: 1230–32. https://doi.org/10.1038/nn.4068.

Kwan, Kenneth Y., Mandy M.S. Lam, Matthew B. Johnson, Umber Dube, Sungbo Shim, Mladen-Roko Rašin, André M.M. Sousa, et al. 2012. "Species-Dependent Posttranscriptional Regulation of NOS1 by FMRP in the Developing Cerebral Cortex." *Cell* 149 (4). Elsevier: 899–911. https://doi.org/10.1016/j.cell.2012.02.060.

Lai, Meng-Chuan, Michael V Lombardo, Bonnie Auyeung, Bhismadev Chakrabarti, and Simon Baron-Cohen. 2015. "Sex/Gender Differences and Autism: Setting the Scene for Future Research." *JAAC* 54: 11–24. https://doi.org/10.1016/j.jaac.2014.10.003.

Langen, Marieke, Sarah Durston, Martien J.H. Kas, Herman van Engeland, and Wouter G. Staal. 2011. "The Neurobiology of Repetitive Behavior: …and Men." *Neuroscience & Biobehavioral Reviews* 35 (3). Pergamon: 356–65. https://www.sciencedirect.com/science/article/pii/S0149763410000291?via%3Dihub.

Langen, Marieke, Martien JH Kas, Wouter G Staal, Herman van Engeland, and Sarah Durston. 2011. "The Neurobiology of Repetitive Behavior: Of Mice…." *Neuroscience & Biobehavioral Reviews* 35 (3): 345–55. https://doi.org/10.1016/j.neubiorev.2010.02.004.

Latham, Naomi, and Georgia Mason. 2004. "From House Mouse to Mouse House: The Behavioural Biology of Free-Living Mus Musculus and Its Implications in the Laboratory." *Applied Animal*

Behaviour Science 86 (3–4): 261–89. https://doi.org/10.1016/j.applanim.2004.02.006.

Lauritsen, Marlene Briciet, Carsten Bocker Pedersen, and Preben Bo Mortensen. 2005. "Effects of Familial Risk Factors and Place of Birth on the Risk of Autism: A Nationwide Register-Based Study." *Journal of Child Psychology and Psychiatry* 46 (9): 963–71. https://doi.org/10.1111/j.1469-7610.2004.00391.x.

Law, Charity W., Yunshun Chen, Wei Shi, and Gordon K. Smyth. 2014. "Voom: Precision Weights Unlock Linear Model Analysis Tools for RNA-Seq Read Counts." *Genome Biology* 15 (February): R29. https://doi.org/10.1186/gb-2014-15-2-r29.

Leblond, Claire S., Jutta Heinrich, Richard Delorme, Christian Proepper, Catalina Betancur, Guillaume Huguet, Marina Konyukh, et al. 2012. "Genetic and Functional Analyses of SHANK2 Mutations Suggest a Multiple Hit Model of Autism Spectrum Disorders." Edited by Matthew State. *PLoS Genetics* 8 (2): e1002521. https://doi.org/10.1371/journal.pgen.1002521.

Leblond, Claire S., Caroline Nava, Anne Polge, Julie Gauthier, Guillaume Huguet, Serge Lumbroso, Fabienne Giuliano, et al. 2014. "Meta-Analysis of SHANK Mutations in Autism Spectrum Disorders: A Gradient of Severity in Cognitive Impairments." *PLoS Genetics* 10 (9). https://doi.org/10.1371/journal.pgen.1004580.

Lee, Bokyoung, Yinhua Zhang, Yoonhee Kim, Shinhyun Kim, Yeunkum Lee, and Kihoon Han. 2017. "Age-Dependent Decrease of GAD65/67 MRNAs but Normal Densities of GABAergic Interneurons in the Brain Regions of Shank3 -Overexpressing Manic Mouse Model." *Neuroscience Letters* 649 (May): 48–54. https://doi.org/10.1016/j.neulet.2017.04.016.

Lee, Eun-Jae, Hyejin Lee, Tzyy-Nan Huang, Changuk Chung, Wangyong Shin, Kyungdeok Kim, Jae-Young Koh, Yi-Ping Hsueh, and Eunjoon Kim. 2015. "Trans-Synaptic Zinc Mobilization Improves Social Interaction in Two Mouse Models of Autism through NMDAR Activation." *Nature Communications* 6 (1). Nature Publishing Group: 7168. https://doi.org/10.1038/ncomms8168.

Lee, Jiseok, Changuk Chung, Seungmin Ha, Dongmin Lee, Do-Young Kim, Hyun Kim, and Eunjoon Kim. 2015. "Shank3-Mutant Mice Lacking Exon 9 Show Altered Excitation/Inhibition Balance, Enhanced Rearing, and Spatial Memory Deficit." *Frontiers in Cellular Neuroscience* 9. Frontiers Media SA: 94. https://doi.org/10.3389/fncel.2015.00094.

Lee, Yeunkum, Sun Gyun Kim, Bokyoung Lee, Yinhua Zhang, Yoonhee Kim, Shinhyun Kim, Eunjoon Kim, Hyojin Kang, and Kihoon Han. 2017. "Striatal Transcriptome and Interactome Analysis of Shank3-Overexpressing Mice Reveals the Connectivity between Shank3 and MTORC1 Signaling." *Frontiers in Molecular Neuroscience* 10 (June): 201. https://doi.org/10.3389/fnmol.2017.00201.

Lee, Yeunkum, Jae Ryun Ryu, Hyojin Kang, Yoonhee Kim, Shinhyun Kim, Yinhua Zhang, Chunmei Jin, et al. 2017. "Characterization of the Zinc-Induced Shank3 Interactome of Mouse Synaptosome." *Biochemical and Biophysical Research Communications* 494 (3–4). Elsevier Ltd: 581–86. https://doi.org/10.1016/j.bbrc.2017.10.143.

Lefebvre, Aline, Anita Beggiato, Thomas Bourgeron, and Roberto Toro. 2015. "Neuroanatomical Diversity of Corpus Callosum and Brain Volume in Autism: Meta-Analysis, Analysis of the Autism Brain Imaging Data Exchange Project, and Simulation." *Biological Psychiatry* 78 (2): 126–34. https://doi.org/10.1016/j.biopsych.2015.02.010.

Leisman, Gerry, Robert Melillo, and Frederick R. 2013. "Clinical Motor and Cognitive Neurobehavioral Relationships in the Basal Ganglia." In *Basal Ganglia - An Integrative View*. InTech. https://doi.org/10.5772/55227.

Lennertz, Leonhard, Michael Wagner, Wolfgang Wölwer, Anna Schuhmacher, Ingo Frommann, Julia Berning, Svenja Schulze-Rauschenbach, et al. 2012. "A Promoter Variant of SHANK1 Affects Auditory Working Memory in Schizophrenia Patients and in Subjects Clinically at Risk for Psychosis." *European Archives of Psychiatry and Clinical Neuroscience* 262 (2). Springer-Verlag: 117–24. https://doi.org/10.1007/s00406-011-0233-3.

Lerma, Juan. 2003. "Roles and Rules of Kainate Receptors in Synaptic Transmission." *Nature Reviews Neuroscience* 4 (6). Nature Publishing Group: 481–95. https://doi.org/10.1038/nrn1118.

Lex, A., N. Gehlenborg, H. Strobelt, R. Vuillemot, and H. Pfister. 2014. "UpSet: Visualization of Intersecting Sets." *IEEE Transactions on Visualization and Computer Graphics* 20 (12): 1983–92. https://doi.org/10.1109/TVCG.2014.2346248.

Leyfer, Ovsanna T., Susan E. Folstein, Susan Bacalman, Naomi O. Davis, Elena Dinh, Jubel Morgan, Helen Tager-Flusberg, and Janet E. Lainhart. 2006. "Comorbid Psychiatric Disorders in Children with Autism: Interview Development and Rates of Disorders." *Journal of Autism and Developmental Disorders* 36 (7): 849–61. https://doi.org/10.1007/s10803-006-0123-0.

Lim, Chae-Seok, Hyopil Kim, Nam-Kyung Yu, Sukjae Joshua Kang, TaeHyun Kim, Hyoung-Gon Ko, Jaehyun Jae-Hyung Jaehyun Lee, et al. 2017. "Enhancing Inhibitory Synaptic Function Reverses Spatial Memory Deficits in Shank2 Mutant Mice." *Neuropharmacology* 112 (Pt A). Pergamon: 104–12. https://doi.org/10.1016/J.NEUROPHARM.2016.08.016.

Lim, Elaine T., Soumya Raychaudhuri, Stephan J. Sanders, Christine Stevens, Aniko Sabo, Daniel G. MacArthur, Benjamin M. Neale, et al. 2013. "Rare Complete Knockouts in Humans: Population Distribution and Significant Role in Autism Spectrum Disorders." *Neuron* 77 (2). Elsevier: 235–42. https://doi.org/10.1016/j.neuron.2012.12.029.

Lim, S, S Naisbitt, J Yoon, J I Hwang, P G Suh, M Sheng, and E Kim. 1999. "Characterization of the Shank Family of Synaptic Proteins. Multiple Genes, Alternative Splicing, and Differential Expression in Brain and Development." *The Journal of Biological Chemistry* 274 (41): 29510–18. http://www.ncbi.nlm.nih.gov/pubmed/10506216.

Liu, Ruijie, Aliaksei Z. Holik, Shian Su, Natasha Jansz, Kelan Chen, Huei San Leong, Marnie E. Blewitt, Marie-Liesse Asselin-Labat, Gordon K. Smyth, and Matthew E. Ritchie. 2015. "Why Weight? Modelling Sample and Observational Level Variability Improves Power in RNA-Seq Analyses." *Nucleic Acids Research* 43 (15): e97. https://doi.org/10.1093/nar/gkv412.

Lord, C, M Rutter, and A Le Couteur. 1994. "Autism Diagnostic Interview-Revised: A Revised Version of a Diagnostic Interview for Caregivers of Individuals with Possible Pervasive Developmental Disorders." *Journal of Autism and Developmental Disorders* 24 (5): 659–85. http://www.ncbi.nlm.nih.gov/pubmed/7814313.

Lord, Catherine, Susan Risi, Linda Lambrecht, Edwin H. Cook, Jr., Bennett L. Leventhal, Pamela C. DiLavore, Andrew Pickles, and Michael Rutter. 2000. "The Autism Diagnostic Observation Schedule—Generic: A Standard Measure of Social and Communication Deficits Associated with the Spectrum of Autism." *Journal of Autism and Developmental Disorders* 30 (3). Kluwer Academic Publishers-Plenum Publishers: 205–23. https://doi.org/10.1023/A:1005592401947.

Lundström, Sebastian, Zheng Chang, Maria Råstam, Christopher Gillberg, Henrik Larsson, Henrik Anckarsäter, and Paul Lichtenstein. 2012. "Autism Spectrum Disorders and Autisticlike Traits." *Archives of General Psychiatry* 69 (1): 46. https://doi.org/10.1001/archgenpsychiatry.2011.144.

Lundström, Sebastian, Abraham Reichenberg, Henrik Anckarsäter, Paul Lichtenstein, and Christopher Gillberg. 2015. "Autism Phenotype versus Registered Diagnosis in Swedish Children: Prevalence Trends over 10 Years in General Population Samples." *BMJ* 350. https://doi.org/10.1136/bmj.h1961.

Luo, Junyu, Qiru Feng, Liping Wei, and Minmin Luo. 2017. "Optogenetic Activation of Dorsal Raphe Neurons Rescues the Autistic-like Social Deficits in Shank3 Knockout Mice." *Cell Research* 27 (7): 950–53. https://doi.org/10.1038/cr.2017.52.

Luo, Weijun, Michael S. Friedman, Kerby Shedden, Kurt D. Hankenson, and Peter J. Woolf. 2009. "GAGE: Generally Applicable Gene Set Enrichment for Pathway Analysis." *BMC Bioinformatics* 10 (May): 161. https://doi.org/10.1186/1471-2105-10-161.

Lyall, Kristen, Lisa Croen, Julie Daniels, M. Daniele Fallin, Christine Ladd-Acosta, Brian K. Lee, Bo Y. Park, et al. 2017. "The Changing Epidemiology of Autism Spectrum Disorders." *Annual Review of Public Health* 38 (1). Annual Reviews : 81–102. https://doi.org/10.1146/annurev-publhealth-031816-044318.

Ma Verhoeven, Willem, Jos Im Egger, Marjolein H Willemsen, Gert Jm De Leijer, and Tjitske Kleefstra. 2012. "Phelan-McDermid Syndrome in Two Adult Brothers: Atypical Bipolar Disorder as Its Psychopathological Phenotype?" *Neuropsychiatric Disease and Treatment* 8: 175–79. https://doi.org/10.2147/NDT.S30506.

Mandell, David S, and Raymond Palmer. 2005. "Differences Among States in the Identification of Autistic Spectrum Disorders." *Arch Pediatr Adolesc Med* 159: 266–69. https://pdfs.semanticscholar.org/cfad/b618cea9d5d63c25d2de85e1931f7767a01e.pdf.

Mansour, Rosleen, Allison T. Dovi, David M. Lane, Katherine A. Loveland, and Deborah A. Pearson. 2017. "ADHD Severity as It Relates to Comorbid Psychiatric Symptomatology in Children with Autism Spectrum Disorders (ASD)." *Research in Developmental Disabilities* 60 (January). Pergamon: 52–64. https://doi.org/10.1016/J.RIDD.2016.11.009.

Maren, Stephen. 2003. "The Amygdala, Synaptic Plasticity, and Fear Memory." *Annals of the New York Academy of Sciences* 985 (April): 106–13.

Martin, Patrick. 2003. "The Epidemiology of Anxiety Disorders: A Review." *Dialogues in Clinical Neuroscience* 5 (3). Les Laboratoires Servier: 281–98. http://www.ncbi.nlm.nih.gov/pubmed/22034470.

Matsuo, Tomohiko, Tatsuya Hattori, Akari Asaba, Naokazu Inoue, Nobuhiro Kanomata, Takefumi Kikusui, Reiko Kobayakawa, and Ko Kobayakawa. 2015. "Genetic Dissection of Pheromone Processing Reveals Main Olfactory System-Mediated Social Behaviors in Mice." *Proceedings of the National Academy of Sciences of the United States of America* 112 (3). National Academy of Sciences: E311-20. https://doi.org/10.1073/pnas.1416723112.

McHenry, Jenna A, James M Otis, Mark A Rossi, J Elliott Robinson, Oksana Kosyk, Noah W Miller, Zoe A McElligott, Evgeny A Budygin, David R Rubinow, and Garret D Stuber. 2017. "Hormonal Gain Control of a Medial Preoptic Area Social Reward Circuit." *Nature Neuroscience* 20 (3). Nature Publishing Group: 449–58. https://doi.org/10.1038/nn.4487.

Mefford, Heather C., Mark L. Batshaw, and Eric P. Hoffman. 2012. "Genomics, Intellectual Disability, and Autism." Edited by W. Gregory Feero and Alan E. Guttmacher. *New England Journal of Medicine* 366 (8): 733–43. https://doi.org/10.1056/NEJMra1114194.

Mei, Yuan, Patricia Monteiro, Yang Zhou, Jin-Ah Kim, Xian Gao, Zhanyan Fu, and Guoping Feng. 2016. "Adult Restoration of Shank3 Expression Rescues Selective Autistic-like Phenotypes." *Nature* 530 (7591). Nature Publishing Group: 481–84. https://doi.org/10.1038/nature16971.

Merner, Nancy, Baudouin Forgeot d'Arc, Scott C. Bell, Gilles Maussion, Huashan Peng, Julie Gauthier, Liam Crapper, et al. 2016. "A de Novo Frameshift Mutation in Chromodomain Helicase DNA-Binding Domain 8 (CHD8): A Case Report and Literature Review." *American Journal of Medical Genetics Part A* 170 (5): 1225–35. https://doi.org/10.1002/ajmg.a.37566.

Moessner, Rainald, Christian R Marshall, James S Sutcliffe, Jennifer Skaug, Dalila Pinto, John Vincent, Lonnie Zwaigenbaum, et al. 2007. "REPORT Contribution of SHANK3 Mutations to Autism Spectrum Disorder." *The American Journal of Human Genetics Genetics and Genome Biology Am. J. Hum. Genet* 8181: 1289–97. https://doi.org/10.1086/522590.

Monteiro, Patricia, and Guoping Feng. 2017. "SHANK Proteins: Roles at the Synapse and in Autism Spectrum Disorder." *Nature Reviews Neuroscience* 18 (3). Nature Publishing Group: 147–57. https://doi.org/10.1038/nrn.2016.183.

Muguruza, Carolina, J. Javier Meana, and Luis F. Callado. 2016. "Group II Metabotropic Glutamate Receptors as Targets for Novel Antipsychotic Drugs." *Frontiers in Pharmacology* 7 (May). Frontiers: 130. https://doi.org/10.3389/fphar.2016.00130.

Naisbitt, Scott, Kim Eunjoon, Jian Cheng Tu, Bo Xiao, Carlo Sala, Juli Valtschanoff, Richard J. Weinberg, Paul F. Worley, and Morgan Sheng. 1999. "Shank, a Novel Family of Postsynaptic Density Proteins That Binds to the NMDA Receptor/PSD-95/GKAP Complex and Cortactin." *Neuron* 23 (3): 569–82. https://doi.org/10.1016/S0896-6273(00)80809-0.

Narita, Masaaki, Akiko Oyabu, Yoshio Imura, Naoki Kamada, Tomomi Yokoyama, Kaori Tano, Atsuko Uchida, and Naoko Narita. 2010. "Nonexploratory Movement and Behavioral Alterations in a Thalidomide or Valproic Acid-Induced Autism Model Rat." *Neuroscience Research* 66 (1): 2–6. https://doi.org/10.1016/j.neures.2009.09.001.

Nelson, E C, A Agrawal, A C Heath, R Bogdan, R Sherva, B Zhang, R Al-Hasani, et al. 2016. "Evidence of CNIH3 Involvement in Opioid Dependence." *Molecular Psychiatry* 21 (5). Nature Publishing Group: 608–14. https://doi.org/10.1038/mp.2015.102.

Nelson, Sacha B., and Vera Valakh. 2015. "Excitatory/Inhibitory Balance and Circuit Homeostasis in Autism Spectrum Disorders." *Neuron* 87 (4). Cell Press: 684–98. https://doi.org/10.1016/J.NEURON.2015.07.033.

Newschaffer, Craig J., Lisa A. Croen, Julie Daniels, Ellen Giarelli, Judith K. Grether, Susan E. Levy, David S. Mandell, et al. 2007. "The Epidemiology of Autism Spectrum Disorders." *Annual Review of Public Health* 28 (1): 235–58. https://doi.org/10.1146/annurev.publhealth.28.021406.144007.

Niswender, Colleen M., and P. Jeffrey Conn. 2010. "Metabotropic Glutamate Receptors: Physiology, Pharmacology, and Disease." *Annual Review of Pharmacology and Toxicology* 50 (1): 295–322. https://doi.org/10.1146/annurev.pharmtox.011008.145533.

Noor, Abdul, Anath C. Lionel, Sarah Cohen-Woods, Narges Moghimi, James Rucker, Alanna Fennell, Bhooma Thiruvahindrapuram, et al. 2014. "Copy Number Variant Study of Bipolar Disorder in Canadian and UK Populations Implicates Synaptic Genes." *American Journal of Medical Genetics Part B: Neuropsychiatric Genetics* 165 (4). Wiley-Blackwell: 303–13. https://doi.org/10.1002/ajmg.b.32232.

Nordahl, Christine Wu, Robert Scholz, Xiaowei Yang, Michael H. Buonocore, Tony Simon, Sally Rogers, and David G. Amaral. 2012. "Increased Rate of Amygdala Growth in Children Aged 2 to 4 Years With Autism Spectrum Disorders." *Archives of General Psychiatry* 69 (1). American Medical Association: 53. https://doi.org/10.1001/archgenpsychiatry.2011.145.

Ornoy, A., L. Weinstein-Fudim, and Z. Ergaz. 2015. "Prenatal Factors Associated with Autism Spectrum Disorder (ASD)." *Reproductive Toxicology* 56 (August). Pergamon: 155–69. https://doi.org/10.1016/J.REPROTOX.2015.05.007.

Owen, Scott F., Sebnem N. Tuncdemir, Patrick L. Bader, Natasha N. Tirko, Gord Fishell, and Richard W. Tsien. 2013. "Oxytocin Enhances Hippocampal Spike Transmission by Modulating Fast-

Spiking Interneurons." *Nature* 500 (7463). Nature Publishing Group: 458–62. https://doi.org/10.1038/nature12330.

Ozonoff, Sally, Ana-Maria Iosif, Fam Baguio, Ian C Cook, Monique Moore Hill, Ted Hutman, Sally J Rogers, et al. 2010. "A Prospective Study of the Emergence of Early Behavioral Signs of Autism." *Journal of the American Academy of Child and Adolescent Psychiatry* 49 (3). NIH Public Access: 256-66.e1-2. http://www.ncbi.nlm.nih.gov/pubmed/20410715.

Pappas, Andrea L., Alexandra L. Bey, Xiaoming Wang, Mark Rossi, Yong Ho Kim, Haidun Yan, Fiona Porkka, et al. 2017. "Deficiency of Shank2 Causes Mania-like Behavior That Responds to Mood Stabilizers." *JCI Insight* 2 (20). American Society for Clinical Investigation. https://doi.org/10.1172/jci.insight.92052.

Peça, João, Cátia Feliciano, Jonathan T. Ting, Wenting Wang, Michael F. Wells, Talaignair N. Venkatraman, Christopher D. Lascola, Zhanyan Fu, and Guoping Feng. 2011. "Shank3 Mutant Mice Display Autistic-like Behaviours and Striatal Dysfunction." *Nature* 472 (7344). Nature Publishing Group: 437–42. https://doi.org/10.1038/nature09965.

Peter, Saša, Michiel M. ten Brinke, Jeffrey Stedehouder, Claudia M. Reinelt, Bin Wu, Haibo Zhou, Kuikui Zhou, et al. 2016. "Dysfunctional Cerebellar Purkinje Cells Contribute to Autism-like Behaviour in Shank2-Deficient Mice." *Nature Communications* 7 (September). Nature Publishing Group: 12627. https://doi.org/10.1038/ncomms12627.

Peykov, S, S Berkel, M Schoen, K Weiss, F Degenhardt, J Strohmaier, B Weiss, et al. 2015. "Identification and Functional Characterization of Rare SHANK2 Variants in Schizophrenia." *Molecular Psychiatry* 20 (12). Nature Publishing Group: 1489–98. https://doi.org/10.1038/mp.2014.172.

Pham, Emiley, Leslie Crews, Kiren Ubhi, Lawrence Hansen, Anthony Adame, Anna Cartier, David Salmon, et al. 2010. "Progressive Accumulation of Amyloid-β Oligomers in Alzheimer's Disease and in Amyloid Precursor Protein Transgenic Mice Is Accompanied by Selective Alterations in Synaptic Scaffold Proteins." *FEBS Journal* 277 (14). NIH Public Access: 3051–67. https://doi.org/10.1111/j.1742-4658.2010.07719.x.

Phelan, K., and H. E. McDermid. 2012. "The 22q13.3 Deletion Syndrome (Phelan-McDermid Syndrome)." *Molecular Syndromology* 2 (3–5): 186–201. https://doi.org/10.1159/000334260.

Pieretti, M, F P Zhang, Y H Fu, S T Warren, B A Oostra, C T Caskey, and D L Nelson. 1991. "Absence of Expression of the FMR-1 Gene in Fragile X Syndrome." *Cell* 66 (4): 817–22. http://www.ncbi.nlm.nih.gov/pubmed/1878973.

Pinto, Dalila, Alistair T. Pagnamenta, Lambertus Klei, Richard Anney, Daniele Merico, Regina Regan, Judith Conroy, et al. 2010. "Functional Impact of Global Rare Copy Number Variation in Autism Spectrum Disorders." *Nature* 466 (7304): 368–72. https://doi.org/10.1038/nature09146.

Pop, Andreea S., Baltazar Gomez-Mancilla, Giovanni Neri, Rob Willemsen, and Fabrizio Gasparini. 2014. "Fragile X Syndrome: A Preclinical Review on Metabotropic Glutamate Receptor 5 (MGluR5) Antagonists and Drug Development." *Psychopharmacology* 231 (6). Springer Berlin Heidelberg: 1217–26. https://doi.org/10.1007/s00213-013-3330-3.

Pope, H G, S L McElroy, P E Keck, and J I Hudson. 1991. "Valproate in the Treatment of Acute Mania. A Placebo-Controlled Study." *Archives of General Psychiatry* 48 (1): 62–68. http://www.ncbi.nlm.nih.gov/pubmed/1984763.

Popik, P, and J M van Ree. 1991. "Oxytocin but Not Vasopressin Facilitates Social Recognition Following Injection into the Medial Preoptic Area of the Rat Brain." *European Neuropsychopharmacology : The Journal of the European College of*

Neuropsychopharmacology 1 (4): 555–60.

Portfors, Christine V., and David J. Perkel. 2014. "The Role of Ultrasonic Vocalizations in Mouse Communication." *Current Opinion in Neurobiology* 28 (October): 115–20. https://www.sciencedirect.com/science/article/pii/S0959438814001287.

Portfors, Christine V. 2007. "Types and Functions of Ultrasonic Vocalizations in Laboratory Rats and Mice." *Journal of the American Association for Laboratory Animal Science : JAALAS* 46 (1): 28–34.

Presti, Michael F., Christopher J. Watson, Robert T. Kennedy, Mark Yang, and Mark H. Lewis. 2004. "Behavior-Related Alterations of Striatal Neurochemistry in a Mouse Model of Stereotyped Movement Disorder." *Pharmacology Biochemistry and Behavior* 77 (3): 501–7. https://doi.org/10.1016/j.pbb.2003.12.004.

Price, Joseph L. 2006. "Comparative Aspects of Amygdala Connectivity." *Annals of the New York Academy of Sciences* 985 (1): 50–58. https://doi.org/10.1111/j.1749-6632.2003.tb07070.x.

Proepper, Christian, Svenja Johannsen, Stefan Liebau, Janine Dahl, Bianca Vaida, Juergen Bockmann, Michael R. Kreutz, Eckart D. Gundelfinger, and Tobias M. Boeckers. 2007. "Abelson Interacting Protein 1 (Abi-1) Is Essential for Dendrite Morphogenesis and Synapse Formation." *EMBO Journal* 26 (5): 1397–1409. https://doi.org/10.1038/sj.emboj.7601569.

Qin, Luye, Kaijie Ma, Zi-Jun Wang, Zihua Hu, Emmanuel Matas, Jing Wei, and Zhen Yan. 2018. "Social Deficits in Shank3-Deficient Mouse Models of Autism Are Rescued by Histone Deacetylase (HDAC) Inhibition." *Nature Neuroscience*, March. https://doi.org/10.1038/s41593-018-0110-8.

Qualmann, B. 2004. "Linkage of the Actin Cytoskeleton to the Postsynaptic Density via Direct Interactions of Abp1 with the ProSAP/Shank Family." *Journal of Neuroscience* 24 (10): 2481–95. https://doi.org/10.1523/JNEUROSCI.5479-03.2004.

R Core Team (R Foundation for Statistical Computing, Vienna,Austria). 2014. "R: A Language and Environment for Statistical Computing."

Raab, M., T.M. M. Boeckers, and W.L. L. Neuhuber. 2010. "Proline-Rich Synapse-Associated Protein-1 and 2 (ProSAP1/Shank2 and ProSAP2/Shank3)-Scaffolding Proteins Are Also Present in Postsynaptic Specializations of the Peripheral Nervous System." *Neuroscience* 171 (2). Elsevier Inc.: 421–33. https://doi.org/10.1016/j.neuroscience.2010.08.041.

Rai, Dheeraj, Brian K Lee, Christina Dalman, Jean Golding, Glyn Lewis, and Cecilia Magnusson. 2013. "Parental Depression, Maternal Antidepressant Use during Pregnancy, and Risk of Autism Spectrum Disorders: Population Based Case-Control Study." *BMJ (Clinical Research Ed.)* 346 (April): f2059. http://www.ncbi.nlm.nih.gov/pubmed/23604083.

Redcay, Elizabeth, and Eric Courchesne. 2005. "When Is the Brain Enlarged in Autism? A Meta-Analysis of All Brain Size Reports." *Biological Psychiatry* 58 (1). Elsevier: 1–9. https://doi.org/10.1016/J.BIOPSYCH.2005.03.026.

Reddy, Kavita S. 2005. "Cytogenetic Abnormalities and Fragile-x Syndrome in Autism Spectrum Disorder." *BMC Medical Genetics* 6 (1): 3. https://doi.org/10.1186/1471-2350-6-3.

Reichenberg, Abraham, Raz Gross, Mark Weiser, Michealine Bresnahan, Jeremy Silverman, Susan Harlap, Jonathan Rabinowitz, et al. 2006. "Advancing Paternal Age and Autism." *Archives of General Psychiatry* 63 (9): 1026. https://doi.org/10.1001/archpsyc.63.9.1026.

Reim, Dominik, Ute Distler, Sonja Halbedl, Chiara Verpelli, Carlo Sala, Juergen Bockmann, Stefan Tenzer, Tobias M. Boeckers, and Michael J. Schmeisser. 2017. "Proteomic Analysis of Post-

Synaptic Density Fractions from Shank3 Mutant Mice Reveals Brain Region Specific Changes Relevant to Autism Spectrum Disorder." *Frontiers in Molecular Neuroscience* 10 (February). Frontiers Media SA: 26. https://doi.org/10.3389/fnmol.2017.00026.

Rilling, James K, and Alan G Sanfey. 2011. "The Neuroscience of Social Decision-Making." *Annual Review of Psychology* 62 (1): 23–48. https://doi.org/10.1146/annurev.psych.121208.131647.

Ritchie, Matthew E., Belinda Phipson, Di Wu, Yifang Hu, Charity W. Law, Wei Shi, and Gordon K. Smyth. 2015. "Limma Powers Differential Expression Analyses for RNA-Sequencing and Microarray Studies." *Nucleic Acids Research* 43 (7): e47–e47. https://doi.org/10.1093/nar/gkv007.

Robinson, Donita L., Dawnya L. Zitzman, and Sarah K. Williams. 2011. "Mesolimbic Dopamine Transients in Motivated Behaviors: Focus on Maternal Behavior." *Frontiers in Psychiatry* 2 (MAY): 1–13. https://doi.org/10.3389/fpsyt.2011.00023.

Rodrigues, Ricardo J, and Juan Lerma. 2012. "Metabotropic Signaling by Kainate Receptors." *WIREs Membr Transp Signal* 1: 399–410. https://doi.org/10.1002/wmts.35.

Roselli, Francesco, Peter Hutzler, Yvonne Wegerich, Paolo Livrea, and Osborne F. X. Almeida. 2009. "Disassembly of Shank and Homer Synaptic Clusters Is Driven by Soluble β-Amyloid1-40 through Divergent NMDAR-Dependent Signalling Pathways." Edited by Hitoshi Okazawa. *PLoS ONE* 4 (6). Public Library of Science: e6011. https://doi.org/10.1371/journal.pone.0006011.

Rothwell, Patrick E., Marc V. Fuccillo, Stephan Maxeiner, Scott J. Hayton, Ozgun Gokce, Byung Kook Lim, Stephen C. Fowler, Robert C. Malenka, and Thomas C. Südhof. 2014. "Autism-Associated Neuroligin-3 Mutations Commonly Impair Striatal Circuits to Boost Repetitive Behaviors." *Cell* 158 (1). Cell Press: 198–212. https://doi.org/10.1016/J.CELL.2014.04.045.

Rothwell, Patrick E. 2016. "Autism Spectrum Disorders and Drug Addiction: Common Pathways, Common Molecules, Distinct Disorders?" *Frontiers in Neuroscience* 10 (February). Frontiers: 20. https://doi.org/10.3389/fnins.2016.00020.

Rubeis, Silvia De, Paige M. Siper, Allison Durkin, Jordana Weissman, François Muratet, Danielle Halpern, Maria del Pilar Trelles, et al. 2018. "Delineation of the Genetic and Clinical Spectrum of Phelan-McDermid Syndrome Caused by SHANK3 Point Mutations." *Molecular Autism* 9 (1). BioMed Central: 31. https://doi.org/10.1186/s13229-018-0205-9.

Rubenstein, J. L. R., and M. M. Merzenich. 2003. "Model of Autism: Increased Ratio of Excitation/Inhibition in Key Neural Systems." *Genes, Brain and Behavior* 2 (5). Wiley/Blackwell (10.1111): 255–67. https://doi.org/10.1034/j.1601-183X.2003.00037.x.

Russo, Scott J., and Eric J. Nestler. 2013. "The Brain Reward Circuitry in Mood Disorders." *Nature Reviews Neuroscience* 14 (9). Nature Publishing Group: 609–25. https://doi.org/10.1038/nrn3381.

Sacco, Roberto, Stefano Gabriele, and Antonio M. Persico. 2015. "Head Circumference and Brain Size in Autism Spectrum Disorder: A Systematic Review and Meta-Analysis." *Psychiatry Research: Neuroimaging* 234 (2). Elsevier: 239–51. https://doi.org/10.1016/J.PSCYCHRESNS.2015.08.016.

Sala, Carlo, Valentin Piëch, Nathan R. Wilson, Maria Passafaro, Guosong Liu, and Morgan Sheng. 2001. "Regulation of Dendritic Spine Morphology and Synaptic Function by Shank and Homer." *Neuron* 31 (1): 115–30. https://doi.org/10.1016/S0896-6273(01)00339-7.

Sala, Carlo, Cinzia Vicidomini, Ilaria Bigi, Adele Mossa, and Chiara Verpelli. 2015. "Shank Synaptic

Scaffold Proteins: Keys to Understanding the Pathogenesis of Autism and Other Synaptic Disorders." *Journal of Neurochemistry* 135 (5): 849–58. https://doi.org/10.1111/jnc.13232.

Sams-Dodd, F. 1996. "Phencyclidine-Induced Stereotyped Behaviour and Social Isolation in Rats: A Possible Animal Model of Schizophrenia." *Behavioural Pharmacology* 7 (1): 3–23. http://www.ncbi.nlm.nih.gov/pubmed/11224390.

Sams-Dodd, Frank. 1998. "Effects of Dopamine Agonists and Antagonists on PCP-Induced Stereotyped Behaviour and Social Isolation in the Rat Social Interaction Test." *Psychopharmacology* 135 (2): 182–93. https://doi.org/10.1007/s002130050500.

Sandin, Sven, Paul Lichtenstein, Ralf Kuja-Halkola, Henrik Larsson, Christina M. Hultman, and Abraham Reichenberg. 2014. "The Familial Risk of Autism." *JAMA* 311 (17). American Medical Association: 1770. https://doi.org/10.1001/jama.2014.4144.

Sarowar, Tasnuva, Resham Chhabra, Antonietta Vilella, Tobias M. Boeckers, Michele Zoli, and Andreas M. Grabrucker. 2016. "Activity and Circadian Rhythm Influence Synaptic Shank3 Protein Levels in Mice." *Journal of Neurochemistry* 138 (6): 887–95. https://doi.org/10.1111/jnc.13709.

Sasanfar, Roksana, Stephen A Haddad, Ala Tolouei, Majid Ghadami, Dongmei Yu, and Susan L Santangelo. 2010. "Paternal Age Increases the Risk for Autism in an Iranian Population Sample." *Molecular Autism* 1 (1): 2. https://doi.org/10.1186/2040-2392-1-2.

Sato, Daisuke, Anath C. C. Lionel, Claire S. S. Leblond, Aparna Prasad, Dalila Pinto, Susan Walker, Irene O'Connor, et al. 2012. "SHANK1 Deletions in Males with Autism Spectrum Disorder." *The American Journal of Human Genetics* 90 (5). Cell Press: 879–87. http://www.cell.com/ajhg/pdf/S0002-9297(12)00161-9.pdf.

Scattoni, M L, L Ricceri, and J N Crawley. 2011. "Unusual Repertoire of Vocalizations in Adult BTBR T+tf/J Mice during Three Types of Social Encounters." *Genes, Brain and Behavior* 10 (1). NIH Public Access: 44–56. https://doi.org/10.1111/j.1601-183X.2010.00623.x.

Schmeisser, Michael J., Elodie Ey, Stephanie Wegener, Juergen Bockmann, A. Vanessa Stempel, Angelika Kuebler, Anna Lena Janssen, et al. 2012. "Autistic-like Behaviours and Hyperactivity in Mice Lacking ProSAP1/Shank2." *Nature* 486 (7402). Nature Publishing Group: 256–60. https://doi.org/10.1038/nature11015.

Schopler, E, R J Reichler, R F DeVellis, and K Daly. 1980. "Toward Objective Classification of Childhood Autism: Childhood Autism Rating Scale (CARS)." *Journal of Autism and Developmental Disorders* 10 (1): 91–103. http://www.ncbi.nlm.nih.gov/pubmed/6927682.

Schubert, D, G J M Martens, and S M Kolk. 2015. "Molecular Underpinnings of Prefrontal Cortex Development in Rodents Provide Insights into the Etiology of Neurodevelopmental Disorders." *Molecular Psychiatry* 20 (7). Nature Publishing Group: 795–809. https://doi.org/10.1038/mp.2014.147.

Schumann, C. M., Julia Hamstra, Beth L Goodlin-Jones, Linda J Lotspeich, Hower Kwon, Michael H Buonocore, Cathy R Lammers, Allan L Reiss, and David G Amaral. 2004. "The Amygdala Is Enlarged in Children But Not Adolescents with Autism; the Hippocampus Is Enlarged at All Ages." *Journal of Neuroscience* 24 (28): 6392–6401. https://doi.org/10.1523/JNEUROSCI.1297-04.2004.

Serret, Sylvie, Susanne Thümmler, Emmanuelle Dor, Stephanie Vesperini, Andreia Santos, and Florence Askenazy. 2015. "Lithium as a Rescue Therapy for Regression and Catatonia Features in Two SHANK3 Patients with Autism Spectrum Disorder: Case Reports." *BMC Psychiatry* 15 (1). BioMed Central: 107. https://doi.org/10.1186/s12888-015-0490-1.

Sesack, Susan R, and Anthony A Grace. 2010. "Cortico-Basal Ganglia Reward Network: Microcircuitry." *Neuropsychopharmacology : Official Publication of the American College of Neuropsychopharmacology* 35 (1). Nature Publishing Group: 27–47. https://doi.org/10.1038/npp.2009.93.

Sheng, M, and E Kim. 2000. "The Shank Family of Scaffold Proteins." *Journal of Cell Science* 113 (Pt 1: 1851–56.

Silverman, Jill L., Sarah M. Turner, Charlotte L. Barkan, Seda S. Tolu, Roheeni Saxena, Albert Y. Hung, Morgan Sheng, and Jacqueline N. Crawley. 2011. "Sociability and Motor Functions in Shank1 Mutant Mice." *Brain Research* 1380 (March). Elsevier: 120–37. https://doi.org/10.1016/J.BRAINRES.2010.09.026.

Silverman, Jill L, Mu Yang, Catherine Lord, and Jacqueline N Crawley. 2010. "Behavioural Phenotyping Assays for Mouse Models of Autism." *Nature Reviews Neuroscience* 11 (7). Nature Publishing Group: 490–502. https://doi.org/10.1038/nrn2851.

Siu, Michelle T., and Rosanna Weksberg. 2017. "Epigenetics of Autism Spectrum Disorder." In *Neuroepigenomics in Aging and Disease*, 63–90. Springer, Cham. https://doi.org/10.1007/978-3-319-53889-1_4.

Soden, Marta E, and Lu Chen. 2010. "Fragile X Protein FMRP Is Required for Homeostatic Plasticity and Regulation of Synaptic Strength by Retinoic Acid." *The Journal of Neuroscience : The Official Journal of the Society for Neuroscience* 30 (50). NIH Public Access: 16910–21. https://doi.org/10.1523/JNEUROSCI.3660-10.2010.

Sorge, Robert E., Loren J. Martin, Kelsey A. Isbester, Susana G. Sotocinal, Sarah Rosen, Alexander H. Tuttle, Jeffrey S. Wieskopf, et al. 2014. "Olfactory Exposure to Males, Including Men, Causes Stress and Related Analgesia in Rodents." *Nature Methods* 11 (6). Nature Publishing Group: 629–32. https://doi.org/10.1038/nmeth.2935.

Sovner, R., A. Stone, and C. Fox. 1996. "Ring Chromosome 22 and Mood Disorders." *Journal of Intellectual Disability Research* 40 (1). Blackwell Publishing Ltd: 82–86. https://doi.org/10.1111/j.1365-2788.1996.tb00607.x.

Speed, Haley E., Mehreen Kouser, Zhong Xuan, Jeremy M. Reimers, Christine F. Ochoa, Natasha Gupta, Shunan Liu, and C. M. Powell. 2015. "Autism-Associated Insertion Mutation (InsG) of Shank3 Exon 21 Causes Impaired Synaptic Transmission and Behavioral Deficits." *Journal of Neuroscience* 35 (26): 9648–65. https://doi.org/10.1523/JNEUROSCI.3125-14.2015.

Spence, Sarah J, and Mark T Schneider. 2009. "The Role of Epilepsy and Epileptiform EEGs in Autism Spectrum Disorders." *Pediatric Research* 65 (6). NIH Public Access: 599–606. https://doi.org/10.1203/PDR.0b013e31819e7168.

Squire, Larry R., and John T. Wixted. 2011. "The Cognitive Neuroscience of Human Memory Since H.M." *Annual Review of Neuroscience* 34 (1): 259–88. https://doi.org/10.1146/annurev-neuro-061010-113720.

State, Matthew W, and Nenad Šestan. 2012. "Neuroscience. The Emerging Biology of Autism Spectrum Disorders." *Science (New York, N.Y.)* 337 (6100). NIH Public Access: 1301–3. https://doi.org/10.1126/science.1224989.

Stotz-Ingenlath, Gabriele. 2000. "Epistemological Aspects of Eugen Bleuler's Conception of Schizophrenia in 1911." *Medicine Health Care and Philosophy* 3: 153–59. https://link.springer.com/content/pdf/10.1023%2FA%3A1009919309015.pdf.

Subramanian, Aravind, Pablo Tamayo, Vamsi K. Mootha, Sayan Mukherjee, Benjamin L. Ebert, Michael A. Gillette, Amanda Paulovich, et al. 2005. "Gene Set Enrichment Analysis: A

Knowledge-Based Approach for Interpreting Genome-Wide Expression Profiles." *Proceedings of the National Academy of Sciences* 102 (43): 15545–50. https://doi.org/10.1073/pnas.0506580102.

Sungur, A. Özge, Magdalena C.E. Jochner, Hani Harb, Ayşe Kılıç, Holger Garn, Rainer K.W. Schwarting, and Markus Wöhr. 2017. "Aberrant Cognitive Phenotypes and Altered Hippocampal BDNF Expression Related to Epigenetic Modifications in Mice Lacking the Post-Synaptic Scaffolding Protein SHANK1: Implications for Autism Spectrum Disorder." *Hippocampus* 27 (8): 906–19. https://doi.org/10.1002/hipo.22741.

Sungur, A. Özge, Rainer K.W. Schwarting, and Markus Wöhr. 2016. "Early Communication Deficits in the *Shank1* Knockout Mouse Model for Autism Spectrum Disorder: Developmental Aspects and Effects of Social Context." *Autism Research* 9 (6). Wiley-Blackwell: 696–709. https://doi.org/10.1002/aur.1564.

Sungur, A. Özge, Karl J. Vörckel, Rainer K.W. Schwarting, and Markus Wöhr. 2014. "Repetitive Behaviors in the Shank1 Knockout Mouse Model for Autism Spectrum Disorder: Developmental Aspects and Effects of Social Context." *Journal of Neuroscience Methods* 234 (August). Elsevier: 92–100. https://doi.org/10.1016/J.JNEUMETH.2014.05.003.

Swanson, L W, and P E Sawchenko. 1983. "Hypothalamic Integration: Organization of the Paraventricular and Supraoptic Nuclei." *Annual Review of Neuroscience* 6 (1). Annual Reviews 4139 El Camino Way, P.O. Box 10139, Palo Alto, CA 94303-0139, USA : 269–324. https://doi.org/10.1146/annurev.ne.06.030183.001413.

Tabet, Anne-Claude, Thomas Rolland, Marie Ducloy, Jonathan Lévy, Julien Buratti, Alexandre Mathieu, Damien Haye, et al. 2017. "A Framework to Identify Contributing Genes in Patients with Phelan-McDermid Syndrome." *Npj Genomic Medicine* 2 (1). Springer US: 32. https://doi.org/10.1038/s41525-017-0035-2.

Tabuchi, Katsuhiko, Jacqueline Blundell, Mark R Etherton, Robert E Hammer, Xinran Liu, Craig M Powell, and Thomas C Südhof. 2007. "A Neuroligin-3 Mutation Implicated in Autism Increases Inhibitory Synaptic Transmission in Mice." *Science (New York, N.Y.)* 318 (5847). American Association for the Advancement of Science: 71–76. https://doi.org/10.1126/science.1146221.

Toro, Roberto, Marina Konyukh, Richard Delorme, Claire Leblond, Pauline Chaste, Fabien Fauchereau, Mary Coleman, Marion Leboyer, Christopher Gillberg, and Thomas Bourgeron. 2010. "Key Role for Gene Dosage and Synaptic Homeostasis in Autism Spectrum Disorders." *Trends in Genetics* 26 (8). Elsevier: 363–72. https://doi.org/10.1016/j.tig.2010.05.007.

Tu, Jian Cheng, Bo Xiao, Scott Naisbitt, Joseph P. Yuan, Ronald S. Petralia, Paul Brakeman, Andrew Doan, et al. 1999. "Coupling of MGluR/Homer and PSD-95 Complexes by the Shank Family of Postsynaptic Density Proteins." *Neuron* 23 (3): 583–92. https://doi.org/10.1016/S0896-6273(00)80810-7.

Turnbull, H. Rutherford. 2005. "Individuals With Disabilities Education Act Reauthorization." *Remedial and Special Education* 26 (6). Sage PublicationsSage CA: Los Angeles, CA: 320–26. https://doi.org/10.1177/07419325050260060201.

Uematsu, Ken, Myriam Heiman, Marina Zelenina, Júlio Padovan, Brian T Chait, Anita Aperia, Akinori Nishi, and Paul Greengard. 2015. "Protein Kinase A Directly Phosphorylates Metabotropic Glutamate Receptor 5 to Modulate Its Function." *Journal of Neurochemistry* 132 (6). NIH Public Access: 677–86. https://doi.org/10.1111/jnc.13038.

Uemura, Takeshi, Hisashi Mori, and Masayoshi Mishina. 2004. "Direct Interaction of GluRδ2 with Shank Scaffold Proteins in Cerebellar Purkinje Cells." *Molecular and Cellular Neuroscience* 26 (2): 330–41. https://doi.org/10.1016/j.mcn.2004.02.007.

Uhlen, M., L. Fagerberg, B. M. Hallstrom, C. Lindskog, P. Oksvold, A. Mardinoglu, A. Sivertsson, et al. 2015. "Tissue-Based Map of the Human Proteome." *Science* 347 (6220): 1260419–1260419. https://doi.org/10.1126/science.1260419.

Veening, Jan G., Lique M. Coolen, Trynke R. De Jong, Henk W. Joosten, Sietze F. De Boer, Jaap M. Koolhaas, and Berend Olivier. 2005. "Do Similar Neural Systems Subserve Aggressive and Sexual Behaviour in Male Rats? Insights from c-Fos and Pharmacological Studies." *European Journal of Pharmacology* 526 (1–3): 226–39. https://doi.org/10.1016/j.ejphar.2005.09.041.

Verhoeven, Willem M.A., Jos I.M. Egger, Ruthy Cohen-Snuijf, Sarina G. Kant, and Nicole de Leeuw. 2013. "Phelan-McDermid Syndrome: Clinical Report of a 70-Year-Old Woman." *American Journal of Medical Genetics Part A* 161 (1). Wiley Subscription Services, Inc., A Wiley Company: 158–61. https://doi.org/10.1002/ajmg.a.35597.

Vicidomini, C, L Ponzoni, D Lim, M J Schmeisser, D Reim, N Morello, D Orellana, et al. 2017. "Pharmacological Enhancement of MGlu5 Receptors Rescues Behavioral Deficits in SHANK3 Knock-out Mice." *Molecular Psychiatry* 22 (5): 689–702. https://doi.org/10.1038/mp.2016.30.

Vucurovic, Ksenija, Emilie Landais, Cécile Delahaigue, Julien Eutrope, Anouck Schneider, Camille Leroy, Hamza Kabbaj, et al. 2012. "Bipolar Affective Disorder and Early Dementia Onset in a Male Patient with SHANK3 Deletion." *European Journal of Medical Genetics* 55: 625–29. https://doi.org/10.1016/j.ejmg.2012.07.009.

Waga, Chikako, Nobuhiko Okamoto, Yumiko Ondo, Reiko Fukumura-Kato, Yu-ichi Goto, Shinichi Kohsaka, and Shigeo Uchino. 2011. "Novel Variants of the SHANK3 Gene in Japanese Autistic Patients with Severe Delayed Speech Development." *Psychiatric Genetics* 21 (4): 208–11. https://doi.org/10.1097/YPG.0b013e328341e069.

Wallace, Gregory L, Briana Robustelli, Nathan Dankner, Lauren Kenworthy, Jay N Giedd, and Alex Martin. 2013. "Increased Gyrification, but Comparable Surface Area in Adolescents with Autism Spectrum Disorders." *Brain : A Journal of Neurology* 136 (Pt 6). Oxford University Press: 1956–67. https://doi.org/10.1093/brain/awt106.

Wang, Fei, Helmut W. Kessels, and Hailan Hu. 2014. "The Mouse That Roared: Neural Mechanisms of Social Hierarchy." *Trends in Neurosciences* 37 (11). Elsevier Ltd: 674–82. https://doi.org/10.1016/j.tins.2014.07.005.

Wang, Hansen, Susan S. Kim, and Min Zhuo. 2010. "Roles of Fragile X Mental Retardation Protein in Dopaminergic Stimulation-Induced Synapse-Associated Protein Synthesis and Subsequent α-Amino-3-Hydroxyl-5-Methyl-4-Isoxazole-4-Propionate (AMPA) Receptor Internalization." *Journal of Biological Chemistry* 285 (28): 21888–901. https://doi.org/10.1074/jbc.M110.116293.

Wang, Tianyun, Hui Guo, Bo Xiong, Holly A.F. Stessman, Huidan Wu, Bradley P. Coe, Tychele N. Turner, et al. 2016. "De Novo Genic Mutations among a Chinese Autism Spectrum Disorder Cohort." *Nature Communications* 7 (November). Nature Publishing Group: 13316. https://doi.org/10.1038/ncomms13316.

Wang, Wenting, Chenchen Li, Qian Chen, Marie-Sophie van der Goes, James Hawrot, Annie Y. Yao, Xian Gao, et al. 2017. "Striatopallidal Dysfunction Underlies Repetitive Behavior in Shank3-Deficient Model of Autism." *The Journal of Clinical Investigation* 127 (5). American Society for Clinical Investigation: 1978–90. https://doi.org/10.1172/JCI87997.

Wang, Xiaoming, Alexandra L. Bey, Brittany M. Katz, Alexandra Badea, Namsoo Kim, Lisa K. David, Lara J. Duffney, et al. 2016. "Altered MGluR5-Homer Scaffolds and Corticostriatal Connectivity in a Shank3 Complete Knockout Model of Autism." *Nature Communications* 7 (May). Nature Publishing Group: 11459. https://doi.org/10.1038/ncomms11459.

Wang, Xiaoming, Portia A. McCoy, Ramona M. Rodriguiz, Yanzhen Pan, H. Shawn Je, Adam C. Roberts, Caroline J. Kim, et al. 2011. "Synaptic Dysfunction and Abnormal Behaviors in Mice Lacking Major Isoforms of Shank3." *Human Molecular Genetics* 20 (15). Oxford University Press: 3093–3108. https://doi.org/10.1093/hmg/ddr212.

Wang, Xiaoming, Qiong Xu, Alexandra L. Bey, Yoonji Lee, and Yong Hui Jiang. 2014. "Transcriptional and Functional Complexity of Shank3 Provides a Molecular Framework to Understand the Phenotypic Heterogeneity of SHANK3 Causing Autism and Shank3 Mutant Mice." *Molecular Autism* 5 (1). BioMed Central: 30. https://doi.org/10.1186/2040-2392-5-30.

Wei, Shu-Chen Chen, Hsin-Fang Fang Yang-Yen, Po-Nien Nien Tsao, Meng-Tzu Tzu Weng, Chien-Chih Chih Tung, Linda C.H. H. Yu, Liang-Chuan Chuan Lai, et al. 2017. "SHANK3 Regulates Intestinal Barrier Function Through Modulating ZO-1 Expression Through the PKCϵ-Dependent Pathway." *Inflammatory Bowel Diseases* 23 (10). Oxford University Press: 1730–40. https://doi.org/10.1097/MIB.0000000000001250.

White, Susan W, Donald Oswald, Thomas Ollendick, and Lawrence Scahill. 2009. "Anxiety in Children and Adolescents with Autism Spectrum Disorders." *Clinical Psychology Review* 29 (3): 216–29. https://doi.org/10.1016/j.cpr.2009.01.003.

Wickham, Hadley. 2009. *Ggplot2: Elegant Graphics for Data Analysis*. Use R! New York: Springer-Verlag.

Wilkins, Jonathan, and Johnny L. Matson. 2009. "A Comparison of Social Skills Profiles in Intellectually Disabled Adults With and Without ASD." *Behavior Modification* 33 (2): 143–55. https://doi.org/10.1177/0145445508321880.

Willemsen, M H, J H M Rensen, H M J Van, Schrojenstein-Lantman De Valk, B C J Hamel, and T Kleefstra. 2011. "Adult Phenotypes in Angelman-and Rett-Like Syndromes." *Mol Syndromol* 2: 217–34. https://doi.org/10.1159/000335661.

Wilson, Heather L., John A. Crolla, Dena Walker, Lina Artifoni, Bruno Dallapiccola, Takako Takano, Pradeep Vasudevan, et al. 2008. "Interstitial 22q13 Deletions: Genes Other than SHANK3 Have Major Effects on Cognitive and Language Development." *European Journal of Human Genetics* 16 (11): 1301–10. https://doi.org/10.1038/ejhg.2008.107.

Wise, Steven P. 2008. "Forward Frontal Fields: Phylogeny and Fundamental Function." *Trends in Neurosciences* 31 (12): 599–608. https://doi.org/10.1016/j.tins.2008.08.008.

Wöhr, Markus, Florence I. Roullet, Albert Y. Hung, Morgan Sheng, and Jacqueline N. Crawley. 2011. "Communication Impairments in Mice Lacking Shank1: Reduced Levels of Ultrasonic Vocalizations and Scent Marking Behavior." Edited by Wim E. Crusio. *PLoS ONE* 6 (6). Public Library of Science: e20631. https://doi.org/10.1371/journal.pone.0020631.

Won, Hyejung, Hye-Ryeon Lee, Heon Yung Gee, Won Mah, Jae-Ick Kim, Jiseok Lee, Seungmin Ha, et al. 2012. "Autistic-like Social Behaviour in Shank2-Mutant Mice Improved by Restoring NMDA Receptor Function." *Nature* 486 (7402). Nature Publishing Group: 261–65. https://doi.org/10.1038/nature11208.

Xiao, Zhou, Ting Qiu, Xiaoyan Ke, Xiang Xiao, Ting Xiao, Fengjing Liang, Bing Zou, et al. 2014. "Autism Spectrum Disorder as Early Neurodevelopmental Disorder: Evidence from the Brain Imaging Abnormalities in 2–3 Years Old Toddlers." *Journal of Autism and Developmental Disorders* 44 (7). Springer US: 1633–40. https://doi.org/10.1007/s10803-014-2033-x.

Xue, Mingshan, Bassam V. Atallah, and Massimo Scanziani. 2014. "Equalizing Excitation–Inhibition Ratios across Visual Cortical Neurons." *Nature* 511 (7511). Nature Publishing Group: 596–600. https://doi.org/10.1038/nature13321.

Yalcin, Binnaz, David J. Adams, Jonathan Flint, and Thomas M. Keane. 2012. "Next-Generation Sequencing of Experimental Mouse Strains." *Mammalian Genome* 23 (9–10): 490–98. https://doi.org/10.1007/s00335-012-9402-6.

Yang, Mu, Ozlem Bozdagi, Maria Luisa Scattoni, Markus Wöhr, Florence I Roullet, Adam M Katz, Danielle N Abrams, et al. 2012. "Reduced Excitatory Neurotransmission and Mild Autism-Relevant Phenotypes in Adolescent Shank3 Null Mutant Mice." *The Journal of Neuroscience : The Official Journal of the Society for Neuroscience* 32 (19). NIH Public Access: 6525–41. https://doi.org/10.1523/JNEUROSCI.6107-11.2012.

Yang, Mu, Jill L. Silverman, and Jacqueline N. Crawley. 2011. "Automated Three-Chambered Social Approach Task for Mice." In *Current Protocols in Neuroscience*, Chapter 8:Unit 8.26. Hoboken, NJ, USA: John Wiley & Sons, Inc. https://doi.org/10.1002/0471142301.ns0826s56.

Yang, Y, Xiaoming Wang, and Yong-hui Jiang. 2018. "SHANK2 -harbors -potentially -pathogenic Mutations -associated -with -bipolar -disorder." *International Society for Bipolar Disorders*, no. Poster. https://onlinelibrary.wiley.com/doi/epdf/10.1111/bdi.12619.

Yin, Shen, and Colleen M. Niswender. 2014. "Progress toward Advanced Understanding of Metabotropic Glutamate Receptors: Structure, Signaling and Therapeutic Indications." *Cellular Signalling* 26 (10). Pergamon: 2284–97. https://doi.org/10.1016/j.cellsig.2014.04.022.

Yizhar, Ofer, Lief E. Fenno, Matthias Prigge, Franziska Schneider, Thomas J. Davidson, Daniel J. O'Shea, Vikaas S. Sohal, et al. 2011. "Neocortical Excitation/Inhibition Balance in Information Processing and Social Dysfunction." *Nature* 477 (7363). Nature Publishing Group: 171–78. https://doi.org/10.1038/nature10360.

Yoon, Seo-Yeon, Soon-Gu Kwon, Yong Ho Kim, Ji-Hee Yeo, Hyoung-Gon Ko, Dae-Hyun Roh, Bong-Kiun Kaang, Alvin J Beitz, Jang-Hern Lee, and Seog Bae Oh. 2017. "A Critical Role of Spinal Shank2 Proteins in NMDA-Induced Pain Hypersensitivity." *Molecular Pain* 13 (January): 174480691668890. https://doi.org/10.1177/1744806916688902.

Young, Allan H., and James I. Newham. 2006. "Lithium in Maintenance Therapy for Bipolar Disorder." *Journal of Psychopharmacology* 20 (2_suppl). SAGE PublicationsSage CA: Thousand Oaks, CA: 17–22. https://doi.org/10.1177/1359786806063072.

Yu, Kevin K, Charlton Cheung, Siew E Chua, and Gráinne M McAlonan. 2011. "Can Asperger Syndrome Be Distinguished from Autism? An Anatomic Likelihood Meta-Analysis of MRI Studies." *Journal of Psychiatry & Neuroscience : JPN* 36 (6). Canadian Medical Association: 412–21. https://doi.org/10.1503/jpn.100138.

Yuen, Ryan K C, Bhooma Thiruvahindrapuram, Daniele Merico, Susan Walker, Kristiina Tammimies, Ny Hoang, Christina Chrysler, et al. 2015. "Whole-Genome Sequencing of Quartet Families with Autism Spectrum Disorder." *Nature Medicine* 21 (2). Nature Publishing Group: 185–91. https://doi.org/10.1038/nm.3792.

Zafeiriou, Dimitrios I., Athina Ververi, Vaios Dafoulis, Efrosini Kalyva, and Euthymia Vargiami. 2013. "Autism Spectrum Disorders: The Quest for Genetic Syndromes." *American Journal of Medical Genetics Part B: Neuropsychiatric Genetics* 162 (4): 327–66. https://doi.org/10.1002/ajmg.b.32152.

Zhang, Hua Anton Maximov, Fang Xu Yu Fu, Tie-Shan Tang, Tatiana Tkatch, D. James Surmeier, Ilya Bezprozvanny, et al. 2005. "Association of CaV1.3 L-Type Calcium Channels with Shank." *Journal of Neuroscience* 25 (5): 1037–49. https://doi.org/10.1523/JNEUROSCI.4554-04.2005.

Zhou, Yongdi Yang Yongdi, Tobias Kaiser, Patrícia Monteiro, Xiangyu Zhang, Marie. S. Van der Goes, Dongqing Wang, Boaz Barak, et al. 2016. "Mice with Shank3 Mutations

Associated with ASD and Schizophrenia Display Both Shared and Distinct Defects." *Neuron* 89 (1). Elsevier: 147–62. https://doi.org/10.1016/j.neuron.2015.11.023.

ANNEXES

I. Article 1: "Social Communication in Mice – Are There Optimal Cage Conditions?

Allain-Thibeault Ferhat[1,2,3], Anne-Marie Le Sourd[1,2,3], Fabrice de Chaumont[4], Jean-Christophe Olivo-Marin[4], Thomas Bourgeron[1,2,3,5], Elodie Ey[1,2,3]

1 Human Genetics and Cognitive Functions, Institut Pasteur, Paris, France,
2 CNRS UMR 3571 'Genes,
Synapses and Cognition', Institut Pasteur, Paris, France,
3 University Paris Diderot, Sorbonne Paris Cité, Human Genetics and Cognitive Functions, Paris, France,
4 Quantitative Image Analysis, URA 2582, InstitutPasteur, Paris, France,
5 FondaMental Foundation, Créteil, France

PLOS | ONE

RESEARCH ARTICLE

Social Communication in Mice – Are There Optimal Cage Conditions?

Allain-Thibeault Ferhat[1,2,3], Anne-Marie Le Sourd[1,2,3], Fabrice de Chaumont[4], Jean-Christophe Olivo-Marin[4], Thomas Bourgeron[1,2,3,5], Elodie Ey[1,2,3]*

1 Human Genetics and Cognitive Functions, Institut Pasteur, Paris, France, **2** CNRS UMR 3571 'Genes, Synapses and Cognition', Institut Pasteur, Paris, France, **3** University Paris Diderot, Sorbonne Paris Cité, Human Genetics and Cognitive Functions, Paris, France, **4** Quantitative Image Analysis, URA 2582, Institut Pasteur, Paris, France, **5** FondaMental Foundation, Créteil, France

* elodie.ey@pasteur.fr

OPEN ACCESS

Citation: Ferhat A-T, Le Sourd A-M, de Chaumont F, Olivo-Marin J-C, Bourgeron T, Ey E (2015) Social Communication in Mice – Are There Optimal Cage Conditions?. PLoS ONE 10(3): e0121802. doi:10.1371/journal.pone.0121802

Academic Editor: Georges Chapouthier, Université Pierre et Marie Curie, FRANCE

Received: October 29, 2014

Accepted: January 29, 2015

Published: March 25, 2015

Data Availability Statement: Data are available from Harvard's Dataverse database under the DOI: doi:10.7910/DVN/29079.

Funding: This work was supported by the Fondation de France; by the ANR FLEXNEURIM [ANR09BLAN034003]; by the ANR [ANR- 08-MNPS-037-01–SynGen]; by Neuron-ERANET (EUHF-AUTISM); by the Fondation Orange; by the Fondation FondaMentale; by the Fondation Bettencourt–Schueller. The research leading to these results has also received support from the Innovative Medicines Initiative Joint Undertaking under grant agreement no. 115300, resources of which are composed of

Abstract

Social communication is heavily affected in patients with neuropsychiatric disorders. Accordingly, mouse models designed to study the mechanisms leading to these disorders are tested for this phenotypic trait. Test conditions vary between different models, and the effect of these test conditions on the quantity and quality of social interactions and ultrasonic communication is unknown. The present study examines to which extent the habituation time to the test cage as well as the shape / size of the cage influence social communication in freely interacting mice. We tested 8 pairs of male mice in free dyadic social interactions, with two habituation times (20 min and 30 min) and three cage formats (rectangle, round, square). We tested the effect of these conditions on the different types of social contacts, approach-escape sequences, follow behavior, and the time each animal spent in the vision field of the other one, as well as on the emission of ultrasonic vocalizations and their contexts of emission. We provide for the first time an integrated analysis of the social interaction behavior and ultrasonic vocalizations. Surprisingly, we did not highlight any significant effect of habituation time and cage shape / size on the behavioral events examined. There was only a slight increase of social interactions with the longer habituation time in the round cage. Remarkably, we also showed that vocalizations were emitted during specific behavioral sequences especially during close contact or approach behaviors. The present study provides a protocol reliably eliciting social contacts and ultrasonic vocalizations in adult male mice. This protocol is therefore well adapted for standardized investigation of social interactions in mouse models of neuropsychiatric disorders.

Introduction

Neuropsychiatric diseases affect heavily the social life of patients. In many cases, social communication is affected and becomes atypical. The patients get isolated in their social environment, due to a lack of interest for social interactions or atypical ways of interacting. Genetic studies of neuropsychiatric diseases led to the identification of several susceptibility genes for autism

financial contribution from the European Union's Seventh Framework Program (FP7/2007-2013) and EFPIA companies' in kind contribution. The funders had no role in study design, data collection and analysis, decision to publish, or preparation of the manuscript.

Competing Interests: This study was partly funded by the EFPIA companies. There are no patents, products in development or marketed products to declare. This does not alter the authors' adherence to all the PLOS ONE policies on sharing data and materials, as detailed online in the guide for authors.

spectrum disorders (ASD) [1,2] or schizophrenia [3]. Mice remain one of the privileged mammalian animal models to study neuropsychiatric disorders, given the relative easiness of genetic modifications in this species.

Mice are social animals using olfactory, visual, tactile and acoustic signals to communicate [4–7]. Acoustic signals are one of the easiest communication signal types to measure and quantify. No convincing evidence of vocal learning in mice exists at the moment, and the contextual usage (especially in adult mice) as well as the perception levels of these acoustic signals remain unclear and need further investigations (reviewed in [8]); however, mouse ultrasonic vocalizations could still be considered as a reliable proxy to model the genetic bases of social communication deficits, excluding vocal learning processes [9,10]. Indeed, usage and structure of ultrasonic vocalizations varied with the contexts of emission and affective states (reviewed in [11]). Therefore, social interactions and vocal communication in mice can be used as proxies to examine the validity of mouse models for neuropsychiatric diseases [10,12–14].

One issue in different tests used to evaluate social interactions and communication is to stimulate free social interactions without forcing them, i.e., favoring voluntary approaches instead of incidental contacts. The aim is to get a maximum of spontaneous affiliative social interactions. For this purpose, the shape of the test cage as well as the time the tested animal is habituated to it are supposed to be determinant (Fig. 1A). A preliminary scanning of the literature of mouse models of ASD was not informative to highlight any relationship between cage size and social contact in free social interactions. Indeed, the duration of the recording had a major influence on the proportion of time spent in contact during that test. The shorter the test, the higher the percentage of time was spent in contact (S1 Table).

To avoid these influences, a standardized test was developed for the characterization of social deficits in mouse models of ASD and is now broadly used [13]. The three-chambered test has been designed in the laboratory of J. N. Crawley to evaluate the interest for a conspecific (constrained under a cup) as well as the preference for an unfamiliar conspecific over a familiar one [15]. Variables measured are usually the time spent in each compartment and the time spent sniffing the cups with the conspecifics (e.g., [16–19]). The advantage of this test is its standardization. Its major weakness is that social interactions are constrained, allowing only a very limited evaluation of social communication even for the sniffing time supposed to be the most representative of social interest [20]. This test allows the detection of social deficits; it gives however no qualitative indication about social interactions and represents only a quantitative estimation for social interest and conspecific recognition. A complementary test to counterbalance this weakness is the same-sex free dyadic interactions test [9,17,18,21,22]. Mice are left free to interact in a test cage. Both mice can be introduced together at the same time (situation not considered here), or one animal (the *occupant*, usually the tested mouse of a specific genotype) can be habituated to the test cage, while the second one is introduced later (the *new-comer*, usually from a commercially available control strain). The last situation allows to distinguish between *occupant* and *new-comer*, i.e., the emitter and the receiver of most interactions, respectively. This test does not encompass as many standardized elements as the three-chambered test since animals are freely interacting and cannot be controlled. The analysis of this type of interactions is more time-consuming and more prone to subjective interpretations. New software nevertheless allow to reduce these subjective elements in the analyses (e.g., EthoVision XT from Noldus Information Technology, The Netherlands, or Mice Profiler from Icy software [23,24]). The elicited interactions are closer to ethological behaviors, even if the motivation of the animals is usually manipulated (through social isolation and habituation to the test cage for the *occupant*, and group housing for the *new-comer*, situation considered in the present study). Data extracted allow a qualitative description of the interactions.

We designed the present study to test specifically the influence of the cage shape/size and the habituation time that vary in a controlled way. We aimed at testing whether same-sex social interactions occurring in a reasonably sized test cage with reduced habituation time are not forced in comparison with social interactions in larger cages with longer habituation time. We used the semi-automated module Mice Profiler from Icy software [23], that allows a comparison over a large panel of events, states and sequences of events within social interactions to get as much details as possible on these interactions in each condition.

We hypothesized that social interactions in the round cage will be the most different from the rectangle and the square cages. Indeed, corners in test cages appear to be very often used by animals (see Fig. 1C), and therefore their absence might lead to major modifications of the interactions. Given our previous experiments, two habituation times have been chosen close enough not to have a large influence on social interactions. The reason of this comparison is very pragmatic: the shorter habituation time will be convenient to spare some time for each animal and to improve testing efficiency.

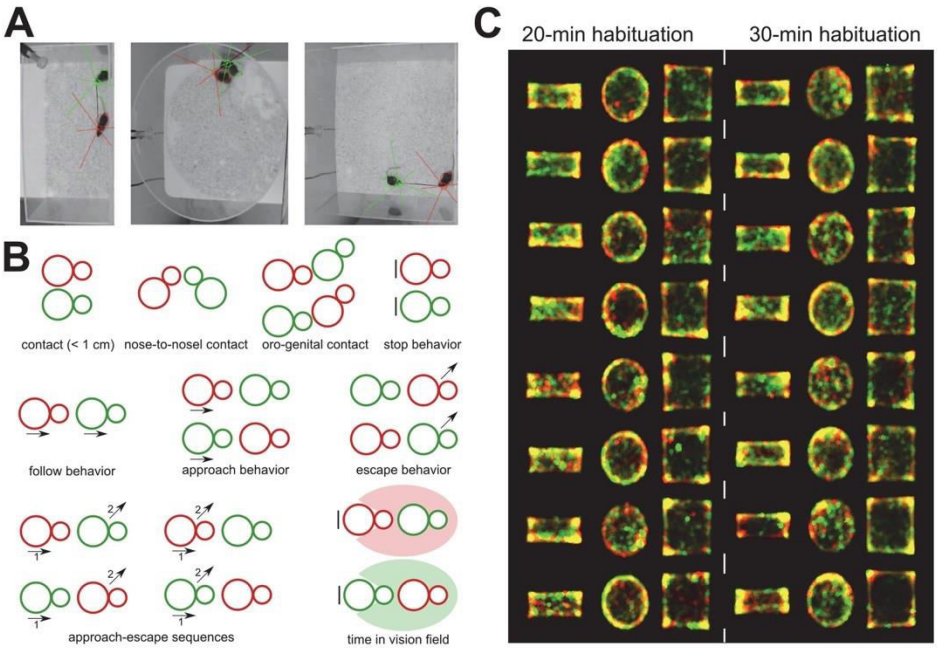

Fig 1. Methods used to examine the influence of cage shape/size on social interactions in mice. (A) Setting used to track with Mice Profiler the *occupant* male (red) and the *new-comer* male (green) during social interactions in a rectangle, a round and a square cage. (B) Behavioral events detected by Mice Profiler during social interactions between the *occupant* (red) and the *new-comer* (green). (C) Spatial occupation of the interaction cage by the *occupant* (red) and the *new-comer* (green) for the eight pairs of mice in the three cage types. Yellow traces represent the overlap of the two spatial occupations.

doi:10.1371/journal.pone.0121802.g001

Material and Methods

Upon arrival, seven-week old C57BL/6J male mice (Charles River Laboratories, L'Arabesle, France) were housed in groups of four in a colony room maintained at 23±1°C on a 12:12 hour light/dark cycle, with lights on at 8:00 AM. Mice had access to food and water *ad libitum*. One week after their arrival, the 48 males considered as *occupants* were socially isolated for 3 weeks before the experiments to increase their social motivation and reduce their aggressiveness [21,22]. The 12 mice used as *new-comers* were kept in groups of four males throughout the experiment. The experiments were conducted when animals were 11 weeks of age. Behavioral experiments were approved by the ethical committee CETEA Institut Pasteur n°89.

All experiments were conducted between 9:30 AM and 6:00 PM. Two pairs of mice were tested simultaneously with an opaque separation between the two cages. Pairs tested together underwent the same habituation time, but cage shape/size was balanced between right and left for each trial. Parameters tested in the experiment were the habituation time to the test cage (20 min or 30 min) and the shape and surface of the experimental Plexiglas cage (rectangle: 50 × 25 cm [1250 cm^2], round: 50 cm diameter [1963.5 cm^2], square: 50 cm side [2500 cm^2]; height: 30 cm in all cases). The *occupant* mouse was left 20 min or 30 min for habituation in the experimental cage (100 lx; clean sawdust bedding [9]). After this time, an unfamiliar male mouse (the *new-comer*) was introduced. The two animals were allowed to freely interact for 8 min [9,21]. Social interactions were videotaped continuously (high-resolution CamTech Super-Hi-Res video camera; 25 fps). Ultrasonic vocalizations were recorded simultaneously (sampling frequency: 250 kHz, 16-bit accuracy). Audio recording hardware (UltraSoundGate 416–200, Condenser ultrasound microphone Polaroid/CMPA) and software (Avisoft SASLab Pro Recorder) were from Avisoft Bioacoustics (Berlin, Germany). Previous experiments suggested that ultrasonic vocalizations were mainly emitted by the *occupant*; the contribution of the *new-comer* (if any) was negligible [22]. At the end of the experiment, mice were returned to their respective home cages and none of the *occupants* were used again. Between each interaction test, the experimental cage was emptied from bedding, and new fresh bedding was used.

Given the important number of conditions tested (6 conditions: habituation time: 20 min or 30 min; cage shape: rectangle, round, or square), we tested and analyzed only 8 pairs of mice per condition to limit the number of animals involved. Mice Profiler provides sufficiently detailed information to extract robust data with such a sample size for each condition (see supplementary information in [23]). The experimenters were blind of the conditions of the tested animals for data analyses (except for video scoring, where the experimenter could see the shape of the cage but was not aware of the habituation time). Social interactions were encoded on compressed video files (704 x 576 pixels; Fig. 1A). Using the plugin Mice Profiler from Icy software [23], we measured several behavioral events (Fig. 1B):

- time spent in contact (threshold: 1 cm),
- types of contacts: nose-to-nose, oro-genital from the *occupant*'s point of view and oro-genital from the *new-comer*'s point of view,
- follow behavior (i.e., the *occupant* follows the *new-comer*, both animals moving),
- approach behavior (i.e., the *occupant* approaches the *new-comer*, the *new-comer* approaches the *occupant*),
- escape behavior (i.e., the *occupant* escapes from the *new-comer*, the *new-comer* escapes from the *occupant*),

- approach-escape sequences (i.e., *occupant* approaches *new-comer* & *new-comer* escapes, *new-comer* approaches *occupant* and *occupant* escapes, *occupant* approaches *new-comer* & *occupant* escapes, *new-comer* approaches *occupant* & *new-comer* escapes),
- the time each animal spent in the vision field of the other one, both for the *occupant* and the *new-comer* when they are not moving.
- stop behavior (i.e., the *occupant* does not move, or the *new-comer* does not move).

We detected manually ultrasonic vocalizations with the software Avisoft SASLab Pro (Avisoft, Germany; FFT-length: 1024 points, 75% overlap; time resolution: 0.853 ms; frequency resolution: 293 Hz; Hamming window). We measured the latency for the first ultrasonic vocalization as well as the total number of ultrasonic vocalization and their duration.

We used non-parametric statistical tests given the non-normal distribution of the data and the small sample-sizes (8 pairs of animals per condition). We used a Kruskal-Wallis rank sum test to evaluate the effect of the cage shape for each habituation time separately. When significant differences emerged, we used Wilcoxon-Mann-Whitney U-tests to identify where the difference stemmed from in 2-by-2 comparisons. To evaluate the effect of the habituation time for each cage shape separately, we used Wilcoxon-Mann-Whitney U-tests. All statistical results are compiled in the S2 Table. All analyses were conducted with the computing and statistical software R (R Developmental Core Team 2009).

Results

We tested the effect of the cage shape/size and the habituation time on different events and sequences of events occurring in affiliative social interactions between adult male mice. Results are presented for the first 4 min of the recordings. Results for the complete 8-min recordings are overall similar to the ones for the first 4-min recordings unless otherwise specified (data not shown; S2 Table for statistical analyses).

The habituation time to the test cage influenced the time spent in contact only in the round cage, with the time spent in contact being significantly longer after 30-min habituation than after 20-min habituation (Mann-Whitney U-test: $U = 10$, $p = 0.021$; Fig. 2). There was no significant effect of the cage shape/size on the time spent in contact after 20-min habituation and after 30-min habituation (Fig. 2).

The effects of the habituation time and of the cage shape/size were also limited in the different types of contacts (Fig. 3). There was a significant effect of habituation time in the round cage only on the total duration of nose-to-nose contacts (Mann-Whitney U-test: $U = 6$, $p = 0.005$; Fig. 3A). This contact was significantly longer after 30-min habituation than after 20-min habituation in the round cage. There was no significant difference due to habituation time in the total duration of the *occupant* sniffing the ano-genital region of the *new-comer* and in the total duration of the *new-comer* sniffing the ano-genital region of the *occupant* (Fig. 3B and 3C). Concerning cage shape/size, we did not find any significant effect neither in the 20-min habituation condition nor in the 30-min habituation condition on the total time spent in nose-to-nose contacts (Fig. 3A), on the total time spent by the *occupant* sniffing the ano-genital region of the *new-comer* (Fig. 3B), and on the total time spent by the *new-comer* sniffing the ano-genital region of the *occupant* (Fig. 3C).

The total duration of the *occupant* following the *new-comer* did not differ significantly according to the cage shape and the habituation time (all p-values >0.05; Fig. 4A). No significant effect of habituation time and cage shape/size had been found on the duration of the stop behaviors (Fig. 4B and 4C). No significant differences between the 20-min and the 30-min habituation conditions had been found in any cage shape/size for the number of occurrences of the

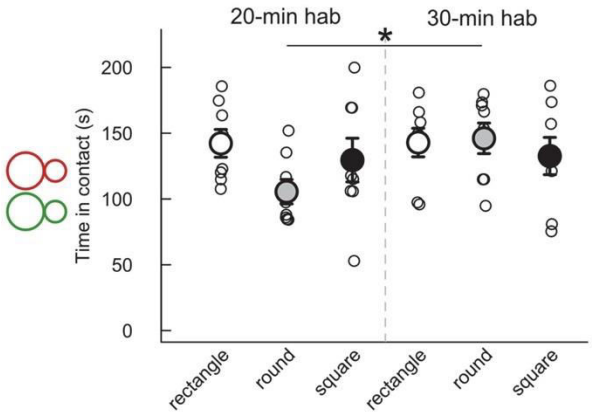

Fig 2. Limited influence of habituation time and cage shape/size on the time spent in contact. Time in contact (< 1 cm) was measured during the first 4 min of interaction after 20 min (left panel) or 30 min (right panel) habituation time in three cage types. (Wilcoxon-Mann-Whitney U-tests: n = 8 pairs of mice per condition; *: p<0.05; data are presented as mean +/- sem).

doi:10.1371/journal.pone.0121802.g002

occupant approaching the *new comer* (Fig. 5A), the number of occurrences of the *new-comer* approaching the *occupant* (Fig. 5B), and the number of occurrences of the *new-comer* escaping from the *occupant* (Fig. 5D). The number of occurrences of the *occupant* escaping from the *new-comer* had been significantly higher after 30-min habituation than after 20-min habituation in the round cage (Mann-Whitney U-test: U = 8 p = 0.013). The number of occurrences of the *occupant* escaping from the *new-comer* had also been significantly lower after 30-min habituation than after 20-min habituation in the square cage (Mann-Whitney U-test: U = 55.5 p = 0.016; Fig. 5C).

The effects of the cage shape/size were not significant in both the 20-min and the 30-min habituation conditions on the number of occurrences of the *occupant* approaching the *new-comer* (Fig. 5A), the number of occurrences of the *new-comer* approaching the *occupant* (Fig. 5B), and the number of occurrences of the *new-comer* escaping from the *occupant* (Fig. 5D). There had been only a significant effect of the cage shape/size in the 30-min habituation condition on the number of occurrences of the *occupant* escaping from the *new-comer* (Kruskal-Wallis test: Df = 2, X = 11.67, p = 0.003; Fig. 5D). Indeed, the *occupant* escaped from the *new-comer* significantly more frequently in the round cage in comparison with the rectangle cage (Mann-Whitney U-test: U = 12, p = 0.040) and in comparison with the square cage (Mann-Whitney U-test: U = 60.5, p = 0.003) after 30-min habituation. The *occupant* also escaped from the *new-comer* significantly more frequently in the rectangle cage in comparison with the square cage after 30-min habituation (Mann-Whitney U-test: U = 51.5, p = 0.045). Results for the duration of the same behavioral events were similar (data not shown).

Very limited influence of the cage shape/size and habituation time had been found on sequences of approach-escape behaviors (Fig. 6). There had been no significant effect of the habituation time on the frequency of occurrence (Fig. 6) and the duration (data not shown) of the three following types of sequences: "*occupant* approaches *new-comer* & *new-comer* escapes" (Fig. 6A), "*new-comer* approaches *occupant* and *occupant* escapes" (Fig. 6B), and "*new-comer* approaches *occupant* & *new-comer* escapes" (Fig. 6D). Only a significant effect of habituation

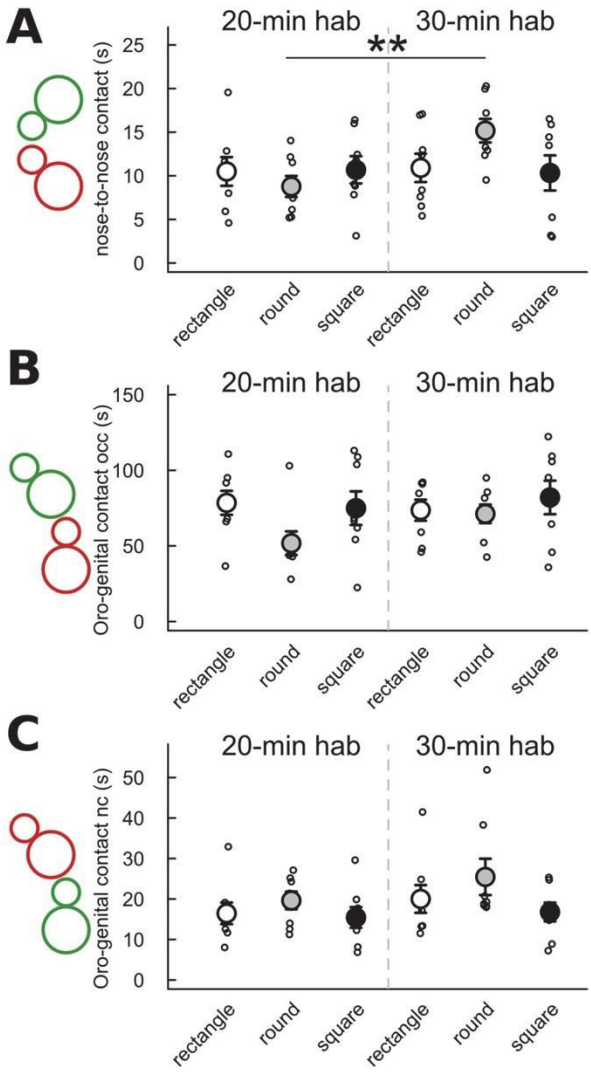

Fig 3. Limited effect of habituation time and cage shape/size on the duration of different types of contact. Contact (< 1 cm) was measured during the first 4 min of interaction after 20 min (left panel) or 30 min (right panel) habituation time in three cage types. (A) Time spent in mouth-to-mouth contact. (B) Time spent by the *occupant* (occ) sniffing the ano-genital region of the *new-comer*. (C) Time spent by the *new-comer* (nc) sniffing the ano-genital region of the *occupant*. (Wilcoxon-Mann-Whitney U-tests: n = 8 pairs of mice per condition; *: $p<0.05$, **: $p<0.01$; data are presented as mean +/- sem).

doi:10.1371/journal.pone.0121802.g003

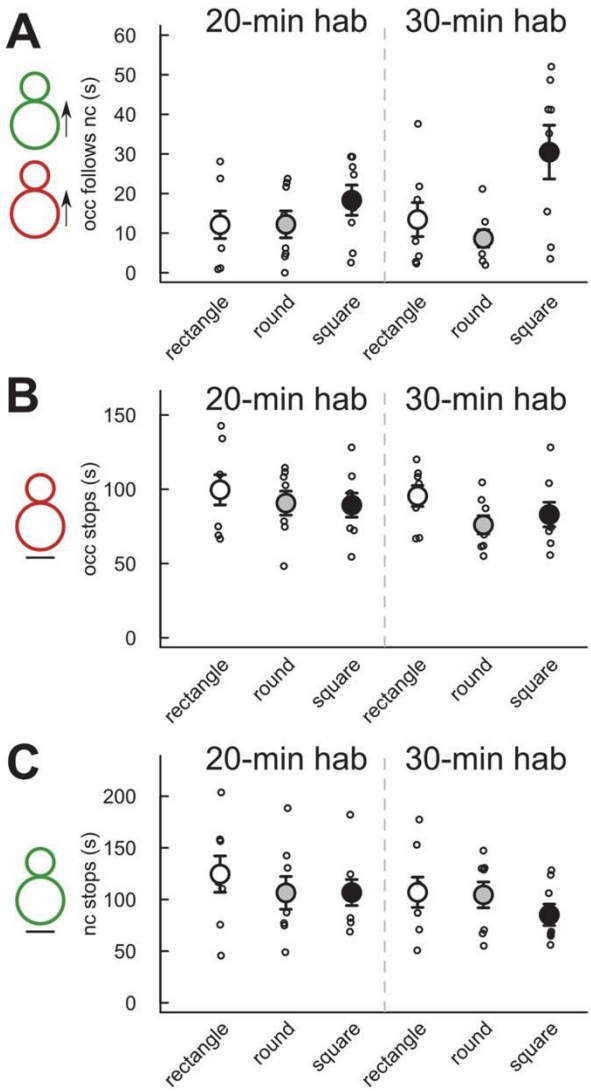

Fig 4. No significant effect of habituation time and cage shape/size on the duration of the follow and stop behaviors. Measures were taken after 20 min (left panel) or 30 min (right panel) habituation time in three cage types. (A) Time spent by the *occupant* (occ) following the *new-comer* (nc) in the first 4 min of interaction. (B) Time spent by the *occupant* (occ) not moving during the first 4 min of interaction. (C) Time spent by the *new-comer* (nc) not moving during the first 4 min of interaction. (Wilcoxon-Mann-Whitney U-tests: n = 8 pairs of mice per condition; data are presented as mean +/- sem).

doi:10.1371/journal.pone.0121802.g004

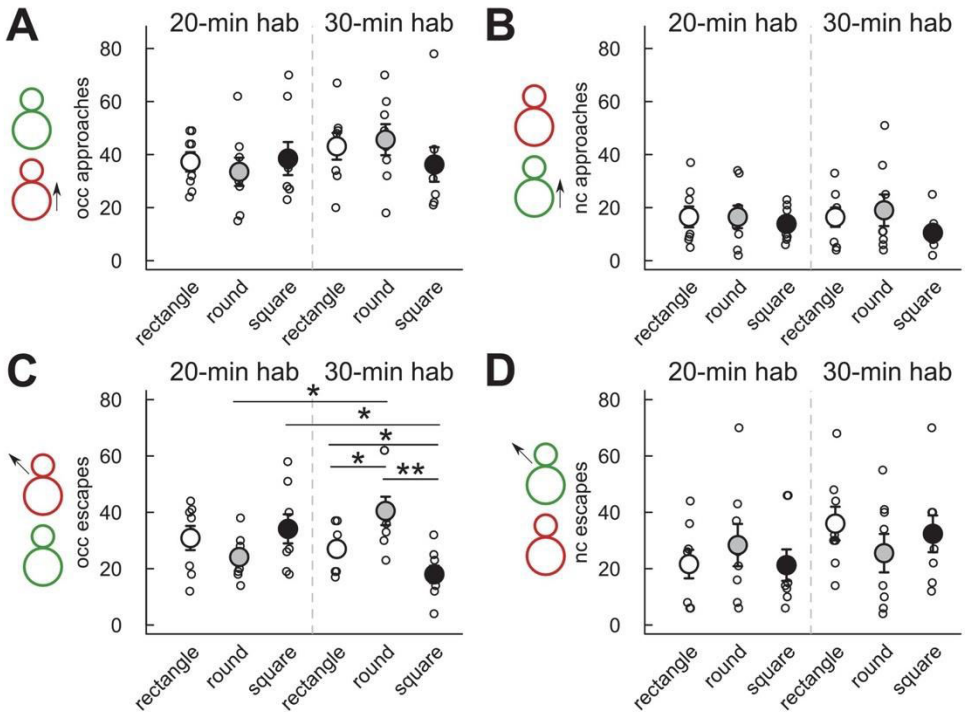

Fig 5. Limited effect of habituation time and cage shape/size on the number of approach or escape behaviors. Measures were taken during the first 4 min of interaction after 20 min (left panel) or 30 min (right panel) habituation time in three cage types. (A) Number of occurrences of the *occupant* (occ) approaching the *new-comer*. (B) Number of occurrences of the *new-comer* (nc) approaching the *occupant*. (C) Number of occurrences of the *occupant* (occ) escaping from the *new-comer*. (D) Number of occurrences of the *new-comer* (nc) escaping from the *occupant*. (Wilcoxon-Mann-Whitney U-tests: n = 8 pairs of mice per condition; *: $p<0.05$, **: $p<0.01$; data are presented as mean +/- sem).

doi:10.1371/journal.pone.0121802.g005

time had been found for the sequence "*occupant* approaches *new-comer* & *occupant* escapes" in the square cage (Fig. 6C). Indeed, the sequence "*occupant* approaches *new-comer* & *occupant* escapes" occurred significantly less frequently in the 30-min habituation condition than in the 20-min habituation condition in the square cage (Mann-Whitney U-test: U = 59.5, p = 0.004). No significant differences in the frequency of occurrences (Fig. 6) and in the duration (data not shown) of the four types of sequences emerged between the cage shapes in the 20-min habituation condition. There had been nevertheless a significant effect of cage shape/size in the 30-min habituation condition for the sequence "*occupant* approaches *new-comer* & *occupant* escapes" (Kruskal-Wallis test: Df = 2, X = 6.33, p = 0.042), which occurred significantly more frequently in the round cage in comparison with the square cage (Mann-Whitney U-test: U = 54, p = 0.023; Fig. 6C).

We also examined the effect of cage shape/size and habituation time on the time spent by the animals in the vision field of each other when the animals are not moving. The *occupant* kept the *new-comer* in its vision field significantly longer after 20-min habituation than after 30-min habituation in the round cage only (Mann-Whitney U-test: U = 51, p = 0.049; Fig. 7A).

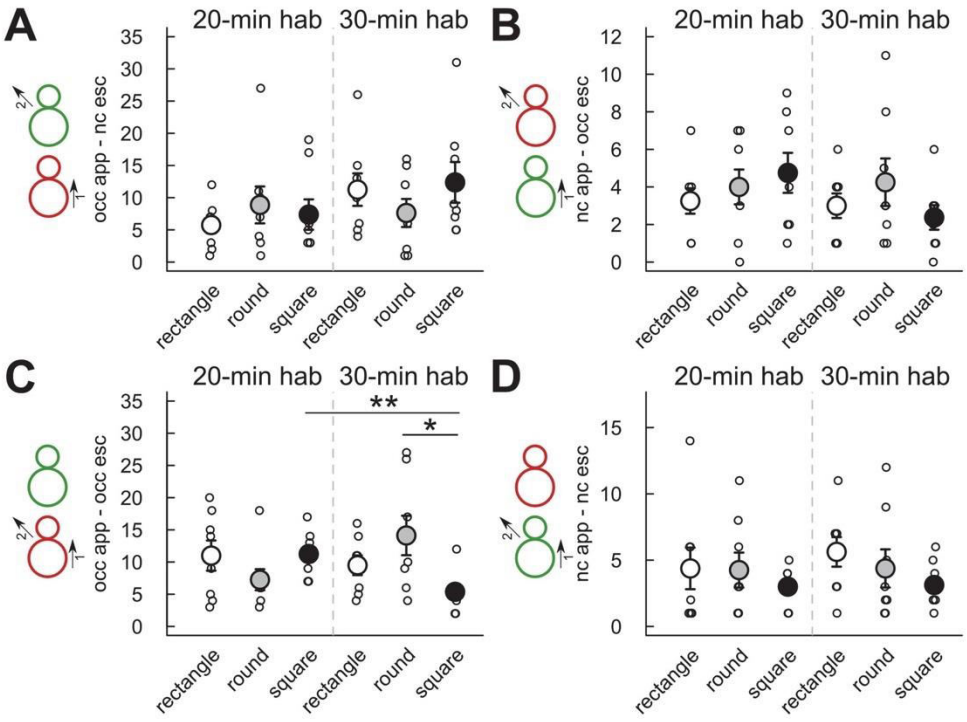

Fig 6. Limited effect of habituation time and cage shape/size on the number of occurrences of different types of approach-escape sequences. Measures were taken during the first 4 min of interaction after 20 min (left panel) or 30 min (right panel) habituation time in three cage types. (A) Number of occurrences of the sequence "*occupant* approaches *new-comer* & *new-comer* escapes". (B) Number of occurrences of the sequence "*new-comer* approaches *occupant* and *occupant* escapes". (C) Number of occurrences of the sequence "*occupant* approaches *new-comer* & *occupant* escapes". (D) Number of occurrences of the sequence "*new-comer* approaches *occupant* & *new-comer* escapes". (Wilcoxon-Mann-Whitney U-tests: n = 8 pairs of mice per condition; *: $p<0.05$, **: $p<0.01$; data are presented as mean +/- sem).

doi:10.1371/journal.pone.0121802.g006

No significant effect of habituation time had been found on the time the *new-comer* kept the *occupant* in its vision field (Fig. 7B). The cage shape/size did not appear to have a significant influence on the time spent by each animal in the vision field of the other one during stop situations for both the 20-min habituation condition and the 30-min habituation condition during the first 4 min of interactions (Fig. 7). In contrast, over the 8 min of interactions, there was a significant effect of cage shape/size on both the time the *occupant* kept the *new-comer* in its vision field (Kruskal-Wallis test: Df = 2, X = 8.14, p = 0.017) and the time the *new-comer* kept the *occupant* in its vision field (Kruskal-Wallis test: Df = 2, X = 7.27, p = 0.026). Both measures were more elevated in the round cage in comparison with the rectangle cage (Mann-Whitney U-tests: U = 5, p = 0.003; U = 11, p = 0.028; data not shown).

Finally, we tested the effect of the cage shape/size and the habituation time on the latency for the first ultrasonic vocalization, the number of ultrasonic vocalizations and the mean duration of the calls. No significant differences emerged between the habituation time conditions for each cage shape and between cage shapes for each habituation time condition for the

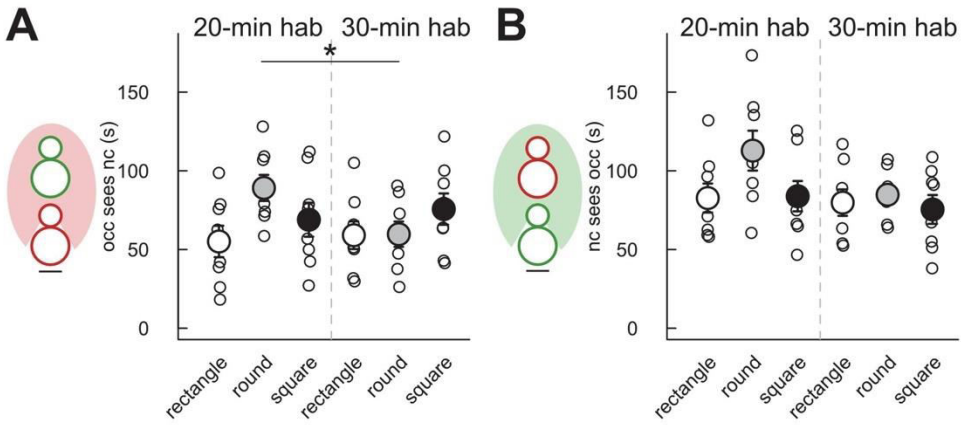

Fig 7. Limited effect of habituation time and cage shape/size on the time spent by one individual in the vision field of the other one. Measures were taken during the first 4 min of interaction after 20 min (left panel) or 30 min (right panel) habituation time in three cage types. (A) Time spent by the *new-comer* in the vision field of the *occupant*. (B) Time spent by the *occupant* in the vision field of the *new-comer*. (Wilcoxon-Mann-Whitney U-tests: n = 8 pairs of mice per condition; *: $p<0.05$; data are presented as mean +/- sem).

doi:10.1371/journal.pone.0121802.g007

latency of the first ultrasonic vocalization (Fig. 8A), the number of ultrasonic vocalizations emitted per minute (Fig. 8B) and the mean duration of ultrasonic vocalizations (Fig. 8C).

The behavioral events during which ultrasonic vocalizations were recorded did not vary significantly with habituation time or cage shape/size (Fig. 9). In all conditions, between 30% and 50% of ultrasonic vocalizations were emitted during social contacts. Many vocalizations were recorded when the *occupant* was behind the *new-comer*, and much fewer in the reverse situation. This would explain why very few vocalizations were recorded during nose-to-nose contacts and when the *new-comer* was sniffing the ano-genital region of the *occupant*, while many vocalizations were recorded when the *occupant* was sniffing the ano-genital region of the *new-comer*. For vocalizations not emitted during contact, a high proportion of vocalizations recorded when the *occupant* was approaching the *new-comer* (with either the *new-comer* or the *occupant* escaping). In contrast, much fewer vocalizations were recorded when the *new-comer* was approaching the *occupant* (with either the *occupant* escaping, or the *new-comer* escaping).

Discussion

Using different settings for cage shape/size and habituation time, we ascertained mouse social behaviors and sequences of social behaviors, as well as ultrasonic vocalizations. We found very little difference caused by the cage shape/size in these features (Fig. 10). Only the habituation time had some minor effect on social behaviors most often in the round cage, with the longer habituation time favoring social interactions.

Previous studies only analyzed the influence of housing conditions on the behavior of the animals (e.g., individually ventilated cages vs. filter-top cages [25], transparent walls vs. cages without view on the room and other cages [26]). In our study, we examined the direct influence of the cage shape/size during a social interaction test. We did not identify major effects of the cage shape/size and the habituation time on the several variables describing social interactions. The present study therefore suggests that the use of a 50 x 25 cm rectangular cage with a 20 min habituation time does not force social interactions, i.e., favor voluntary social approaches.

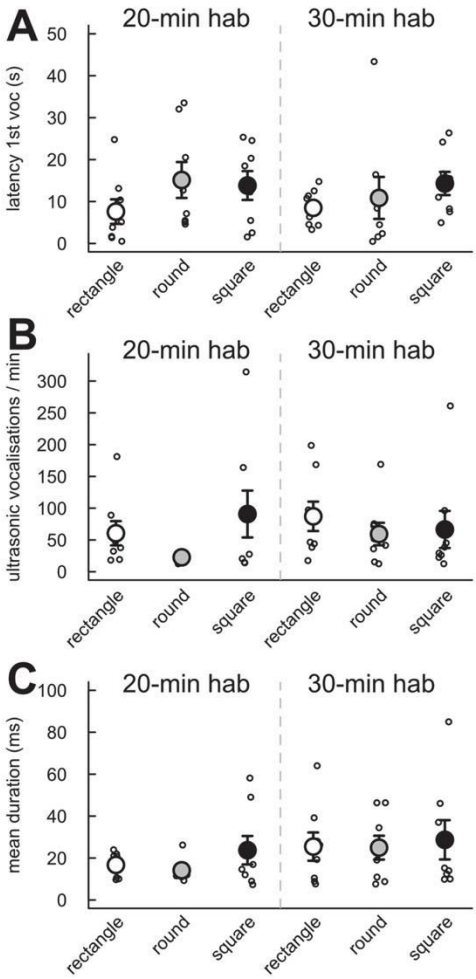

Fig 8. No significant effect of habituation time and cage shape/size on the vocal behavior of the pairs of interacting mice. Measures were taken during the first 4 min of interaction after 20 min (left panel) or 30 min (right panel) habituation time in three cage types. (A) Latency for the first ultrasonic vocalization. (B) Number of ultrasonic vocalizations emitted by minute. (C) Mean duration of ultrasonic vocalizations. (Wilcoxon-Mann-Whitney U-tests: n = 8 pairs of mice per condition; data are presented as mean +/- sem).

doi:10.1371/journal.pone.0121802.g008

This forcing of social interactions would come from a too small space. In such conditions, mice would come in contact incidentally much more often than in larger spaces during the exploration of the cage. What is still unknown and would need further investigation is to what extent interactions would be forced in a smaller space. Further study should also compare the quantity

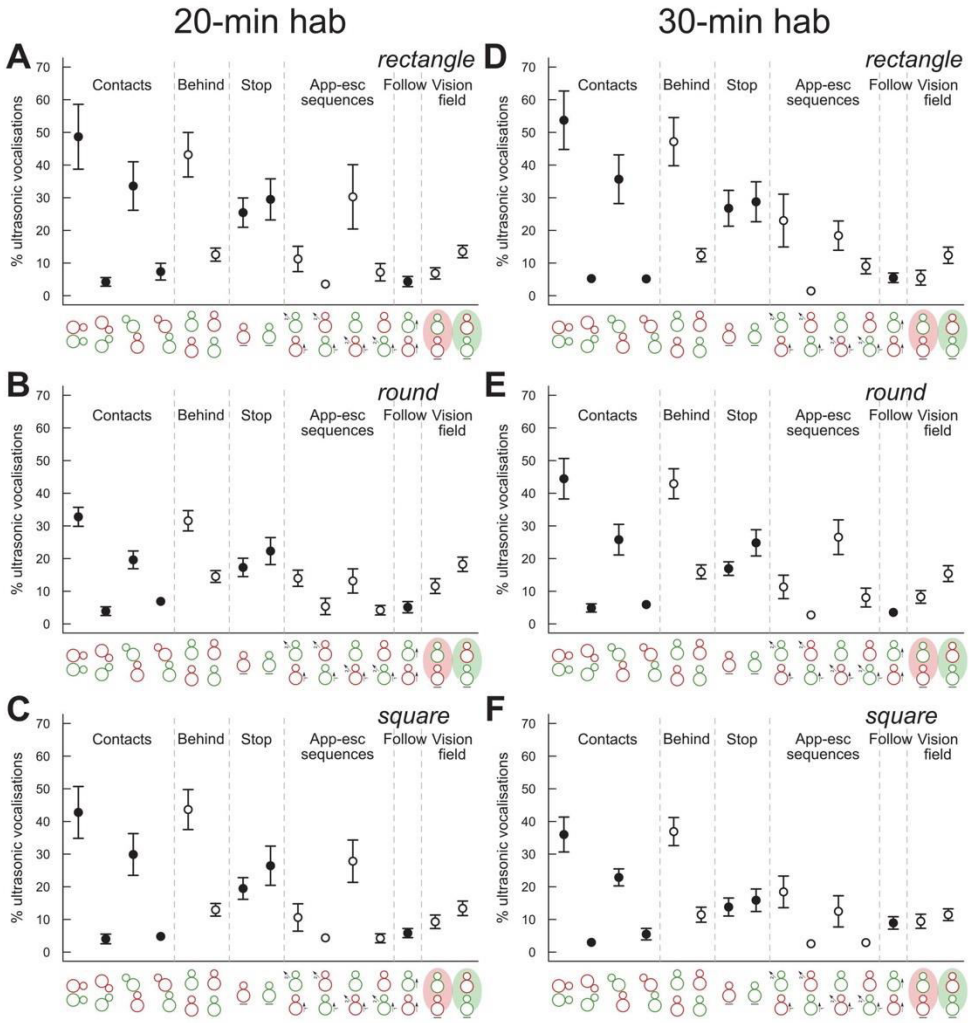

Fig 9. Contexts of ultrasonic vocalization emission during social interactions. Proportion of ultrasonic vocalizations emitted during social events during the first 4 min of interactions (A) after 20 min habituation in the rectangular cage, (B) after 20 min habituation in the round cage, (C) after 20 min habituation in the square cage, (D) after 30 min habituation in the rectangular cage, (E) after 30 min habituation in the round cage, (F) after 30 min habituation in the square cage. Social events are presented in the following order: contact < 1 cm, nose-to-nose contact, *occupant* sniffing ano-genital region of *new-comer*, *occupant* sniffing ano-genital region of *new-comer*, *occupant* behind *new-comer*, *new-comer* behind *occupant*, *occupant* not moving, *new-comer* not moving, *occupant* approaches *new-comer* & *new-comer* escapes, *new-comer* approaches *occupant* and *occupant* escapes, *occupant* approaches *new-comer* & *occupant* escapes, *new-comer* approaches *occupant* & *new-comer* escapes, *occupant* following *new-comer*, *new-comer* in the vision field of *occupant*, *occupant* in the vision field of *new-comer* (n = 8 pairs of mice per condition; data are presented as mean +/- sem).

doi:10.1371/journal.pone.0121802.g009

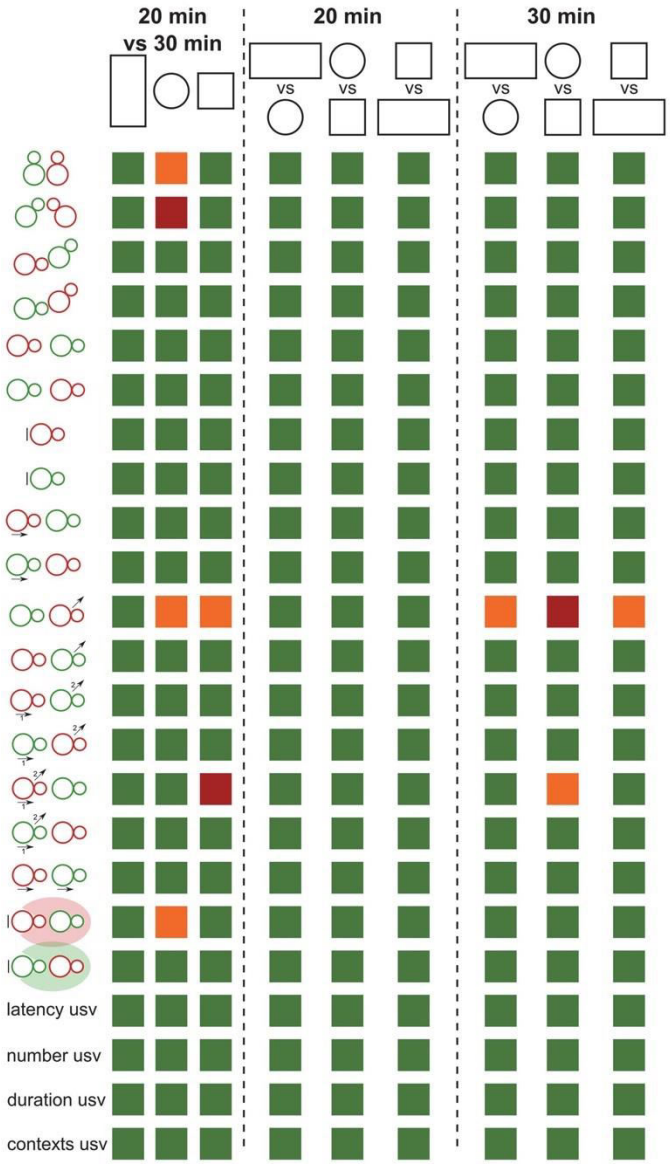

Fig 10. Limited effects of habituation time and cage shape/size on behavioral events during adult male mouse social interactions. Most comparisons were non-significant (green boxes: $p > 0.05$), while only a few effects of habituation time and cage shape/size were detected (orange boxes: $p < 0.05$, red boxes: $p < 0.01$).

doi:10.1371/journal.pone.0121802.g010

and quality of spontaneous social interactions with and without habituation to the test cage for the *occupant*.

We would have expected major differences in the round cage in comparison with the square and the rectangle ones given the absence of corners. Indeed corners are used very often (Fig. 1C) and might represent stop zones, where animals can get stuck. We thought this would lead to major differences for instance in approach/escape sequences and in stop behaviors. Such major differences were not observed. Only a slight increase of escape behaviors of the *occupant* from the *new-comer* has been found in the round cage in comparison with other cage types. This suggests that corners in test cages are not leading to major perturbations of social sequences in mice. They are not used as preferred places for stop behaviors, and their absence does not favor follow behavior or impair the different types of social investigations (nose-to-nose, ano-genital sniffing). In contrast, the habituation time had some effect on social interactions mostly in the round cage. This might suggest that the lack of corners renders it more difficult to the animals (used to cages with corners throughout their life) to habituate to such environments. The exploratory phase might last longer in round cages than in cages with corners, delaying the social investigation.

The Mice Profiler module of Icy software from de Chaumont and colleagues [23] was originally tested on mice interacting with a similar protocol as ours, with a rectangular cage and 30 min habituation to the test cage. We compared our data within the rectangular cage and after 30 min habituation to these data for C57Bl/6J male mice. The duration of the follow behavior was slightly shorter in our experiment in comparison with the de Chaumont and colleagues' study both during the first 4 min of interaction and during the 8 min of interaction [23]. The duration of nose-to-nose contact was lower in our study in comparison with the de Chaumont study, while the total duration of oro-genital sniffing (from both the *occupant* and the *new-comer*) was similar between the two studies during the first 4 min of interaction. Overall, most discrepancies were found for the nose-to-nose contact, while data for other behaviors were similar. The fact that mice from the present study were isolated for 3 weeks and those from the de Chaumont study for 4 weeks might explain some of the differences between the durations of the follow behavior and of the types of contacts.

Ultrasonic vocalizations were recorded in all conditions, confirming that two interacting males vocalize together and do not show overt aggressive behaviors during 4 min (and even 8 min) of interactions if the *occupant* has been isolated for 3 weeks before the test. To what extent social communication is affected by this long period of social isolation remains to be quantified, given the high stress level probably generated by social isolation (that needs to be much shorter or absent in juvenile[27] and in female [18] mice). Spontaneous ultrasonic vocalizations of same-sex groups of males are very rare and usually very simple and short in structure (E. Ey, unpublished data). The present protocol should then be considered as an artificial but reliable way (and not as an ethological way) to evoke ultrasonic vocalizations and affiliative interactions in males, which might be useful in the behavioral characterization of mouse models of neuropsychiatric disorders. It is probably the craving for social contacts that triggers these complex ultrasonic vocalizations. Moreover, a similar amount of ultrasonic vocalizations was recorded in the three cage types. This absence of difference in the amount of vocalizations detected suggests that even in the largest cages (square and round cages), where the microphone has to cover a large surface, the level of detection of ultrasonic vocalizations is not different from the smallest cage (rectangle cage). This indication of the recording surface of the ultrasonic microphone used will be helpful to design new recording cages for 24 h continuous recordings in complex environments, including more than two individuals. Such environments will have a more ethological design, more similar to burrows and tunnels, to allow a complete expression of the natural behavioral repertoire of mice [28]. Continuous recordings using

synchronized advanced technologies (RFID tracking, triangulation for audio recordings, 3D video recordings) will allow to gather data about spontaneous social communication in groups of mice, during daylight (presumably very reduced) and during nighttime (presumably much more complex than in the artificial classical laboratory settings). Spontaneous social interactions might substantially differ in quality and temporal distribution from the ones evoked in artificial laboratory conditions as in the present study.

For the first time, we manage to correlate the emission of ultrasonic vocalizations and the detailed social events extracted from Mice Profiler. We confirmed that ultrasonic vocalizations are not emitted randomly and therefore provide further support for their role in social communication. At the moment, it is still not possible to identify clearly the emitter. The fact that ultrasonic vocalizations are rarely emitted during nose-to-nose contacts could justify using triangulation to localize the emitter since the noses of the two animals are usually not close to one another during ultrasonic vocalization emission.

Ultrasonic vocalizations are supposedly mostly emitted by the *occupant* during social contacts (especially ano-genital sniffing) and during approach behaviors. The present study also suggested an effect of the emission of ultrasonic vocalizations on the outcome of an approach. The escape behavior of the *new-comer* or the *occupant* was often correlated with the emission of ultrasonic vocalizations. When the *occupant* approaches the *new-comer*, the later is often less likely to escape and end the contact if more vocalizations were emitted. The correlation between the ultrasonic vocalizations emitted and the type of social interactions described in this study is the first step towards a better understanding of the relationship between the types of vocalizations [29] and the relative positions of mice during social interactions. Future studies should concentrate on identifying call types that are specific to social events and sequences described here. In addition, new social experiments with long term continuous recordings of spontaneous interactions and playback studies should complement these aspects on the functions of these ultrasonic vocalizations, and more specifically on the identification of any sequences of ultrasonic vocalizations triggering specific behaviors in the receiver.

Overall, the present study suggest that a rectangular cage (50 x 25 cm) with 20-min habituation to the test cage is sufficient to elicit non-aggressive interactions between an isolated "*occupant*" adult male and a socially-housed "*new-comer*" adult male. A large amount of ultrasonic vocalizations can even be recorded in these conditions. Such a protocol will be useful in a better evaluation of social communication deficits in mouse models of neuropsychiatric disorders.

Supporting Information

S1 Table. Non-exhaustive review of the literature on free social interactions in mouse models of autism spectrum disorders. Information about the habituation time, the cage shape, the duration of the test, the background of the wild-type strain studied is compiled. Selected articles: [13,16–19,22,30–49].
(PDF)

S2 Table. Statistical tests conducted for all variables describing social interactions and vocal behaviors. Comparisons were made to identify the effect of habituation time and cage shape/size.
(PDF)

Acknowledgments

We thank Guillaume Dumas for valuable comments on the manuscript. We are also grateful to the two reviewers whose comments noticeably improved the manuscript.

Author Contributions

Conceived and designed the experiments: EE TB. Performed the experiments: EE AMLS. Analyzed the data: ATF AMLS FDC JCOM TB EE. Contributed reagents/materials/analysis tools: ATF AMLS FDC JCOM TB EE. Wrote the paper: ATF AMLS FDC JCOM TB EE.

References

1. Huguet G, Ey E, Bourgeron T. The Genetic Landscapes of Autism Spectrum Disorders. In: Chakravarti A, Green E, editors. Annual Review of Genomics and Human Genetics, Vol 14. 2013. pp. 191–213.
2. Jeste SS, Geschwind DH. Disentangling the heterogeneity of autism spectrum disorder through genetic findings. Nat Rev Neurol. 2014; 10: 74–81. doi: 10.1038/nrneurol.2013.278 PMID: 24468882
3. Ripke S, Neale BM, Corvin A, Walters JTR, Farh K-H, Holmans PA, et al. Biological insights from 108 schizophrenia-associated genetic loci. Nature. 2014; 511: 421–427. doi: 10.1038/nature13595 PMID: 25056061
4. Palanza P, Della Seta D, Ferrari PF, Parmigiani S. Female competition in wild house mice depends upon timing of female/male settlement and kinship between females. Anim Behav. 2005; 69: 1259–1271. doi: 10.1016/j.anbehav.2004.09.014
5. Brennan PA, Kendrick KM. Mammalian social odours: attraction and individual recognition. Philos Trans R Soc B-Biol Sci. 2006; 361: 2061–2078. doi: 10.1098/rstb.2006.1931 PMID: 17118924
6. Latham N, Mason G. From house mouse to mouse house: the behavioural biology of free-living Mus musculus and its implications in the laboratory. Appl Anim Behav Sci. 2004; 86: 261–289. doi: 10.1016/j.applamin.2004.02.006
7. Portfors CV. Types and functions of ultrasonic vocalizations in laboratory rats and mice. J Am Assoc Lab Anim Sci. 2007; 46: 28–34. PMID: 17203913
8. Portfors CV, Perkel DJ. The role of ultrasonic vocalizations in mouse communication. Curr Opin Neurobiol. 2014; 28: 115–120. doi: 10.1016/j.conb.2014.07.002 PMID: 25062471
9. Bourgeron T, Jamain S, Granon S. Animal Models of Autism—Proposed Behavioral Paradigms and Biological Studies. In: Fisch GS, Flint J, editors. Contemporary Clinical Neuroscience: Transgenic and Knockout Models of Neuropsychiatric Disorders. Totowa: Humana Press Inc.; 2006. pp. 151–174.
10. Scattoni ML, Crawley J, Ricceri L. Ultrasonic vocalizations: A tool for behavioural phenotyping of mouse models of neurodevelopmental disorders. Neurosci Biobehav Rev. 2009; 33: 508–515. doi: 10.1016/j.neubiorev.2008.08.003 PMID: 18771687
11. Lahvis GP, Alleva E, Scattoni ML. Translating mouse vocalizations: prosody and frequency modulation1. Genes Brain Behav. 2011; 10: 4–16. doi: 10.1111/j.1601-183X.2010.00603.x PMID: 20497235
12. O'Tuathaigh CMP, Moran PM, Waddington JL. Genetic models of schizophrenia and related psychotic disorders: progress and pitfalls across the methodological "minefield." Cell Tissue Res. 2013; 354: 247–257. doi: 10.1007/s00441-013-1652-4 PMID: 23715722
13. Silverman JL, Yang M, Lord C, Crawley JN. Behavioural phenotyping assays for mouse models of autism. Nat Rev Neurosci. 2010; 11: 490–502. doi: 10.1038/nrn2851 PMID: 20559336
14. Michetti C, Ricceri L, Scattoni ML. Modelling social communication deficits in mouse models of autism. Autism. 2012; S1:007. doi: 10.4172/2165-7890.S1-007
15. Nadler JJ, Moy SS, Dold G, Simmons N, Perez A, Young NB, et al. Automated apparatus for quantitation of social approach behaviors in mice. Genes Brain Behav. 2004; 3: 303–314. doi: 10.1111/j.1601-183X.2004.00071.x PMID: 15344923
16. McFarlane HG, Kusek GK, Yang M, Phoenix JL, Bolivar VJ, Crawley JN. Autism-like behavioral phenotypes in BTBR T+tf/J mice. Genes Brain Behav. 2008; 7: 152–163. doi: 10.1111/j.1601-183X.2007.00330.x PMID: 17559418
17. Ey E, Yang M, Katz AM, Woldeyohannes L, Silverman JL, Leblond CS, et al. Absence of deficits in social behaviors and ultrasonic vocalizations in later generations of mice lacking neuroligin4. Genes Brain Behav. 2012; 11: 928–941. doi: 10.1111/j.1601-183X.2012.00849.x
18. Schmeisser MJ, Ey E, Wegener S, Bockmann J, Stempel AV, Kuebler A, et al. Autistic-like behaviours and hyperactivity in mice lacking ProSAP1/Shank2. Nature. 2012; 486: 256–+. doi: 10.1038/nature11015 PMID: 22699619
19. Peça J, Feliciano C, Ting JT, Wang W, Wells MF, Venkatraman TN, et al. Shank3 mutant mice display autistic-like behaviours and striatal dysfunction. Nature. 2011; 472: 437–442. doi: 10.1038/nature09965 PMID: 21423165

20. Fairless AH, Shah RY, Guthrie AJ, Li H, Brodkin ES. Deconstructing Sociability, An Autism-Relevant Phenotype, in Mouse Models. Anat Rec Adv Integr Anat Evol Biol. 2011; 294: 1713–1725. doi: 10.1002/ar.21318 PMID: 21905241

21. Granon S, Faure P, Changeux J-P. Executive and social behaviors under nicotinic receptor regulation. Proc Natl Acad Sci. 2003; 100: 9596–9601. doi: 10.1073/pnas.1533498100 PMID: 12876201

22. Chabout J, Serreau P, Ey E, Bellier L, Aubin T, Bourgeron T, et al. Adult Male Mice Emit Context-Specific Ultrasonic Vocalizations That Are Modulated by Prior Isolation or Group Rearing Environment. Plos One. 2012; 7: e29401. doi: 10.1371/journal.pone.0029401 PMID: 22238608

23. De Chaumont F, Coura RD-S, Serreau P, Cressant A, Chabout J, Granon S, et al. Computerized video analysis of social interactions in mice. Nat Methods. 2012; 9: 410–U134. doi: 10.1038/nmeth.1924 PMID: 22388289

24. De Chaumont F, Dallongeville S, Chenouard N, Hervé N, Pop S, Provoost T, et al. Icy: an open bioimage informatics platform for extended reproducible research. Nat Methods. 2012; 9: 690–696. doi: 10.1038/nmeth.2075 PMID: 22743774

25. Logge W, Kingham J, Karl T. Behavioural consequences of IVC cages on male and female C57BL/6J mice. Neuroscience. 2013; 237: 285–293. doi: 10.1016/j.neuroscience.2013.02.012 PMID: 23415791

26. Harris AP, D'Eath RB, Healy SD. A cage without a view increases stress and impairs cognitive performance in rats. Anim Welf. 2010; 19: 235–241.

27. Panksepp JB, Jochman KA, Kim JU, Koy JJ, Wilson ED, Chen Q, et al. Affiliative Behavior, Ultrasonic Communication and Social Reward Are Influenced by Genetic Variation in Adolescent Mice. Plos One. 2007; 2. doi: 10.1371/journal.pone.0000351

28. Blanchard RJ, Blanchard DC. Bringing natural behaviors into the laboratory: a tribute to Paul MacLean. Physiol Behav. 2003; 79: 515–524. doi: 10.1016/S0031-9384(03)00157-4 PMID: 12954446

29. Ey E, Torquet N, Le Sourd A-M, Leblond CS, Boeckers TM, Faure P, et al. The Autism ProSAP1/Shank2 mouse model displays quantitative and structural abnormalities in ultrasonic vocalisations. Behav Brain Res. 2013; 256: 677–689. doi: 10.1016/j.bbr.2013.08.031 PMID: 23994547

30. Pearson BL, Defensor EB, Pobbe RLH, Yamamoto LHL, Bolivar VJ, Blanchard DC, et al. Mecp2 Truncation in Male Mice Promotes Affiliative Social Behavior. Behav Genet. 2012; 42: 299–312. doi: 10.1007/s10519-011-9501-2 PMID: 21909962

31. Harper KM, Hiramoto T, Tanigaki K, Kang G, Suzuki G, Trimble W, et al. Alterations of social interaction through genetic and environmental manipulation of the 22q11.2 gene Sept5 in the mouse brain. Hum Mol Genet. 2012; 21: 3489–3499. doi: 10.1093/hmg/dds180 PMID: 22589251

32. Hammerschmidt K, Radyushkin K, Ehrenreich H, Fischer J. The Structure and Usage of Female and Male Mouse Ultrasonic Vocalizations Reveal only Minor Differences. Plos One. 2012; 7. doi: 10.1371/journal.pone.0041133

33. Goorden SMI, van Woerden GM, van der Weerd L, Cheadle JP, Elgersma Y. Cognitive deficits in Tsc1 +/– mice in the absence of cerebral lesions and seizures. Ann Neurol. 2007; 62: 648–655. doi: 10.1002/ana.21317 PMID: 18067135

34. Silverman JL, Smith DG, Rizzo SJS, Karras MN, Turner SM, Tolu SS, et al. Negative Allosteric Modulation of the mGluR5 Receptor Reduces Repetitive Behaviors and Rescues Social Deficits in Mouse Models of Autism. Sci Transl Med. 2012; 4: 131ra51–131ra51. doi: 10.1126/scitranslmed.3003501

35. Radyushkin K, Hammerschmidt K, Boretius S, Varoqueaux F, El-Kordi A, Ronnenberg A, et al. Neuroligin-3-deficient mice: model of a monogenic heritable form of autism with an olfactory deficit. Genes Brain Behav. 2009; 8: 416–425. doi: 10.1111/j.1601-183X.2009.00487.x PMID: 19243448

36. Jamain S, Radyushkin K, Hammerschmidt K, Granon S, Boretius S, Varoqueaux F, et al. Reduced social interaction and ultrasonic communication in a mouse model of monogenic heritable autism. Proc Natl Acad Sci U S A. 2008; 105: 1710–1715. doi: 10.1073/pnas.0711555105 PMID: 18227507

37. El-Kordi A, Winkler D, Hammerschmidt K, K√§stner A, Krueger D, Ronnenberg A, et al. Development of an autism severity score for mice using Nlgn4 null mutants as a construct-valid model of heritable monogenic autism. Behav Brain Res. 2013; 251: 41–49. doi: 10.1016/j.bbr.2012.11.016 PMID: 23183221

38. Wang X, McCoy PA, Rodriguiz RM, Pan Y, Je HS, Roberts AC, et al. Synaptic dysfunction and abnormal behaviors in mice lacking major isoforms of Shank3. Hum Mol Genet. 2011; 20: 3093–3108. doi: 10.1093/hmg/ddr212 PMID: 21558424

39. Dahlhaus R, El-Husseini A. Altered neuroligin expression is involved in social deficits in a mouse model of the fragile X syndrome. Behav Brain Res. 2009; 208: 96–105. doi: 10.1016/j.bbr.2009.11.019 PMID: 19932134

40. Nakatani J, Tamada K, Hatanaka F, Ise S, Ohta H, Inoue K, et al. Abnormal Behavior in a Chromosome-Engineered Mouse Model for Human 15q11–13 Duplication Seen in Autism. Cell. 2009; 137: 1235–1246. doi: 10.1016/j.cell.2009.04.024 PMID: 19563756

41. Moretti P. Abnormalities of social interactions and home-cage behavior in a mouse model of Rett syndrome. Hum Mol Genet. 2004; 14: 205–220. doi: 10.1093/hmg/ddi016 PMID: 15548546

42. Fyffe SL, Neul JL, Samaco RC, Chao H-T, Ben-Shachar S, Moretti P, et al. Deletion of Mecp2 in Sim1-Expressing Neurons Reveals a Critical Role for MeCP2 in Feeding Behavior, Aggression, and the Response to Stress. Neuron. 2008; 59: 947–958. doi: 10.1016/j.neuron.2008.07.030 PMID: 18817733

43. Etherton MR, Blaiss CA, Powell CM, Sudhof TC. Mouse neurexin-1 deletion causes correlated electrophysiological and behavioral changes consistent with cognitive impairments. Proc Natl Acad Sci. 2009; 106: 17998–18003. doi: 10.1073/pnas.0910297106 PMID: 19822762

44. Moretti P. Learning and Memory and Synaptic Plasticity Are Impaired in a Mouse Model of Rett Syndrome. J Neurosci. 2006; 26: 319–327. doi: 10.1523/JNEUROSCI.2623-05.2006 PMID: 16399702

45. Chadman KK, Gong S, Scattoni ML, Boltuck SE, Gandhy SU, Heintz N, et al. Minimal Aberrant Behavioral Phenotypes of Neuroligin-3 R451C Knockin Mice. Autism Res. 2008; 1: 147–158. doi: 10.1002/aur.22 PMID: 19360662

46. Brielmaier J, Matteson PG, Silverman JL, Senerth JM, Kelly S, Genestine M, et al. Autism-relevant social abnormalities and cognitive deficits in engrailed-2 knockout mice. Plos One. 2012; 7: e40914–e40914. doi: 10.1371/journal.pone.0040914 PMID: 22829897

47. Yang M, Bozdagi O, Scattoni ML, Woehr M, Roullet FI, Katz AM, et al. Reduced Excitatory Neurotransmission and Mild Autism-Relevant Phenotypes in Adolescent Shank3 Null Mutant Mice. J Neurosci. 2012; 32: 6525–6541. doi: 10.1523/jneurosci.6107-11.2012 PMID: 22573675

48. Scattoni ML, Ricceri L, Crawley JN. Unusual repertoire of vocalizations in adult BTBR T plus tf/J mice during three types of social encounters. Genes Brain Behav. 2010; 10: 44–56. doi: 10.1111/j.1601-183X.2010.00623.x

49. Rotschafer SE, Trujillo MS, Dansie LE, Ethell IM, Razak KA. Minocycline treatment reverses ultrasonic vocalization production deficit in a mouse model of Fragile X Syndrome. Brain Res. 2010; 1439: 7–14. doi: 10.1016/j.brainres.2011.12.041

model	publication	test	habituation	cage size	cage area	observation time	time of interaction	time of interaction (%)	background & sex
Adult same-sex social interactions									
Mecp2 308/Y (truncat	Pearson et al. (2012)	free social interactions with 2 adults (interactor: C57BL/6J)	no	7' x 14' x 30 cm	98 cm²	NA	per oct types	per oct types	C57BL/6J, males
Sept8-KO	Harper et al. (2012)	free social interactions with 2 adults (pairs of 1 mutant and 1 C57BL/6 mouse)	both 30 min in a fresh home cage (different from test cage)	NA (27 x 16 x 12.5 cm?)	432 cm²?	5 min + 5 min separated by 30 min	30 s (trial 1)	10% (trial 1)	C57BL/6J, males
BTBR T+tf/J	Scattoni et al. (2010)	free social interactions with 2 adults	individual housing for 5 days	36.9 x 15.6 x 13.2 cm	575.64 cm²	3 min	67 s (m), 25 s (f)	37.2% (m), 13.9% (f)	C57BL/6J, males & females
C57BL/6N	Hammerschmidt et al. (2012)	free social interactions with 2 adults	60 s	36 x 20 cm?	720 cm²?	3 min	NA	NA	C57BL/6N, males & females
Tsc1-HZ	Goorden et al. (2007)	free social interactions with 2 adults (2 interactors: 129P2-C57BL/6)	15 min	45 x 20 cm	900 cm²	2 min + 2 min + 2 min	58% (trial 1)	58% (trial 1)	C57BL/6J*C57BL/6N, females
BTBR T+tf/J	Silverman et al. (2012)	free social interactions with 2 adults (interactor: 129/SvImJ)	no hab tot the test cage (1h individual housing before the test)	Noldus PhenoTyper 3000 arena (30 x 30 x 30 cm)	900 cm²	10 min	150 s	25%	C57BL/6J, males?
Mgs3-KO	Radyushkin et al. (2009)	free social interactions with 2 adults (same genotype)	hab to the test cage 10-min for 2 days before the test	neutral cage (30 x 30 x 30 cm)	900 cm²	10 min	75 s	12.5%	C57BL/6N, males
Mgn4-KO	Jamain et al. (2008)	free social interactions with 2 adults (same genotype)	hab to the test cage 10-min for 2 days before the test	neutral cage (gray Plexiglas box, 30 x 30 x 30 cm)	900 cm²	10 min	115 s	19.2%	C57BL/6J, males
Mgn4-KO	El-Kordi et al. (2013)	free social interactions with 2 adults (same genotype)	10 min on two consecutive days before testing	30 x 30 x 30 cm	900 cm²	10 min	87 s (m), 66 s (f)	14.5% (m), 11% s (f)	C57BL/6J, males & females
Shank3-KO	Wang et al. (2011)	free social interactions with 2 adults (interactor: C3H)	5 min (in a partitionned cage, after 14 days of individual housing)	48 x 26 x 20 cm	1248 cm²	NA	21 s (m), 29 s (f)	NA	C57BL/6J, males & females
Mgn4-KO	Ey et al. (2012)	free social interactions with 2 adults (interactor: WT)	30 min	50 x 25 x 30 cm	1250 cm²	4 min	NA	NA	C57BL/6J, males & females
Shank2-KO	Schmeisser et al. (2012)	free social interactions with 2 adults (interactor: WT)	30 min	50 x 25 x 30 cm	1250 cm²	4 min	85 s (m), 135 s (f)	35.4% (m), 56.3% (f)	C57BL/6, males & females
Shank3-KO	Peça et al. (2011)	free social interactions with 2 adults (interactor: WT)	1h in the room	40 x 40 x 30 cm	1600 cm²	10 min	96 s	14.3%	hybrid background, males
Fmr1-KO & TgN1F	Dahlhaus & El-Husseini (2009)	free social interactions with 2 adults (interactor: WT)	10 min (in a cage separated in 2)	40 x 60 cm	2400 cm²	10 min	relative changes	relative changes	C57BL/6, males
C57BL/6J	Chaboud et al. (2012)	free social interactions with 2 adults (same genotype)	30 min	50 x 30 x 30 cm	1500 cm²	4 min	NA	NA	C57BL/6J, males
Dup(15q11-13 (ch 7 in mice)	Nakatani et al. (2009)	free social interactions with 2 adults (same genotype)	no hab in the test cage	40 x 40 x 30 cm	1600 cm²	10 min	133 s	22.2%	129SvJ x C57BL/6, males
Mecp2 308/Y (truncation)	Moretti et al. (2004)	resident-intruder test (intruder=129S6/SvEv)	resident in its home cage	28.5 x 17.5 x 12 cm	498.75 cm²	10 min (3 consecutive days)	48% of time	48%	129SvEv, males
Mecp2 conditional KO (in hypothalamus)	Fyffe et al. (2008)	resident-intruder test (intruder=C57BL/6)	resident in its home cage for 2 weeks	NA (45 x 24 x 17 cm?)	1080 cm²?	10 min	per oct types	per oct types	129/SvEv x FVB, males
Juvenile same-sex social interactions									
Nlvn1a-KO	Etherton et al. (2009)	free social interactions with a juvenile	no hab in the test cage (only to the room)	same size as home cage (27 cm x 16 cm x 12 cm?; from Kogan et al. 2000)	432 cm²?	2 min	38 s	31.6%	NA, males & females
Mecp2 308/Y (truncation)	Moretti et al. (2004)	free social interactions with a juvenile (129S6/SvEv)	15 min	28.5 x 17.5 x 12 cm	498.75 cm²	2 min	70 s	58.3%	129SvEv, males
Mecp2 308/Y (truncation)	Moretti et al. (2006)	free social interactions with a juvenile (C57BL/6J)	15 min	28.5 x 17.5 x 12 cm	498.75 cm²	2 min	78 s	65%	129SvEv, males
Mgn4-KO	Ey et al. (2012)	free social interactions with 2 juveniles (interactor: C57BL/6J)	1h in isolation before testing (in a different cage)	Noldus PhenoTyper arena (25 x 25 x 35 cm)	625 cm²	10 min	per oct types	per oct types	C57BL/6J, males & females
Mgn3-KI (R451C)	Chadman et al. (2008)	juvenile social play	10 min of habituation one day before testing	Noldus PhenoTyper arena (30 x 30 x 30 cm)	900 cm²	30 min observation	per oct types	per oct types	C57BL/6J, males & females
BTBR T+tf/J	MacFarlane et al. (2008)	juvenile social play	10 min	Noldus PhenoTyper arena (30 x 30 x 30 cm)	900 cm²	30 min	per oct types	per oct types	C57BL/6J, males & females
Shank1-KO	Silverman et al. (2011)	juvenile social play	no (individual housing for 1h)	Noldus PhenoTyper 3000 arena (30 x 30 x 30 cm)	900 cm²	10 min	per oct types	per oct types	C57BL/6J*129S6/SvJae, males & females
engrailed-2-KO	Brielmaier et al. (2012)	free social interactions with 2 juveniles (interactor: C57BL/6J)	housing in individual standard mouse cages 1h before testing	Noldus PhenoTyper arena (30 x 30 x 30 cm)	900 cm²	10 min	per oct types	per oct types	129S2/SvPas
Shank3-KO	Yang et al. (2012)	free social interactions with 2 juveniles (interactor: C57BL/6J)	no (individual housing for 1h)	Noldus PhenoTyper 3000 arena (25 x 25 x 35 cm)	900 cm²	10 min	per oct types	per oct types	C57BL/6, males & females
Male-female interactions									
C57BL/6J	Yang et al. (2013)	male-female interactions	no	35 x 14 x 36 cm	490 cm²	5 min + 3 min separated by 3 min	18 s / min	30%	C57BL/6J, males
BTBR T+tf/J	Scattoni et al. (2010)	male-female interactions	individual housing for 5 days	36.9 x 15.6 x 13.2 cm	575.64 cm²	5 min	45 s	15%	C57BL/6J, males & females
Fmr1-KO	Rotschafer et al. (2012)	male-female interactions (same genotype)	no hab in the test cage	28.8 x 21.8 x 28.8 cm	822.1 cm²	until mating occurred (or max of 20 min)	NA	NA	FVB/129P2, males
C57BL/6N	Hammerschmidt et al. (2012)	male-female interactions	60 s	36 x 20 cm?	720 cm²?	3 min	NA	NA	C57BL/6N, males
Mgn4-KO	Ey et al. (2012)	male-female interactions (B6 female)	10 min	50 x 25 x 30 cm	1250 cm²	3 min	130 s	72.2%	C57BL/6J, males
Shank2-KO	Schmeisser et al. (2012)	male-female interactions (B6 female)	10 min	50 x 25 x 30 cm	1250 cm²	3 min	120 s	66.7%	C57BL/6, males

	4-min				8-min			
time in contact								
Habituation time			Mann-Whitney U-test				Mann-Whitney U-test	
			20-min vs 30-min				*20-min vs 30-min*	
rectangle			W = 33, p = 0.959				W = 31, p = 0.959	
round			W = 10, p = 0.021				W = 3, p = 0.001	
square			W = 28, p = 0.721				W = 30, p = 0.879	
Cage shape	Kruskal-Wallis rank sum test		Mann-Whitney U-test		Kruskal-Wallis rank sum test		Mann-Whitney U-test	
		rectangle vs round	*round vs square*	*rectangle vs square*		*rectangle vs round*	*round vs square*	*rectangle vs square*
20-min habituation	X = 5.055, df = 2, p = 0.080	NA	NA	NA	X = 4.085, df = 2, p = 0.130	NA	NA	NA
30-min habituation	X = 0.455, df = 2, p = 0.797	NA	NA	NA	X = 1.095, df = 2, p = 0.578	NA	NA	NA
nose-to-nose contact (duration)								
Habituation time			Mann-Whitney U-test				Mann-Whitney U-test	
			20-min vs 30-min				*20-min vs 30-min*	
rectangle			W = 29, p = 0.798				W = 33.5, p = 0.916	
round			W = 6, p = 0.005				W = 9, p = 0.015	
square			W = 32, p = 1				W = 29, p = 0.798	
Cage shape	Kruskal-Wallis rank sum test		Mann-Whitney U-test		Kruskal-Wallis rank sum test		Mann-Whitney U-test	
		rectangle vs round	*round vs square*	*rectangle vs square*		*rectangle vs round*	*round vs square*	*rectangle vs square*
20-min habituation	X = 1.085, df = 2, p = 0.581	NA	NA	NA	X = 0.992, df = 2, p = 0.609	NA	NA	NA
30-min habituation	X = 3.505, df = 2, p = 0.173	NA	NA	NA	X = 2.885, df = 2, p = 0.236	NA	NA	NA
oro-genital contact (duration) from the occupant								
Habituation time			Mann-Whitney U-test				Mann-Whitney U-test	
			20-min vs 30-min				*20-min vs 30-min*	
rectangle			W = 37, p = 0.645				W = 31.5, p = 1	
round			W = 15, p = 0.083				W = 6, p = 0.005	
square			W = 28, p = 0.721				W = 30, p = 0.879	
Cage shape	Kruskal-Wallis rank sum test		Mann-Whitney U-test		Kruskal-Wallis rank sum test		Mann-Whitney U-test	
		rectangle vs round	*round vs square*	*rectangle vs square*		*rectangle vs round*	*round vs square*	*rectangle vs square*
20-min habituation	X = 5.46, df = 2, p = 0.065	NA	NA	NA	X = 4.781, df = 2, p = 0.092	NA	NA	NA
30-min habituation	X = 0.945, df = 2, p = 0.623	NA	NA	NA	X = 1.755, df = 2, p = 0.416	NA	NA	NA
oro-genital contact (duration) from the new-comer								
Habituation time			Mann-Whitney U-test				Mann-Whitney U-test	
			20-min vs 30-min				*20-min vs 30-min*	
rectangle			W = 24, p = 0.442				W = 21, p = 0.279	
round			W = 30, p = 0.879				W = 34, p = 0.875	
square			W = 25, p = 0.505				W = 29, p = 0.798	
Cage shape	Kruskal-Wallis rank sum test		Mann-Whitney U-test		Kruskal-Wallis rank sum test		Mann-Whitney U-test	
		rectangle vs round	*round vs square*	*rectangle vs square*		*rectangle vs round*	*round vs square*	*rectangle vs square*
20-min habituation	X = 1.685, df = 2, p = 0.431	NA	NA	NA	X = 5.497, df = 2, p = 0.064	NA	NA	NA
30-min habituation	X = 2.78, df = 2, p = 0.249	NA	NA	NA	X = 1.900, df = 2, p = 0.387	NA	NA	NA
follow behaviour (duration)								
Habituation time			Mann-Whitney U-test				Mann-Whitney U-test	
			20-min vs 30-min				*20-min vs 30-min*	
rectangle			W = 30, p = 0.879				W = 31, p = 0.959	
round			W = 39, p = 0.505				W = 38, p = 0.574	
square			W = 18, p = 0.161				W = 18, p = 0.161	
Cage shape	Kruskal-Wallis rank sum test		Mann-Whitney U-test		Kruskal-Wallis rank sum test		Mann-Whitney U-test	
		rectangle vs round	*round vs square*	*rectangle vs square*		*rectangle vs round*	*round vs square*	*rectangle vs square*
20-min habituation	X =2.547, df = 2, p = 0.280	NA	NA	NA	X = 0.965, df = 2, p = 0.617	NA	NA	NA
30-min habituation	X = 5.415, df = 2, p = 0.067	NA	NA	NA	X = 5.345, df = 2, p = 0.069	NA	NA	NA
occupant approaches new-comer (occurrences)								
Habituation time			Mann-Whitney U-test				Mann-Whitney U-test	
			20-min vs 30-min				*20-min vs 30-min*	
rectangle			W = 21.5, p = 0.292				W = 24.5, p = 0.462	
round			W = 17.5, p = 0.141				W = 21, p = 0.279	
square			W = 35, p = 0.793				W = 30.5, p = 0.916	
Cage shape	Kruskal-Wallis rank sum test		Mann-Whitney U-test		Kruskal-Wallis rank sum test		Mann-Whitney U-test	
		rectangle vs round	*round vs square*	*rectangle vs square*		*rectangle vs round*	*round vs square*	*rectangle vs square*
20-min habituation	X = 0.452, df = 2, p = 0.798	NA	NA	NA	X = 1.905, df = 2, p = 0.386	NA	NA	NA
30-min habituation	X = 2.324, df = 2, p = 0.313	NA	NA	NA	X = 2.143, df = 2, p = 0.343	NA	NA	NA
new-comer approaches occupant (occurrences)								
Habituation time			Mann-Whitney U-test				Mann-Whitney U-test	
			20-min vs 30-min				*20-min vs 30-min*	
rectangle			W = 34.5, p = 0.834				W = 35.5, p = 0.752	
round			W = 30.5, p = 0.916				W = 30.5, p = 0.916	
square			W = 41, p = 0.370				W = 45.5, p = 0.171	
Cage shape	Kruskal-Wallis rank sum test		Mann-Whitney U-test		Kruskal-Wallis rank sum test		Mann-Whitney U-test	
		rectangle vs round	*round vs square*	*rectangle vs square*		*rectangle vs round*	*round vs square*	*rectangle vs square*
20-min habituation	X = 0.117, df = 2, p = 0.943	NA	NA	NA	X = 0.905, df = 2, p = 0.636	NA	NA	NA
30-min habituation	X = 1.043, df = 2, p = 0.594	NA	NA	NA	X = 3.723, df = 2, p = 0.156	NA	NA	NA
occupant escapes from new-comer (occurrences)								
Habituation time			Mann-Whitney U-test				Mann-Whitney U-test	
			20-min vs 30-min				*20-min vs 30-min*	
rectangle			W = 42, p = 0.318				W = 30, p = 0.875	
round			W = 8, p = 0.013				W = 12, p = 0.040	
square			W = 55.5, p = 0.016				W = 52, p = 0.040	
Cage shape	Kruskal-Wallis rank sum test		Mann-Whitney U-test		Kruskal-Wallis rank sum test		Mann-Whitney U-test	
		rectangle vs round	*round vs square*	*rectangle vs square*		*rectangle vs round*	*round vs square*	*rectangle vs square*
20-min habituation	X = 2.312, df = 2, p = 0.315	NA	NA	NA	X = 5.462, df = 2, p = 0.065	NA	NA	NA
30-min habituation	X = 11.667, df = 2, p = 0.003	W = 12, p = 0.040	W = 60.5, p = 0.003	W = 51.5, p = 0.046	X = 8.562, df = 2, p = 0.014	W = 34, p = 0.875	W = 53.5, p = 0.027	W = 58, p = 0.007
new-comer escapes from occupant (occurrences)								
Habituation time			Mann-Whitney U-test				Mann-Whitney U-test	
			20-min vs 30-min				*20-min vs 30-min*	
rectangle			W = 15.5, p = 0.092				W = 21.5, p = 0.293	
round			W = 35.5, p = 0.753				W = 28, p = 0.713	
square			W = 19.5, p = 0.207				W = 17.5, p = 0.140	
Cage shape	Kruskal-Wallis rank sum test		Mann-Whitney U-test		Kruskal-Wallis rank sum test		Mann-Whitney U-test	
		rectangle vs round	*round vs square*	*rectangle vs square*		*rectangle vs round*	*round vs square*	*rectangle vs square*
20-min habituation	X = 0.499, df = 2, p = 0.779	NA	NA	NA	X = 0.857, df = 2, p = 0.652	NA	NA	NA
30-min habituation	X = 1.100, df = 2, p = 0.577	NA	NA	NA	X = 0.420, df = 2, p = 0.810	NA	NA	NA
occupant approaches new-comer & new-comer escapes (occurrences)								
Habituation time			Mann-Whitney U-test				Mann-Whitney U-test	
			20-min vs 30-min				*20-min vs 30-min*	
rectangle			W = 16.5, p = 0.115				W = 22, p = 0.315	
round			W = 33.5, p = 0.916				W = 32, p = 1	
square			W = 16, p = 0.1				W = 14.5, p = 0.073	
Cage shape	Kruskal-Wallis rank sum test		Mann-Whitney U-test		Kruskal-Wallis rank sum test		Mann-Whitney U-test	
		rectangle vs round	*round vs square*	*rectangle vs square*		*rectangle vs round*	*round vs square*	*rectangle vs square*
20-min habituation	X = 0.704, df = 2, p = 0.703	NA	NA	NA	X = 0.969, df = 2, p = 0.616	NA	NA	NA
30-min habituation	X =1.421, df = 2, p = 0.492	NA	NA	NA	X = 1.568, df = 2, p = 0.457	NA	NA	NA

new-comer approaches occupant & occupant escapes (occurrences)									
Habituation time			Mann-Whitney U-test					Mann-Whitney U-test	
			20-min vs 30-min					*20-min vs 30-min*	
rectangle			W = 32.5, p = 1					W = 39.5, p = 0.460	
round			W = 33, p = 0.958					W = 28.5, p = 0.751	
square			W = 47, p = 0.124					W = 49.5, p = 0.073	
Cage shape	Kruskal-Wallis rank sum test		Mann-Whitney U-test		Kruskal-Wallis rank sum test			Mann-Whitney U-test	
		rectangle vs round	*round vs square*	*rectangle vs square*		*rectangle vs round*	*round vs square*	*rectangle vs square*	
20-min habituation	X = 1.232, df = 2, p = 0.540	NA	NA	NA	X = 1.554, df = 2, p = 0.460	NA	NA	NA	
30-min habituation	X = 1.317, df = 2, p = 0.518	NA	NA	NA	X = 2.287, df = 2, p = 0.319	NA	NA	NA	

occupant approaches new-comer & occupant escapes (occurrences)									
Habituation time			Mann-Whitney U-test					Mann-Whitney U-test	
			20-min vs 30-min					*20-min vs 30-min*	
rectangle			W = 35, p = 0.792					W = 30.5, p = 0.916	
round			W = 15, p = 0.081					W = 12.5, p = 0.046	
square			W = 59.5, p = 0.004					W = 53.5, p = 0.027	
Cage shape	Kruskal-Wallis rank sum test		Mann-Whitney U-test		Kruskal-Wallis rank sum test			Mann-Whitney U-test	
		rectangle vs round	*round vs square*	*rectangle vs square*		*rectangle vs round*	*round vs square*	*rectangle vs square*	
20-min habituation	X = 3.478, df = 2, p = 0.176	NA	NA	NA	X = 4.805, df = 2, p = 0.091	NA	NA	NA	
30-min habituation	X = 6.329, df = 2, p = 0.042	W = 23, p = 0.370	W = 54, p = 0.023	W = 48.5, p = 0.090	X = 5.857, df = 2, p = 0.053	NA	NA	NA	

new-comer approaches occupant & new-comer escapes (occurrences)									
Habituation time			Mann-Whitney U-test					Mann-Whitney U-test	
			20-min vs 30-min					*20-min vs 30-min*	
rectangle			W = 20.5, p = 0.241					W = 28, p = 0.712	
round			W = 31, p = 0.957					W = 27, p = 0.634	
square			W = 32, p = 1					W = 32.5, p = 1	
Cage shape	Kruskal-Wallis rank sum test		Mann-Whitney U-test		Kruskal-Wallis rank sum test			Mann-Whitney U-test	
		rectangle vs round	*round vs square*	*rectangle vs square*		*rectangle vs round*	*round vs square*	*rectangle vs square*	
20-min habituation	X = 0.099, df = 2, p = 0.952	NA	NA	NA	X = 1.172, df = 2, p = 0.557	NA	NA	NA	
30-min habituation	X = 2.714, df = 2, p = 0.257	NA	NA	NA	X = 2.030, df = 2, p = 0.363	NA	NA	NA	

new-comer in vision field of occupant (duration)									
Habituation time			Mann-Whitney U-test					Mann-Whitney U-test	
			20-min vs 30-min					*20-min vs 30-min*	
rectangle			W = 28, p = 0.721					W = 29, p = 0.798	
round			W = 51, p = 0.049					W = 64, p < 0.001	
square			W = 27, p = 0.645					W = 35, p = 0.798	
Cage shape	Kruskal-Wallis rank sum test		Mann-Whitney U-test		Kruskal-Wallis rank sum test			Mann-Whitney U-test	
		rectangle vs round	*round vs square*	*rectangle vs square*		*rectangle vs round*	*round vs square*	*rectangle vs square*	
20-min habituation	X = 4.995, df = 2, p = 0.082	NA	NA	NA	X = 8.135, df = 2, p = 0.017	W = 5, p = 0.003	W = 48, p = 0.105	W = 22, p = 0.328	
30-min habituation	X = 1.815, df = 2, p = 0.404	NA	NA	NA	X = 2.205, df = 2, p = 0.332	NA	NA	NA	

occupant in vision-field of new-comer (duration)									
Habituation time			Mann-Whitney U-test					Mann-Whitney U-test	
			20-min vs 30-min					*20-min vs 30-min*	
rectangle			W = 34, p = 0.879					W = 29, p = 0.798	
round			W = 49, p = 0.083					W = 60, p = 0.002	
square			W = 35, p = 0.798					W = 36, p = 0.721	
Cage shape	Kruskal-Wallis rank sum test		Mann-Whitney U-test		Kruskal-Wallis rank sum test			Mann-Whitney U-test	
		rectangle vs round	*round vs square*	*rectangle vs square*		*rectangle vs round*	*round vs square*	*rectangle vs square*	
20-min habituation	X = 4.145, df = 2, p = 0.126	NA	NA	NA	X = 7.265, df = 2, p = 0.026	W = 11, p = 0.028	W = 55, p = 0.015	W = 32, p = 1	
30-min habituation	X = 0.455, df = 2, p = 0.797	NA	NA	NA	X = 0.665, df = 2, p = 0.717	NA	NA	NA	

occupant stops (duration)									
Habituation time			Mann-Whitney U-test					Mann-Whitney U-test	
			20-min vs 30-min					*20-min vs 30-min*	
rectangle			W = 33, p = 0.959					W = 30, p = 0.879	
round			W = 45, p = 0.195					W = 43, p = 0.279	
square			W = 38.5, p = 0.528					W = 34, p = 0.879	
Cage shape	Kruskal-Wallis rank sum test		Mann-Whitney U-test		Kruskal-Wallis rank sum test			Mann-Whitney U-test	
		rectangle vs round	*round vs square*	*rectangle vs square*		*rectangle vs round*	*round vs square*	*rectangle vs square*	
20-min habituation	X = 0.555, df = 2, p = 0.758	NA	NA	NA	X = 3.02, df = 2, p = 0.221	NA	NA	NA	
30-min habituation	X = 3.515, df = 2, p = 0.173	NA	NA	NA	X = 1.985, df = 2, p = 0.371	NA	NA	NA	

new-comer stops (duration)									
Habituation time			Mann-Whitney U-test					Mann-Whitney U-test	
			20-min vs 30-min					*20-min vs 30-min*	
rectangle			W = 41, p = 0.382					W = 34, p = 0.879	
round			W = 33.5, p = 0.916					W = 36, p = 0.721	
square			W = 46, p = 0.161					W = 41.5, p = 0.344	
Cage shape	Kruskal-Wallis rank sum test		Mann-Whitney U-test		Kruskal-Wallis rank sum test			Mann-Whitney U-test	
		rectangle vs round	*round vs square*	*rectangle vs square*		*rectangle vs round*	*round vs square*	*rectangle vs square*	
20-min habituation	X = 1.085, df = 2, p = 0.581	NA	NA	NA	X =1.134, df = 2, p = 0.567	NA	NA	NA	
30-min habituation	X = 2.375, df = 2, p = 0.305	NA	NA	NA	X = 0.965, df = 2, p = 0.617	NA	NA	NA	

latency for first vocalization									
Habituation time			Mann-Whitney U-test					Mann-Whitney U-test	
			20-min vs 30-min					*20-min vs 30-min*	
rectangle			W = 23, p = 0.382					NA	
round			W = 43, p = 0.279					NA	
square			W = 31, p = 0.959					NA	
Cage shape	Kruskal-Wallis rank sum test		Mann-Whitney U-test		Kruskal-Wallis rank sum test			Mann-Whitney U-test	
		rectangle vs round	*round vs square*	*rectangle vs square*		*rectangle vs round*	*round vs square*	*rectangle vs square*	
20-min habituation	X = 3.02, df = 2, p = 0.221	NA	NA	NA	NA	NA	NA	NA	
30-min habituation	X = 3.255, df = 2, p = 0.196	NA	NA	NA	NA	NA	NA	NA	

nb of vocalizations / min									
Habituation time			Mann-Whitney U-test					Mann-Whitney U-test	
			20-min vs 30-min					*20-min vs 30-min*	
rectangle			W = 24, p = 0.442					W = 23, p = 0.382	
round			W = 13.5, p = 0.059					W = 13, p = 0.050	
square			W = 33, p = 0.959					W = 31, p = 0.959	
Cage shape	Kruskal-Wallis rank sum test		Mann-Whitney U-test		Kruskal-Wallis rank sum test			Mann-Whitney U-test	
		rectangle vs round	*round vs square*	*rectangle vs square*		*rectangle vs round*	*round vs square*	*rectangle vs square*	
20-min habituation	X = 3.528, df = 2, p = 0.171	NA	NA	NA	X = 5.013, df = 2, p = 0.082	NA	NA	NA	
30-min habituation	X = 1.735, df = 2, p = 0.420	NA	NA	NA	X = 0.455, df = 2, p = 0.797	NA	NA	NA	

mean duration of vocalizations									
Habituation time			Mann-Whitney U-test					Mann-Whitney U-test	
			20-min vs 30-min					*20-min vs 30-min*	
rectangle			W = 26, p = 0.574					W = 34, p = 0.879	
round			W = 25, p = 0.505					W = 29, p = 0.798	
square			W = 30, p = 0.879					W = 38, p = 0.574	
Cage shape	Kruskal-Wallis rank sum test		Mann-Whitney U-test		Kruskal-Wallis rank sum test			Mann-Whitney U-test	
		rectangle vs round	*round vs square*	*rectangle vs square*		*rectangle vs round*	*round vs square*	*rectangle vs square*	
20-min habituation	X = 0.645, df = 2, p = 0.724	NA	NA	NA	X = 2.445, df = 2, p = 0.295	NA	NA	NA	
30-min habituation	X = 0.035, df = 2, p = 0.983	NA	NA	NA	X = 0.095, df = 2, p = 0.954	NA	NA	NA	

II. Article 2: "Recording Mouse Ultrasonic Vocalizations to Evaluate Social Communication"

Allain-Thibeault Ferhat[1], Nicolas Torquet[2], Anne-Marie Le Sourd[1], Fabrice de Chaumont[3], Jean-Christophe Olivo-Marin[3], Philippe Faure[2],Thomas Bourgeron[1], Elodie Ey[1]

1 Human Genetics and Cognitive Functions, University Paris Diderot, CNRS UMR 3571, Institut Pasteur
2 Neurophysiology and Behavior, University Pierre et Marie Curie Paris 6, CNRS UMR 7102
3 Bio Image Analysis, CNRS URA 2582, Institut Pasteur

Video Article

Recording Mouse Ultrasonic Vocalizations to Evaluate Social Communication

Allain-Thibeault Ferhat[1], Nicolas Torquet[2], Anne-Marie Le Sourd[1], Fabrice de Chaumont[3], Jean-Christophe Olivo-Marin[3], Philippe Faure[2], Thomas Bourgeron[1], Elodie Ey[1]

[1]Human Genetics and Cognitive Functions, University Paris Diderot, CNRS UMR 3571, Institut Pasteur

[2]Neurophysiology and Behavior, University Pierre et Marie Curie Paris 6, CNRS UMR 7102

[3]Bio Image Analysis, CNRS URA 2582, Institut Pasteur

Correspondence to: Elodie Ey at elodie.ey@pasteur.fr

URL: http://www.jove.com/video/53871
DOI: doi:10.3791/53871

Keywords: Behavior, Issue 112, neuroscience, mouse, social communication, ultrasonic vocalization, pup isolation calls, male vocalizations, female-female interactions, neuropsychiatric disorders, mouse models

Date Published: 6/5/2016

Citation: Ferhat, A.T., Torquet, N., Le Sourd, A.M., de Chaumont, F., Olivo-Marin, J.C., Faure, P., Bourgeron, T., Ey, E. Recording Mouse Ultrasonic Vocalizations to Evaluate Social Communication. *J. Vis. Exp.* (112), e53871, doi:10.3791/53871 (2016).

Abstract

Mice emit ultrasonic vocalizations in different contexts throughout development and in adulthood. These vocal signals are now currently used as proxies for modeling the genetic bases of vocal communication deficits. Characterizing the vocal behavior of mouse models carrying mutations in genes associated with neuropsychiatric disorders such as autism spectrum disorders will help to understand the mechanisms leading to social communication deficits. We provide here protocols to reliably elicit ultrasonic vocalizations in pups and in adult mice. This standardization will help reduce inter-study variability due to the experimental settings. Pup isolation calls are recorded throughout development from individual pups isolated from dam and littermates. In adulthood, vocalizations are recorded during same-sex interactions (without a sexual component) by exposing socially motivated males or females to an unknown same-sex conspecific. We also provide a protocol to record vocalizations from adult males exposed to an estrus female. In this context, there is a sexual component in the interaction. These protocols are established to elicit a large amount of ultrasonic vocalizations in laboratory mice. However, we point out the important inter-individual variability in the vocal behavior of mice, which should be taken into account by recording a minimal number of individuals (at least 12 in each condition). These recordings of ultrasonic vocalizations are used to evaluate the call rate, the vocal repertoire and the acoustic structure of the calls. Data are combined with the analysis of synchronous video recordings to provide a more complete view on social communication in mice. These protocols are used to characterize the vocal communication deficits in mice lacking *ProSAP1/Shank2*, a gene associated with autism spectrum disorders. More ultrasonic vocalizations recordings can also be found on the *mouseTube* database, developed to favor the exchange of such data.

Video Link

The video component of this article can be found at http://www.jove.com/video/53871/

Introduction

Patients with neuropsychiatric disorders usually display deficits in social communication (*e.g.*, patients with autism spectrum disorders, schizophrenia, or Alzheimer disease)[1]. Genetically engineered mice are more and more frequently used to model genetic causes of these disorders[2]. Studying social communication in these mouse models is of high interest for understanding the mechanisms of genetic mutations leading to atypical social dysfunctions and for testing new therapies. Since mice are social animals and communicate with each others using olfactory, tactile, visual and acoustic signals, they are suitable models to evaluate social communication.

Mouse ultrasonic vocalizations are now currently used as a proxy for modeling the genetic bases of vocal communication deficits[3,4] (but the existence of vocal learning in this species is still debated[5,6], even if most recent studies argue for the absence of vocal learning[7]). Laboratory mice have been found to emit ultrasonic vocalizations in mother-infant relationships, in male-female socio-sexual interactions, in same-sex social interactions (reviewed in reference[8]) and in juvenile-juvenile social interactions[9]. Mouse pups emit isolation calls during their first two weeks of life when isolated from dam and littermates[10]. Males emit ultrasonic vocalizations when in presence of an estrus female (or urinary cues from her)[11,12]. Males and females emit ultrasonic vocalization when interacting with an unknown conspecific of the same sex[13,14]. The organization and functions of these vocalizations are not completely clear and need further investigations. Current knowledge on the functional aspect is limited to the elicitation of retrieval behavior in mothers hearing pup isolation calls, the facilitation of proximity of adult females toward adult male vocalizations[15] and the increased exploratory behavior of adult males hearing adult female vocalizations[16].

Characterizing the abnormalities in vocal communication in mouse models of neuropsychiatric disorders should be conducted in standardized conditions to rule out major contribution of the experimental conditions. Such characterizations, combined with the evaluation of simultaneous social interactions and neurobiological studies, in various genetic models should improve our knowledge on the genetic contribution to the different aspects of mouse ultrasonic communication. Over a long term, it should give further light on some neurobiological bases of social communication in humans. We presently aim at providing simple protocols to reliably elicit ultrasonic vocalizations during development and in adulthood for both male and female mice in the laboratory. Such protocols should ease the standardization of recordings to more reliably

compare ultrasonic vocalization emissions between strains and laboratories. It should also facilitate the setting up of such recordings in laboratories having no prior experience with mouse ultrasonic vocalizations recordings. We also highlight the current possibility to combine ultrasonic vocalizations data with detailed behavioral data collected simultaneously during social interactions in adult mice, to obtain crucial information on social impairments as well as on the context of emission of ultrasonic vocalizations. Such analyses will shed new light on the organization and functions of mouse ultrasonic vocalizations. Finally, we also advertise the possibility to share ultrasonic vocalization recordings with the whole scientific community on the *mouseTube* database (http://mousetube.pasteur.fr). Open access to audio recording data should boost knowledge on mouse ultrasonic communication by allowing scientists to compare their own data with ultrasonic vocalizations recorded in other laboratories (with similar or different strains/protocols), and/or to challenge their analysis methods with files recorded under different conditions.

Protocol

Ethics statement: Procedures involving animal subjects have been approved by the Comité d'Ethique en Expérimentation animale (CETEA) n°89 at the Institut Pasteur, Paris.

1. Animal Preparation

1. To record pup isolation calls, obtain pregnant females from the mouse strain of interest. Note: Breed heterozygous males and females to obtain at least 10 litters including wild-type, heterozygous and knock-out pups to obtain robust control animals.
2. Obtain two categories of adult mice to record vocalizations during same-sex interactions.
    1. Obtain at least 12 males or 12 females of each genotype as test mice from the strain of interest (to take into account inter-individual variability). Note: This protocol is well-adapted for adults, but it can be adjusted to juveniles, with reduced isolation time before the experiment[9]. This test works for males or females. However, avoid testing males from mouse strains that display a clear aggressive phenotype in the male-male social interaction test.
    2. To maximize the amount of affiliative interactions, isolate the test animals before the experiments. House males individually for 3 weeks (to reduce aggressive interactions to a minimum[14,17]) and females for 3 days (E. Ey, unpublished data) to increase their social motivation.
    3. Obtain males or females from strains representative of the genetic background of the test strain to use them as new-comers (*e.g.,* as interacting mice, see 3.1.3). For instance, if the mutant strain being studied has been generated on the C57BL/6J background, use C57BL/6J mice as new-comers. Calculate the number of animals needed so that each of these mice is not used more than 2 times a day as new-comer. House them in groups.

3. Obtain two categories of adult mice to record male vocalizations in presence of an estrus female.
    1. Obtain at least 12 sexually mature males from each genotype of the strain of interest (to take into account inter-individual variability). Note: If the males have never had experience with females before, put them in individual cages and leave them spend one night with a female two days before the test to increase their motivation to emit ultrasonic vocalizations[6].
    2. Obtain sexually mature females from the background strain of the recorded males. For instance, if the mutant males being studied have been generated on the C57BL/6J background, use C57BL/6J females. Calculate the number of females needed so that each of these mice is not used more than 3 times a day. House them in groups.

2. Pup Isolation Calls

1. Pup Identification
    1. Three days before the predicted day of birth, isolate the pregnant females.
    2. Check the females for birth every morning and every evening. Note the day of birth as P0.
    3. Identify the pups at P1 using long-lasting paw tattoos (subcutaneous injection of green tattoo paste with a 0.3 mm x 13 mm [30 G ½"] needle). Create a code with one, two, three or four paws marked. Be as quick as possible, to minimally disturb the pups, and put them back in the nest as soon as possible.

2. Set up the Cage to Record Pup Isolation Calls.
    1. Use either a self-made soundproof chamber (**Figure 1A**) or a simple Styrofoam box. Place a thermometer within the box to monitor the temperature for each recording. Make sure that the temperature remains between 18 °C and 22 °C.
    2. Place a microphone at the top (through a hole in the top of the box). Adjust the height of the microphone so that the membrane of the microphone is 12-15 cm above the bottom of the box where the pup will lie down. Connect the microphone to the sound card, and the sound card to the computer.
    3. To adjust the gain of the sound card, conduct a recording trial with a pup that will not be used in the experiment. Put the pup in the same conditions as in the experiment (see 2.3.1). Close the door. Adjust the gain on the sound card, so that it is on the maximum value (to have the highest amplitude possible for the vocalizations) but without overloading (check on the live spectrogram display on the recording software).
    Note: A few calls might be overloaded if the amplitude of the majority of the calls is kept at the highest level possible.
    4. Register the gain level for each recording session and do not change it between pups/litters/sessions. Variations in gain levels would lead to inaccurate call detection and acoustic variables measures with the same thresholds in the analyses using automatic detection and measurements (see 5.1 to 5.4).

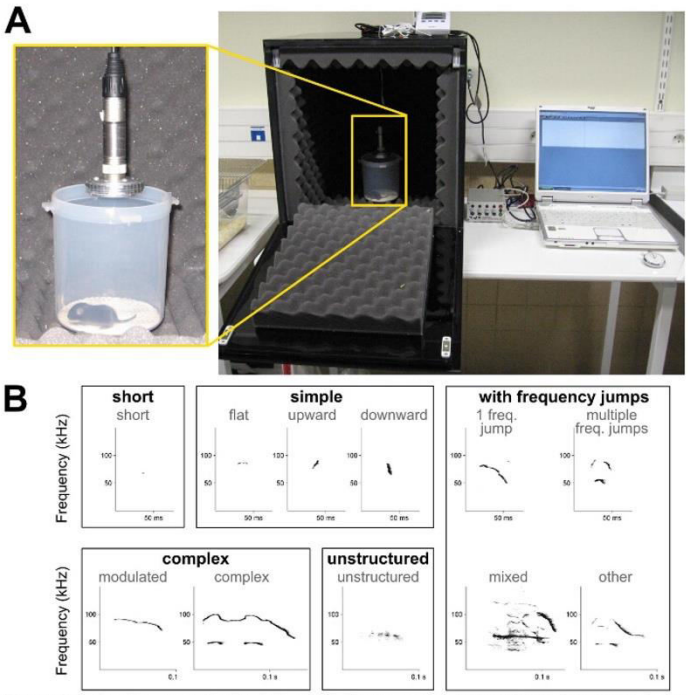

Figure 1: Set up for recording isolation calls from mouse pups and spectrograms of ultrasonic vocalizations. (**A**) Example of a self-made sound-proof chamber to record pup isolation calls. (**B**) Spectrograms of the different call types used in the present call type classification; see description in Table 1. Please click here to view a larger version of this figure.

3. Conduct the recording of pup isolation calls every two days. Conduct recordings in the morning for pups born in the night, and in the afternoon for pups born during the day to avoid categorizing in the same age class pups with half a day of age difference. This is most noticeable for the very young stages P2 and P4.
    1. Take one pup in the litter. Place it as quickly and gently as possible in a plastic recipient washed with ethanol 10% and dried (diameter: 9 cm; height: 10 cm to prevent older pups from escaping from the area covered by the microphone). Put the recipient just under the microphone.
    2. Close the box as quickly and silently as possible. Start the recording of pup ultrasonic vocalizations in the recording software (16-bit format, 300 kHz sampling frequency to capture sound amplitude up to 150 kHz with a high quality).
    3. After the required time of recording has elapsed (up to 5 min), stop the recording. Take the pup out of the box. Write down the paw tattoos of the pup.
    4. Take the axillary temperature of the pup with a probe-thermometer. Mark the pup on its back with a tiny point with a smell-less pen (water ink), to recognize more easily the already recorded pups in the nest when the next one is chosen and to avoid manipulating all pups each time a new one is chosen. Put the pup back in the nest.
    5. Wash the plastic recipient and the plastic covering its bottom with 10% ethanol and dry it well before putting the next pup inside.
    6. Choose the next pup in the litter and repeat 2.3.

4. Check body weight, motor coordination, negative geotaxis, and developmental marks (for details of the reduced test battery please see the method sections in Schmeisser *et al.*[18] and in Ey *et al.*[19]) after a period of rest of 1 hr to allow the pups to recover after the exhausting emission of ultrasonic vocalizations. Use another cohort of animals if the complete developmental test battery such as in Chadman *et al.*[20] and Scattoni *et al.*[21] is conducted.
5. Repeat these recordings every two days between P2 and P12 to characterize pup vocal behavior and development throughout their first two weeks of life.

3. Ultrasonic Vocalizations during Same-sex Social Interactions

1. Vocalization Recordings
    1. Prepare a test cage (50 x 25 cm x 30 cm^3; Plexiglas, 100 lux [low intensity white light]) cleaned with soap water, dried and filled with 2 cm fresh bedding in the soundproof chamber.

1. Place the microphone so that vocalizations emitted from all corners of the cage can be recorded. Fix the microphone in a corner of the test cage (either on the cage or on a tripod) and adjust the angle microphone-cage bottom to cover the cage's entire surface.
   Note: Ultrasounds are very directional.
2. Place a video camera on the top of the soundproof chamber to capture the whole surface of the test cage.
   Note: Check that the microphone is not hiding a corner of the test cage on the video.
3. Before testing, adjust the gain of the soundcard with a spare male and a spare female that will not be used in the experiment later. Put these animals in the test cage in the recording chamber. Adjust the gain level on the sound card to maximize the amplitude of the recorded vocalizations but to minimize overloading as seen in the live spectrogram display on the recording software.
   Note: The gain depends on the distance between the microphone and the vocalizing animals.

2. Introduce the animal to be tested (male or female; it will be called the "occupant") in the test cage on fresh bedding. Leave it habituate to the test cage in the soundproof chamber for 20 min to maximize its interest for the unknown conspecific introduced in 3.1.3.
3. After this habituation time, introduce the 2nd animal for the interaction (male or female, same sex as the occupant, but different ear marks / paw tattoo to identify them later; it will be called the "new-comer").
   1. Start recording the ultrasonic vocalizations (16-bit format, 300 kHz sampling frequency to capture sound amplitude up to 150 kHz with a high quality) and the video to capture the introduction of the new-comer in the test cage. Start recording the ultrasonic vocalizations during habituation (occupant alone) if a comparison between the baseline level of vocalization emission during cage exploration and the social interaction is needed.
   2. Synchronize manually/visually the audio and video recordings by pressing on the time watch ("bip" sound near the microphone) exactly when the hind paws of the new-comer mouse touch the ground.
   3. Leave the two animals interact for the desired time (for instance 4 min, a duration sufficient to collect enough ultrasonic vocalizations).

4. Put the occupant and the new-comer back in their respective home cages. Empty the used bedding from the test cage, wash it with soap water and dry it with paper towels. Put fresh bedding and place it back in the soundproof chamber for the next test.

4. Male Vocalizations During Interaction with an Estrus Female

1. Early in the morning the day of testing the males, take vaginal smears from each female to determine their sexual status within the estrus cycle.
   1. Hold the female by the tail and maintain her on the cage grid. Use a pipette to rinse the vagina several times with 20 µl PBS (*i.e.*, inject and recollect the same 20 µl PBS several times). Recollect the 20 µl PBS with the same pipette tip. Use sterile PBS, to avoid any infection if females are to be tested for several consecutive days.
   2. Spread the PBS containing the suspension of vaginal cells on a slide. Put four samples on one slide (identify the individuals at the side of the slide with a pencil). Let the slides dry before conducting the staining.
   3. Work under the laboratory fume hood.
      1. Prepare one bath of pure May-Grünwald, one bath of phosphate buffer solution (0.1 M) and one bath of Giemsa R (1/20 in phosphate buffer solution).
      2. Put the slides in the bath of pure May-Grünwald for 3 min, then rinse them in the bath of phosphate buffer solution for 1 min and finally transfer them for 10 min in the bath of Giemsa R (1/20 in phosphate buffer solution).
      3. After that, rinse the slides again in the bath of phosphate buffer solution for 10 sec and let them dry.

   4. Examine the stained slides under the microscope. Females that can be used during the day are those whose samples present only large cornified epithelial cells (without nucleus, stained in blue; full estrus).

2. Put the males in the test room at least 30 min before testing them.
3. Vocalization Recordings
   1. Repeat 3.1 if necessary.
   2. Introduce the male to be tested (on fresh bedding). Leave him habituate to the test cage in the soundproof chamber for 10 min.
   3. After this habituation time, introduce a female in estrus (among the ones selected from the staining).
      1. Start recording the ultrasonic vocalizations and the video to capture the introduction of the female in the test cage. Start recording the ultrasonic vocalizations during habituation (male alone) if a comparison between the baseline level of vocalization emission during cage exploration and the social interaction is needed.
      2. Synchronize manually/visually the audio and video recordings by pressing on the time watch ("bip" sound near the microphone) exactly when the hind paws of the female mouse touch the ground.
      3. Leave the two animals interact for the desired time (for instance 4 min, a duration sufficient to collect enough ultrasonic vocalizations).

   4. Put the male and the female back in their respective home cages. Empty the used bedding from the test cage, wash it with soap water and dry it with paper towels. Put fresh bedding and place it back in the soundproof chamber for the next test.
      Note: It is optimal to use each estrus female only one time each day (but if necessary it can be used up to 3 times on the same day but not in a row).

5. Variables to Be Extracted

1. Prepare audio files for the analyses. Note: The procedure below is specific to A*visoft SASLab Pro* and may change according to the software used.
    1. Cut the files so that they start exactly at the "bip" of the time watch, and end after the desired duration (5 min for pup recordings, 4 min for adult recordings).
    2. Filter out the amplitude under 30 kHz by using a high-pass filter (Edit>Filter>FIR Time Domain Filter; High Pass with 30 kHz frequency cut off). Use batch processing to filter all files of interest (Actions>Batch Processing>FIR filter).
    3. Identify each ultrasonic vocalization by labelling them with the software.
        1. Use automatic detection for pup recordings (Tools>Labels>Create section labels from waveform events). Adjust threshold, hold time and margin for the most accurate detection. Manually check the detection and adjust labels if necessary (recommended).
        2. Use visual detection (manual insertion of labels) for adult recordings with background noise (select the vocalizations, click right, and insert section label from marker).
    4. Create the spectrogram. Activate automatic parameter measurements (Tools>Automatic Parameter Measurements>Automatic Parameter Measurements Set up).
    5. Check the "Enable automatic measurements", the "Compute parameters from entire spectrogram", and the "Automatic update" boxes. Select "Element separation": interactively (section labels).
    6. Check boxes to calculate the desired temporal parameters (Duration of element, Interval, Start/End time) and spectrum-based parameters (Peak frequency), and the location of measurements (Start of element, End of element, Mean, Max, Min).
    7. Copy the measurements and paste them in a spreadsheet.
    Note: For recordings conducted with adults, measurements of spectrum-based parameters might be impossible because of background noise. Use manual measurements of peak frequency by clicking on the different frequency values directly on the spectrogram and pasting the values manually in a table.
2. Determine call rate, *i.e.,* number of calls per minute by first determining the number of vocalizations emitted (total number of labels). Then, calculate the call rate by dividing the total number of vocalizations recorded by the duration (in minutes) of the file.
3. Determine temporal organization, *i.e.*, distribution of time intervals between calls to determine sequence organization.
    1. Calculate the time intervals between the end of the vocalization n and the start of the vocalization n+1 using the start/end time of each label.
    2. Establish the distribution density of the time intervals between ultrasonic vocalizations.
4. Determine call repertoire, *i.e.,* define the call types present in the recording. Use the example of classification presented in **Table 1** and **Figure 1B**.
    1. When labeling each vocalization in 5.1.3, write the name of the call type in the label.
    2. Calculate the exact number and the proportion of each call type to build the vocal repertoire.
5. Determine acoustic characteristics for each vocalization, *i.e.,* duration, peak frequency (*i.e.,* frequency with the highest amplitude) at the beginning and the end of the call, maximum and minimum peak frequency, and mean frequency if automatic measurement is possible (**Figure 1B**).
    1. Use the automatic parameter measurements function in the software to measure automatically duration, peak frequency characteristics (*e.g.*, start, end, mean, maximum, minimum) in pup recordings.
    2. Use the duration of the label as the duration of the vocalization for adult recordings. Measure manually on the spectrogram window the peak frequency characteristics (*e.g.,* start, end, maximum, minimum).
6. Couple ultrasonic vocalization data and social interaction data (*MiceProfiler* plugin from the ICY platform[22]).
    1. Make sure to synchronize as precisely as possible the audio and the video recordings as described in the protocol.
    2. Encode the video of the social interaction using the *Mice Profiler Tracker* plugin of the ICY platform as described in de Chaumont *et al.*[22]. Start the tracking exactly when the hind paws of the introduced animal touch the ground.
    3. Upload the encoded video file and its corresponding xml file (generated by *Mice Profiler Tracker*) in the *Mice Profiler Video Label Maker* plugin of the ICY platform as described in de Chaumont *et al.*[22].
    Note: The *Mice Profiler Video Label Maker* plugin will automatically link the video file and the text file generated from the analysis of the audio file if they have the same name (see: http://icy.bioimageanalysis.org/plugin/Mice_Profiler_Video_Label_Maker).
    4. After checking that the mouse scale is correct, click on "Create USV stats" for each file to obtain the number and the proportion of vocalizations emitted during each social event in a separated file.

6. Uploading Files on the *mouseTube* Database

1. Make sure the files are on a storage server which can be accessed from outside the institution.
Note: Servers hosted in some institutions with high security levels will need a specific configuration to be accessible by people connecting from outside the institution.
2. Go to the *mouseTube* website (http://mousetube.pasteur.fr). Log in (login and password are attributed to each user by the administrators).
3. Check whether the mouse strain recorded already exists in the *mouseTube* database by clicking on the "Strains" button. If not, ask the administrators to create it.
4. Create subjects using the "Subjects>Create" button. Enter the identification codes of the animals recorded. Gather them in groups to ease later retrieval of data.
5. Enter the description of the protocol used to record ultrasonic vocalizations using the "Protocols>Create" button.

6. Create an experiment for each recording session using the "Experiments>Create" button. Specify the protocol, the group of individuals which has been recorded, the hardware and software used and their specificities.
   Note: The experiment gathers all the metadata corresponding to the vocalization files.
7. Create the link to the vocalization files using the "Vocalisations>Create" button. Select the experiment within the list. Copy and paste the url of the vocalization file (this link begins with http://…) into the corresponding field of the "Files to link" column. Validate the entries by clicking on the button "Create a link between mouseTube and the files".
   Note: It is not required to fill each box for each file at the same time.
8. If necessary, modify the links entered at any moment, and add details in the "Notes" section. Do not hesitate to write down notes to give more details. For instance, if a link toward a video file that was recorded simultaneously with the audio file has been entered, this can be specified in the "Notes".

Representative Results

With the present protocols, we characterized the vocal behavior of mice lacking *ProSAP1/Shank2*, a gene associated with autism spectrum disorders (ASD)[23-25]. ASD are characterized by deficits in social communication and stereotyped behaviors[1]. Our *Shank2*$^{-/-}$ mice displayed hyperactivity, increased anxiety and atypical vocal communication[18,26]. Indeed, we noted that *Shank2*$^{-/-}$ mice displayed an atypical developmental profile in their emission rate of pup isolation calls in comparison with the typical inverted U-shaped curve in their wild-type littermates. *Shank2*$^{-/-}$ mice displayed an increased call rate at P4 and decreased call rate at P6 in comparison with their wild-type littermates (**Figure 2**). We also observed a decreased call rate in female interactions involving a *Shank2*$^{-/-}$ female in comparison with interactions involving a wild-type littermate (**Figure 2**). We examined the repertoire of the 5 different call categories. It appeared to be different between pups (for instance here P2, P6 and P10) and adults (**Figure 3**). Genotype-related differences were significant mostly in adulthood. During social interactions involving adult *Shank2*$^{-/-}$ males or females with a C57BL/6N female, more short calls and unstructured calls were recorded in comparison with interactions involving their wild-type littermates (**Figure 3D** and **E**). Less complex calls and frequency jumps calls were also recorded during interactions with a C57BL/6N female involving adult *Shank2*$^{-/-}$ females in comparison with interactions involving *Shank2*$^{+/+}$ females (**Figure 3E**). Finally, we also measured manually acoustic variables. There was no significant genotype-related difference during development. In contrast, the duration of calls recorded during interactions involving adult *Shank2*$^{-/-}$ females were shorter than those recorded during interactions involving their wild-type littermates (**Figure 4A**). We also highlighted that the peak frequency of ultrasonic vocalizations increased during pup development without significant genotype-related difference[26]. During interactions involving *Shank2*$^{-/-}$ males or females with a C57BL/6N female, ultrasonic vocalizations had a lower peak frequency in comparison with calls recorded during interactions involving their wild-type littermates (**Figure 4B**).

In addition, the present protocol also allowed to study the context of emission of ultrasonic vocalizations by combining the data from audio recordings to the behavioral data extracted from *MiceProfiler* (ICY software, Institut Pasteur, Paris). For instance, in female-female interactions, most ultrasonic vocalizations were emitted when animals were in contact and more specifically the occupant sniffing the new-comer's ano-genital region, or at least the occupant being behind the new-comer. Mice also emitted many ultrasonic vocalizations when the occupant approached the new-comer (**Figure 5**, upper panel). Less vocalizations were recorded when the occupant *Shank2*$^{-/-}$ mice were in physical contact with the new-comer (*e.g.*, sniffing the ano-genital region of the new-comer) than when the occupant was a wild-type mouse. Less vocalizations were triggered when the occupant behind the new-comer was a *Shank2*$^{-/-}$ mouse than when it was a wild-type mouse. More vocalizations were also recorded when the new-comer was in the visual field of the occupant mouse, and more so in the wild-types than in the mutants (**Figure 5**, lower panel).

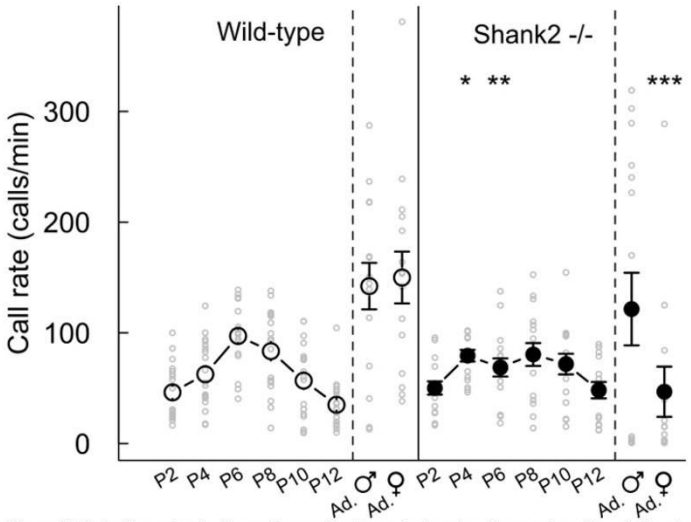

Figure 2: Emission rate of ultrasonic vocalizations during development and in adult male and female *Shank2*$^{-/-}$ mice and wild-type littermates. Call rate of pups (every two days from P2 to P12, n = 18-19 *Shank2*$^{+/+}$, n = 15-16 *Shank2*$^{-/-}$) and adults during male-estrus female interactions (n = 15 *Shank2*$^{+/+}$, n = 16 *Shank2*$^{-/-}$) and female-female interactions (n = 15 *Shank2*$^{+/+}$, n = 13 *Shank2*$^{-/-}$) in wild-type mice (left panel) and *Shank2*$^{-/-}$ mice (right panel). Data are presented as mean+/-SEM and individual points (non-paired Wilcoxon tests: *p <0.05, **p <0.01, ***p <0.001). Please click here to view a larger version of this figure.

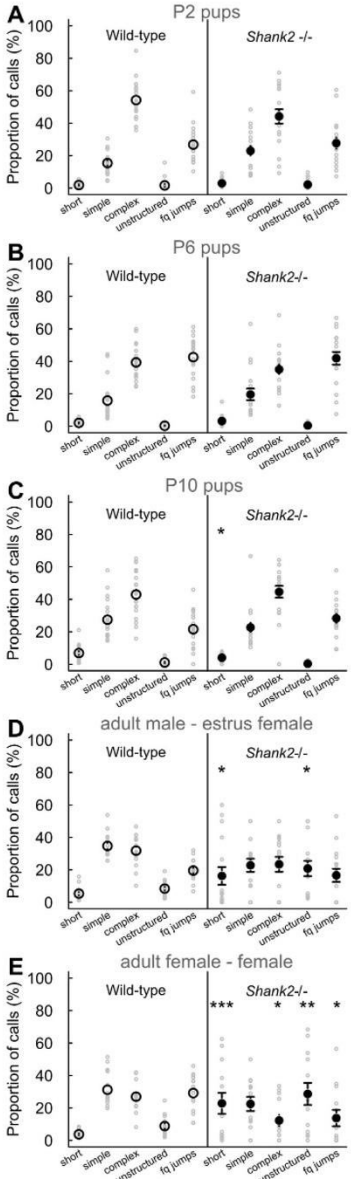

Figure 3: Vocal repertoire of *Shank2*$^{-/-}$ mice and wild-type littermates. Proportions of the five different call types emitted by P2 pups (**A**; n = 20 *Shank2*$^{+/+}$, n = 18 *Shank2*$^{-/-}$), P6 pups (**B**; n = 19 *Shank2*$^{+/+}$, n = 18 *Shank2*$^{-/-}$), P10 pups (**C**; n = 20 *Shank2*$^{+/+}$, n = 18 *Shank2*$^{-/-}$), adult males with an estrus female (**D**; n = 16 *Shank2*$^{+/+}$, n=16 *Shank2*$^{-/-}$) and adult females with another female (**E**; n = 15 *Shank2*$^{+/+}$, n=13 *Shank2*$^{-/-}$) in wild-type mice (left panels) and *Shank2*$^{-/-}$ mice (right panels). Data are presented as mean+/-SEM and individual points (chi-squared tests: *p <0.05, **p <0.01, ***p <0.001). Please click here to view a larger version of this figure.

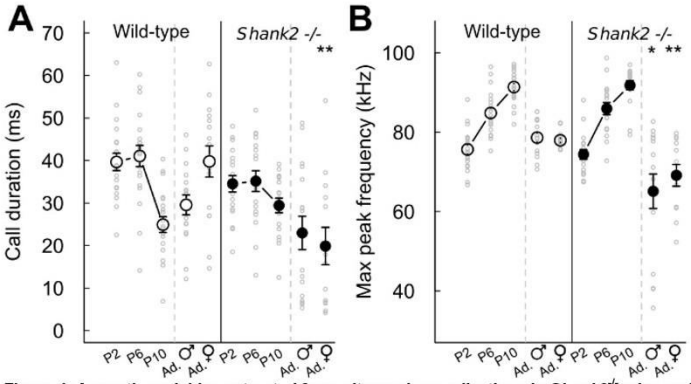

Figure 4: Acoustic variables extracted from ultrasonic vocalizations in *Shank2*$^{-/-}$ mice and wild-type littermates. (**A**) Duration of all call types confounded emitted by P2 pups (n = 20 *Shank2*$^{+/+}$, n = 18 *Shank2*$^{-/-}$), P6 pups (n = 19 *Shank2*$^{+/+}$, n = 18 *Shank2*$^{-/-}$), P10 pups (n = 20 *Shank2*$^{+/+}$, n = 18 *Shank2*$^{-/-}$), adult males with an estrus female (n = 16 *Shank2*$^{+/+}$, n = 16 *Shank2*$^{-/-}$) and adult females with another female (n = 15 *Shank2*$^{+/+}$, n = 13 *Shank2*$^{-/-}$) in wild-type mice (left panel) and *Shank2*$^{-/-}$ mice (right panel). (**B**) Maximum peak frequency measured on all call types confounded in P2 pups, P6 pups, P10 pups, adult males with an estrus female and adult female with another female (same Ns as above). Data are presented as mean+/-SEM and individual points (non-paired Wilcoxon tests: *p <0.05, **p <0.01, ***p <0.001). Please click here to view a larger version of this figure.

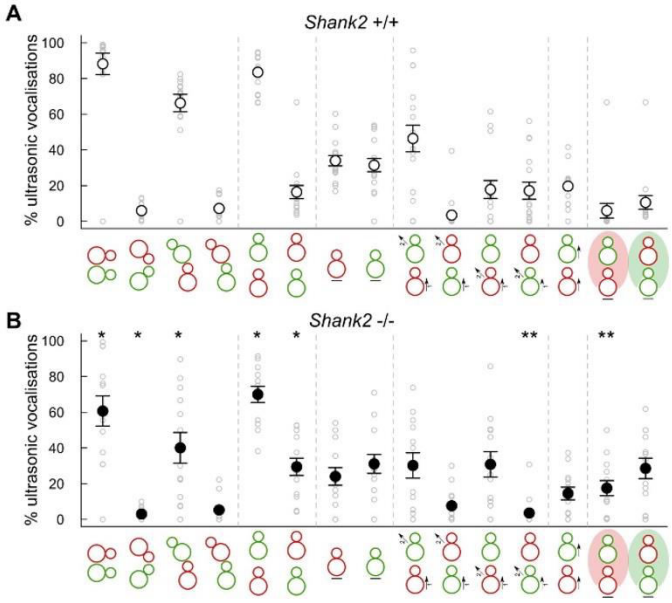

Figure 5: Contexts of emission of mouse ultrasonic vocalizations in female-female adult social interactions. Proportion of ultrasonic vocalizations emitted by pairs involving a *Shank2*$^{+/+}$ with a C57BL/6N mouse (n = 16, **A**) and pairs involving a *Shank2*$^{-/-}$ with a C57BL/6N mouse (n = 13, **B**) during the following types of behavioral events (red: occupant, green: new-comer): social contacts, oro-oral contact, ano-genital sniffing from the occupant mouse, ano-genital sniffing from the new-comer mouse, occupant behind new-comer, new-comer behind occupant, immobility of occupant, immobility of new-comer, approach from the occupant & escape from the new-comer, approach from the new-comer & escape from the occupant, approach & escape from the occupant, approach & escape from the new-comer, occupant following the new-comer, new-comer in the vision field of occupant, occupant in the vision field of new-comer. Data are presented as mean+/-SEM and individual points (non-paired Wilcoxon tests: *p <0.05, **p <0.01). Unpublished data. Please click here to view a larger version of this figure.

Call types	Description
short	duration ≤5 msec and frequency range ≤6.25 kHz
simple	duration >5 msec and frequency range ≤6.25 kHz (flat), or frequency modulation in only one direction (upward or downward) with frequency range >6.25 kHz
complex	frequency modulations in more than one direction and frequency range >6.25 kHz (modulated), or inclusion of one or more additional frequency component (harmonic or non-linear phenomena, but no saturation) but no constraint on frequency range (complex)
frequency jumps	inclusion of one jump (one frequency jump) or more jumps (frequency jumps, others) in frequency without time gap between the consecutive frequency components, with (mixed) or without any noisy part within the pure tone call
unstructured	no pure tone component identifiable; "noisy" calls

Table 1: Characteristics of five types of mouse ultrasonic vocalizations. Examples of criteria of duration, frequency range, frequency modulations and frequency jumps used to determine 5 different call types within mouse ultrasonic vocalizations.

Discussion

The protocol presented here provides standardized and reliable ways to collect mouse ultrasonic vocalizations in the laboratory. These very constrained situations present the advantage of standardization. They are used with success to compare strains or genotypes within strains[18,19,26,27]. As presented in the representative results, these methods allow the identification of atypical social communication in mice mutated for *Shank2*, a gene associated with autism spectrum disorders. Comparisons between mouse strains, between different contexts or even between laboratories will be triggered by the availability of larger datasets on the *mouseTube* database. This tool should boost studies on mouse ultrasonic vocalizations by allowing multivariate analyzes.

The protocols described here are optimized to test mice of different genotypes within a strain, as it is done in the majority of studies modeling the genetic contribution to neuropsychiatric disorders. It is recommended to experimentally design each study to have the best controls possible. Indeed, litter effects might mask or artificially inflate genetic effects[28,29]. It is therefore advisable to include littermate controls for each genotype. Breeding heterozygous parents should therefore be favored, since it will allow the correct matching of mutant and control mice within a litter. This justifies the paw tattoo marking of all pups (blinded to genotype) to track individuals throughout the recordings every two days. Genotyping is done at weaning, by taking tail samples. When recording pup isolation calls from P2 on, we would not recommend taking tail samples already in pups, since this operation includes supplementary manipulation and stress very close in time to a recording session.

The protocols suggested here to elicit ultrasonic vocalizations in adults does not allow clear identification of the emitter of the vocalizations. This explains why we manipulate the motivation of the test animal. Indeed, the test mice are isolated and not the new-comer and the test animals habituate for a long time to the test cage during same-sex interactions. In male-female interactions, the introduced female is not isolated and the test male habituates for shorter time since motivation might be higher in this sexual context. These manipulations of motivation should maximize the probability of the test mouse emitting the vocalizations and not the introduced one. To record male ultrasonic vocalizations in a sexual context, a simple cotton swab with fresh (*i.e.*, not frozen) urine of an estrus female can also be introduced in the cage[30]. This method allows the assignment of ultrasonic vocalizations to the test male with 100% certainty but it prevents collecting any specific information about the actual social context of emission of these vocalizations. Therefore, we favor the protocol described here (with a freely-moving estrus female). We also recommend to always use introduced mice from the same strain when testing mice from a mutant strain and to analyze the data as a pair of mice vocalizing. One recent study promotes the use of triangulation to localize the emitter[31]. In this study, females were found to also emit ultrasonic vocalizations during encounters with a male. This might be explained by the fact that they were isolated for at least two weeks before the recording session. The generalization of the use of the triangulation proposed in this study should nevertheless allow identification of the emitter of the vocalizations in most cases if video recordings are properly synced.

The isolation calls from pups recorded during development are not disturbed by background noise from the bedding. Usually an automatic analysis works very well to extract the main variables. In contrast, vocalizations recorded from adults are disturbed by background noise from the animals moving in the bedding. Automatic analysis might fail, and therefore manual analysis should be used. Nevertheless, adding bedding in the test cage should provide conditions that are less stressful for the animals than bare soil (that mice do not like). Further efforts in the community are concentrated on improving the automatic detection of ultrasonic vocalizations under various conditions, even those implying background noises. For instance, the VoICE software allows to analyze vocalizations that had been manually selected for the absence of background noise[32]. In this software, the extraction of the acoustic variables is automatic but needs the initial manual selection.

It should be noted that the inter-individual variability is very important in the vocal behavior of mice. For instance, the call rate of adult males in presence of an estrus female is very distributed (**Figure 1**). We suggest these standardized protocols to elicit ultrasonic vocalizations already to limit the variability related to the experimental context. Nevertheless, we would like to point out the importance of presenting not only the mean and SEM for the data, but most importantly the individual points in samples of small size[33]. It is also very relevant — if not necessary — to record at least 12 individuals of each group/genotype to gather representative data. In many cases, the inter-individual variability should not be hidden (usually it cannot be), and it might be of high importance to identify individuals carrying the genetic mutation studied but not displaying any atypical phenotype. Such individuals could provide clues about compensations, which might open new pathways for therapies of genetic disorders.

In most behavioral characterizations of mouse models for neuropsychiatric disorders, vocal behavior and social contacts are considered apart (*e.g.*,[19,27,34,35]). Recent analysis methods now provide a semi-automatic detailed characterization of the social events and sequences of events during an interaction (using *MiceProfiler* for instance)[36], as well as the possibility to combine this analysis with data from audio recordings. The main advantage of this method is to provide a comprehensive view of the social communication in mouse models of ASD, to more precisely identify which aspects of social communication are affected. In the present protocol the synchronization is still manual but this can be improved by triggering the video recording through the audio recording software. This type of analyses should become the standard to provide a more comprehensive view of social communication deficits in mouse models of neuropsychiatric disorders. In addition, up to now, vocal signals are mostly analyzed from the emitter side (*i.e.*, tests are built to favor the emission of vocal signals by the tested mouse, as in the present protocols). The focus should now also be set on the receiver of these signals, to better identify the functions of these acoustic signals. This should be done by evaluating also the behavior of the new-comer mice in the present protocols in adults (using *MiceProfiler* for instance)[36], by using playback experiments[16], or by setting up new protocols. Indeed, the present protocols provide very constrained situations that might not reflect the exact ethological conditions of vocalization emission in mice. The spontaneous emission of ultrasonic vocalizations will have to be better-characterized using continuous audio and video recordings to shed more light on the spontaneous vocal behavior of mice.

Disclosures

The authors have nothing to disclose.

Acknowledgements

This work was supported by the Fondation de France; by the ANR FLEXNEURIM [ANR09BLAN034003]; by the ANR [ANR- 08-MNPS-037-01-SynGen]; by Neuron-ERANET (EUHF-AUTISM); by the Fondation Orange; by the Fondation FondaMentale; by the Fondation de France; by the Fondation Bettencourt-Schueller. The research leading to this article has also received support from the Innovative Medicine Initiative Joint Undertaking under grant agreement no. 115300, resources of which are composed of financial contribution from the European Union's Seventh Framework Program (FP7/2007-2013) and EFPIA companies' in kind contribution. We thank Julie Lévi-Strauss for helpful comments on the manuscript and six anonymous reviewers whose comments noticeably improved the manuscript.

References

1. American Psychiatric Association. *Diagnostic and Statistical Manual of Mental Disorders, Fifth Edition (DSM-V).* (2013).
2. Ey, E., Leblond, C. S., & Bourgeron, T. Behavioral Profiles of Mouse Models for Autism Spectrum Disorders. *Autism Res.* **4** (1), 5-16 (2011).
3. Bourgeron, T., Jamain, S., & Granon, S. Animal Models of Autism - Proposed Behavioral Paradigms and Biological Studies. *Contemporary Clinical Neuroscience: Transgenic and Knockout Models of Neuropsychiatric Disorders.* 151-174 (2006).
4. Scattoni, M. L., Crawley, J., & Ricceri, L. Ultrasonic vocalizations: A tool for behavioural phenotyping of mouse models of neurodevelopmental disorders. *Neurosci. Biobehav. Rev.* **33** (4), 508-515 (2009).
5. Portfors, C. V., & Perkel, D. J. The role of ultrasonic vocalizations in mouse communication. *Cur. Opin. Neurobiol.* **28**, 115-120 (2014).
6. Arriaga, G., Zhou, E. P., & Jarvis, E. D. Of mice, birds, and men: the mouse ultrasonic song system has some features similar to humans and song-learning birds. *PLOS ONE.* **7**, e46610 (2012).
7. Hammerschmidt, K., Schreiweis, C., Minge, C., Pääbo, S., Fischer, J., & Enard, W. A humanized version of Foxp2 does not affect ultrasonic vocalization in adult mice: Ultrasonic vocalization of "humanized" FoxP2 mice. *Genes Brain Behav.* (2015).
8. Portfors, C. V. Types and functions of ultrasonic vocalizations in laboratory rats and mice. *J. Am. Assoc. Lab. Anim. Sci.* **46**, 28-34 (2007).
9. Panksepp, J. B., *et al.* Affiliative Behavior, Ultrasonic Communication and Social Reward Are Influenced by Genetic Variation in Adolescent Mice. *PLOS ONE.* **2** (2007).
10. Zippelius, H.-M., & Schleidt, W. M. Ultraschall-Laute bei jungen Mäusen. *Naturwissenschaften.* **43**, 502 (1956).
11. Whitney, G., Coble, J. R., Stockton, M. D., & Tilson, E. F. Ultrasonic emissions: do they facilitate courtship of mice. *J. Comp. Physiol. Psychol.* **84**, 445-452 (1973).
12. Holy, T. E., & Guo, Z. S. Ultrasonic songs of male mice. *PLOS Biol.* **3**, 2177-2186 (2005).
13. Maggio, J. C., & Whitney, G. Ultrasonic vocalizing by adult female mice (Mus musculus). *J. Comp. Psychol.* **99**, 420-436 (1985).
14. Chabout, J., *et al.* Adult Male Mice Emit Context-Specific Ultrasonic Vocalizations That Are Modulated by Prior Isolation or Group Rearing Environment. *PLOS ONE.* **7** (1), e29401 (2012).
15. Hammerschmidt, K., Radyushkin, K., Ehrenreich, H., & Fischer, J. Female mice respond to male ultrasonic "songs" with approach behaviour. *Biol. Lett.* **5**, 589-592 (2009).
16. Wöhr, M., Moles, A., Schwarting, R. K. W., & D'Amato, F. R. Lack of social exploratory activation in male -opioid receptor KO mice in response to playback of female ultrasonic vocalizations. *Soc. Neurosci.* **6**, 76-87 (2011).
17. Granon, S., Faure, P., & Changeux, J.-P. Executive and social behaviors under nicotinic receptor regulation. *Proc. Nat. Acad. Sci.* **100** (16), 9596-9601 (2003).
18. Schmeisser, M. J., *et al.* Autistic-like behaviours and hyperactivity in mice lacking ProSAP1/Shank2. *Nature* **486** (7402), 256-260 (2012).
19. Ey, E., *et al.* Absence of Deficits in Social Behaviors and Ultrasonic Vocalizations in Later Generations of Mice Lacking Neuroligin4. *Genes Brain Behav.* **11**, 928-941 (2012).
20. Chadman, K. K., *et al.* Minimal Aberrant Behavioral Phenotypes of Neuroligin-3 R451C Knockin Mice. *Autism Res.* **1**, 147-158 (2008).
21. Scattoni, M. L., Gandhy, S. U., Ricceri, L., & Crawley, J. N. Unusual Repertoire of Vocalizations in the BTBR T plus tf/J Mouse Model of Autism. *PLOS ONE.* **3** (2008).
22. De Chaumont, F., Coura, R. D.-S., *et al.* Computerized video analysis of social interactions in mice. *Nat. Methods* **9**, 410-417 (2012).
23. Leblond, C. S., *et al.* Genetic and Functional Analyses of SHANK2 Mutations Suggest a Multiple Hit Model of Autism Spectrum Disorders. *PLOS Genet.* **8** (2), e1002521 (2012).
24. Berkel, S., *et al.* Mutations in the SHANK2 synaptic scaffolding gene in autism spectrum disorder and mental retardation. *Nat. Genet.* **42**, 489-491 (2010).

25. Pinto, D., *et al.* Functional impact of global rare copy number variation in autism spectrum disorders. *Nature* **466**, 368-372 (2010).
26. Ey, E., *et al.* The autism ProSAP1/Shank2 mouse model displays quantitative and structural abnormalities in ultrasonic vocalisations. *Behav. Brain Res.* **256**, 677-689 (2013).
27. Scattoni, M. L., Ricceri, L., & Crawley, J. N. Unusual repertoire of vocalizations in adult BTBR T plus tf/J mice during three types of social encounters. *Genes Brain Behav.* **10**, 44-56 (2010).
28. Zorrilla, E. P. Multiparous species present problems (and possibilities) to developmentalists. *Dev. Psychobiol.* **30** (2), 141-150 (1997).
29. Lazic, S. E., & Essioux, L. Improving basic and translational science by accounting for litter-to-litter variation in animal models. *BMC Neurosci.* **14** (1), 37 (2013).
30. Hoffmann, F., Musolf, K., & Penn, D. J. Freezing urine reduces its efficacy for eliciting ultrasonic vocalizations from male mice. *Physiol. Behav.* **96**, 602-605 (2009).
31. Neunuebel, J. P., Taylor, A. L., Arthur, B. J., & Egnor, S. R. Female mice ultrasonically interact with males during courtship displays. *eLife.* **4** (2015).
32. Burkett, Z. D., Day, N. F., Peñagarikano, O., Geschwind, D. H., & White, S. A. VoICE: A semi-automated pipeline for standardizing vocal analysis across models. *Sci. Rep.* **5**, 10237 (2015).
33. Weissgerber, T. L., Milic, N. M., Winham, S. J., & Garovic, V. D. Beyond Bar and Line Graphs: Time for a New Data Presentation Paradigm. *PLOS Biol.* **13** (4), e1002128 (2015).
34. Jamain, S., *et al.* Reduced social interaction and ultrasonic communication in a mouse model of monogenic heritable autism. *Proc. Nat. Acad. Sci. U. S. A.* **105**, 1710-1715 (2008).
35. Won, H., *et al.* Autistic-like social behaviour in Shank2-mutant mice improved by restoring NMDA receptor function. *Nature* **486**, 261-265 (2012).
36. Ferhat, A.-T., Le Sourd, A.-M., de Chaumont, F., Olivo-Marin, J.-C., Bourgeron, T., & Ey, E. Social Communication in Mice - Are There Optimal Cage Conditions? *PLOS ONE.* **10** (3), e0121802 (2015).

III. Review: “Chapter 5: Behavioural Phenotypes and Neural Circuit Dysfunctions in Mouse Models of Autism Spectrum Disorder”

Allain-Thibeault Ferhat, Sonja Halbedl, Michael J. Schmeisser, Martien J. Kas, Thomas Bourgeron, and Elodie Ey

Chapter 5
Behavioural Phenotypes and Neural Circuit Dysfunctions in Mouse Models of Autism Spectrum Disorder

Allain-Thibeault Ferhat, Sonja Halbedl, Michael J. Schmeisser, Martien J. Kas, Thomas Bourgeron, and Elodie Ey

5.1 Introduction

Autism spectrum disorder (ASD) represents a heterogeneous group of neurodevelopmental disorders characterised by alterations in social behaviours including social interaction and social communication and stereotyped behavioural patterns and restricted interests (American Psychiatric Association 2013). These

---

Allain-Thibeault Ferhat and Sonja Halbedl are equally contributing authors.

A.-T. Ferhat • E. Ey (✉)
Human Genetics and Cognitive Functions Unit, Institut Pasteur, Paris, France

CNRS UMR 3571 Genes, Synapses and Cognition, Institut Pasteur, Paris, France

Human Genetics and Cognitive Functions, University Paris Diderot, Sorbonne Paris Cité, Paris, France
e-mail: elodie.ey@pasteur.fr

S. Halbedl
Institute for Anatomy and Cell Biology, Ulm University, Ulm, Germany

International Graduate School in Molecular Medicine, Ulm University, Ulm, Germany

M.J. Schmeisser
Institute for Anatomy and Cell Biology, Ulm University, Ulm, Germany

Division of Neuroanatomy, Institute of Anatomy, Otto-von-Guericke University Magdeburg, Magdeburg, Germany

Leibniz Institute for Neurobiology, Magdeburg, Germany

M.J. Kas
Department of Translational Neuroscience, Brain Center Rudolf Magnus, University Medical Center Utrecht, Utrecht, The Netherlands

Groningen Institute for Evolutionary Life Sciences, University of Groningen, Groningen, The Netherlands

M.J. Schmeisser, T.M. Boeckers (eds.), *Translational Anatomy and Cell Biology of Autism Spectrum Disorder*, Advances in Anatomy, Embryology and Cell Biology 224, DOI 10.1007/978-3-319-52498-6_5

disorders affect more than one person in a hundred (Elsabbagh et al. 2012; US Department of Health and Human Services 2014). The most frequent comorbidities are epilepsy, attention deficit and hyperactivity disorder (ADHD) and sleep and anxiety disorders. Several hundred genes have been associated with ASD, and the majority of them encode chromatin remodelling and synaptic proteins (Toro et al. 2010; Huguet et al. 2013; Bourgeron 2015). These proteins are involved in neuronal activity-dependent gene regulation and synaptic plasticity (Bourgeron 2015). At the synapse, mutations affect cell adhesion molecules (*NLGN1-4*, *NRXN1-2*, *CNTN4-6*, *CNTNAP2-4*), scaffolding proteins (*SHANK1-3*) or channels and receptors involved in synaptic transmission (*CACNA1*, *GRIN2B*, *GABRB3*, *GABRA3*).

Mouse models carrying mutations in the murine orthologous genes were generated to better understand the mechanisms leading to ASD-like traits (Crawley 2012). These models should also facilitate the understanding of the different neuronal circuits mediating ASD-related phenotypes. At the behavioural level, two core symptoms of ASD can be evaluated in mice, namely, impaired social interactions and stereotyped behaviours (Silverman et al. 2010). Adding to a previous review on mouse models of ASD (Ey et al. 2011), we will focus on social behaviours and stereotyped behaviours and will further aim at linking them with functional and structural impairments.

5.2 Social Behaviours

In social interactions, two aspects can be distinguished. First, social motivation reflects the interest to interact with a conspecific, as shown by the active seeking of social contacts. This is usually measured by the time spent in contact with another mouse. Second, social recognition reflects the ability to distinguish between conspecifics as shown by different behavioural reactions to different individuals. This is usually measured by the decrease of sniffing duration over successive presentations of a conspecific. Social interactions are regulated by social signals, forming social communication. In mice, these signals include ultrasonic vocalisations, odours, pheromones, tactile stimuli involving whisking and body contacts and visual signals using body postures (Latham and Mason 2004; Brennan and Kendrick 2006; Portfors 2007).

Thomas Bourgeron
Human Genetics and Cognitive Functions Unit, Institut Pasteur, Paris, France

CNRS UMR 3571 Genes, Synapses and Cognition, Institut Pasteur, Paris, France

Human Genetics and Cognitive Functions, University Paris Diderot, Sorbonne Paris Cité, Paris, France

FondaMental Foundation, Créteil, France

Gillberg Neuropsychiatry Centre, Sahlgrenska Academy, University of Gothenburg, Gothenburg, Sweden

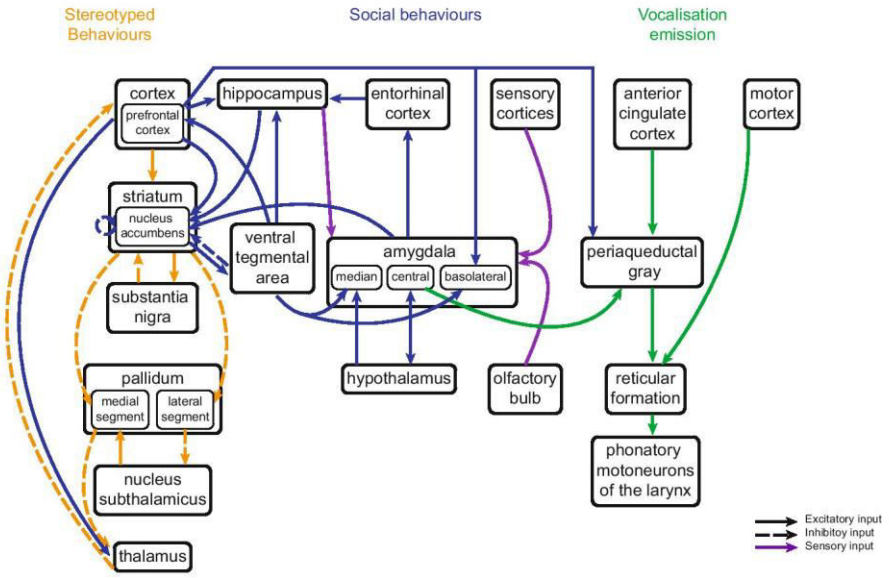

Fig. 5.1 Cortical and subcortical neuronal circuits involved in stereotyped behaviour (*left panel*), social behaviours (*central panel*) and vocal behaviour (*right panel*)

Social behaviours involve complex structural connections within the brain (Fig. 5.1; summary based on Kas et al. 2014; Wang et al. 2014a, b; Soden et al. 2016 for social interactions, and Jürgens 2002, 2009; Arriaga et al. 2012 for ultrasonic vocalisation emission).

Social interactions can have a positive or negative valence. The amygdala plays a crucial role in processing this valence in emotion-based social interactions, such as arousal, freezing and aggression. The medial amygdala is activated by positive or negative socially relevant stimuli, used in social recognition (Bosch and Neumann 2012). Oxytocin, one of the major neurotransmitters in the amygdala, favours social recognition and social bonding (Ferguson et al. 2000). The medial amygdala receives sensory information from the olfactory bulb (Keverne 1999), the preoptic area or the septum (Popik and van Ree 1991). The basolateral amygdala is involved in the processing of emotional stimuli like fear (Maren 2003). This structure projects to the mesolimbic system via the nucleus accumbens to reinforce social stimuli. It also projects to the brainstem, the entorhinal cortex (involved in the assessment of familiarity in stimuli), the prefrontal cortex (social hierarchy), the midbrain reticular formation and the periaqueductal grey (Price 2006). The activity of the amygdala is modulated by reciprocal connections with the hypothalamus.

The hypothalamus integrates cues about the external social environment and the internal evaluation of the affective state (Kruk et al. 1979). It is involved in the choice of the appropriate type of interaction that should be initiated. The medial amygdala projects to the hypothalamus, sending information about the valence of the stimuli, while the hypothalamus projects back on the medial amygdala and the

central amygdala to switch between aggressive and affiliative responses (Veening et al. 2005). The hypothalamus also projects to the nucleus accumbens.

The nucleus accumbens is part of the mesolimbic dopamine system, which reinforces functional social behaviours (Chevallier et al. 2012). It has reciprocal connections with the ventral tegmental area and the ventromedial prefrontal cortex, two other parts of the mesolimbic dopamine system (Russo and Nestler 2013). This system, also called the reward system, is involved in the mediation of social investigation, mating, maternal behaviour and formation of pair bonds (Robinson et al. 2011; Kohls et al. 2013).

The prefrontal cortex organises the temporal sequences of actions, taking into account the rapid changes in the social environment and in the emotional state of the animal (Fuster 2008). The dorsomedial prefrontal cortex, one of the major structures implicated in the establishment and maintenance of social hierarchy and dominance among littermates, projects to the basolateral amygdala (Wang et al. 2014a).

In mice, ultrasonic vocalisations are considered to be innate with very few if any evidence of learning (Hammerschmidt et al. 2012; Portfors and Perkel 2014). Mice voluntarily control the emission or absence of emission of a vocalisation through the anterior cingulate cortex, projecting to the periaqueductal grey, which itself projects to the reticular formation towards phonatory motoneurons. It is still unclear whether mouse ultrasonic vocalisations can be voluntarily modulated by the motor cortex (acting on phonatory motoneurons) (Hammerschmidt et al. 2015).

5.3 Stereotyped Behaviours

Stereotyped behaviours occur in mice under different forms: excessive self-grooming, repetitive climbing, rearing or jumping in specific locations of the cage and atypical digging in the bedding (Kelley 2001; Lewis et al. 2007). Stereotyped behaviours vary in kind but also in degree. For instance, some mouse strains mutated in ASD-risk genes perform self-grooming behaviours to such an extent that they get self-injured (e.g. *Shank3* mutant mice, Peça et al. 2011).

The basal ganglia play a crucial role in the development of stereotyped behaviours (Fig. 5.1). These structures include the striatum (caudate nucleus and putamen; e.g. Langen et al. 2011), the pallidum (globus pallidus), the nucleus subthalamus and the substantia nigra and are functionally interconnected. The basal ganglia are involved in fine-tuning of the motor impulse. Cortical and subcortical structures such as the hippocampus and the amygdala are also involved in the emergence of stereotyped behaviours (Bachevalier 1996). Cortico-striatal circuits receive multiple inputs, and each loop consists of two distinct pathways: the striatonigral "direct pathway" and the striatopallidal "indirect pathway". Activation of the direct pathway results in an increase in thalamic activity, whereas activation of the indirect pathway results in thalamic inhibition. This means that under normal circumstances the direct pathway enhances specific movement behaviour, while the

indirect pathway inhibits specific movement. The cortico-striatal circuitry can be manipulated by targeting agents, which bind to inhibitory GABA receptors or to excitatory glutamate receptors (e.g. Presti et al. 2004). Dopaminergic drugs can also modulate stereotypic behaviours by stimulating the direct pathway or inhibiting the indirect pathway (Presti et al. 2003; Mason and Rushen 2006). Taken together, the basal ganglia are involved in fine-tuning of the required movement via the direct (activation) and indirect (inhibition) pathways. Any imbalance in those circuits can result in the emergence of stereotyped behaviours.

5.4 Meta-Analysis of ASD Mouse Models

For our meta-analysis, we scanned and collected literature from the PubMed (NCBI) database and from Web of Science. We used combinations of the following keywords: "*Nrxn1*", "*Nrxn2*", "*Nlgn1*", "*Nlgn2*", "*Nlgn3*", "*Nlgn4*", "*Shank1*", "*Shank2*", "*Shank3*", "*Cntnap2*", "*Cntnap4*", "*Cntn4*", "*Big2*", "*Cntn5*", "*NB-2*", "*Cntn6*", "*NB-3*", "*Cacna1*", "*Grin2b*", "*Gabrb3*", "*Gabra3*", "*Glra2*", "autism", "ASD", "behaviour", "mouse model" and "social". We only gathered and analysed the main studies for mouse models carrying mutations in synaptic channels and receptors, given the high number of articles for these models. For the present study, we gathered data from all age classes (pups, juveniles, adults), even if data were unbalanced for each age class.

We synthesised data on behavioural, structural and functional aspects into a table (available upon request to the corresponding author), according to the construction characteristics of the model (e.g. knockout, conditional knockout, knock-in, duplication, deletion and overexpression), the genetic background (using the MGI database) and the phenotypical traits studied. For the structural and functional aspects, we examined brain anatomy, protein expression in the different brain regions and synaptic physiology. For the behavioural aspects, we took into account social interactions (motivation and recognition) and communication as well as stereotypes.

To conduct a clustering analysis, we scored the data with the following criteria. When the trait was not examined in the model, the score was NA. These missing data were not considered. When the mutant mice did not differ significantly from wild-type animals, the score was 1. When the mutant mice differed significantly from wild-type animals (either significantly higher and/or lower performances/scores in mutant than in wild-type animals), the score was 2. When differences between mutant and wild-type mice diverged between studies (no significant difference and significantly higher and/or lower performances/scores in mutant than in wild-type animals), the score was 1.5.

Clustering was performed with the statistical software R (R Core Team (2016)) by using the *heatmap.2* function. This function connects the most similar mouse models according to the scoring of each trait. In the complete data set, the amount of missing data was large. To reduce the bias of clustering according to missing data,

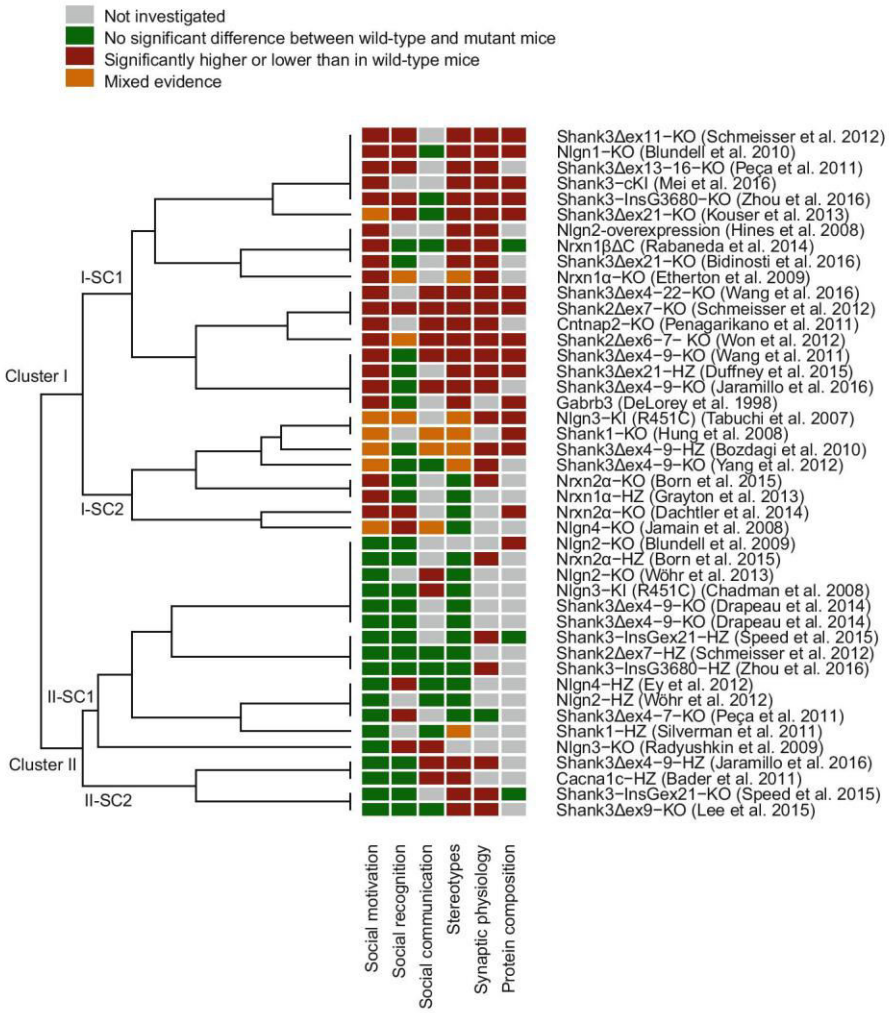

Fig. 5.2 Heatmap representation of the clustering of mouse models for ASD carrying mutations in synaptic proteins and their phenotypic traits as indicated (social interest/motivation, social recognition, social communication, stereotypes, synaptic physiology, protein composition)

we conducted the clustering analysis with the most extensively studied models (three or more behavioural and/or structural and functional traits tested). Most models with mutations in genes encoding synaptic channels and receptors failed to reach the threshold. The most extensively studied mouse models carried mutations in cell adhesion and scaffolding proteins. The heatmap (Fig. 5.2) distinguished two main clusters. The first one encompassed two subclusters (I-SC1 and I-SC2) and the second one also two subclusters (II-SC1 and II-SC2).

5.4.1 Cluster I

Cluster I includes mouse models affected in almost all traits examined. Compared to wild-type littermates, the majority of these mutant mice display reduced social interest, increased stereotyped behaviours and impaired synaptic physiology and atypical synaptic protein composition in the brain regions examined.

The *subcluster I-SC1* includes 18 animal models [*Shank3-cKI* (Mei et al. 2016), *Nlgn1-KO* (Blundell et al. 2010), *Shank3Δex11-KO* (Schmeisser et al. 2012; Vicidomini et al. 2016), *Shank3-InsG3680* (Zhou et al. 2016), *Shank3Δex13-16-KO* (Peça *et al*. 2011), *Shank3Δex21-KO* (Kouser et al. 2013; Duffney et al. 2015), *Nlgn2* overexpression (Hines et al. 2008), *Nrxn1βΔC* (Rabaneda et al. 2014), *Shank3Δex21-KO* (Bidinosti et al. 2016), *Nrxn1α-KO* (Etherton et al. 2009; Grayton et al. 2013), *Shank3Δex4-22-KO* (Wang et al. 2016), *Shank2Δex7-KO* (Schmeisser et al. 2012; Ey et al. 2013; Ferhat et al. 2016), *Cntnap2-KO* (Peñagarikano et al. 2011, 2015), *Shank2Δex6-7-KO* (Won et al. 2012; Lee et al. 2015a), *Shank3Δex4-9*-KO (Wang et al. 2011, 2014b), *Shank3Δex21-HZ*, *Shank3Δex4-9-KO* (Jaramillo et al. 2016), *Gabrb3-KO* (DeLorey et al. 1998, 2008)]. All models of the subcluster I-SC1 displayed a decrease in social interest; only one of the *Shank3Δex21-KO* mutant lines (Kouser et al. 2013; Duffney et al. 2015) displayed mixed evidence for impairment in social motivation in comparison with wild-type mice. Furthermore, only *Shank3Δex11-KO* (Schmeisser et al. 2012; Vicidomini et al. 2016), *Shank3-InsG3680* (Zhou et al. 2016), *Shank3Δex13-16-KO* (Peça et al. 2011) and both *Shank2Δex7-KO* (Schmeisser et al. 2012; Won et al. 2012; Ey et al. 2013; Lee et al. 2015a; Ferhat et al. 2016), *Nlgn1-KO* (Blundell et al. 2010), *Shank3Δex21-KO* (Kouser et al. 2013; Duffney et al. 2015) and *Nrxn1α-KO* (Etherton et al. 2009; Grayton et al. 2013) models displayed significant (or limited) decrease in social recognition in comparison with wild-type littermates.

All models also displayed high level of stereotypy such as self-grooming or jumping behaviour. Synaptic physiology was predominantly analysed in defined areas of the cortex or in the hippocampus. Most models displayed a decrease in miniature excitatory postsynaptic current (mEPSC) or field excitatory postsynaptic potential (fEPSP), except for *Nlgn2*-overexpression (Hines et al. 2008) that showed an increase in miniature inhibitory postsynaptic currents (mIPSC), in comparison with wild-type littermates. Six out of ten models investigated for social communication displayed a significantly lower call rate in comparison with wild-type littermates [*Shank3Δex4-9-KO* (Wang et al. 2011; Wang et al. 2014b), *Shank3Δex4-9-KO* (Jaramillo et al. 2016), *Shank3Δex4-22-KO* (Wang et al. 2016), *Cntnap2-KO* (Peñagarikano et al. 2011, 2015)]. Interestingly, the characterisation of the *Nrxn1α-KO* model (Etherton et al. 2009; Grayton et al. 2013) resulted in divergent results between laboratories for social recognition and stereotyped behaviours.

The *subcluster I-SC2* includes eight well-characterised mouse models [*Nlgn3-R451-KI* (Tabuchi et al. 2007; Ellegood et al. 2011; Etherton et al. 2011; Karvat and Kimchi 2012; Kumar et al. 2014; Steadman et al. 2014; Burrows et al. 2015),

Shank1-KO (Hung et al. 2008; Roullet et al. 2009; Silverman et al. 2011; Sungur et al. 2014; Wöhr 2014), *Shank3Δex4-9-HZ* (Bozdagi et al. 2010; Yang et al. 2012; Drapeau et al. 2014), *Shank3Δex4-9-KO* (Yang et al. 2012), *Nrxn2α-KO* (Born et al. 2015), *Nrxn1α-HZ* (Grayton et al. 2013), *Nrxn2α-KO* (Dachtler et al. 2014) and *Nlgn4-KO* (Jamain et al. 2008; Ey et al. 2012; Ju et al. 2014)]. These models are the ones with either divergent behavioural characterisation between studies or impaired social interactions, but non-significant or divergent differences in stereotyped behaviours. Interestingly, the divergences between studies mostly concern behavioural phenotypes (social interactions, communication, stereotyped behaviours), while results for synaptic physiology and protein composition were frequently convergent.

5.4.2 Cluster II

Cluster II includes mouse models with limited social impairments and stereotyped behaviours. Protein expression was rarely investigated in these models, and the majority of them was not characterised for synaptic physiology.

The *subcluster II-SC1* includes 14 mouse models with no significant impairment in social motivation and in stereotyped behaviours and a very limited characterisation of synaptic physiology [*Nlgn2-KO* (Blundell et al. 2009), *Nrxn2α-HZ* (Born et al. 2015), *Nlgn2-HZ and Nlgn2-KO* (Wöhr et al. 2013), *Nlgn3-R451-KI* (Chadman 2011), two models of *Shank3Δex4-9-KO* (Drapeau et al. 2014), *Shank3-InsGex21-HZ* (Speed et al. 2015), *Shank2Δex7-HZ* (Schmeisser et al. 2012; Ey et al. 2013), *Shank3-InsG3680-HZ (Zhou et al. 2016), Nlgn4-HZ* (Ey et al. 2012), *Shank3Δex4-7-KO* (Peça et al. 2011), *Shank1-HZ* (Silverman et al. 2011; Sungur et al. 2014) and *Nlgn3-KO* (Radyushkin et al. 2009)]. Surprisingly, only three models [*Nlgn3-KO* (Radyushkin et al. 2009), *Shank3Δex4-7-KO* (Peça et al. 2011), *Nlgn4-HZ* (Ey et al. 2012)] showed impaired social recognition, and three of them displayed a decreased rate of emission of ultrasonic vocalisations in comparison with wild-type mice [*Nlgn2-KO* (Wöhr et al. 2013), *Nlgn3-R451-KI* (Chadman 2011), *Nlgn3-KO* (Radyushkin et al. 2009)]. With respect to synaptic physiology, only two models displayed decreased basal transmission [*Nrxn2-HZ* mice (Born et al. 2015), *Shank3Δex4-7-KO* (Peça et al. 2011)].

The *subcluster II-SC2* includes *Shank3Δex4-9-HZ* (Jaramillo et al. 2016), *Cacna1c-HZ* (Bader et al. 2011), *Shank3Δex9-KO* (Lee et al. 2015b) and *Shank3-InsGex21-KO* (Speed et al. 2015). Two of these studies were performed on heterozygous mice. Impairments of synaptic physiology were detected in *Shank3Δex4-9-HZ* (Jaramillo et al. 2016), *Shank3Δex9-KO* (Lee et al. 2015b) and *Shank3-InsGex21-KO* (Speed et al. 2015). Stereotyped behaviours were also increased in comparison with wild-type mice in all of these models in three different tests, respectively, rearing, marbles burying and self-grooming.

Our meta-analysis provides an overview of the most extensively characterised mouse models carrying mutations in ASD-risk genes. Overall, atypical synaptic

physiology was coupled with increased stereotyped behaviours and to a lesser extent with atypical social motivation in most cases. This relationship did not hold for social recognition. Interestingly, the clustering using phenotypes did not cluster the mouse models according to their mutated genes.

5.5 Relating Behavioural Phenotypes with Structural and Functional Characteristics

One of our aims was to relate the different behavioural and structural aspects measured in mouse models of ASD to extract relevant relationships. The comparison of *Cluster I* and *Cluster II* leads to discuss the connection between the different traits measured. *Cluster I* includes models highly impaired in social interest, stereotyped behaviours, synaptic physiology and protein composition, while Cluster II includes much less impaired models. Only three models display impaired social interest without increased stereotyped behaviours [*Nrxn2α-KO* (Born et al. 2015), *Nrxn1α-HZ* (Grayton et al. 2013), *Nrxn2α-KO* (Dachtler et al. 2014)], and the four models from *II-SC2* display stereotyped behaviour without social interest impairment [*Shank3Δex4-9-HZ* (Jaramillo et al. 2016), *Cacna1c-HZ* (Bader et al. 2011), *Shank3Δex9-KO* (Lee et al. 2015b), *Shank3InsGex21-KO* (Speed et al. 2015)]. Social recognition impairments seem more variable, i.e., impaired social motivation does not mean impaired social recognition. Reversely, mouse models displaying abnormalities in synaptic physiology also display increased stereotyped behaviours. This relationship is weaker between impaired synaptic physiology and impaired social motivation. This observation can suggest that when basal circuits are deeply affected, the social motivation, but not social recognition domain, becomes affected.

We also aimed at identifying specific brain regions associated with either atypical social interactions or increased stereotyped behaviours. This was hindered by the fact that most studies analysed both structural and functional aspects only in the hippocampus (CA1, CA3 and dentate gyrus) and the cortex (sensorimotor area and prefrontal cortex). This is unfortunate especially because these brain structures are not the major ones implicated in social interactions and stereotyped behaviours. We therefore could not extract defined information about the links between brain regions and behavioural phenotypes. To link anatomical and physiological impairments with behaviours, other brain structures should be studied in the future, more specifically the striatum including the nucleus accumbens, the mesencephalon including the ventral tegmental area, the amygdala and the diencephalon. These brain regions represent relevant nodes forming a network involved in social and stereotyped behaviours. In most models, only one brain structure was studied; only few studies presented results obtained in several brain regions at the time. Standardised analyses from different brain regions and from different mouse models should allow a better understanding of the circuits affected.

5.6 Mouse Models Carrying Mutations in the *Shank* Genes

Over the last years, several mouse models with mutations in the family of *Shank* genes were published since approximately one per cent of patients with ASD carry a mutation in the *SHANK* gene family (Leblond et al. 2014). In this meta-analysis, 25 well-characterised and independent mouse models exhibited genetic disruption of *Shank1* (one knockout model and one heterozygous model), *Shank2* (two knockout models and one heterozygous model) or *Shank3* (14 knockout models, 1 knock-in and 5 heterozygous models). We tested whether phenotypic traits displayed some similarities between models carrying different mutations in the same gene family.

To date, only one *Shank1* mutant strain was reported (Hung et al. 2008). The heterozygous animals do not display any significant impairment in social interaction and communication but show a slight increase in stereotyped behaviours in old adults in comparison with wild-type littermates. In contrast, the homozygous mutant mice for *Shank1* display reduced scent-marking behaviour and atypical ultrasonic vocalisations but typical social interactions in comparison with wild-type littermates.

Two independent *Shank2* mutant strains display increased stereotyped behaviours, reduced social motivation and recognition as well as atypical social communication (Schmeisser et al. 2012; Won et al. 2012; Ey et al. 2013; Lee et al. 2015a; Ferhat et al. 2016). Although increased GluN1 expression was biochemically detected in both models at the juvenile stage (3–4 weeks), the lines display opposite results in synaptic physiology at CA1 synapses. While Won et al. (2012) and Lee et al. (2015a) identified a reduction in long-term potentiation (LTP), Schmeisser et al. (2012) highlighted an increase of LTP in comparison with wild-type littermates. These divergences remain to be elucidated.

The large panel of *Shank3* mutant models is highly interesting given that only the recent *Shank3Δex4-22-KO* is a complete knockout (Jiang and Ehlers 2013; Wang et al. 2016). The *Shank3* gene is transcribed from six promoters (Jiang and Ehlers 2013; Wang et al. 2014b), and therefore in most models some *Shank3* isoforms remain. The complete knockout model displays impairments in behavioural and synaptic traits examined (Wang et al. 2016), but the phenotypic difference with other *Shank3* mutant mice was not dramatic. Overall, the two traits observed in almost all *Shank3* mutant models are an increase in stereotyped behaviours, especially increased self-grooming, and reduced glutamatergic synaptic transmission tested mostly in the CA1 hippocampus. The presence of stereotyped behaviours seems to be more prominent in models expressing less isoforms (Peça et al. 2011; Schmeisser et al. 2012; Kouser et al. 2013; Bidinosti et al. 2016; Mei et al. 2016; Wang et al. 2016). Abnormalities in social interest are subtle, while reduced performances in social recognition do not appear to be a robust trait in these models. Protein composition at the synapse is disorganised, but it is not clearly related to the number of remaining isoforms.

Overall, *Shank3* mutant mice are best characterised by increased stereotyped behaviours and reduced glutamatergic synaptic transmission, while *Shank2* mutants are best characterised by increased stereotyped behaviours and reduced social motivation, but less obvious phenotypes in synaptic physiology. The stereotyped behaviours appear to be the trait most impacted by the modulation of the number of remaining isoforms in the *Shank3* mutant mice.

5.7 Refining the Analysis to Describe Behavioural Impairments

In mouse behavioural testing, different protocols are supposed to measure similar traits. For example, interest for social interactions or social motivation can be quantified in the three-chambered test or in free same-sex interaction. However, some studies conducting these different experiments on identical mouse models did not lead to the same conclusions. For example, *Shank2* mutant mice (Schmeisser et al. 2012) display a reduction of the interest for a conspecific during free interaction, but no significant reduction of this social interest during the first phase of three-chambered test in comparison with wild-type mice. The use of different protocols can explain the divergence between results obtained in the same models (Etherton et al. 2011; Schmeisser et al. 2012; Jaramillo et al. 2014). These divergences suggest that the interpretation of the tests should be refined to identify what each protocol actually measures. More specifically, the paradigms should be classified according to the Panksepp's system of emotional systems (Panksepp 2006) taking into account their emotional valence, positive emotions (seeking, care and playfulness) or negative emotions (fear, anger, sadness). This Panksepp's model was applied to patients with ASD, who displayed decreased playfulness and increased fear (Carré et al. 2015). Such an approach can be applied to mouse models in order to refine the characterisation of the phenotypic impairments caused by genetic mutations.

Innovative methods should also be developed to provide more ethological contexts allowing the expression of a more complete behavioural repertoire to characterise social interactions, communication and stereotyped behaviours over different age classes (pups, juveniles and adults). In such a context, both the active form (initiating social communication) and the passive form (receiving social communication) of social behaviour could be examined, the latter usually being neglected in mouse models of ASD. These innovative methods should take into account not only all the information gathered in previous experiments but also potential biases such as the different human experimenters (Sorge et al. 2014), the test cage conditions and habituation time (Ferhat et al. 2015). These biases could be reduced in complex environments where the behaviour of the individual mice is recorded continuously with few or any human intervention (Howerton et al. 2012; Ohayon et al. 2013; Weissbrod et al. 2013). In such settings, the different sensory

modalities can also be studied in more ethological conditions, with limited manipulation of the motivations of the tested animals.

As an example, focusing on social recognition in such testing conditions will be of high interest to evaluate how social cues are perceived in mouse models of ASD. New protocols should be developed to disentangle perception (whisking, sniffing or body postures during social contacts) and social cues processing deficits from common memory deficits. If mutant mice do not investigate a conspecific with all sensory modalities, they might be impaired in their ability to differentiate two individuals. Indeed, some models display social recognition deficits, but display normal spatial learning or object working memory (Peça et al. 2011; Schmeisser et al. 2012; Won et al. 2012). In this context, Engelmann and colleagues proposed to evaluate the free interactions between a tested mouse and two more or less familiar conspecifics (Engelmann et al. 2011).

5.8 Conclusions

Overall, the diversity of the mouse models carrying mutations in ASD-risk genes plays a crucial role in unravelling the links between genes, neuronal circuits and behaviour. New multi-scale approaches that include genetics, biochemistry, electrophysiology and a refinement of behavioural characterisation methods will help to dissect out biological pathways associated with ASD such as those involved in social communication and stereotyped behaviours. Altogether, it will favour a better understanding of the mechanisms behind ASD that should orient the identification of knowledge-based treatments.

Acknowledgements We thank Jean-Pierre Bourgeois for his helpful comments and discussion on the manuscript. This work was supported by the Fondation de France, the ANR FLEXNEURIM [ANR09BLAN034003], the ANR [ANR-08-MNPS-037-01–SynGen], the Neuron-ERANET (EUHF-AUTISM), the Fondation Orange, the Fondation FondaMental, the Fondation de France and the Fondation Bettencourt Schueller. The research leading to this article has also received support from EU-AIMS, which receives support from the Innovative Medicines Initiative Joint Undertaking under grant agreement no.115300, resources of which are composed of financial contributions from the European Union's Seventh Framework Programme (P7/2007–2013), from EFPIA companies in kind contribution and from Autism Speaks. MJS was further supported by the Baustein programme of Ulm University (L.SBN.0081), the Care-for-Rare Foundation, the Elite programme of the Baden-Wuerttemberg Foundation and together with EE by the PROCOPE programme.

References

American Psychiatric Association, W. D. (2013) Diagnostic and statistical manual of mental disorders, 5th edn (DSM-V)

Arriaga G, Zhou EP, Jarvis ED (2012) Of mice, birds, and men: the mouse ultrasonic song system has some features similar to humans and song-learning birds. PLoS One. doi:10.1371/journal.pone.0046610

Bachevalier J (1996) Brief report: medial temporal lobe and autism: a putative animal model in primates. J Autism Dev Disord 26:217–220

Bader PL, Faizi M, Kim LH et al (2011) Mouse model of Timothy syndrome recapitulates triad of autistic traits. Proc Natl Acad Sci USA 108:15432–15437. doi:10.1073/pnas.1112667108

Bidinosti M, Botta P, Krüttner S et al (2016) CLK2 inhibition ameliorates autistic features associated with SHANK3 deficiency. Science 351:1199–1203. doi:10.1126/science.aad5487

Blundell J, Tabuchi K, Bolliger MF et al (2009) Increased anxiety-like behavior in mice lacking the inhibitory synapse cell adhesion molecule neuroligin 2. Genes Brain Behav 8:114–126. doi:10.1111/j.1601-183X.2008.00455.x

Blundell J, Blaiss CA, Etherton MR et al (2010) Neuroligin-1 deletion results in impaired spatial memory and increased repetitive behavior. J Neurosci 30:2115–2129. doi:10.1523/JNEUROSCI.4517-09.2010

Born G, Grayton HM, Langhorst H et al (2015) Genetic targeting of NRXN2 in mice unveils role in excitatory cortical synapse function and social behaviors. Front Synaptic Neurosci 7:1–16. doi:10.3389/fnsyn.2015.00003

Bosch OJ, Neumann ID (2012) Both oxytocin and vasopressin are mediators of maternal care and aggression in rodents: from central release to sites of action. Horm Behav 61:293–303. doi:10.1016/j.yhbeh.2011.11.002

Bourgeron T (2015) From the genetic architecture to synaptic plasticity in autism spectrum disorder. Nat Rev Neurosci 16:551–563. doi:10.1038/nrn3992

Bozdagi O, Sakurai T, Papapetrou D et al (2010) Haploinsufficiency of the autism-associated Shank3 gene leads to deficits in synaptic function, social interaction, and social communication. Mol Autism 1:15. doi:10.1186/2040-2392-1-15

Brennan PA, Kendrick KM (2006) Mammalian social odours: attraction and individual recognition. Philos Trans R Soc Lond B Biol Sci 361:2061–2078. doi:10.1098/rstb.2006.1931

Burrows EL, Laskaris L, Koyama L et al (2015) A neuroligin-3 mutation implicated in autism causes abnormal aggression and increases repetitive behavior in mice. Mol Autism 6:62. doi:10.1186/s13229-015-0055-7

Carré A, Chevallier C, Robel L et al (2015) Tracking social motivation systems deficits: the affective neuroscience view of autism. J Autism Dev Disord 45:3351–3363. doi:10.1007/s10803-015-2498-2

Chadman KK (2011) Fluoxetine but not risperidone increases sociability in the BTBR mouse model of autism. Pharmacol Biochem Behav 97:586–594. doi:10.1016/j.pbb.2010.09.012

Chevallier C, Kohls G, Troiani V et al (2012) The social motivation theory of autism. Trends Cogn Sci 16:231–238. doi:10.1016/j.tics.2012.02.007

Crawley JN (2012) Translational animal models of autism and neurodevelopmental disorders. Dialogues Clin Neurosci 14:293–305

Dachtler J, Glasper J, Cohen RN et al (2014) Deletion of α-neurexin II results in autism-related behaviors in mice. Transl Psychiatry 4:e484. doi:10.1038/tp.2014.123

DeLorey TM, Handforth A, Anagnostaras SG et al (1998) Mice lacking the β3 subunit of the GABAA receptor have the epilepsy phenotype and many of the behavioral characteristics of Angelman syndrome. J Neurosci 18:8505–8514. doi:10.1097/00000542-199809130-00006

DeLorey TM, Sahbaie P, Hashemi E et al (2008) Gabrb3 gene deficient mice exhibit impaired social and exploratory behaviors, deficits in non-selective attention and hypoplasia of cerebellar vermal lobules: a potential model of autism spectrum disorder. Behav Brain Res 187:207–220. doi:10.1016/j.bbr.2007.09.009

Drapeau E, Dorr NP, Elder GA, Buxbaum JD (2014) Absence of strong strain effects in behavioral analyses of Shank3-deficient mice. Dis Model Mech 7:667–681. doi:10.1242/dmm.013821

Duffney LJ, Zhong P, Wei J et al (2015) Autism-like deficits in Shank3-deficient mice are rescued by targeting actin regulators. Cell Rep 11:1400–1413. doi:10.1016/j.celrep.2015.04.064

Ellegood J, Lerch JP, Henkelman RM (2011) Brain abnormalities in a Neuroligin3 R451C knockin mouse model associated with autism. Autism Res 4:368–376. doi:10.1002/aur.215

Elsabbagh M, Divan G, Koh YJ et al (2012) Global prevalence of autism and other pervasive developmental disorders. Autism Res 5:160–179. doi:10.1002/aur.239

Engelmann M, Hädicke J, Noack J (2011) Testing declarative memory in laboratory rats and mice using the nonconditioned social discrimination procedure. Nat Protoc 6:1152–1162. doi:10.1038/nprot.2011.353

Etherton MR, Blaiss CA, Powell CM, Südhof TC (2009) Mouse neurexin-1alpha deletion causes correlated electrophysiological and behavioral changes consistent with cognitive impairments. Proc Natl Acad Sci USA 106:17998–18003. doi:10.1073/pnas.0910297106

Etherton M, Földy C, Sharma M et al (2011) Autism-linked neuroligin-3 R451C mutation differentially alters hippocampal and cortical synaptic function. Proc Natl Acad Sci USA 108:13764–13769. doi:10.1073/pnas.1111093108

Ey E, Leblond CS, Bourgeron T (2011) Behavioral profiles of mouse models for autism spectrum disorders. Autism Res 4:5–16. doi:10.1002/aur.175

Ey E, Yang M, Katz AM et al (2012) Absence of deficits in social behaviors and ultrasonic vocalizations in later generations of mice lacking neuroligin4. Genes Brain Behav 11:928–941. doi:10.1111/j.1601-183X.2012.00849.x

Ey E, Torquet N, Le Sourd AM et al (2013) The autism ProSAP1/Shank2 mouse model displays quantitative and structural abnormalities in ultrasonic vocalisations. Behav Brain Res 256:677–689. doi:10.1016/j.bbr.2013.08.031

Ferguson JN, Young LJ, Hearn EF et al (2000) Social amnesia in mice lacking the oxytocin gene. Nat Genet 25:284–288. doi:10.1038/77040

Ferhat A-T, Le Sourd AM, De Chaumont F et al (2015) Social communication in mice—Are there optimal cage conditions? PLoS One 10:1–19. doi:10.1371/journal.pone.0121802

Ferhat A-T, Torquet N, Le Sourd AM et al (2016) Recording mouse ultrasonic vocalizations to evaluate social communication. J Vis Exp:1–12. doi:10.3791/53871

Fuster JM (2008) The prefrontal cortex, 4th edn. Academic Press, San Diego. ISBN:9780123736444

Grayton HM, Missler M, Collier DA, Fernandes C (2013) Altered social behaviours in neurexin 1a knockout mice resemble core symptoms in neurodevelopmental disorders. PLoS One. doi:10.1371/journal.pone.0067114

Hammerschmidt K, Radyushkin K, Ehrenreich H, Fischer J (2012) The structure and usage of female and male mouse ultrasonic vocalizations reveal only minor differences. PLoS One 7:1–7. doi:10.1371/journal.pone.0041133

Hammerschmidt K, Whelan G, Eichele G, Fischer J (2015) Mice lacking the cerebral cortex develop normal song: Insights into the foundations of vocal learning. Sci Rep 5:8808. doi:10.1038/srep08808

Hines RM, Wu L, Hines DJ et al (2008) Synaptic imbalance, stereotypies, and impaired social interactions in mice with altered neuroligin 2 expression. J Neurosci 28:6055–6067. doi:10.1523/JNEUROSCI.0032-08.2008

Howerton CL, Garner JP, Mench JA (2012) A system utilizing radio frequency identification (RFID) technology to monitor individual rodent behavior in complex social settings. J Neurosci Methods 209:74–78. doi:10.1016/j.jneumeth.2012.06.001

Huguet G, Ey E, Bourgeron T (2013) The genetic landscapes of autism spectrum disorders. Annu Rev Genomics Hum Genet 14:191–213. doi:10.1146/annurev-genom-091212-153431

Hung AY, Futai K, Sala C et al (2008) Smaller dendritic spines, weaker synaptic transmission, but enhanced spatial learning in mice lacking Shank1. J Neurosci 28:1697–1708. doi:10.1523/JNEUROSCI.3032-07.2008

Jamain S, Radyushkin K, Hammerschmidt K et al (2008) Reduced social interaction and ultrasonic communication in a mouse model of monogenic heritable autism. Proc Natl Acad Sci USA 105:1710–1715. doi:10.1073/pnas.0711555105

Jaramillo TC, Liu S, Pettersen A et al (2014) Autism-related neuroligin-3 mutation alters social behavior and spatial learning. Autism Res 7:264–272. doi:10.1002/aur.1362

Jaramillo TC, Speed HE, Xuan Z et al (2016) Altered striatal synaptic function and abnormal behaviour in Shank3 Exon4-9 deletion mouse model of autism. Autism Res 9:350–375. doi:10.1002/aur.1529

Jiang YH, Ehlers MD (2013) Modeling autism by SHANK gene mutations in mice. Neuron 78:8–27. doi:10.1016/j.neuron.2013.03.016

Ju A, Hammerschmidt K, Tantra M et al (2014) Juvenile manifestation of ultrasound communication deficits in the neuroligin-4 null mutant mouse model of autism. Behav Brain Res 270:159–164. doi:10.1016/j.bbr.2014.05.019

Jürgens U (2002) Neural pathways underlying vocal control. Neurosci Biobehav Rev 26:235–258. doi:10.1016/S0149-7634(01)00068-9

Jürgens U (2009) The neural control of vocalization in mammals: a review. J Voice 23:1–10. doi:10.1016/j.jvoice.2007.07.005

Karvat G, Kimchi T (2012) Systematic autistic-like behavioral phenotyping of 4 mouse strains using a novel wheel-running assay. Behav Brain Res 233:405–414. doi:10.1016/j.bbr.2012.05.028

Kas MJ, Modi ME, Saxe MD, Smith DG (2014) Advancing the discovery of medications for autism spectrum disorder using new technologies to reveal social brain circuitry in rodents. Psychopharmacology (Berl) 231:1147–1165. doi:10.1007/s00213-014-3464-y

Kelley A (2001) Measurement of rodent stereotyped behavior. Curr Protoc Neurosci Chapter 8: Unit 8.8. doi:10.1002/0471142301.ns0808s04

Keverne EB (1999) The vomeronasal organ. Science 286:716–720. doi:10.2307/2899372

Kohls G, Schulte-Rüther M, Nehrkorn B et al (2013) Reward system dysfunction in autism spectrum disorders. Soc Cogn Affect Neurosci 8:565–572. doi:10.1093/scan/nss033

Kouser M, Speed HE, Dewey CM et al (2013) Loss of predominant Shank3 isoforms results in hippocampus-dependent impairments in behavior and synaptic transmission. J Neurosci 33:18448–18468. doi:10.1523/JNEUROSCI.3017-13.2013

Kruk MR, De Vos-Frerichs TP, Van Der Poel AM (1979) The induction of aggressive behaviour by electrical stimulation in the hypothalamus of male rats. Behaviour 70:292–322. doi:10.1163/156853979X00106

Kumar M, Duda JT, Hwang W-T et al (2014) High resolution magnetic resonance imaging for characterization of the neuroligin-3 knock-in mouse model associated with autism spectrum disorder. PLoS One 9:e109872. doi:10.1371/journal.pone.0109872

Langen M, Durston S, Kas MJH et al (2011) The neurobiology of repetitive behavior: ...and men. Neurosci Biobehav Rev 35:356–365. doi:10.1016/j.neubiorev.2010.02.005

Latham N, Mason G (2004) From house mouse to mouse house: the behavioural biology of free-living Mus musculus and its implications in the laboratory. Appl Anim Behav Sci 86:261–289. doi:10.1016/j.applanim.2004.02.006

Leblond CS, Nava C, Polge A et al (2014) Meta-analysis of SHANK mutations in autism spectrum disorders: a gradient of severity in cognitive impairments. PLoS Genet. doi:10.1371/journal.pgen.1004580

Lee E-J, Lee H, Huang T-N et al (2015a) Data sup Trans-synaptic zinc mobilization improves social interaction in two mouse models of autism through NMDAR activation. Nat Commun 6:7168. doi:10.1038/ncomms8168

Lee J, Chung C, Ha S et al (2015b) Shank3-mutant mice lacking exon 9 show altered excitation/inhibition balance, enhanced rearing, and spatial memory deficit. Front Cell Neurosci 9:94. doi:10.3389/fncel.2015.00094

Lewis MH, Tanimura Y, Lee LW, Bodfish JW (2007) Animal models of restricted repetitive behavior in autism. Behav Brain Res 176:66–74. doi:10.1016/j.bbr.2006.08.023

Maren S (2003) The amygdala, synaptic plasticity, and fear memory. Ann N Y Acad Sci 985:106–113

Mason G, Rushen J (2006) Stereotypic animal behaviour:fundamentals and applications to welfare. CABI, Wallingford

Mei Y, Monteiro P, Zhou Y et al (2016) Adult restoration of Shank3 expression rescues selective autistic-like phenotypes. Nature 530:481–484. doi:10.1038/nature16971

Ohayon S, Avni O, Taylor AL et al (2013) Automated multi-day tracking of marked mice for the analysis of social behaviour. J Neurosci Methods 219:10–19. doi:10.1016/j.jneumeth.2013.05.013

Panksepp J (2006) Emotional endophenotypes in evolutionary psychiatry. Prog Neuro-Psychopharmacol Biol Psychiatry 30:774–784. doi:10.1016/j.pnpbp.2006.01.004

Peça J, Feliciano C, Ting JT et al (2011) Shank3 mutant mice display autistic-like behaviours and striatal dysfunction. Nature 472:437–442. doi:10.1038/nature09965

Peñagarikano O, Abrahams BS, Herman EI et al (2011) Absence of CNTNAP2 leads to epilepsy, neuronal migration abnormalities, and core autism-related deficits. Cell 147:235–246. doi:10.1016/j.cell.2011.08.040

Peñagarikano O, Lázaro MT, Lu X-H et al (2015) Exogenous and evoked oxytocin restores social behavior in the Cntnap2 mouse model of autism. Sci Transl Med 7:271ra8. doi:10.1126/scitranslmed.3010257

Popik P, van Ree JM (1991) Oxytocin but not vasopressin facilitates social recognition following injection into the medial preoptic area of the rat brain. Eur Neuropsychopharmacol 1:555–560

Portfors CV (2007) Types and functions of ultrasonic vocalizations in laboratory rats and mice. J Am Assoc Lab Anim Sci 46:28–34

Portfors CV, Perkel DJ (2014) The role of ultrasonic vocalizations in mouse communication. Curr Opin Neurobiol 28:115–120. doi:10.1016/j.conb.2014.07.002

Presti MF, Mikes HM, Lewis MH (2003) Selective blockade of spontaneous motor stereotypy via intrastriatal pharmacological manipulation. Pharmacol Biochem Behav 74:833–839. doi:10.1016/S0091-3057(02)01081-X

Presti MF, Watson CJ, Kennedy RT et al (2004) Behavior-related alterations of striatal neurochemistry in a mouse model of stereotyped movement disorder. Pharmacol Biochem Behav 77:501–507. doi:10.1016/j.pbb.2003.12.004

Price JL (2006) Comparative aspects of amygdala connectivity. Ann N Y Acad Sci 985:50–58. doi:10.1111/j.1749-6632.2003.tb07070.x

Rabaneda LG, Robles-Lanuza E, Nieto-González J, Scholl FG (2014) Neurexin dysfunction in adult neurons results in autistic-like behavior in mice. Cell Rep 8:338–346. doi:10.1016/j.celrep.2014.06.022

Radyushkin K, Hammerschmidt K, Boretius S et al (2009) Neuroligin-3-deficient mice: model of a monogenic heritable form of autism with an olfactory deficit. Genes Brain Behav 8:416–425. doi:10.1111/j.1601-183X.2009.00487.x

R Core Team (2016) R: a language and environment for statistical computing. R Foundation for Statistical Computing, Vienna. https://www.R-project.org/

Robinson DL, Zitzman DL, Williams SK (2011) Mesolimbic dopamine transients in motivated behaviors: focus on maternal behavior. Front Psychiatry 2:1–13. doi:10.3389/fpsyt.2011.00023

Roullet FI, Wöhr M, Yang M, Crawley JN (2009) Scent marking and countermarking behaviors as a measure of olfactory communication in the BTBR T+tf/J inbred strain, a mouse model of autism. Chem Senses 34:A23. doi:10.1093/chemse/bjp032

Russo S, Nestler E (2013) The brain reward circuitry in mood disorders. Nat Rev Neurosci 625:609–625. doi:10.1038/nrn3381

Schmeisser MJ, Ey E, Wegener S et al (2012) Autistic-like behaviours and hyperactivity in mice lacking ProSAP1/Shank2. Nature 486:256–260. doi:10.1038/nature11015

Silverman JL, Yang M, Lord C, Crawley JN (2010) Behavioural phenotyping assays for mouse models of autism. Nat Rev Neurosci 11:490–502. doi:10.1038/nrn2851

Silverman JL, Turner SM, Barkan CL et al (2011) Sociability and motor functions in Shank1 mutant mice. Brain Res 1380:120–137. doi:10.1016/j.brainres.2010.09.026

Soden ME, Miller SM, Burgeno LM et al (2016) Genetic isolation of hypothalamic neurons that regulate context-specific male social behavior. Cell Rep 16:304–313. doi:10.1016/j.celrep.2016.05.067

Sorge RE, Martin LJ, Isbester KA et al (2014) Olfactory exposure to males, including men, causes stress and related analgesia in rodents. Nat Methods 11:629–632. doi:10.1038/nmeth.2935

Speed HE, Kouser M, Xuan Z et al (2015) Autism-associated insertion mutation (InsG) of Shank3 Exon 21 causes impaired synaptic transmission and behavioral deficits. J Neurosci 35:9648–9665. doi:10.1523/JNEUROSCI.3125-14.2015

Steadman PE, Ellegood J, Szulc KU et al (2014) Genetic effects on cerebellar structure across mouse models of autism using a magnetic resonance imaging atlas. Autism Res 7:124–137. doi:10.1002/aur.1344

Sungur AÖ, Vörckel KJ, Schwarting RKW, Wöhr M (2014) Repetitive behaviors in the Shank1 knockout mouse model for autism spectrum disorder: developmental aspects and effects of social context. J Neurosci Methods 234:92–100. doi:10.1016/j.jneumeth.2014.05.003

Tabuchi K, Blundell J, Etherton MR et al (2007) A neuroligin-3 mutation implicated in autism increases inhibitory synaptic transmission in mice. Science 318:71–76. doi:10.1126/science.1146221

Toro R, Konyukh M, Delorme R et al (2010) Key role for gene dosage and synaptic homeostasis in autism spectrum disorders. Trends Genet 26:363–372. doi:10.1016/j.tig.2010.05.007

U.S. Department of Health and Human Services (2014) Prevalence of autism spectrum disorder among children aged 8 years—autism and developmental disabilities monitoring network, 11 sites, United States, 2010. MMWR Surveill Summ 63:1–21

Veening JG, Coolen LM, De Jong TR et al (2005) Do similar neural systems subserve aggressive and sexual behaviour in male rats? Insights from c-Fos and pharmacological studies. Eur J Pharmacol 526:226–239. doi:10.1016/j.ejphar.2005.09.041

Vicidomini C, Ponzoni L, Lim D et al (2016) Pharmacological enhancement of mGlu5 receptors rescues behavioral deficits in SHANK3 knock-out mice. Mol Psychiatry:1–14. doi:10.1038/mp.2016.30

Wang X, McCoy PA, Rodriguiz RM et al (2011) Synaptic dysfunction and abnormal behaviors in mice lacking major isoforms of Shank3. Hum Mol Genet 20:3093–3108. doi:10.1093/hmg/ddr212

Wang F, Kessels HW, Hu H (2014a) The mouse that roared: neural mechanisms of social hierarchy. Trends Neurosci 37:674–682. doi:10.1016/j.tins.2014.07.005

Wang X, Xu Q, Bey AL et al (2014b) Transcriptional and functional complexity of Shank3 provides a molecular framework to understand the phenotypic heterogeneity of SHANK3 causing autism and Shank3 mutant mice. Mol Autism 5:30. doi:10.1186/2040-2392-5-30

Wang X, Bey AL, Katz BM et al (2016) Altered mGluR5-Homer scaffolds and corticostriatal connectivity in a Shank3 complete knockout model of autism. Nat Commun 7:11459. doi:10.1038/ncomms11459

Weissbrod A, Shapiro A, Vasserman G et al (2013) Automated long-term tracking and social behavioural phenotyping of animal colonies within a semi-natural environment. Nat Commun 4:2018. doi:10.1038/ncomms3018

Wöhr M (2014) Ultrasonic vocalizations in Shank mouse models for autism spectrum disorders: detailed spectrographic analyses and developmental profiles. Neurosci Biobehav Rev 43:199–212. doi:10.1016/j.neubiorev.2014.03.021

Wöhr M, Silverman JL, Scattoni ML et al (2013) Developmental delays and reduced pup ultrasonic vocalizations but normal sociability in mice lacking the postsynaptic cell adhesion protein neuroligin2. Behav Brain Res 251:50–64. doi:10.1016/j.bbr.2012.07.024

Won H, Lee H-R, Gee HY et al (2012) Autistic-like social behaviour in Shank2-mutant mice improved by restoring NMDA receptor function. Nature 486:261–265. doi:10.1038/nature11208

Yang M, Bozdagi O, Scattoni ML et al (2012) Reduced excitatory neurotransmission and mild autism-relevant phenotypes in adolescent Shank3 null mutant mice. J Neurosci 32:6525–6541. doi:10.1523/JNEUROSCI.6107-11.2012

Zhou Y, Kaiser T, Monteiro P et al (2016) Mice with Shank3 mutations associated with ASD and Schizophrenia display both shared and distinct defects. Neuron 89:147–162. doi:10.1016/j.neuron.2015.11.023

Study on the neurobiological bases of autism spectrum disorders: Behavioural and molecular characterisation of Shank3 mutant mice

Autism spectrum disorders (ASD) are neurodevelopmental psychiatric disorders characterised by alterations in social interactions and communications as well as stereotyped behaviours and restricted interests. Mutations in genes coding synaptic proteins are strongly associated with ASD and more specifically *SHANK3,* encoding for a scaffolding protein in the post-synaptic density of glutamatergic synapses. The aim of the present PhD thesis is to characterise a mouse model deleted for exon 11 in *Shank3* and to better understand the brain regions affected by this mutation. We characterised the mice at the behavioural level (a longitudinal study between three and twelve months of age) and at the molecular level (transcriptome analysis using mRNA sequencing). At three months of age, we observed a decreased locomotor activity, increased stereotyped behaviour and increased social motivation during free interaction in *Shank3*-/- mice compared to *Shank3*+/+ mice. When testing animals at 3, 8, and 12 months of age, we noticed a worsening of the phenotype in *Shank3*-/- mice while ageing, especially in self-grooming behaviour. When exploring the transcriptomic, we revealed an impairment of gene expression of striatal neurons sensitive to dopamine, the medium spiny neurons, as well as post-synaptic signalling in striatum. Altogether, this project provides a comprehensive characterisation of a mouse model of ASD. It sheds some light on the molecular mechanisms possibly involved in patients with ASD mutated in *SHANK3*. This insight could reveal new therapeutic approaches targeting the imbalance in dopaminosensitive neurons.

Étude des bases neurobiologiques des troubles du spectre autistique : Caractérisation comportementale et moléculaire de souris invalidées pour *Shank3*.

Les troubles du spectre autistique (TSA) sont des troubles psychiatriques neuro-développementaux caractérisés par des altérations de l'interaction et de la communication sociales ainsi que des comportements stéréotypés et des intérêts restreints. Les TSA sont fortement associés à des composantes génétiques et en particulier avec le gène *SHANK3*, codant pour une protéine d'échafaudage dans la densité post-synaptique des synapses glutamatergiques.

L'objectif de ce doctorat est de caractériser un modèle de souris *Shank3* et de mieux comprendre les régions du cerveau affectées par la délétion de *Shank3*. Nous avons caractérisé les souris au niveau comportemental (une étude longitudinale entre trois et douze mois) et au niveau moléculaire (analyse du transcriptome en utilisant le séquençage de l'ARNm).

À l'âge de trois mois, nous avons observé une diminution de l'activité locomotrice, une augmentation des comportements stéréotypés et une motivation sociale accrue au cours d'interaction libre chez les souris *Shank3*-/- en comparant aux souris *Shank3*+/+. Lorsque nous avons testé les animaux à l'âge de 8 et 12 mois, nous avons observé une détérioration du phénotype chez les souris *Shank3*- / - en vieillissant, en particulier pour les comportements stéréotypés.

Lors de l'analyse du transcriptome, nous avons révélé, au niveau du striatum, une altération de l'expression génique des neurones sensibles à la dopamine, les neurones épineux moyens, ainsi que des problèmes de la signalisation post-synaptique.

Ainsi, ce projet fournit une caractérisation complète d'un modèle murin de l'autisme. Il met en lumière les mécanismes moléculaires éventuellement impliqués chez les patients atteints de TSA et portant une mutation dans *SHANK3*. Cette idée pourrait révéler une nouvelle approche thérapeutique pour les patients ciblant le déséquilibre dans les neurones du striatum.